Universidad Autónoma de Madrid

Departamento de Bioquímica

Caracterización funcional de ING4: implicaciones en supresión tumoral

Alberto Moreno de la Gándara

Madrid, 2012

Departamento de Bioquímica
Facultad de Medicina
Universidad Autónoma de Madrid

Caracterización funcional de ING4: implicaciones en supresión tumoral

Alberto Moreno de la Gándara
Licenciado en Bioquímica

Director de Tesis: Dr. Ignacio Palmero Rodríguez

Instituto de Investigaciones Biomédicas “Alberto Sols”
CSIC-UAM

MINISTERIO
DE CIENCIA E
INNOVACIÓN

CSIC

UAM
UNIVERSIDAD AUTONOMA
DE MADRID

INSTITUTO DE INVESTIGACIONES BIOMÉDICAS
"ALBERTO SOLS"

Ignacio Palmero, PhD
Instituto de Investigaciones Biomédicas
Arturo Duperier, 4.
E-28029 Madrid, SPAIN
Tel: 34 91 585 4491
Fax: 34 91 585 4401
email: ipalmero@iib.uam.es

IGNACIO PALMERO RODRÍGUEZ, Científico Titular del Instituto de Investigaciones Biomédicas "Alberto Sols" CSIC-UAM,

certifico que:

ALBERTO MORENO DE LA GÁNDARA, Licenciado en Bioquímica por la Universidad Autónoma de Madrid ha realizado, bajo mi dirección, el trabajo de investigación titulado:

"Caracterización funcional de ING4: implicaciones en supresión tumoral"

Considero que el mencionado trabajo reúne la originalidad y calidad científica requeridas para poder ser presentado para optar al grado de Doctor por la Universidad Autónoma de Madrid.

Y para que conste a todos los efectos, firmo el presente certificado,
en Madrid, a 28 de Noviembre de 2011.

Fdo: Ignacio Palmero
Científico Titular, CSIC

Vº Bº: Miguel Campanero
Prof. Honorario
Dpto. Bioquímica, UAM

C/Arturo Duperier, nº 4
28029 MADRID ESPAÑA
TEL.: 91 585 4400
FAX: 91 585 4401

A mis padres

Lo que sabemos es una gota de agua, lo que ignoramos es el océano.

Isaac Newton

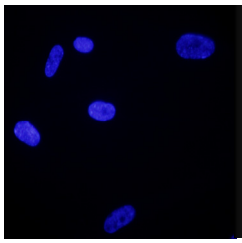

Agradecimientos

Finalmente llega el momento de cerrar una etapa y hacer balance de lo vivido durante estos últimos cinco años. Son tantos recuerdos, anécdotas y experiencias las que pasan por la cabeza que no hay forma de plasmar en un papel el agradecimiento a tanta gente que ha contribuido a que esto sea posible. Al fin y al cabo, han sido unos años muy intensos de gran crecimiento personal y profesional los que han hecho de esta tesis una experiencia estupenda.

En estos momentos en los que se afronta el futuro con incertidumbre y nerviosismo por el que será de ti, a que te dedicarás o dónde acabarás hace que se afronte con cierta tristeza el momento de dejar esto atrás. Pero también hace sonreír y llena de alegría el pensar en toda la gente que has conocido y que de una forma u otra ha estado a tu lado durante todo este tiempo.

En primer lugar quería dar las gracias a Ignacio Palmero por darme la oportunidad de formar parte del laboratorio y en su apoyo para sacar adelante este proyecto. En todo momento he sentido tu dedicación y tu ayuda en los momentos difíciles. Tu capacidad de razonamiento y de motivación en los momentos en los que crees que todo va a salir mal me ha hecho aprender a disfrutar de este trabajo y ver que todo tiene una explicación. Me siento muy afortunando de haber contado con un gran director de tesis.

Gracias a todos los compañeros con los que he compartido el 1.4. durante estos años, con los que me he sentido como en mi casa y por los que he pasado de ser “pequeño lechón” a “mamá pato”. No son pocas personas, pero de todas guardo un recuerdo imborrable: Esther llamándome Antonio desde el primer día, Ana matándonos de la vergüenza, Bea y sus despistes, Laura con su viaje en globo, Alicia con nuestros paseos a Cantoblanco, Agatha con el vodka que aún no nos hemos tomado, Simone y el cuadrilátero del amor, Weronika con sus resacas brutales, Adrián con sus desates fiesteros, Marta con su risa loca intentando hacerme destripar un ratón descompuesto y con nuestras charlas trascendentales. Mis vecinos, identificados con las locuras de Héctor, las paridas de Álvaro, las tonterías de Rosa, los palabros raros de Mónica…Pero especialmente me acuerdo de Lara, porque a pesar de haber coincidido poco, le dió tiempo a identificar mi primera contaminación por “champiñones” y a mi vivir lo estresante que es escribir una tesis. También de Camino, porque a pesar de nuestras diferencias ha sido muy importante para mí. Me enseñó todo lo que supo y también pasamos muy buenos momentos con el cruce de mi ratón@. Flopy, mi boluda favorita, por todos nuestros planes de futuro con BF y por nuestras risas con el diccionario hispano-porteño. David por hacerme pensar todos los días que le “habían atropellao”, por su misterio y por esa cantidad de cosas raras que nos envía. Yenny por ser capaz de pasar frío a 40ºC y ponerse al sol por la mañana como los lagartos. Rafa, por ser el manchego perfecto, por sus ideas imperialistas y por su empeño en poner a los caracoles en lo más alto de la escala evolutiva. Por supuesto de Carmela, por todo el interés que ha mostrado en mí, por sus consejos y por hacerme la berrea tantas veces. Y finalmente de Irma, porque desde el momento en el que entró en el laboratorio quiso aprender lo más rápido posible para ayudarme. Recordaré tus chillidos con los ratones que casi me matan del susto y tu paciencia con mis prisas finales.

Además, quería mencionar a todas las personas del centro que me han ayudado durante esta etapa. La gente de seguridad, Carlos, Ruth y Diego, por poner esa cara de “que c…haces

aquí" al venir los fines de semana. Los de informática, Alex, Gema y Nani por ser únicos, Javi por sus achuchones y Guti por su ayuda en los momentos de pánico y por sus sabios consejos. También los de imagen, Javi, Antonio y Ricardo, por estar siempre dispuestos a echar un cable y a Estrella, Diego y Lucía por los días en el citómetro y en el microscopio. Mis compañeras de comedor del 0.2, por no desesperar cuando se nos olvidaba avisarlas para comer, por ser capaces de hablar de tantas chorradas por minuto como nosotros. Esther con su risa contagiosa, Anna soportando mi italiano básico, Natalia por no dejarme ir a China y por vivir en una cueva y Pilar por dejar meterme con ella y con su pueblo. Merche y Toño por no bajarse nunca del podio en las competiciones del iib. Los vecinos del fondo, Diana, Jose, Sandra y Marina por nuestra rivalidad "sana" haciendo videos ridículos. La gente que ha pasado por el 2.4, Miguel, Teresa, Celia, Andrea, Alonso, Raúl, Irene, Josué, por las cenas de navidad. Jose, Asun y Benilde por nuestras colaboraciones. A mis compañeros políticos del B15, Irene y sus lloros memorables en las bodas y los aún más memorables bailes de Carlos. A mis compañer@s del viaje a Oslo, Vero, María, Vanessa, María, Cristina, Blanca y Jaime, porque pensaba que "las de Perona" eran la fiesta y me demostraron que son unas personas geniales pero con las pilas gastadas (excepto Jaime). También a Laura por su maestría en el padel. A los vecinos del 1.8, Amparo por ser una persona muy especial por la que siento mucho cariño, Pablo porque compartimos mucho tiempo juntos e Irene, porque es mi zurda favorita, mi compañera de siempre y a la que siempre he recurrido cuando he tenido un problema. Y aunque llegaron más tarde, los vecinos "de enfrente". No han sido pocos los desahogos y las historias surrealistas con la tecnología vividas con María, los chistes malos de Jose en cultivos que a mí tanto me gustan y María descubriéndome detalles escondidos de series frikis.

Mis compañeros de la facultad, con los que empecé este camino y a los que aún tengo la suerte de disfrutar. Porque aunque nos vemos poco, siempre compartimos experiencias, consejos y apoyo como si no hubiera pasado el tiempo. Dani, por ser mi compañero "perita", Nacho por sentirte siempre cerca, incluso desde el escenario, Teresa porque eres única y porque me encantan tus vestidos de lunares y tus tobillos, Tefi por tu característica y adorable locura, Celia por tus risas, Cris por los míticos y tradicionales días en Aranjuez y Sali porque de una forma u otra, desde los cuatro años siempre has estado pendiente de mi.

A mis amigos de siempre, mis "amantes". Sabéis que os tengo un cariño especial y que aunque siempre esté dando por c…, y me cueste demostrar mis sentimientos os quiero un montón y sois muy necesarios para mí. Hugo, porque aunque me desquicias…en el fondo me encanta tu carácter, tu forma de ser y la alegría que transmites. Nadia, porque estar contigo es sinónimo de que pase algo diferente, porque siempre tienes alguna historia, porque te sabes hacer querer. Javi, porque eres un máquina, y aunque no te acuerdes de nada y haces cosas raras, estando a tu lado nada puede pasar, vales para todo. Ana, porque tu frágil salud es desconcertante, pero siempre das con la tecla, tienes esa capacidad de analizar las cosas que me encanta y que muchas veces me ha abierto los ojos. Alberto, porque son miles las cosas que hemos vivido y miles los kilómetros que hemos pedaleado juntos, porque me has enseñado muchas cosas y porque siempre he admirado tu perseverancia y las ganas que le pones a todo lo que haces. Ana,

por ser mi compañera de fatigas, la única que me comprende cuando estoy cabreado, porque me encanta tu sinceridad y porque me encanta tu "fino" sentido del humor. Kike, porque siempre has estado presente en los viajes, en los paseos con las pipas, en las huidas de los gitanos...eres muy especial para mí, la persona a la que siempre he recurrido ante el mínimo problema. Eres único.

A mis compañeros más especiales, los que me han acompañado a lo largo de esta aventura. La mayor parte de lo que he aprendido ha sido gracias a ellos y de los que me llevo una amistad llena de recuerdos que espero sigan creciendo. Isa, fuiste la última en llegar, pero desde el principio hemos pasado muy buenos ratos y parece como siempre hubieras estado ahí. Me encantan tus locuras, tus bailes, tus chistes…da gusto llegar a trabajar y dar con una persona tan alegre y optimista todas las mañanas. Cuando te hagas coaching, me llamas. Bárbara, porque ha sido genial contar con una amiga como tú, hemos conectado mucho porque tenemos una forma muy parecida de ver la vida. Desde que te fuiste se ha notado mucho tu falta, tu alegría, tu capacidad de hablar de mil cosas a la vez y no enterarme de nada, de asustarme y matarme de la risa a la vez. Leti, mi compañera de principio a fin. Me has enseñado todo acerca del mundo de las drogas, de las enfermedades y de los barrios chungos de Madrid. Vales un montón, siempre lo he pensado. En todo momento de "túnel" ahí estabas tú, sabiendo como arrancarme una sonrisa y consiguiendo que me olvidara de todo. Dani, mi compañero de fatigas. Si no hubiera sido por tí no se si habría sobrevivido entre tanta fiera. Me ensañaste a despedazar bichos, a diferenciar entre lápiz y lapicero, a que no me timaran con un cheque…Eres una persona que admiro mucho, por tu arrojo, por tu fuerza para salir adelante en los momentos difíciles…un ejemplo para mi. María, porque fuiste la que se encargó de mí cuando llegué y no sabía más que dejar mi mochila debajo de la poyata. Porque te dejaba todo el trabajo cuando me tenía que ir a clase, porque alucinabas cuando pintaba las bandas de los western…siempre te he sentido cerca, incluso en estos años en los que ya no estabas, eres el espejo en el que me he mirado desde que entré y la que me ha dado fuerzas y ánimos en todo momento.

Por supuesto, gracias a mis abuelos. Porque aunque no han sabido bien lo que hacía, han mostrado un gran cariño e interés por mí en todo momento. A Irene, porque siempre has estado dispuesta a echarme una mano si he necesitado algo. Me alegro mucho de que hayas podido hacer un esfuerzo, dejar alguna fiesta de lado, y estar conmigo hasta el final.

A mis padres. Por todo el esfuerzo y atención que me habéis dedicado. Porque a pesar de no ser una persona muy comunicativa, habéis estado siempre arropándome y dispuestos a darme todo lo que necesitará. Gracias por transmitirme todo lo que sabéis, aconsejarme y enseñarme a sacar las cosas adelante. Gracias por todo vuestro cariño y por esos desayunos de interactuación. Sois los mejores padres del mundo.

Y finalmente a Marta. Por tu comprensión, por tu paciencia con mis indecisiones torturantes. Por esperarme cuando te decía que tardaba cinco minutos y luego era media hora, por compartir tantas dudas y tantos momentos filosofales que me han ayudado en el trabajo y en la vida. Por todos los momentos difíciles que hemos pasado y superado juntos y por todos los buenos que nos quedan por vivir en adelante. Gracias por estar siempre a mi lado.

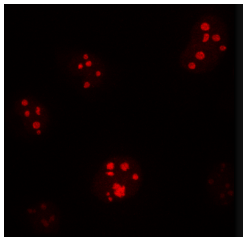

Resumen

Las proteínas de la familia ING juegan un papel importante en respuestas relacionadas con mecanismos de supresión tumoral como apoptosis, parada de ciclo celular y reparación de daño en ADN, en conexión con las vías de p53 y NFκB y con la maquinaria de remodelación de cromatina. Además de estas funciones comunes, ING4 posee funciones específicas relacionadas con progresión tumoral como control de migración, angiogénesis e invasión. Existen alteraciones de ING4 en tumores humanos que se han asociado con mayor malignidad, de acuerdo con un papel importante en progresión tumoral. Con estos antecedentes, en este trabajo hemos analizado el papel de ING4 como supresor tumoral, usando distintos abordajes. En primer lugar, hemos analizado el impacto de mutaciones de ING4 asociadas a tumores humanos, mediante distintos ensayos funcionales y estructurales. Hemos demostrado que una mutación de ING4 asociada a cáncer reduce su estabilidad e inhibe su capacidad de controlar proliferación y migración. Por otro lado, hemos realizado el análisis funcional de ING4 en un sistema de fibroblastos primarios. Hemos comprobado que ING4 tiene un efecto antiproliferativo en estas células, que requiere del reconocimiento de marcas de cromatina, y que es dependiente de p53. Además, hemos identificado el perfil de expresión génica asociado a la expresión de ING4 en células primarias. Nuestros datos muestran que ING4 regula un grupo de genes con una fuerte representación de factores solubles (citoquinas y quimioquinas) y de genes de la vía de NFκB. Análisis *in vitro* e *in vivo* han revelado un papel diferencial de ING4 en proliferación, mediado por factores solubles, potenciando el crecimiento de células tumorales y no de células primarias. Estos resultados resaltan la importancia de ING4 en tumorogénesis y muestran un papel importante en la regulación y liberación de factores solubles que pueden influir en el crecimiento y progresión tumoral a través de la comunicación del tumor con el microentorno.

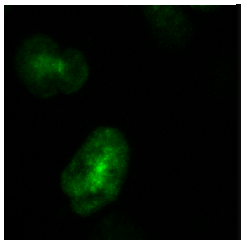

Abstract

The ING family of proteins plays an important role in responses related to tumor suppression mechanisms such as apoptosis, cell cycle arrest and DNA damage response in connection with the p53 and NFκB pathways and the chromatin remodeling machinery. In addition to these common functions, ING4 has specific functions related to tumor progression such as control of migration, angiogenesis and invasion. There are ING4 alterations in human tumors that have been associated with increased malignancy, in agreement with an important role in tumor progression. With this background, in this work we analyzed the role of ING4 as a tumor suppressor using different approaches. First, we have analyzed the impact of mutations of ING4 associated with human tumors by different functional and structural assays. We have shown that a mutation of ING4 associated with cancer reduces its stability, and inhibits its ability to control proliferation and migration. In addition, we performed functional analysis of ING4 in a system of primary fibroblasts. We found that ING4 has an antiproliferative effect on these cells, which requires recognition of chromatin marks and is p53 dependent. In addition, we identified the gene expression profile associated with the expression of ING4 in primary cells. Our data show that ING4 regulates a group of genes with a strong representation of soluble factors (cytokines and chemokines) and genes of the NFκB pathway. Analysis *in vitro* and *in vivo* revealed a differential role of ING4 on proliferation, mediated by soluble factors, enhancing the growth of tumor cells and not of primary cells. These results highlight the importance of ING4 on tumorigenesis and show an important role in the regulation and release of soluble factors that can influence the tumor growth and progression through the communication of the tumor with the microenvironment.

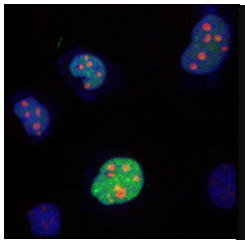

Índice

Agradecimientos III

Resumen IX

Abstract XIII

Índice 3

Clave de Abreviaturas 7

Introducción 11

1. La familia de proteínas ING 12

2. ING4 13

2.1. Estructura y localización 13

2.2. Función biológica de ING4 14

2.3. ING4 y cromatina 16

2.4. Alteraciones de ING4 asociadas a tumores 19

3. Microentorno tumoral 20

Objetivos 25

Materiales y Métodos 29

1. Mutagénesis dirigida 29

2. Cultivos celulares 29

3. Transfección 29

4. Infección retroviral 30

5. Inmunoblot 30

6. RT-QPCR 30

7. Inmunofluorescencia 31

8. Determinación de la tasa de síntesis de ADN 31

9. Migración celular 32

10. Ensayos de migración en transwell 32

11. Ensayos de crecimiento en agar blando 32

12. Espectroscopía por RMN y determinación de la estructura 33

13. Ensayos de viabilidad celular 33

14. Ensayos de vida media de proteína 33

15. Curvas de crecimiento 33

16. Actividad β-Galactosidasa asociada a senescencia (SA-β-Gal) 33

17. Perfil de expresión génica 34
18. Ensayos de medio condicionado 34
19. ELISA y array de quimioquinas 34
20. Ensayo de tumorogénesis en ratones 35
21. Ensayos de migración y metástasis en pez cebra 35
22. Vectores de expresión 36
23. Anticuerpos 37

Resultados 41

1. Impacto funcional de mutaciones de ING4 asociadas a tumores 41
1.1. Generación de formas mutantes de ING4 41
1.2. Efecto de mutantes de ING4 en proliferación celular 42
1.3. Efecto de mutantes de ING4 en migración celular 43
1.4. Efecto de mutantes de ING4 en crecimiento independiente de anclaje 44
1.5. Efecto de mutantes de ING4 en viabilidad celular 45
1.6. Impacto del mutante N214D en la estructura de la proteína y unión a marcas de histonas 46
1.7. Efecto del mutante N214D en la estabilidad de la proteína 47

2. Caracterización de ING4 en fibroblastos primarios humanos 50
2.1. Efecto de ING4 y mutantes en proliferación celular en fibroblastos primarios 51
2.2. Efecto de ING4 y mutantes en inducción de senescencia y daño en ADN 52
2.3. Conexión de ING4 con las vías de supresión tumoral de p53 y Rb 54
2.4. Análisis del perfil de expresión regulados por ING4 56
2.5. Efectos de ING4 mediados por factores solubles 60
2.6. Efecto de ING4 en tumorogénesis *in vivo* 62

3. Efectos de ING4 en inducción de metástasis en pez cebra 63

Discusión 67

Conclusiones 79

Bibliografía 83

Anexo 95

Clave de abreviaturas

BrdU: Bromodeoxiuridina

CAFs: Fibroblastos asociados a carcinoma *(Carcinoma Associated Fibroblasts)*

CHX: Cicloheximida

DDR: Respuesta a daño en ADN *(DNA damage response)*

ELISA: *Enzyme-Linked ImmunoSorbent Assay*

H3K4me3: Histona H3 trimetilada en lisina 4

HA: Hemaglutinina

HAT: Histona acetil transferasa *(Histone Acetyl Transferase)*

HDAC: Histona deacetilasa *(Histone Deacetylase)*

HMVEC: Células endoteliales microvasculares humanas *(Human Microvascular Endothelial Cells)*

ING: *Inhibitor of Growth*

Kd: Constante de disociación

LPS: Lipopolisacárido

LZL: Cremallera de leucinas *(Leucine Zipper-Like)*

miRNA: Micro ARN

NCR: Nueva región conservada *(Novel Conserved Region)*

NLS: Secuencia de localización nuclear *(Nuclear Localization Sequence)*

NMR: Resonancia magnética nuclear *(Nuclear Magnetic Resonance)*

PHD: *Plant Homeo Domain*

Rb: Retinoblastoma

ROS: Especies reactivas de oxígeno *(Reactive Oxygen Species)*

RT-QPCR: PCR cuantitativa *(Real Time Quantitative-Polymerase Chain Reaction)*

SAHFs: Focos de heterocromatina asociados a senescencia *(Senescence Associated Heterochromatin Foci)*

SASP: Fenotipo secretor asociado a senescencia *(Senescence Associated Secretory Phenotype)*

SA-β-Gal: Actividad β-Gal asociada a senescencia *(Senescence Associated β-Gal Activity)*

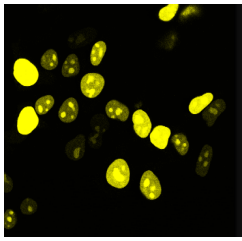

Introducción

El cáncer es una enfermedad compleja que resulta de la acumulación de modificaciones genéticas y epigenéticas, que alteran la homeostasis celular (Berdasco and Esteller, 2010; Hanahan and Weinberg, 2000). Las células de organismos superiores están sometidas continuamente a estímulos potencialmente oncogénicos, procedentes tanto del medio ambiente como del interior de la célula. Sin embargo, existen mecanismos de protección que limitan la formación de tumores. Entre estos mecanismos destacan la muerte celular programada o apoptosis, la senescencia celular, y la reparación del ADN (Lowe et al., 2004). El fallo de estos mecanismos supone la pérdida de la barrera antitumoral y la adquisición de las características que definen la transformación neoplásica: señalización proliferativa sostenida, resistencia a la muerte celular, inmortalidad replicativa, inducción de angiogénesis, activación de invasión y metástasis y conexión con el microentorno tumoral (Hanahan and Weinberg, 2011).

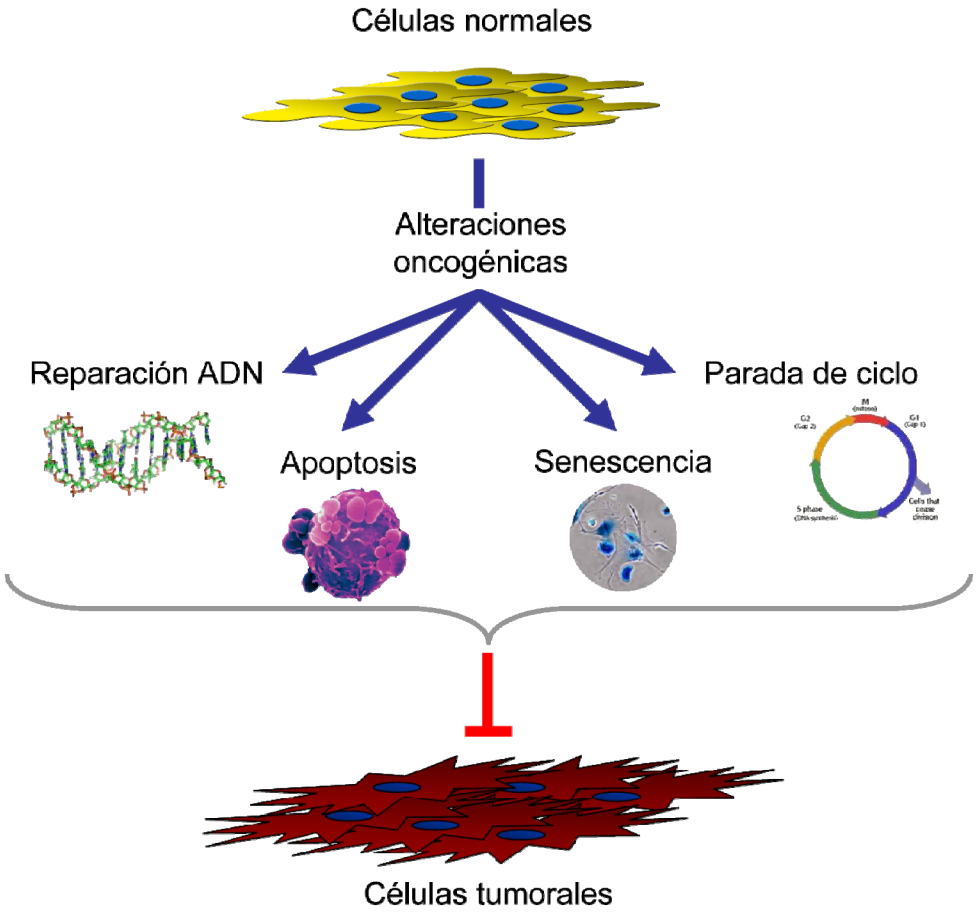

Fig. 1. Esquema de los principales mecanismos de supresión tumoral.

1. La familia de proteínas ING

La familia de proteínas ING (*Inhibitor of Growth*) constituye una familia conservada durante la evolución, desde levaduras hasta humanos. A finales de los 90 se descubrió ING1 gracias a un abordaje en el que se buscaban genes con expresión disminuida en células de cáncer de mama, siendo este el miembro fundador de la familia (Garkavtsev et al., 1996). Mediante técnicas de homología de secuencia, se identificaron el resto de miembros de esta familia de supresores tumorales. En mamíferos, esta familia comprende varios miembros, productos de cinco loci (ING1 – ING5) Algunos miembros de la familia (ING1, ING3 e ING4) tienen variantes por procesamiento alternativo.

Los miembros de la familia tienen una estructura similar, conteniendo un extremo N-terminal variable, una región conservada (NCR) que se ha relacionado con Lamina A en ING1 (Han et al., 2008), una secuencia de localización nuclear (NLS) en la zona central y una región C-terminal altamente conservada que contiene un dominio PHD (*Plant HomeoDomain*), relacionado con la interacción proteína-proteína y con procesos de remodelación de cromatina (Aguissa-Toure et al., 2011; Shi and Gozani, 2005; Soliman and Riabowol, 2007). Los loci de los cinco *ING* humanos se encuentran en cromosomas diferentes, localizándose todos ellos en la región subtelomérica, excepto en

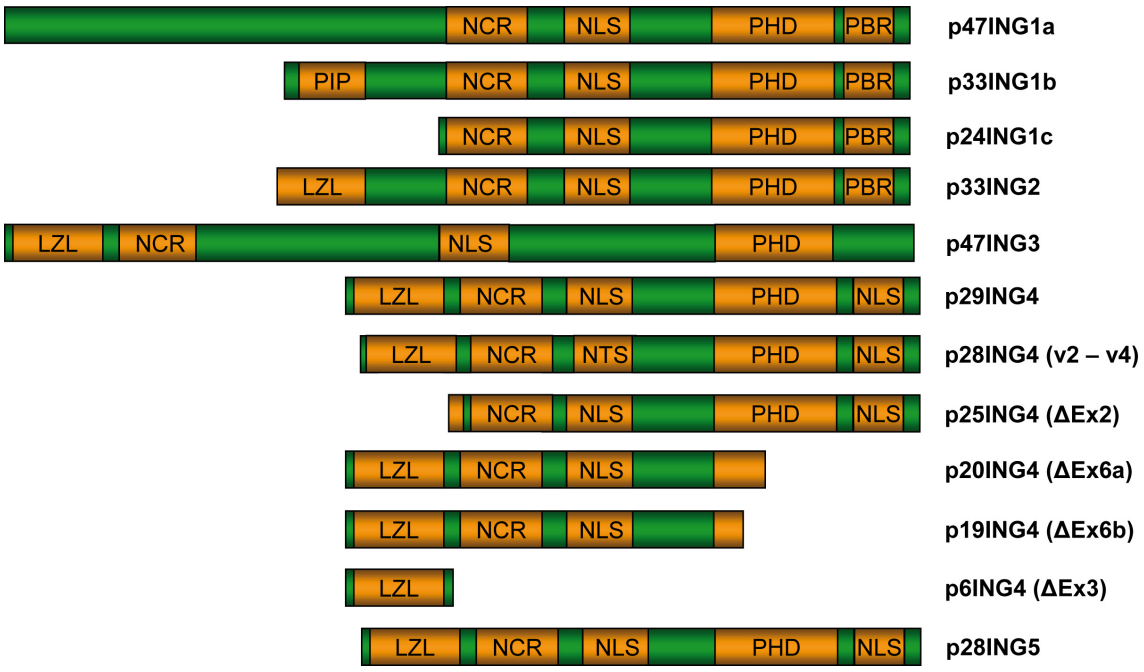

Fig. 2. La familia de proteínas ING. Representación de las proteínas conocidas y sus características estructurales. PIP: Dominio de interacción con PCNA; LZL: Cremalleras de leucinas; NCR: Nueva región conservada; NLS: Secuencias de localización nuclear; NTS: Señal de localización nuclear truncada; PHD: *Plant HomeoDomain*; PBR: Región polibásica.

el caso de ING3 que se localiza en la zona intermedia del brazo largo (He et al., 2005). Todos los miembros de la familia se expresan de forma ubicua en tejidos fetales y adultos, aunque el grado de expresión varía en función del órgano y de la fase del desarrollo (Walzak et al., 2008).

La familia de proteínas ING está relacionada con procesos relacionados con supresión tumoral tales como regulación negativa de la proliferación celular, inducción de apoptosis, senescencia celular, reparación de ADN, inhibición por contacto e inhibición de angiogénesis. Los miembros de la familia llevan a cabo estas funciones principalmente regulando la transcripción de genes a partir del reconocimiento de marcas de cromatina a través de su dominio PHD y mediante el reclutamiento de complejos modificadores que conllevan la activación o represión transcripcional (Shi and Gozani, 2005). Estas funciones se realizan en conexión con p53 y con la vía de NFκB (Garkavtsev et al., 2004; Guo and Fast, 2011; Nozell et al., 2008; Zhang et al., 2005).

2. ING4

2.1. Estructura y localización

El locus ING4 se encuentra en el cromosoma 12p13.31, una región con frecuente pérdida de heterozigosidad en tumores humanos (Gunduz et al., 2005). La proteína ING4 humana tiene 249 aminoácidos, y un peso molecular de 29kDa. Existen distintas variantes de procesamiento que difieren entre sí en unos pocos aminoácidos localizados en la zona central (ING4_v1 ING4_v4). La localización de ING4 es mayoritariamente nuclear (Ythier et al., 2008). Se ha sugerido que algunas variantes presentan diferencias en cuanto a localización subcelular y a nivel funcional, aunque esto, actualmente, aún está cuestionado (Raho et al., 2007; Tsai et al., 2008; Unoki et al., 2006). Además existen otras variantes de procesamiento que suponen la pérdida de exones completos. Algunas de estas, provocan cambios en la pauta de lectura y dan lugar a proteínas truncadas (-Δ2, -Δ3, -Δ6a y -Δ6b). Ninguna de ellas presenta cambios en localización subcelular, ni alteraciones a nivel funcional excepto en el caso de la variante -Δ6a (Raho et al., 2007). ING4 tiene un alto grado de homología entre ratón y humano, compartiendo una misma estructura. En cambio, no todas las variantes de procesamiento identificadas en humanos se han caracterizado en ratón.

El extremo N-terminal de la proteína contiene un dominio de cremalleras de leucinas por donde ha sido descrito que es capaz de homodimerizar. El resto de proteínas de la familia ING, excepto ING1, también tienen este dominio, por lo que la capacidad de formar heterodímeros es una posibilidad que incrementaría la diversidad de funciones de estas proteínas (Palacios et al., 2010). A continuación, presenta el dominio NCR, conservado entre los distintos miembros de la familia ING y en la zona central de la proteína se encuentra el dominio de localización nuclear, región también muy conservada y que además contiene una señal de localización nucleolar (Tsai et al., 2008). En el extremo C-terminal de la proteína se encuentra el dominio más conservado de la familia, el dominio PHD. Este dominio contiene un motivo de dedos de zinc tipo C_4HC_3 y está relacionado con interacciones proteína-proteína, implicadas en procesos de remodelación de cromatina (Baker et al., 2008; Soliman and Riabowol, 2007). En el caso de ING4 e ING5, se ha descrito otro posible dominio de localización nuclear tras el dominio PHD. Estas dos proteínas están relacionadas filogenéticamente y son las que más homología tienen entre sí de la familia, por lo que parece que pueden estar relacionadas funcionalmente (Shiseki et al., 2003).

2.2. Funciones biológicas de ING4

Desde su descubrimiento, la familia de proteínas ING ha sido relacionada con mecanismos de supresión tumoral. ING4 comparte funciones con el resto de miembros de la familia como parada de ciclo celular e inducción de apoptosis (Coles and Jones, 2009). Además de estar implicada en estas funciones comunes, numerosos estudios indican que ING4 juega un papel específico en progresión tumoral, ejerciendo funciones que no se han descrito en otras proteínas ING como son la inhibición por contacto (Kim et al., 2004), inhibición de la migración (Li et al., 2008), inhibición de la angiogénesis (Li and Li, 2010), aunque hay trabajos que sugieren la implicación de ING1b en esta última (Tallen et al., 2009), y respuesta a hipoxia (Colla et al., 2007).

La desregulación de la división celular es básica en el proceso de formación de un tumor. La sobreexpresión de ING4 en líneas tumorales tiene un efecto antiproliferativo, que se produce a través de la parada de ciclo con acumulación en la fase G2/M y disminución de la fase G1 (Li et al., 2010; Shiseki et al., 2003; Zhang et al., 2004). Asimismo, ING4 ha sido relacionado con la regulación del inhibidor de ciclo celular p21CIP1, implicado entre otras funciones, en la inhibición de la actividad del complejo CDK2/Ciclina B1, necesario para la transición por G2 (Bates et al., 1998; Medema et al., 1998).

La muerte celular programada o apoptosis es un proceso fisiológico que contribuye al mantenimiento del balance celular. La expresión de ING4 induce apoptosis, mediante la regulación de proteínas esenciales para esta respuesta, ya que provoca un aumento del factor pro-apoptótico Bax y una disminución del factor anti-apoptótico Bcl-2 (Cai et al., 2009; Li et al., 2009b; Zhang et al., 2004). Además, ING4 también sensibiliza a apoptosis en respuesta a factores que provocan daño en ADN, como etopósido o doxorrubicina, (Hung et al., 2009; Zhang et al., 2004).

ING4 fue identificada en una búsqueda de genes que revirtieran la pérdida de inhibición por contacto típica de células transformadas. De este modo se ha comprobado que la expresión de ING4 inhibe la capacidad de crecer de forma independiente de anclaje, aunque no se conoce cual es el mecanismo que subyace a esta función (Hung et al., 2009; Kim et al., 2004).

Durante la progresión tumoral ocurren cambios morfológicos en la célula, como la polarización celular y la formación de filopodios y lamelipodios que otorgan motilidad a la célula, favoreciendo de este modo un fenotipo invasivo. ING4 ha sido relacionado con este fenotipo, mediante la regulación transcripcional de la GTPasa RhoA, mediadora de la reorganización de las fibras de estrés durante la migración celular, en conexión con la vía de NFκB (Li et al., 2008). Además de las funciones como regulador de transcripción en el núcleo, también se ha demostrado que ING4 actúa en citoplasma y membrana a través de la interacción y colocalización en lamelipodios con la proteína Liprinα1/PPFIA1, que juega un papel importante en la regulación de las adhesiones focales, y que recluta a ING4 a los lamelipodios, donde reprime la migración celular mediante la inhibición de la polimerización de los filamentos de actina (Shen et al., 2007). Estas funciones suponen un papel adicional de la proteína como modulador de motilidad en la membrana plasmática.

La angiogénesis es un proceso fisiológico consistente en la formación de vasos sanguíneos a partir de otros preexistentes. Es un mecanismo requerido por los tumores para su crecimiento, y está relacionado con los procesos de migración, invasión y metástasis. Este proceso está mediado por la acción de factores de crecimiento, proteasas, supresores tumorales, oncogenes y citoquinas (Carmeliet and Jain, 2000; Kerbel and Folkman, 2002). ING4 inhibe la angiogénesis mediante la regulación transcripcional de genes en conexión con la vía de NFκB. En ensayos realizados en células de glioblastoma *in vivo* e *in vitro* se identificó a IL-6, IL-8 y COX2 como genes regulados por ING4 relacionados con angiogénesis y vascularización. Se observó que en estos tumores, bajos niveles de ING4 correlacionaban con elevada vascularización, y con vasos más densos y hemorrágicos (Garkavtsev et al., 2004). Por tanto ING4 ejerce

un papel importante en la regulación de la angiogénesis durante el desarrollo tumoral en conexión con la vía de NFκB.

ING4 también se ha relacionado con respuesta a hipoxia. En el contexto de un tumor, la disponibilidad de oxígeno disminuye según va aumentando el tamaño del mismo, produciéndose una situación de hipoxia que activa mecanismos de respuesta en las células tumorales. Uno de los genes principales implicados en esta respuesta es el regulador transcripcional HIF1α (Smith et al., 2008). ING4 está implicado en la regulación mediada por HIF1α en hipoxia, modulando su actividad mediante la regulación de la proteína hidroxilasa HPH-2, que regula la hidroxilación y consecuente degradación de HIF1α (Hung et al., 2009; Ozer and Bruick, 2005). De acuerdo con esto, se ha comprobado que dos de los genes regulados por HIF-1α, como IL-8 y OPN, están aumentados en tumores que expresan poco ING4 (Colla et al., 2007).

La expresión de ING4 es ubicua en el embrión y en el adulto, aunque los niveles varían según el tejido (Walzak et al., 2008). Se conoce poco acerca de la regulación de ING4, aunque se ha descrito recientemente que está controlada a nivel de ARN y de proteína por el gen supresor de metástasis BRMS1 (Li and Li, 2010). Igualmente se ha observado que la expresión del oncogen Myc en células de meduloblastoma podría regular ING4 (Zhou et al., 2010). Además, existen datos que conectan el papel de algunos microARNs (miRNAs) en supresión de la función de ING4. La expresión de los miRNAs miR-650 y miR-214 se ha asociado con disminución de los niveles de ING4 en tumores gástricos y de páncreas respectivamente (Zhang et al., 2010a; Zhang et al., 2010b). También se ha publicado un estudio que relaciona el aumento de los niveles de ING4 con el tratamiento con curcumina en células de glioma (Liu et al., 2007).

2.3. ING4 y cromatina

El mecanismo por el que ING4 y el resto de proteínas ING participan en regulación transcripcional es a través del reconocimiento de marcas de histonas y del reclutamiento de complejos con actividad modificadora de cromatina. ING4, al igual que el resto de miembros de la familia ING, reconoce específicamente la histona H3 trimetilada en la lisina 4 (H3K4me3), marcador de promotores activos, a través del dominio PHD (Hung et al., 2009; Palacios et al., 2008; Pena et al., 2006; Shi et al., 2006). La afinidad con la que ING4 reconoce a la cola N-terminal de la H3 aumenta con el grado de metilación de la lisina 4 (Hung et al., 2009), al igual que en otras proteínas con dominios PHD como RAG2 o BPTF y en otros miembros de la familia ING (Li et al., 2006;

Matthews et al., 2007). A pesar de esto, el grado de reconocimiento de metilación en la histona 3 en los distintos miembros de la familia ING es diferente, ya que se ha observado que existen variaciones en la afinidad de unión de los dominios PHD de ING4 e ING2 a la marca H3K4me3 (Hung et al., 2009; Palacios et al., 2008).

Los residuos esenciales para el reconocimiento de H3K4me3 en la proteína ING4 humana son la tirosina 198, el triptófano 221 y el aspártico 213. Los dos primeros forman un bolsillo aromático responsable del reconocimiento de la lisina trimetilada, y están conservados en ING1 e ING2 (Abad et al., 2011; Hung et al., 2009; Pena et al., 2006). El aspártico 213 no está directamente relacionado con el bolsillo aromático sino con el mantenimiento del complejo H3/ING4 mediante la estabilización de una arginina de la cola de la histona. La mutación de cualquiera de estos tres residuos provoca un cambio que altera la afinidad de la proteína por la marca e impide la unión a H3K4me3. Además, en el caso de la mutación D213, se ha comprobado que no modifica la capacidad de unión a complejos histona acetil transferasa (HAT) ni varia la acetilación de la H4 (Hung et al., 2009).

El mecanismo de regulación transcripcional por ING4 incluye además del reconocimiento de marcas de histonas a través del dominio PHD, la unión a factores de transcripción como p53 o NFκB y el reclutamiento a cromatina de complejos modificadores (Nozell et al., 2008; Shiseki et al., 2003). La modulación de la estructura de la cromatina resulta fundamental para la regulación de la expresión génica. Esta se lleva a cabo mediante numerosos complejos proteicos encargados de modificar el ADN y las histonas. Los primeros datos que relacionaban a la familia ING con histonas se obtuvieron en levaduras, donde se identificó la conexión de los ortólogos Yng1, Yng2 y Pho23 con complejos con actividad HAT (Loewith et al., 2000). Posteriormente, se ha demostrado en células de mamífero que ING4 y otras proteínas ING forman parte de complejos multiproteicos con actividad HAT, histona deacetilasa (HDAC) y ADN metil transferasa (sólo en el caso de ING1b, Scott et al., 2001), responsables de la activación o represión transcripcional. Mediante proteómica se ha identificado a ING4 en un complejo con actividad HAT asociado a HBO1, hEaf6, y proteínas JADE (Doyon et al., 2006). También se ha descrito su unión física a la HAT p300 mediante inmunoprecipitación (Shiseki et al., 2003). La conexión de ING4 con HDACs no está tan clara, pero se ha sugerido que ING4 puede cooperar con complejos HDAC en la represión de genes diana de NFκB (Nozell et al., 2008).

ING4 coopera con factores de transcripción como p53 o NFκB (Shi and Gozani, 2005; Soliman and Riabowol, 2007). La vía de p53 juega un papel esencial en supresión

tumoral, regulando una variedad de respuestas frente a señales de estrés procedentes del interior celular o su entorno, y se encuentra alterada en la mayor parte de los tumores humanos (Polager and Ginsberg, 2009; Millau et al., 2009; Vousden and Prives, 2009). Se ha descrito que ING4 y p53 pueden interaccionar físicamente (Shiseki et al., 2003) a través de una secuencia localizada en el dominio de localización nuclear (Zhang et al., 2005). Además, funciones características de ING4 como regulación de apoptosis y de la proliferación celular son dependientes de p53 (Shiseki et al., 2003; Zhang et al., 2004). En estudios recientes sobre el mecanismo de ING4 se han identificado dos proteínas que impiden su unión a p53: EBNA3C y PAD4. La primera está codificada por el virus de Epstein-Barr y se une a ING4 en la misma zona que p53 (Saha et al., 2010). La segunda, se une físicamente a ING4 a través del dominio PHD y está encargada de su citrulinación, una modificación post-traducional que también ocurre en la zona de unión de p53 (Guo and Fast, 2011). Además, ING4 puede modular la actividad de p53 a través de la acetilación de la lisina 382, sin afectar sobre los niveles de proteína, y actuando como co-activador transcripcional a través del reclutamiento de complejos con actividad HAT (Doyon et al., 2006; Shiseki et al., 2003; Zhang et al., 2005).

La vía de NFκB está implicada en la regulación de la respuesta inmune innata y adaptativa, supervivencia celular, angiogénesis, tumorogénesis y metástasis (Ruland, 2011). NFκB es un regulador esencial de la respuesta inflamatoria a través de la regulación transcripcional de numerosos genes, muchos de ellos citoquinas pro-inflamatorias (Karin et al., 2002). En una situación basal, los dímeros de NFκB se encuentran localizados en citoplasma interaccionando con las proteínas de la familia IκB. La fosforilación y degradación de estas proteínas conlleva la translocación de NFκB a núcleo, donde regula la transcripción de sus genes diana (Hayden and Ghosh, 2008).

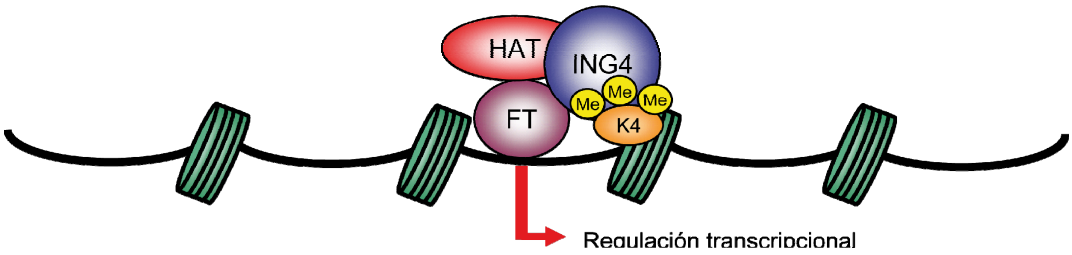

Fig. 3. Modelo de acción de ING4 en cromatina.

Distintas evidencias indican una conexión entre ING4, y otras proteínas de la familia ING, con regulación transcripcional por NFκB (Garkavtsev et al., 2004; Gomez-Cabello et al., 2010; Nozell et al., 2008). Resultados con líneas tumorales humanas y modelos animales indican que ING4 puede modular la expresión de genes diana de NFκB. Sin embargo, los efectos de ING4 sobre la expresión de estos genes y el mecanismo por el que puede

estar actuando no están bien definidos (Coles et al., 2010; Garkavtsev et al., 2004; Nozell et al., 2008).

La capacidad de dimerizar de ING4 también podría ser relevante en su papel como regulador transcripcional. El dímero de ING4 se caracteriza porque cada uno de los monómeros se pliega de forma individual, formando una estructura alargada que contiene dos dominios de unión a H3K4me3, que actuarían de forma independiente. El mecanismo por el que estos dímeros reconocen a la marca modificada de histonas H3K4me3 es aún desconocido, pero puede suponer una intensificación del reclutamiento de complejos HAT a cromatina, modulando la acción de ING4 como regulador transcripcional (Palacios et al, 2010).

2.4. Alteraciones de ING4 asociadas a tumores

Las proteínas ING están desreguladas en diferentes tipos de cáncer humano. En algunos casos se ha correlacionado la baja expresión de las proteínas ING con progresión tumoral y disminución de la tasa de supervivencia. La pérdida de heterozigosidad, el reordenamiento génico, la hipermetilación de promotores y los cambios de localización se han propuesto como mecanismos que alteran la función de proteínas ING en tumores (Campos et al., 2004a; Gong et al., 2005; Nouman et al., 2003).

Las alteraciones del locus ING4 asociadas a tumores humanos, incluyen principalmente la disminución de expresión y localización subcelular aberrante, además de deleciones y mutaciones puntuales (Garkavtsev et al., 2004; Kim et al., 2004; Wang et al., 2010). Estas alteraciones, se han observado en distintos tipos tumorales como neuroblastomas, adenocarcinomas de pulmón, glioblastomas, y carcinomas de pulmón, colorectales o escamosos de cuello y cabeza entre otros (Gunduz et al., 2005; Kim et al., 2004; Nozell et al., 2008). En casos de glioblastoma y mieloma se ha asociado la disminución de la expresión de ING4 con alto grado de malignidad y angiogénesis, y en el caso del mieloma se asoció igualmente a un incremento en los niveles de IL-8 y OPN (Colla et al., 2007; Garkavtsev et al., 2004). También se han identificado niveles disminuidos de ING4 en melanomas malignos en comparación con nevus displásicos, lo que se ha determinado como un factor de mal pronóstico en estos pacientes (Li et al., 2008). El patrón de localización subcelular de ING4 es mayoritariamente nuclear en todos los tejidos. Aunque con menos frecuencia que en otras proteínas ING, se han identificado patrones de localización aberrante de ING4 en tumores de pulmón humanos, relacionados con aumentos de la proteína en citoplasma. Aunque no se conoce cual es

el mecanismo, este puede estar relacionado con los niveles de expresión de las distintas variantes de procesamiento (Wang et al., 2010), ya que estos cambios se han demostrado *in vitro* por otros grupos (Unoki et al., 2006). Las mutaciones puntuales de ING4 en tumores son menos frecuentes. Se han identificado mutantes puntuales de la proteína en varias líneas tumorales: la mutación M50V en la línea de adenocarcinoma colorrectal ACHN, la mutación Y121N en la línea de adenocarcinoma de pulmón H23 y la mutación N214D en la línea de adenocarcinoma de pulmón de células pequeñas H82 (Kim et al., 2004).

3. Microentorno tumoral

El estudio de la biología del tumor se ha centrado tradicionalmente en el estudio de las propiedades de las propias células tumorales, pero esta idea ha ido evolucionando y actualmente se reconoce la importancia del microentorno durante la tumorogénesis. El microentorno tumoral está formado por distintos tipos de células no tumorales y componentes del tejido conectivo que contribuyen por diferentes mecanismos al crecimiento y diseminación del tumor. En el microentorno se encuentran vasos sanguíneos y linfáticos, fibroblastos y células inflamatorias, además de una gran cantidad de moléculas extracelulares y de factores solubles que proporcionan un soporte estructural al tumor, y que componen un complejo sistema de comunicación entre los distintos componentes del microentorno (Egeblad et al., 2010; Hanahan and Weinberg, 2011; Lazennec and Richmond, 2010; Pietras and Ostman, 2010).

Las células tumorales liberan al medio extracelular factores solubles como hormonas, factores de crecimiento y citoquinas y quimioquinas, además de componentes de la matriz extracelular, responsables del reclutamiento de distintos tipos celulares al microentorno tumoral. Estos a su vez proporcionan una segunda fuente de factores solubles, formando un mecanismo de comunicación entre células tumorales y entorno que contribuye a la progresión tumoral (Lazennec and Richmond, 2010; Mantovani et al., 2009).

Un componente importante del microentorno tumoral está formado por una población de fibroblastos con características distintivas, denominados fibroblastos asociados a carcinoma o CAFs (Rasanen and Vaheri, 2010; Xing et al., 2010). Estos pueden proceder de fibroblastos locales, de células progenitoras derivadas de médula ósea o de células epiteliales transdiferenciadas (Haviv et al., 2009; Pietras and Ostman,

2010). Los CAFs favorecen el crecimiento tumoral a través de la secreción al medio de componentes de la matriz extracelular y factores solubles. Entre otros efectos, la secreción de estos factores provoca inflamación, atrayendo al microentorno tumoral células del sistema inmune y activando a las células endoteliales, favoreciendo así el crecimiento tumoral, invasión y metástasis (Kalluri and Zeisberg, 2006; Lazennec and Richmond, 2010; Shimoda et al., 2010).

La vasculatura también es un componente importante dentro del microentorno tumoral. Los vasos sanguíneos facilitan el aporte de nutrientes a la masa del tumor, y favorecen la intravasación de células tumorales en el sistema circulatorio favoreciendo los procesos de invasión y metástasis (Raza et al., 2010). Según va creciendo un tumor, las células endoteliales quiescentes se reactivan para permitir la formación de nuevos vasos sanguíneos, en un proceso mediado por distintas vías de señalización pro-angiogénica como VEGF, angiopoyetina y otros (Carmeliet and Jain, 2000; Dejana et al., 2009; Pasquale, 2010), y con la cooperación de señales paracrinas procedentes de los pericitos, células contráctiles en contacto con las células endoteliales (Gaengel et al., 2009).

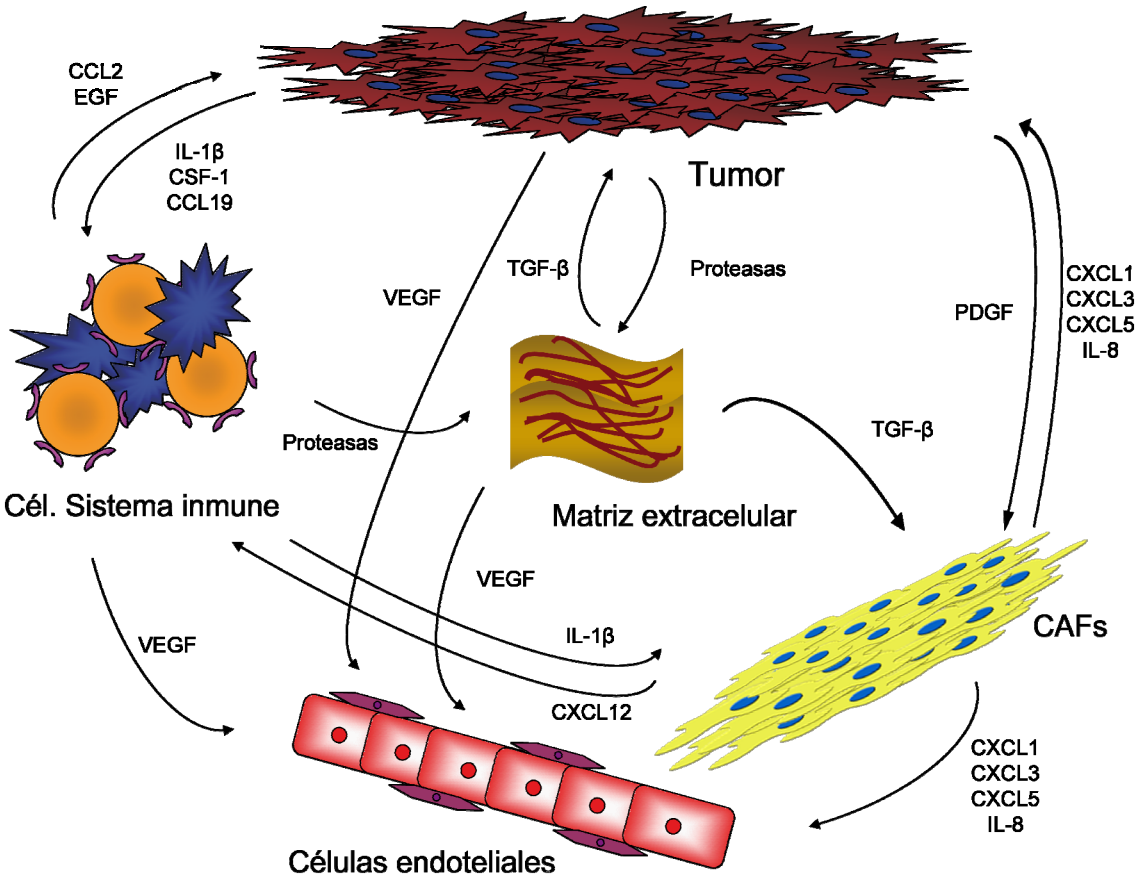

Fig. 4. Microentorno tumoral. Interacción entre los distintos componentes: células cancerígenas, fibroblastos asociados a carcinoma (CAFs), células del sistema inmune, células endoteliales y factores solubles. Las células del tumor producen una gran variedad de estos factores, que modulan las propias células cancerígenas y las que lo rodean.

Las células del sistema inmune también participan de una manera importante en la formación, mantenimiento y diseminación de un tumor. En el microentorno tumoral se encuentran macrófagos, mastocitos, neutrófilos y linfocitos B y T, que son atraídos por citoquinas, quimioquinas y factores de crecimiento que se producen en el microentorno. Las células inflamatorias han mostrado un papel en la angiogénesis, estimulación de la proliferación celular, motilidad e invasión de células cancerígenas (Egeblad et al., 2010; Joyce and Pollard, 2009; Mantovani et al., 2008).

Con estos antecedentes, en este trabajo, nos propusimos estudiar el papel de ING4 en diferentes aspectos del proceso de tumorogénesis para entender su contribución a los mecanismos de supresión tumoral. Para ello, se han utilizado diferentes modelos celulares en los que se ha analizado el efecto de la expresión ectópica de ING4 y formas mutantes, en diferentes ensayos funcionales *in vitro* e *in vivo*. Estos experimentos nos han permitido demostrar la importancia de la función de ING4 en tumorogénesis.

Objetivos

1. Caracterizar el impacto funcional de mutaciones de ING4 asociadas a tumores humanos.

2. Analizar el papel de ING4 en fibroblastos primarios humanos y su conexión con las vías de supresión tumoral de p53 y Rb.

3. Estudiar la firma genética asociada a la expresión de ING4 en células primarias.

4. Analizar la conexión de ING4 con el microentorno tumoral.

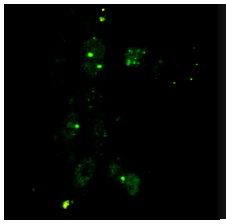

Materiales y métodos

1. Mutagénesis dirigida

Para la construcción de los distintos mutantes se utilizó el kit Quick Change Site-Directed Mutagenesis Kit (Stratagene), utilizando como molde el ADNc de la proteína ING4 humana clonada dentro del vector retroviral pLPC. Las mutaciones se incorporaron por PCR empleando la ADN polimerasa Pfu Turbo (Stratagene), y posterior digestión con DpnI que elimina la banda parental (metilada). Los oligos utilizados fueron:

Y121N Fw: 5'-CAGATTGAGTCAAGTGACAATGACAGCTCTTCCAGC-3'

Y121N Rv: 5'-GCTGGAAGAGCTGTCATTGTCACTTGACTCAATCTG-3'

N214D Fw: 5'-AGAGATGATTGGCTGTGACGACCCTGATTGCATTGAGTGG-3'

N214D Rv: 5'- CCACTCAATGCAATCAGGGTCGTCACAGCCAATCATCTCT-3'

D213A Fw: 5'-AGAGATGATTGGCTGTGCCAACCCTGATTGTTCCATTGAGTGG-3'

D213A Rv: 5'-CCACTCAATGGAACAATCAGGGTTGGCACAGCCAATCATCTCT-3'

2. Cultivos celulares

Se utilizaron fibroblastos primarios humanos IMR90 procedentes de la ATCC de pase temprano y fibroblastos inmortalizados de ratón (NIH3T3) además de las líneas celulares humanas U2OS (osteosarcoma), HT1080 (fibrosarcoma), MDA-MB-231 (cáncer de mama) y 293T (riñón embrionario), que fueron cultivadas en medio DMEM (Gibco), suplementado con 10% suero fetal bovino (Gibco), en presencia de penicilina-estreptomicina, a 37ºC y 5% CO_2. Las líneas H23 y H82 (carcinoma de pulmón) se cultivaron con medio RPMI (Gibco) en las mismas condiciones.

También se utilizaron células endoteliales microvasculares humanas (HMVEC), que se crecieron en medio MCDB 131 (Sigma), suplementado con 10% de suero fetal bovino, 2mM L-glutamina, 10ng/ml de factor de crecimiento epidérmico, 10ng/ml de hidrocortisona y 16,32 µg/ml de extracto de pituitaria bovina (Invitrogen).

3. Transfección

Las transfecciones transitorias en células 293T se realizaron mediante el método de transfección por precipitados de fosfato cálcico, siguiendo el protocolo descrito previamente (Goeman et al., 2005; Palmero and Serrano, 2001) y las realizadas en células U2OS se llevaron a cabo mediante transfección por FuGENE (Roche), siguiendo el protocolo de transfección descrito por la casa comercial.

4. Infección retroviral

Para las infecciones retrovirales se utilizaron células NIH3T3, HT1080, IMR90 y MDA-MB-231. Se usó el protocolo de infección descrito previamente en (Abad et al., 2011). Las células se sometieron a selección con antibiótico (Puromicina a 2µg/ml, Higromicina 75µg/ml, Blasticidina 10µg/ml), durante un periodo de 3 a 6 días.

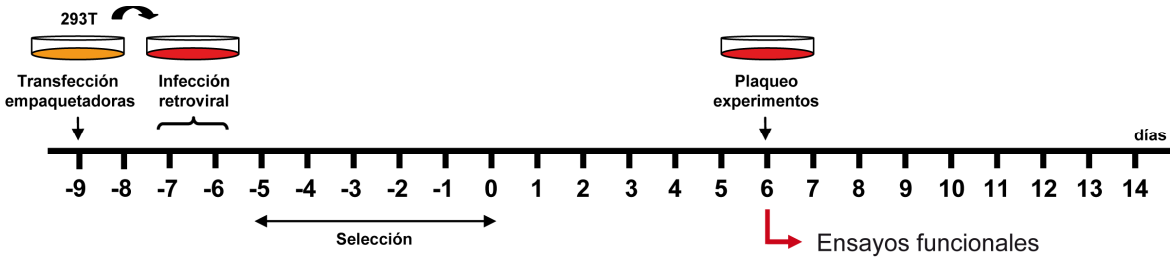

Fig. 5. Diseño experimental para la transducción retroviral. Para la producción de partículas virales se utilizaron células 293T como empaquetadoras. Se hicieron tres rondas de infección retroviral dos días después de la transfección con los vectores retrovirales. Se recogió el sobrenadante viral y se añadió al cultivo. Las células se sometieron a selección con antibiótico y al finalizar la selección, se dejaron crecer seis días, momento en el que se usaron para realizar los distintos experimentos.

5. Inmunoblot

La preparación de los lisados totales celulares utilizados para la detección de proteínas se realizo como se describió previamente en (Palmero et al., 2002). Los lisados se cuantificaron mediante la técnica de Lowry (Lowry Protein Assay, BioRad). Posteriormente, se resolvieron 30µg de los lisados totales por electroforesis en geles de poliacrilamida con SDS (SDS-PAGE), en los que la fracción separadora se preparó al 12%. Tras la electroforesis, las proteínas se transfirieron a membranas de nitrocelulosa (0,2 µM de tamaño de poro, BioRad), mediante transferencia húmeda durante 1 hora a 200mA. Las membranas se bloquearon en leche en polvo (Fluka) disuelta al 5% en TBS-Tween 0,2%, durante al menos una hora. Tras el bloqueo, las membranas se incubaron con los anticuerpos primarios (Tabla 2) diluidos en leche al 5% en TBS-Tween 0,2%. Se sometieron a tres lavados con TBS-Tween 0,2% y se incubaron con el anticuerpo secundario correspondiente acoplado a actividad peroxidada (Tabla 3). Las membranas se revelaron mediante quimioluminiscencia tras tres lavados con TBS-Tween 0,2% e incubación con el reactivo ECL (Amersham).

6. RT-QPCR

Se preparó ARN total utilizando Tri Reagent (Sigma) a partir de células U2OS o IMR90 creciendo asincrónicamente. Se utilizaron 2µg del ARN total para sintetizar ADNc

usando la transcriptasa reversa M-MLV (Promega). 1 µl de la reacción fue utilizado para llevar a cabo reacciones de PCR. Los oligos utilizados fueron:
ING4 Fw: 5'- ATTGCCTTTGTCACCAGGTC-3';
ING4 Rv: 5´-GGCACGAATTCTCACTATTTCTTCTTCCG-3´.

Para la validación de los resultados del microarray, se utilizaron los siguientes oligos:
IL-6 Fw: 5'-GATGAGTACAAAAGTCCTGATCCA-3'
IL-6 Rv: 5'-CTGCAGCCACTGGTTCTGT-3'
IL-8 Fw: 5'-AGACAGCAGAGCACACAAGC-3'
IL-8 Rv: 5'-ATGGTTCCTTCCGGTGGT-3'
CXCL1 Fw: 5'-CATCGAAAAGATGCTGAACAGT-3'
CXCL1 Rv: 5'-CTTCAGGAACAGCCACCAGT-3'
CXCL2 Fw: 5'-CATCGAAAAGATGCTGAAAAATG-3'
CXCL2 Rv: 5'-TTCAGGAACAGCCACCAATA-3'
El ARN ribosomal 18S se utilizó como referencia. Los ensayos se realizaron usando sondas de Universal Probe Library en una máquina ABI9700.

7. Inmunofluorescencia

Las células IMR90 y U2OS se plaquearon en cámaras de 8 pocillos de cristal (LabTek) a una densidad de 20000 células por pocillo. Al día siguiente se procesaron para inmunofluorescencia, como se describe en (Gonzalez et al., 2006), con ligeras modificaciones. Las células se fijaron con paraformaldehido al 4% en PBS durante 20 minutos, se permeabilizaron con Tritón X100 al 0,1% en PBS durante 15 minutos y se incubaron en solución de bloqueo (2% BSA en PBS) toda la noche a 4ºC. Al día siguiente, se incubaron al menos durante 2 horas con los anticuerpos primarios correspondientes (Tabla 2) en la solución de bloqueo, a temperatura ambiente. Las células se lavaron dos veces con PBS-Tritón 0,1% y se incubaron con los anticuerpos secundarios conjugados con fluorocromos, en solución de bloqueo (Tabla 3). Tras dos lavados, las muestras se montaron con Vectashield con DAPI (Santa Cruz) y se analizaron en un microscopio de fluorescencia Leica Leitz DM RB o en un microscopio confocal Leica TCSSP2 DMIRE 2.

8. Determinación de la tasa de síntesis de ADN

Para medir la incorporación de BrdU en las células NIH3T3, HT1080, IMR90 y MDA-MB-231 se plaquearon 20000 células en cámaras de 8 pocillos de cristal (LabTek)

y 24 horas después se incubaron con BrdU a una concentración final de 10μM durante 4 horas. Las células BrdU positivas se detectaron mediante inmunofluorescencia, siguiendo el protocolo descrito en el apartado 7, incluyendo un tratamiento con HCl 2M durante 5 minutos antes del bloqueo. Para la detección se utilizó el anticuerpo anti-BrdU (Megabase Research Products). Las muestras fueron teñidas a la vez con DAPI (Santa Cruz) para visualizar el núcleo. Se contaron al menos 200 células para cada condición.

9. Migración celular

Se sembraron células NIH3T3, infectadas con las distintas construcciones de ING4, en placas de 6 pocillos y se dejó que llegaran a confluencia. Se hizo una incisión con una punta de pipeta de un lado a otro del pocillo y se hicieron fotos al microscopio a distintos tiempos midiendo la anchura de la herida en cada uno de ellos para determinar la velocidad de cerramiento.

10. Ensayos de migración en transwell

La migración en transwell se realizó usando cámaras Boyden (transwell) con membranas de policarbonato (Corning) tratadas con gelatina al 0,5%. Para la obtención de los medios condicionados, se crecieron células NIH3T3 infectadas hasta un 90% de confluencia, posteriormente se lavaron varias veces con PBS y se mantuvieron en medio sin suero durante 48 horas. Posteriormente se recogieron los medios y se concentraron 60 veces con el uso de concentradores Ultra-15 (Millipore Corporation). Para los ensayos de migración, se plaquearon células HMVEC crecidas durante 16 horas sin suero en la parte superior de la cámara ($1,2x10^5$ células endoteliales en medio sin suero), mientras que en la parte inferior se puso el medio condicionado en medio sin suero a una concentración final de proteína de 15 μg/ml. A las 18 horas de incubación a 37ºC, se retiraron las células de la parte superior con un bastoncillo, y las células migradas se fijaron y tiñeron con Diff-Quick (Dade Behring). La migración se determinó contando veinte campos de máxima migración por transwell usando un microscopio a 40 aumentos.

11. Ensayos de crecimiento en agar blando

Células NIH3T3 infectadas con ING4 salvaje y mutantes, se volvieron a infectar con un vector con la versión mutada del oncogén Ha-Ras (pWZL Hygro RasV12) y con vector vacío como control (pWZL Hygro). Las células infectadas y seleccionadas se

resuspendieron en una matriz de agarosa al 0,3% y medio DMEM completo, y se plaquearon en placas de 60mm sobre una capa de agarosa al 0,5%. Se dejaron crecer y se contaron las colonias visualmente a los 15 días.

12. Espectroscopía por RMN y determinación de la estructura

Los experimentos de resonancia magnética nuclear (RMN) fueron realizados en el CICbioGUNE (Bilbao), utilizando espectrómetros Brujwe AVANCEII 600Mhz (con criosondas) y 700Mhz a 25ºC en 20mM fosfato sódico pH 6.5, 50mM NaCl, 1mM DTT y 9%(vol/vol) $2H_2O$. La asignación de la resonancia del esqueleto y de la cadena lateral se obtuvieron usando un set de NMR 2D y 3D grabado en una muestra 0,5 PHD^{N214D} uniformemente enriquecida en ^{15}N. La distancia de restricción recogida del espectro NOESY se usó para calcular un conjunto de modelos utilizando las dinámicas de ángulos de torsión.

13. Ensayos de viabilidad celular

Las células NIH3T3 y HT1080 infectadas se plaquearon a una densidad de $1,5x10^5$ por pocillo. Al día siguiente se les añadió doxorrubicina a concentraciones crecientes y se incubaron durante 24 horas a 37ºC. Tras ese tiempo se recogieron y se tiñeron con azul de tripano para su contaje directo al microscopio.

14. Ensayos de vida media de proteína

Las células 293T fueron transfectadas transitoriamente con las distintas construcciones de ING4. A las 36 horas post-transfección se añadió cicloheximida a una concentración final de 50 µg/ml en medio DMEM completo para inhibir la síntesis de proteínas. Los inhibidores del proteasoma MG132 (Sigma) o lactacistina (Calbiochem) se añadieron una hora después de empezar el tratamiento con cicloheximida a una concentración final de 20µM o 10µM respectivamente. Los lisados totales celulares se analizaron por inmunoblot usando el anticuerpo anti-HA, y el anticuerpo anti-actina como control de carga. La cuantificación de la intensidad de las bandas se llevó a cabo por densitometría, utilizando el programa Analysis (Olympus).

15. Curvas de crecimiento

Las células IMR90 y MDA-MB-231 infectadas se sembraron por duplicado a una densidad de 20000 células en placas de 24 pocillos. Se dejaron crecer y se tripsinizaron y contaron a los distintos puntos.

16. Actividad β-Galactosidasa asociada a senescencia (SA β-Gal)

Las células IMR90 infectadas y seleccionadas se plaquearon en placas de 6 pocillos a una densidad de 40000 células por pocillo. Al día siguiente se fijaron y tiñeron para SA-β-Gal como se describió previamente (Dimri et al., 1995). Para hallar el porcentaje de células SA β-Gal positivas, se contaron al menos 200 células de cada condición.

17. Perfil de expresión génica

Los experimentos de microarrays se llevaron a cabo utilizando un array G4112F de 4x44K del Genoma Humano Completo (Agilent Technologies). Se realizaron dos infecciones retrovirales independientes en células IMR90 de pase temprano con ING4 salvaje, el mutante N214D y el vector vacío como control. El ARN se obtuvo como se describió previamente en (Moreno-Bueno et al., 2009). El ARN fue marcado e hibridado a los arrays usando el *Low RNA Linear Amplification Kit* y el *In Situ Hybridization Kit Plus* (Agilent Technologies) respectivamente. Se realizó la hibridación competitiva para cada una de las muestras, usando como referencia una muestra de las células con vector vacío marcada de forma inversa. Tras la hibridación y los lavados, se escanearon los portas en un *Axon GenePix Scanner* (Axon Instruments Inc) y se analizaron utilizando el programa *Feature Extraction Software 10.0* (Agilent Technologies). Además, se realizó una hibridación más usando el marcaje con los fluorocromos recíprocos. Para la identificación de genes con expresión diferencial en células IMR90 que expresaban ING4 salvaje en comparación con las que expresaban el vector vacío, usamos el GEPAS (*Gene Expression Analysis Package,* http://gepas3.bioinfo.cipf.es) y se seleccionaron aquellos genes que diferían en al menos 2 veces en todas las muestras con una desviación estándar de menos de 0,5. El grupo de genes que salió de este análisis se analizó más profundamente respecto a su expresión en el resto de muestras. El grado de enriquecimiento por categorías funcionales se llevó a cabo usando la aplicación FatiGO (http://babelomics.bioinfo.cipf.es).

18. Ensayos de medio condicionado

Para determinar los efectos en proliferación de los factores secretados por la expresión ectópica de ING4, se llevaron a cabo ensayos de medio condicionado. La obtención del medio condicionado de células IMR90 infectadas se hizo de la misma manera que para los ensayos de migración en transwell con células NIH3T3 (ver apartado 10), excepto que las células se crecieron en medio sin suero durante 72 horas. Tras ese tiempo se recogió, centrifugo y conservó a -80ºC. El medio condicionado se colocó sobre células IMR90 y MDA-MB-231 salvajes añadiendo suero a una concentración final del 1%. En el caso de los experimentos con anticuerpo bloqueante de IL-8, también se añadió anticuerpo anti-IL-8 a distintas concentraciones: 0, 0,1, 1 y 10 µg/ml.

19. ELISA y array de quimioquinas

El medio obtenido para los ensayos de medio condicionado en IMR90 (ver apartado 18) se utilizó para ensayos de ELISA de IL-8 (R&D Systems) y para hibridar sobre un array de quimioquinas (Ray Biotech; Humano Cat #AAH-CHE-1) siguiendo las instrucciones del fabricante en ambos casos.

20. Ensayo de tumorogénesis en ratones

Para analizar el efecto de ING4 sobre el microentorno tumoral se crecieron células IMR90 infectadas con ING4 salvaje y vector vacío, y células MDA-MB-231 TGL. Posteriormente se tripsinizaron, contaron y mezclaron una proporción de 3 a 1 ($6x10^5$ y $2x10^5$ respectivamente). Se resuspendieron en un volumen final de 100µl de PBS por inyección, y se pincharon subcutáneamente en los costados de ratones nu/nu.

La bioluminiscencia se midió utilizando el gen reportero TGL (Minn et al., 2005). Se inyectaron 200µl de D-luciferina (15mg/ml en PBS) intraperitonealmente a los ratones previamente anestesiados. Las imágenes se obtuvieron pasados 5 minutos tras la inyección con un aparato Xenogen IVIS (IVIS^R Lumina II) acoplado al programa Living Image Adquisition and Analysis Software (Xenogen Corporation). Para analizar la intensidad de bioluminiscencia se definió el área de interés y se calculó como el flujo de fotones/seg. Este valor se analizó en cada medida realizada cada 7 días, relativizándolo en función al valor obtenido en la primera medida. El volumen del tumor se calculó a los mismos tiempos que la bioluminiscencia a partir de medidas con un calibre, usando la fórmula $V= AxB^2/2$ (mm^3), donde A es el diámetro mayor y B el diámetro perpendicular. A

las 5 semanas los ratones fueron sacrificados y analizados. Se les extrajeron los tumores para pesarlos y procesarlos para análisis por histología e inmunofluorescencia.

21. Ensayos de migración y metástasis en pez cebra

La capacidad migratoria de las células MDA 231-TGL infectadas con las distintas construcciones de ING4 se determinó mediante el xenotransplante de células en pez cebra. Los experimentos se realizaron siguiendo el protocolo utilizado en el Hospital Universitario Virgen de la Arrixaca (Murcia). Para ello se obtuvieron los huevos 48 horas antes del transplante. A las 24 horas se descorionaron con pronasa y se mantuvieron en la estufa a 28,5ºC en vasos de cristal con E3 y PTU (1-fenil-2-tiourea al 0,2mM). El día del xenotransplante se resuspendieron las células a una concentración de $5x10^4$ células/µl en 67% DPBS (Gibco) y 5% FBS, añadiendo rojo fenol a una concentración final del 10%. Los embriones se anestesiaron con tricaina y se colocaron en placas Petri con capa solidificada al 2% de agarosa por grupos pequeños. Se microinyectaron 3nl de suspensión celular (150 células) en el vitelo de cada embrión y se incubaron durante 1 hora a 31ºC en E3 y PTU y posteriormente a 35ºC. Se observó la presencia de células a las 2 horas post-transplante y se descartaron los embriones con células fluorescentes fuera del lugar de implantación (falsos positivos). Finalmente, se observó la invasión de células a los 2 días post-transplante, y la formación de masas de células tumorales a los 3 días post-transplante.

22. Vectores de expresión

CONSTRUCCIÓN	INSERTO	ORIGEN
pLPC AU5-ING4	ING4 humano Proteína completa	Clonado durante este trabajo
pLPC AU5-ING4 Y121N	ING4 humano Mutación Y121N	Clonado durante este trabajo
pLPC AU5-ING4 N214D	ING4 humano Mutación N214D	Clonado durante este trabajo
pLPC HA-ING4	ING4 humano Proteína completa	Clonado durante este trabajo
pLPC HA-ING4 N214D	ING4 humano Mutación N214D	Clonado durante este trabajo

pLPC HA-ING4 D213A	ING4 humano Mutación D213A	Clonado durante este trabajo
pLPC RasV12	Ha-Ras humano Mutación G12V	(Serrano et al., 1997)
pWZL RasV12	Ha-Ras humano Mutación G12V	(Serrano et al., 1997)
pCL Eco	gag, pol, env^{eco}	(Naviaux et al., 1996)
pCL Ampho	gag, pol, env^{ampho}	(Naviaux et al., 1996)
pRS shp53 Blast	Interferencia p53 humano	Daniel S Peeper, NKI Amsterdam
pRS shRb Hygro	Interferencia Rb humano	Daniel S Peeper, NKI Amsterdam

Tabla 1. Lista de vectores de expresión retroviral utilizados en este trabajo.

23. Anticuerpos

PROTEÍNA / EPÍTOPO	ANTICUERPO	ORIGEN	DILUCIÓN	PROCEDENCIA
AU5	MMS-135R	Monoclonal ratón	1:500	Babco
HA	12CA5	Monoclonal ratón	1:500	ROCHE
ING4	ab3714	Policlonal cabra	1:500	Abcam
Histona γ-H2AX	JBW301 (05-636)	Monoclonal ratón	1:500 (IF)	Upstate
p53	DO-1 (sc-126)	Monoclonal ratón	1:500	Santa Cruz
Rb	554136	Monoclonal ratón	1:1000	BD Pharmigen
p14ARF	54-75	Policlonal conejo	1:1000 (IF)	David Parry, DNAX Research Institute
BrdU	BP40250	Policlonal conejo	1:1000	Megabase
β-Actina	AC-15 (A5441)	Monoclonal ratón	1:10000	SIGMA

Tabla 2. Lista de anticuerpos primarios utilizados en este trabajo. La concentración de los anticuerpos fue la utilizada para las técnicas de inmunoblot e inmunofluorescencia, excepto los únicamente utilizados para inmunofluorescencia que aparecen indicados como (IF).

ANTICUERPO	ORIGEN	DILUCIÓN	PROCEDENCIA
Anti-Ig ratón-HRP (P 0447)	Policlonal cabra	1:5000	Dako
Anti-Ig conejo-HRP (NA934)	Policlonal burro	1:5000	Amersham
Anti-Ig cabra-HRP (P 0160)	Policlonal conejo	1:3000	Dako
Anti-Ig ratón-Alexa 488 (A11059)	Policlonal cabra	1:500	Invitrogen
Anti-Ig conejo-Alexa 488 (A11029)	Policlonal ratón	1:500	Invitrogen
Anti-Ig conejo-Alexa 594 (A11062)	Policlonal cabra	1:500	Invitrogen

Tabla 3. Lista de anticuerpos secundarios utilizados en este trabajo para inmunoblot e inmunofluorescencia

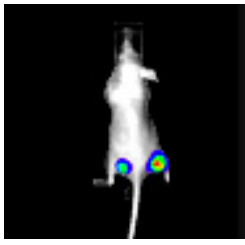

Resultados

1. Impacto funcional de mutaciones de ING4 asociadas a tumores

1.1. Generación de formas mutantes de ING4

En estudios previos se han descrito alteraciones de ING4 en tumores humanos. Nuestro primer objetivo fue caracterizar el efecto de mutaciones puntuales de ING4 asociadas a tumores (Kim et al., 2004) y conocer su implicación funcional en los mecanismos de supresión tumoral. Para ello se generaron dos mutantes puntuales de la proteína ING4 identificados en líneas celulares derivadas de adonocarcinoma de pulmón (Y121N y N214D) fusionados a los epítopos AU5 y HA en el extremo N-terminal de la proteína. La mutación Y121N se encuentra próxima al dominio de localización nuclear (NLS), mientras que la N214D está dentro del dominio conservado PHD (*Plant*

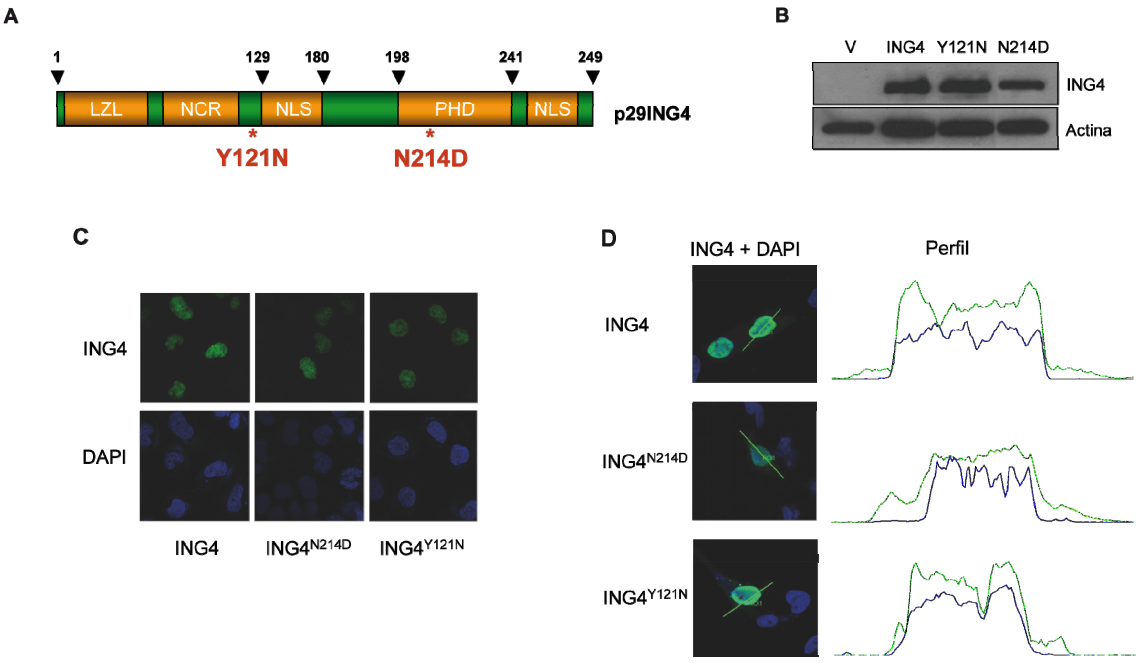

Fig. 6. Caracterización de formas mutantes de ING4. A) Diagrama de la proteína ING4 humana. La posición de las mutaciones se indica con asteriscos. **B)** Inmunoblot que muestra la sobreexpresión de ING4 salvaje ectópico y de los mutantes en células U2OS transfectadas de forma transitoria, usando un anticuerpo anti-ING4. **C)** Análisis por inmunofluorescencia de la localización de las versiones de ING4 en células U2OS transfectadas de forma transitoria. Se utilizó un anticuerpo anti-AU5 para visualizar ING4 ectópico **D)** Perfil de localización de ING4 en células U2OS.

Homeodomain), cercano a un residuo implicado en la interacción con histonas metiladas (D213) (Hung et al., 2009) y de dos cisteínas (C212 y C217), responsables del mantenimiento de la estructura del dominio PHD (Fig. 6A).

Los niveles de expresión de las distintas construcciones se comprobaron por inmunoblot, transfectando de forma transitoria células U2OS. Se observó que los niveles de expresión de la proteína ectópica eran similares entre ING4 salvaje y el mutante

Y121N, mientras que en el caso del mutante N214D se observaba de forma generalizada unos niveles inferiores de proteína (Fig. 6B y ver más adelante). Se ha identificado que ING4 se encuentra deslocalizado en tumores de pulmón (Wang et al., 2010). La presencia de una mutación próxima al dominio de localización nuclear (Y121N) nos hizo plantearnos que pudiera darse un cambio en la localización de ING4 debido a esta alteración, para ello se analizó la localización de los mutantes mediante inmunofluorescencia. Observamos que los dos mutantes de ING4 mostraban el mismo patrón de sublocalización celular que la forma salvaje, siendo esta mayoritariamente nuclear (Fig. 6C y 6D).

1.2. Efecto de mutantes de ING4 en proliferación celular

Se ha descrito previamente que la sobreexpresión de ING4 reduce la tasa de división celular (Zhang et al., 2004). Este fenotipo es uno de los mejor caracterizados para ING4, por lo que decidimos evaluar si se encontraba alterado en los mutantes asociados a tumores. Para la caracterización funcional generamos fibroblastos inmortalizados de ratón (NIH3T3) que expresaban la forma salvaje y los mutantes de ING4 mediante transducción retroviral.

La tasa de síntesis de ADN se estimó a través de ensayos de incorporación de BrdU en células NIH3T3 infectadas con vector vacío, ING4 salvaje y los dos mutantes. Determinamos el grado de incorporación de esté análogo de timidina al ADN mediante inmunofluorescencia y como esperábamos, la expresión ectópica de ING4 salvaje redujo

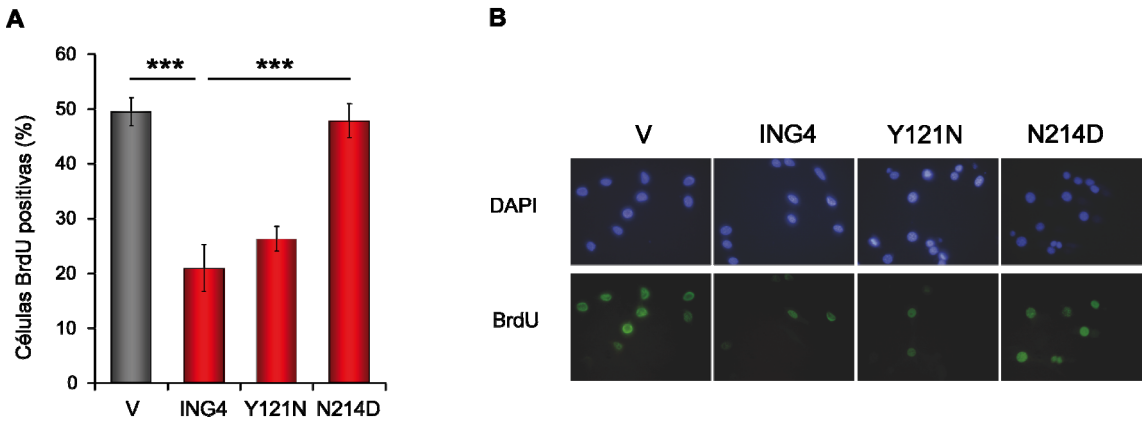

Fig. 7. El mutante N214D pierde el efecto antiproliferativo de ING4. Células NIH3T3 se infectaron con plásmidos de ING4, mutantes y vector vacío como control. A los seis días post-selección se plaquearon y se sometieron a un pulso de BrdU de 4 horas. **A)** Cuantificación del porcentaje de células positivas para BrdU. Se muestra la media y la desviación estándar de tres experimentos independientes (***P<0,001). **B)** Detección de la incorporación de BrdU por inmunofluorescencia usando DAPI para la tinción nuclear (azul) y anti-BrdU (verde) para detectar las células que estaban proliferando.

el porcentaje de células positivas para BrdU a aproximadamente el 50% del control. El mutante Y121N mostró un efecto similar a la forma salvaje, mientras que en el caso del mutante N214D se obtuvo una tasa de incorporación de BrdU similar a las células infectadas con vector vacío (Fig. 7A y 7B). Por lo tanto, el efecto antiproliferativo de ING4 se mantiene en el mutante Y121N pero se pierde en el caso del mutante N214D. Resultados similares se obtuvieron al utilizar la línea de fibrosarcoma HT1080 (datos no mostrados).

1.3. Efecto de mutantes de ING4 en migración celular

El aumento en la migración celular, la invasión y la angiogénesis son características distintivas de las células tumorales, asociadas a su capacidad metastásica. ING4 es la única de las proteínas de la familia ING para la que se ha descrito un efecto inhibitorio de angiogénesis, migración e invasión en estas células (Li et al., 2008; Shen et al., 2007; Unoki et al., 2006;). Por tanto, decidimos determinar si estas propiedades estaban alteradas en los mutantes de ING4. La capacidad antimigratoria de ING4 es llevada a cabo principalmente a través de la regulación de factores solubles promigratorios (Colla et al., 2007; Garkavtsev et al., 2004; Nozell et al., 2008; Xie et al., 2008). Por este motivo, se llevaron a cabo ensayos de migración celular usando medio condicionado de células NIH3T3 que expresaban las distintas construcciones de ING4 para comprobar su capacidad como sustrato quimiotáctico de células endoteliales microvasculares, HMVEC (Fig. 8A). Consistente con el papel descrito de ING4 como regulador negativo de la migración celular y de la angiogénesis, el medio condicionado de células que expresaban la forma salvaje de ING4 fue menos eficiente en la inducción de migración celular (~60% de las células control). En cambio, el efecto en migración celular del medio condicionado de células que expresaban el mutante N214D no se distinguía del de células que expresaban el vector vacío. En este ensayo, el mutante Y121N no tuvo un impacto funcional significativo, ya que presentaba unos niveles de migración similares a los obtenidos por ING4 salvaje, al igual que ocurría en los ensayos de proliferación celular. Se obtuvieron resultados similares en migración celular cuando se utilizaron otras construcciones de ING4 que llevaban fusionado un epítopo diferente, HA en vez de AU5 (Fig. 8B). De este modo, el efecto antimigratorio de ING4 se mantiene en el mutante Y121N, mientras que está capacidad está disminuida en células que expresan el mutante N214D.

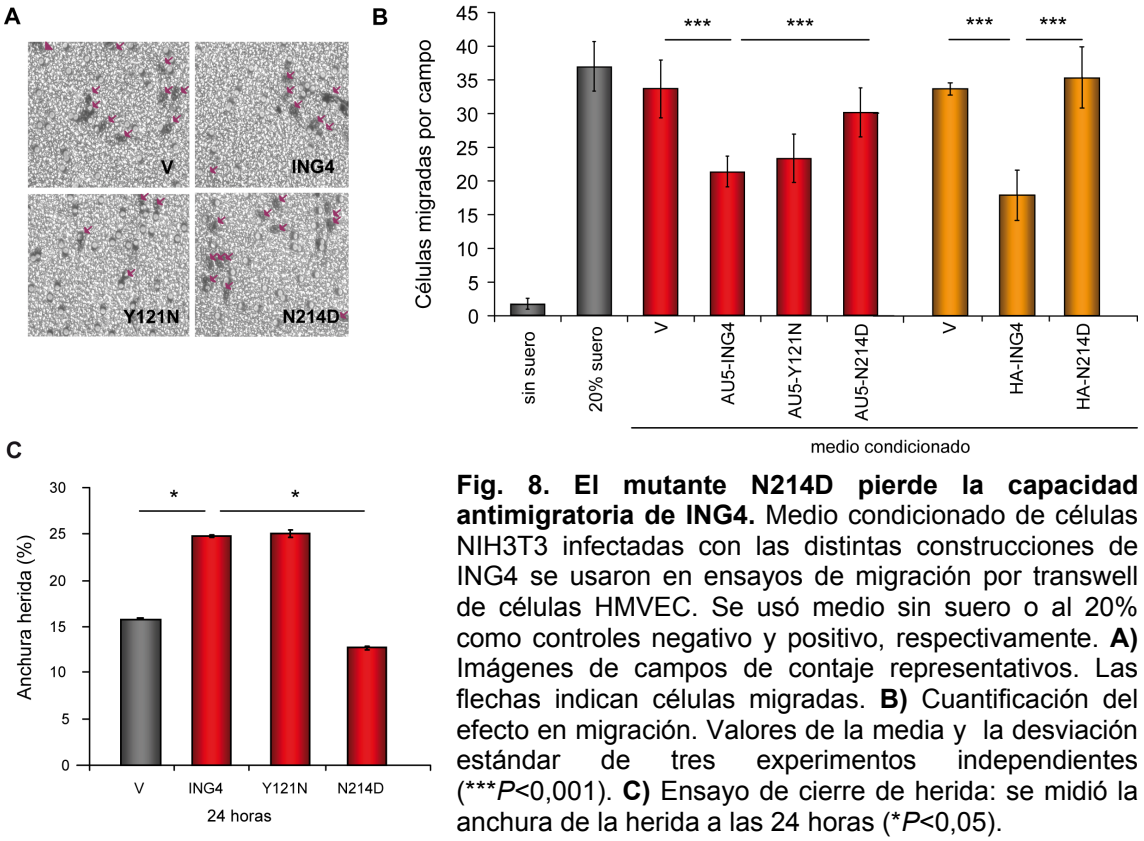

Fig. 8. El mutante N214D pierde la capacidad antimigratoria de ING4. Medio condicionado de células NIH3T3 infectadas con las distintas construcciones de ING4 se usaron en ensayos de migración por transwell de células HMVEC. Se usó medio sin suero o al 20% como controles negativo y positivo, respectivamente. **A)** Imágenes de campos de contaje representativos. Las flechas indican células migradas. **B)** Cuantificación del efecto en migración. Valores de la media y la desviación estándar de tres experimentos independientes (***P<0,001). **C)** Ensayo de cierre de herida: se midió la anchura de la herida a las 24 horas (*P<0,05).

El efecto en migración celular de ING4 y los mutantes sobre las propias células fue determinado mediante ensayos de cierre de herida en células NIH3T3 infectadas. Las células se dejaron llegar a confluencia, momento en el que se hizo la herida con una punta de pipeta y se fue midiendo la anchura a lo largo del tiempo. A las 24 horas se observó una mayor capacidad de cierre de herida del mutante N214D, similar a la que se daba en las células control. El resultado muestra que la capacidad antimigratoria de ING4 sobre las propias células que expresan la proteína está disminuida en el caso de la proteína mutante ING4^{N214D} (Fig. 8C).

1.4. Efecto de mutantes de ING4 en crecimiento independiente de anclaje

ING4 fue identificada en una búsqueda de proteínas capaces de inhibir el crecimiento independiente de sustrato, característica de células transformadas (Hung et al., 2009). Para analizar el impacto de mutaciones asociadas a tumores de ING4 en este efecto, se utilizaron células NIH3T3 infectadas con las construcciones de ING4 y con el vector vacío, que se transformaron al infectar con la forma activada del oncogén Ha-Ras (RasV12). Las células se dejaron crecer en agar blando durante 15 días, momento en el que se contó el número de colonias. La proteína mutante ING4^{Y121N} se dejó de analizar

en este punto ya que en los ensayos realizados previamente mostraba un fenotipo similar al de la proteína salvaje. La capacidad de formar colonias de células NIH3T3 infectadas con RasV12 se redujo aproximadamente un 30% cuando también se sobreexpresaba la proteína ING4 salvaje, comparado con el vector vacío. Sin embargo, este efecto inhibitorio se perdía en fibroblastos NIH3T3 con RasV12 que coexpresaban la proteína mutante ING4^{N214D}, los cuales mostraban una capacidad de formar colonias similar a las células que llevaban el vector vacío (Fig. 9).

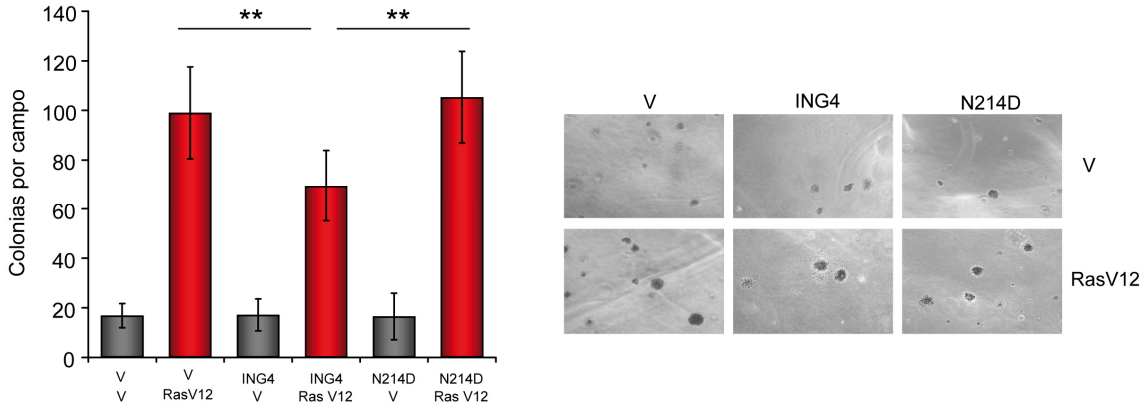

Fig. 9. El mutante N214D pierde la capacidad de ING4 de reducir el crecimiento independiente de anclaje. Células NIH3T3 fueron infectadas en primer lugar con ING4 o el vector vacío. Tras la selección, las células se crecieron en agar blando durante 15 días y se contó el número de colonias. Se muestra la media y la desviación estándar de dos experimentos (**P<0,01) (izquierda). También se muestran imágenes representativas de las colonias obtenidas en un microscopio de campo claro a 200 aumentos (derecha).

1.5. Efecto de mutantes de ING4 en viabilidad celular

La expresión de ING4 provoca muerte celular, efecto que se potencia en presencia de agentes que provocan daño en ADN (Hung et al., 2009). Para analizar el efecto de mutaciones asociadas a tumores en la función de ING4, realizamos un ensayo

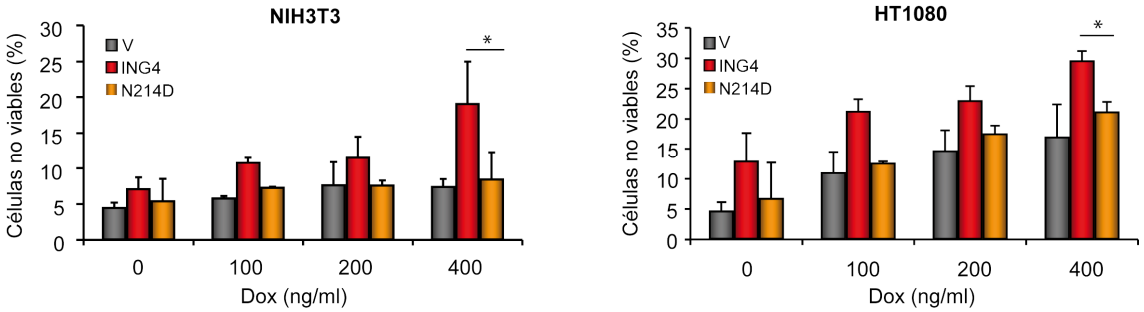

Fig. 10. Sensibilización de ING4 a muerte celular. Fibroblastos de ratón NIH3T3 y células HT1080 que expresaban ING4, el mutante N214D y el vector vacío de forma estable, se trataron con doxorrubicina a las dosis indicadas. A las 24 horas se calculó el porcentaje de células no viables por tinción con azul de tripano. Las gráficas muestran la media y la desviación estándar de dos experimentos independientes (*P<0,05).

de viabilidad en fibroblastos NIH3T3 infectados con ING4 salvaje y el mutante N214D. Las células fueron tratadas con doxorrubicina, agente que causa daño en ADN, y se midió la capacidad de ING4 y del mutante en sensibilizar a muerte en presencia de este agente. Como esperábamos, la expresión de ING4 salvaje provocaba un incremento de aproximadamente tres veces de la muerte celular por daño genotóxico, mientras que este efecto no se daba en fibroblastos que expresaban la forma mutante ING4^{N214D}. Se obtuvieron datos similares utilizando la línea de fibrosarcoma HT1080 (Fig. 10)

1.6. Impacto del mutante N214D en la estructura de la proteína y unión a marcas de histonas

Dado que la mutación N214D de ING4 tenía consecuencias en diversos aspectos a nivel funcional, quisimos determinar el mecanismo molecular que subyacía esta aparente pérdida de función. Primero, investigamos los efectos de la mutación N214D en el plegamiento de la molécula de ING4 y en el reconocimiento de marcas de histonas. Estos estudios se llevaron a cabo en colaboración con el Dr. Francisco Blanco (CIC bioGUNE). Para estudiar el impacto en la estructura de la proteína, el dominio PHD del mutante N214D se analizó en solución por resonancia magnética nuclear (NMR). Los resultados mostraron que la estructura tridimensional de los residuos 195-244 era esencialmente la misma que para la proteína salvaje (Fig. 11A, Palacios et al., 2008). También usamos NMR para analizar la capacidad de unir marcas de histonas del mutante de ING4. Al igual que otras proteínas de la familia, ING4 puede reconocer específicamente la marca de histonas H3K4me3 mediante su dominio PHD (Hung et al., 2009; Palacios et al., 2006; Palacios et al., 2008). Observamos que el mutante ING4-PHD^{N214D} también se une preferentemente a la marca H3K4me3, usando los mismos sitios que el dominio PHD de la proteína salvaje (Fig. 11B), con una afinidad y especificidad muy similar. La constante de disociación (*Kd*) para el N214D y la marca H3K4me3 fue de 3 ± 1μM comparado con la de 4 ± 1μM que se obtenía para ING4 salvaje (Fig. 11C, Palacios et al., 2006). Conjuntamente, este grupo de ensayos biofísicos indican que la mutación N214D no tiene un impacto significativo en el plegamiento o en la capacidad de reconocer marcas de ING4.

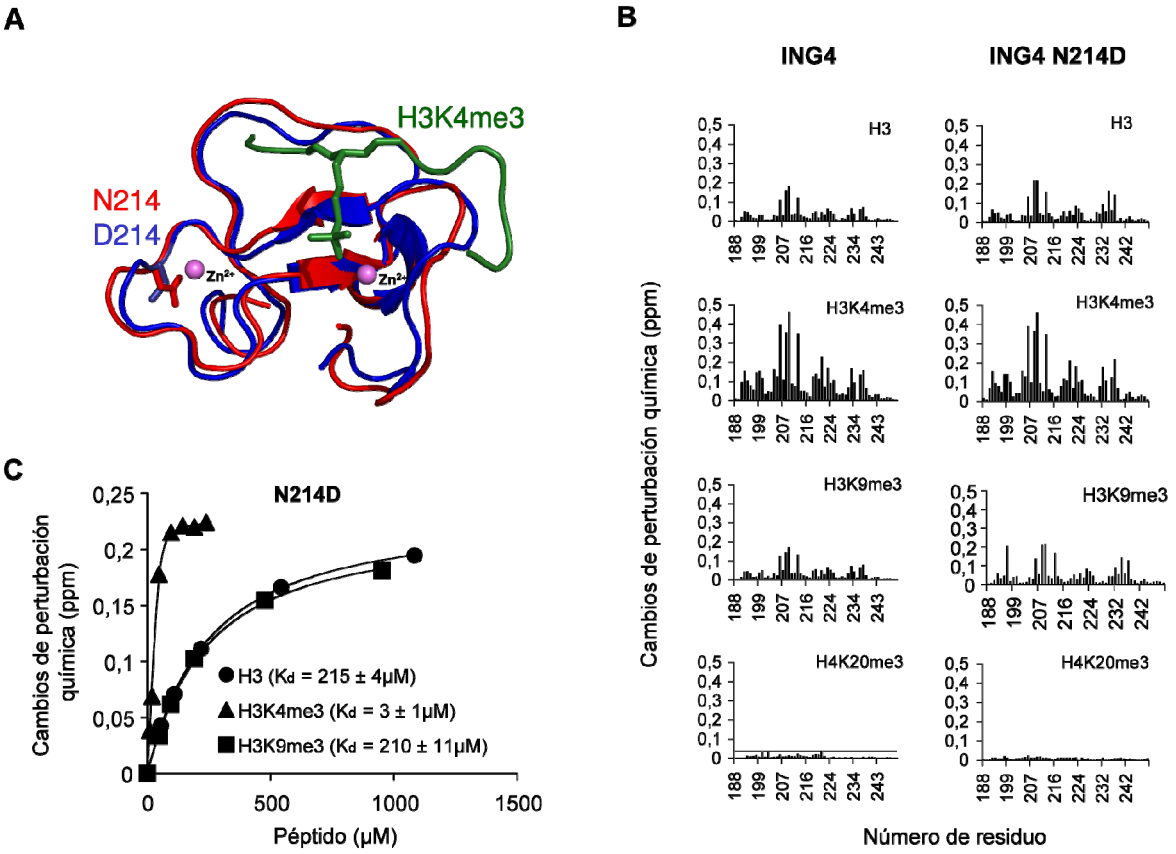

Fig. 11. Plegamiento de la proteína ING4^{N214D} y unión a marcas de histonas no difiere de la proteína salvaje. A) Sobreposición de las estructuras de los dominios PHD de la proteína salvaje (rojo) y el mutante N214D (azul). Los esqueletos de los residuos 195-244 (excluyendo la cadena terminal flexible) se muestran como cintas o hélices. Las cadenas laterales del residuo 214 (N o D) se muestran como barras. En verde se encuentra el péptido de la cisteína H3K4me3, con el residuo de lisina trimetilada mostrada en barras. Los dos cationes Zn^{2+} unidos al PHD del mutante se muestran como esferas en color violeta. **B)** Gráfica de barras de los cambios en la perturbación química observados para cada residuo del dominio PHD de ING4 salvaje y del mutante. El error experimental estimado (±0,012 ppm) se indica con una línea en el gráfico correspondiente al péptido H4K20me3. **C)** Gráfica de los cambios en la perturbación química de la resonancia de la amida W237 del PHD (50μM) como una función de la concentración de los distintos péptidos.

1.7. Efecto del mutante N214D en la estabilidad de la proteína

Durante el transcurso de estos experimentos, observamos de manera consistente unos niveles reducidos de la proteína ING4^{N214D} en comparación a los niveles de la proteína salvaje, en fibroblastos y líneas que expresaban de manera estable o transitoria las dos proteínas (Fig. 12A izquierda, ver también Fig. 6B). Sin embargo, ambas construcciones presentaban niveles similares de transcritos, habiendo incluso niveles algo superiores en el caso del mutante N214D (Fig. 12A derecha). Estos resultados sugerían que la mutación N214D podría causar una deficiencia en la estabilidad de la proteína. Para investigar los efectos de esta mutación en la vida media de ING4, se

transfectaron células 293T de forma transitoria con la proteína ING4 salvaje y el mutante N214D y posteriormente, se trataron las células con cicloheximida, un inhibidor de la síntesis de proteínas (Fig. 12B y C).

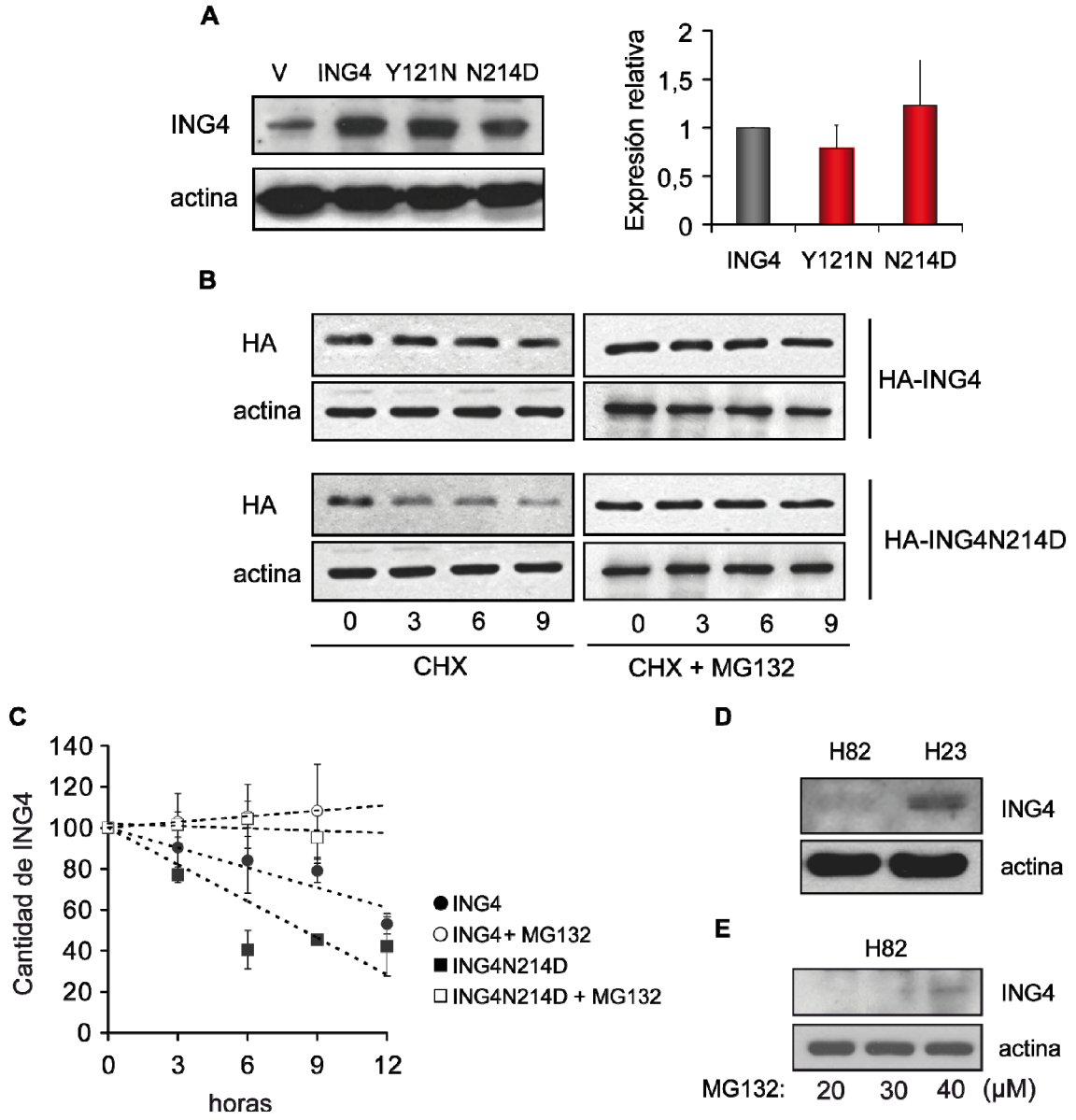

Fig. 12. La vida media de la proteína mutante ING4 N214D está disminuida. A) Análisis de la cantidad de proteína (izquierda) y de transcrito (derecha) de las variantes de ING4 en NIH3T3 por inmunoblot (anticuerpo contra ING4) y por RT-QPCR (media y desviación estándar de tres ensayos independientes. El valor de ING4 salvaje se usó como referencia). **B)** Transfección transitoria de células 293T con los vectores mostrados y tratamiento con cicloheximida (CHX) o combinada con el inhibidor MG132. Las muestras fueron tomadas en los tiempos mostrados y analizadas por inmunoblot utilizando un anticuerpo anti-hemaglutinina (HA) y usando la actina como control de carga. **C)** Cuantificación de los experimentos de vida media. En cada punto, la señal de ING4 ectópico fue cuantificada y normalizada en función a la señal de actina. La gráfica muestra la media y la desviación estándar de tres experimentos independientes. **D)** Análisis por inmunoblot de ING4 endógeno en las líneas humanas de cáncer de pulmón H82 y H23. **E)** Tratamiento de células H82 con distintas concentraciones del inhibidor del proteasoma MG132. Se utilizó un anticuerpo anti-ING4 para la detección y actina como control de carga.

La disminución de la cantidad de proteína N214D resultó ser considerablemente más rápida que el de la proteína salvaje (Fig. 12B izquierda y 12C). Se ha demostrado recientemente que los niveles de proteína de ING4 están regulados por degradación vía proteasoma (Tsai et al., 2008). Para evaluar la conexión de esta reducida estabilidad de la proteína mutante N214D con la vía del proteasoma, se realizaron experimentos de vida media en presencia del inhibidor MG132. Este inhibidor revertía las deficiencias en la estabilidad de la proteína mutante, habiendo un incremento de la vida media tanto de la proteína salvaje como del mutante N214D (Fig. 12B derecha y 12C). Resultados similares se obtuvieron utilizando otro inhibidor del proteasoma, la lactacistina (datos no mostrados). Nuestros datos se confirmaron utilizando la línea celular que expresaba el mutante N214D de forma endógena. Observamos niveles reducidos de ING4 en la línea de carcinoma de pulmón de células pequeñas H82, que tiene el alelo mutante N214D, mientras que esto no se daba en la línea H23 que tiene la mutación Y121N (Kim et al., 2004) (Fig. 12D). Los niveles reducidos de ING4 endógeno en esta línea celular se revirtieron cuando se trataron las células con el inhibidor del proteasoma MG132. Por tanto, en este conjunto de experimentos se muestra que la mutación N214D conlleva una reducción en la estabilidad de la proteína ING4 (Fig. 12E).

Anteriormente, se había sugerido que la estabilidad de ING4 dependía de su

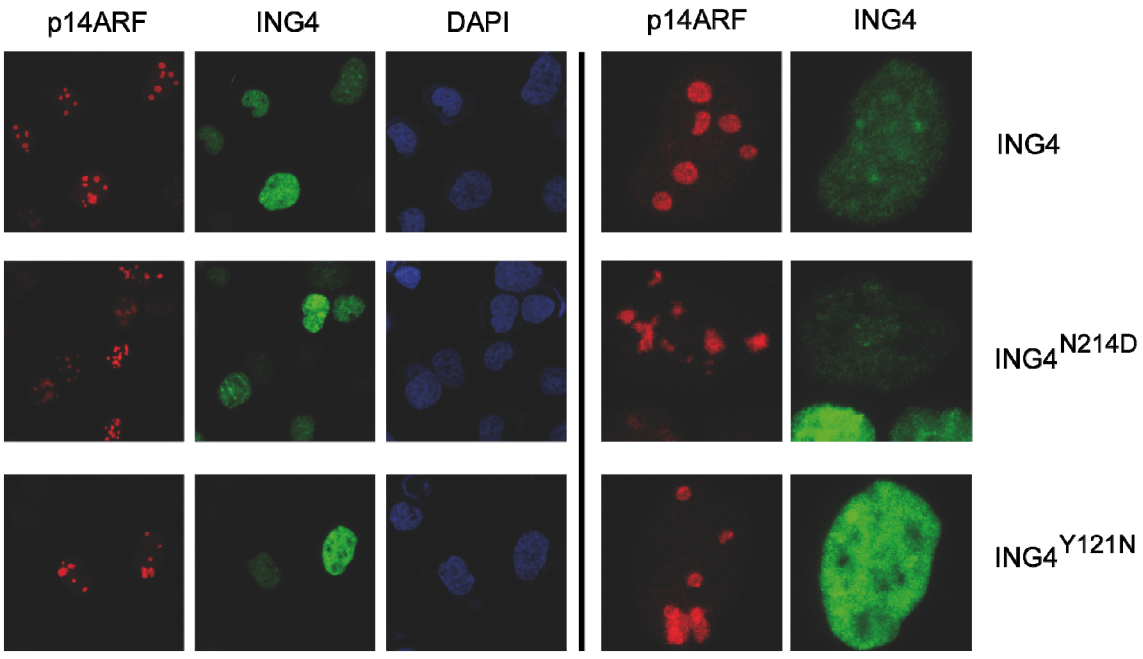

Fig. 13. ING4 y ARF no colocalizan en nucleolo. Análisis por inmunofluorescencia de células NARF2 (línea derivada de U2OS con p14ARF inducible, Stott et al., 1998) transfectadas transitoriamente con los vectores de ING4 salvaje y mutantes marcados con AU5 y tratadas con IPTG (1mM durante 24 horas) para inducir la expresión de p14ARF. Para la detección de la proteína ectópica se utilizó un anticuerpo contra AU5, para la de p14 se realizó con el anticuerpo policlonal de conejo 54-75. Los núcleos se detectaron con DAPI. El panel de la derecha muestra imágenes representativas a un mayor aumento.

acumulación en nucleolo, asociándose al supresor tumoral ARF (*Alternative Reading Frame*) (Tsai et al., 2008). En cambio, nuestros análisis por inmunofluorescencia mostraban de manera consistente una localización de la proteína ING4 predominantemente nuclear tanto para la proteína salvaje como para la mutante, sin acumulación apreciable en nucleolo, incluso estando excluido de él en algunos casos (Fig. 13). Por lo tanto no se observó colocalización de ninguna de las versiones de ING4 con la proteína nucleolar ARF, que permita establecer una correlación entre estabilidad e interacción con p14ARF.

2. Caracterización de ING4 en fibroblastos primarios humanos

En la segunda parte de este trabajo, decidimos llevar a cabo el análisis funcional de ING4 en un sistema de células primarias, utilizando fibroblastos embrionarios de pulmón (IMR90) de pase temprano. Estas son células genéticamente definidas sin ninguna mutación, que poseen los mecanismos de supresión tumoral intactos. Con este sistema pretendíamos caracterizar la función de ING4 en el contexto de células primarias no transformadas.

En estos experimentos, además del mutante N214D asociado a tumores ya descrito, también utilizamos un mutante artificial que impide el reconocimiento de marcas de histonas (D213A), para determinar la importancia del reconocimiento en nuestros

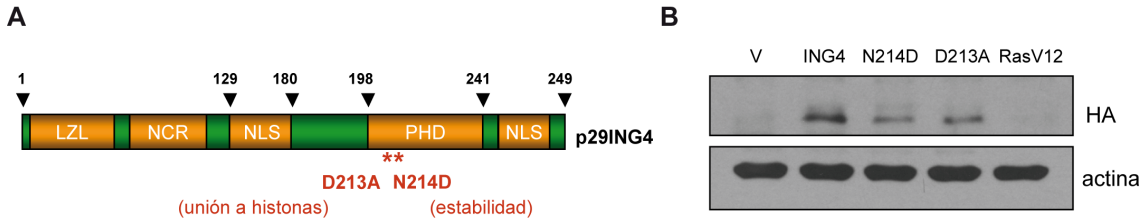

Fig. 14. Esquema de la localización de las mutaciones de ING4 utilizadas en IMR90 y control de expresión A) Diagrama de la proteína ING4 humana. La posición de las mutaciones se indica con asterisco. **B)** Inmunoblot que muestra la sobreexpresión de ING4 salvaje ectópico y de los mutantes N214D y D213A en células IMR90 infectadas retroviralmente, usando un anticuerpo anti-HA.

ensayos (Fig. 14A). Está descrito que en el dominio PHD de ING4, la tirosina 198, el aspártico 213 y el triptófano 221 son los tres residuos esenciales para el reconocimiento de la lisina 4 trimetilada, ya que la mutación de cualquiera de ellos provoca que ING4 no sea capaz de unirse a la marca H3K4me3 (Pena et al., 2006) (Abad et al., 2011). En nuestro caso decidimos utilizar el mutante D213A ya que es el presentaba los efectos

más elevados a nivel funcional y además no alteraba la unión de ING4 a los complejos de histona acetil transferasa (HAT) (Hung et al., 2009). Los niveles de expresión de las distintas construcciones se comprobaron por inmunoblot, mediante infección retroviral de células IMR90. Se observó que los niveles de expresión de los dos mutantes eran inferiores a los de la proteína salvaje (Fig. 14B).

2.1. Efecto de ING4 y mutantes en proliferación celular en fibroblastos primarios

Para determinar el efecto de ING4 y los mutantes D213A y N214D en proliferación celular, se llevaron a cabo ensayos de incorporación de BrdU y curvas de crecimiento en células IMR90 de pase temprano. Mediante infección retroviral se generaron células IMR90 que expresaban las distintas construcciones de ING4, y como controles el vector vacío y RasV12, que provoca parada de ciclo celular. En los experimentos de BrdU, al igual que en los resultados obtenidos en los fibroblastos inmortalizados de ratón, el nivel de incorporación de BrdU se redujo aproximadamente al 50% con la forma salvaje. Sin embargo, ninguno de los mutantes mostró este efecto antiproliferativo, manteniendo unos niveles similares a las células infectadas con vector vacío (Fig. 15A). En el caso de las curvas de crecimiento, también se observaba una reducción en el crecimiento, aunque de una manera menos clara, de las células que

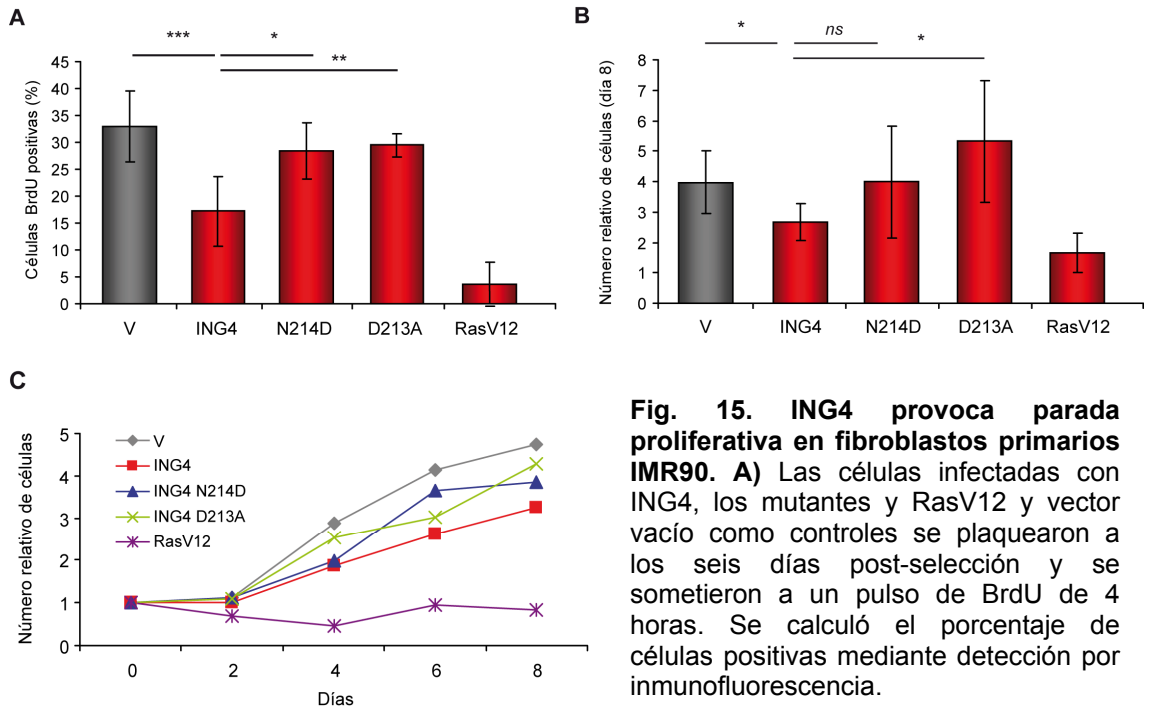

Fig. 15. ING4 provoca parada proliferativa en fibroblastos primarios IMR90. A) Las células infectadas con ING4, los mutantes y RasV12 y vector vacío como controles se plaquearon a los seis días post-selección y se sometieron a un pulso de BrdU de 4 horas. Se calculó el porcentaje de células positivas mediante detección por inmunofluorescencia. **B)** Tasa de crecimiento. Las células se tripsinizaron y contaron cada dos días y se determinó su crecimiento relativo. **C)** Curva de crecimiento. Experimento representativo. En las gráficas A y B se muestra la media y la desviación estándar de tres experimentos (***P<0,001; **P0,01; *P<0,05).

sobreexpresaban ING4 salvaje a lo largo del periodo analizado. El efecto de parada proliferativa se perdía en el caso de los mutantes (Fig. 15B y 15C). En ambos experimentos se comprobó que las células control que sobreexpresaban el oncogén RasV12 reducían su proliferación de manera drástica. Por tanto, la expresión de ING4 en fibroblastos primarios tiene capacidad antiproliferativa, que requiere el reconocimiento de marcas de histonas.

2.2. Efecto de ING4 y mutantes en inducción de senescencia y daño en ADN

La senescencia es un mecanismo esencial de supresión tumoral, por el que las células entran en un estado de parada de ciclo (generalmente en G1) de carácter irreversible (Prieur and Peeper, 2008; Rodier and Campisi, 2011). Miembros de la familia ING han sido identificados como mediadores de la respuesta senescente en conexión con la vía de p53 (ING1 e ING2) y en organización de cromatina (ING1b) (Abad et al., 2011; Kumamoto et al., 2008; Menendez et al., 2009; Pedeux et al., 2005), pero no existían datos previos acerca de la conexión de ING4 con este mecanismo. Con estos antecedentes, quisimos determinar el posible papel de ING4 en senescencia celular mediante el análisis de distintos marcadores como actividad SA-β-Gal (*Senescence Associated Beta Galactosidase Activity*) (Collado and Serrano, 2006; Dimri et al., 1995), aparición de SAHFs (*Senescence Heterochromatin Associated Foci*) o cambios de

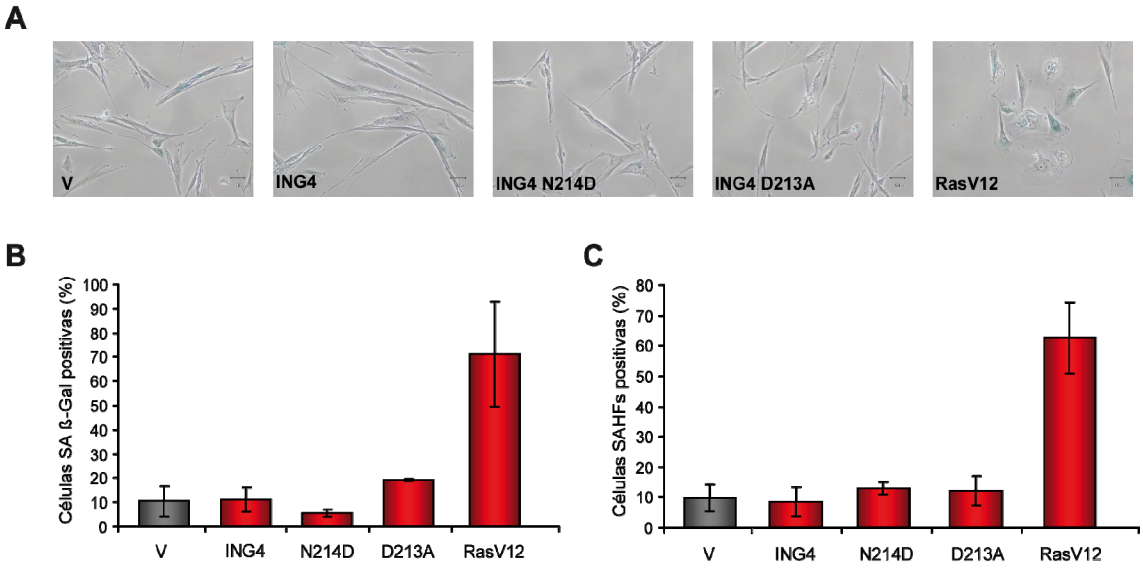

Fig. 16. ING4 no induce un fenotipo senescente. A) Imágenes de contraste de fase donde se muestra la morfología y la tinción SA β-Gal de las células infectadas y sembradas a baja densidad. **B)** Contaje de la tinción SA β-Gal. **C)** Porcentaje de células que muestran SAHFs. En las gráficas B y C se muestra la media y la desviación estándar de tres experimentos independientes.

morfología. Para estos ensayos se utilizaron células IMR90 de pase temprano infectadas con ING4 salvaje y los mutantes puntuales, además del vector vacío y RasV12, característico por la capacidad de inducir senescencia en este tipo celular (Serrano et al., 1997). No se observaron cambios morfológicos típicos de senescencia (citoplasma extendido, forma plana o nucleolos marcados) (Fig. 16A) y tampoco observamos aumento de la actividad SA-β-Gal con ninguna de las construcciones de ING4 (Fig. 16B). También analizamos los efectos en la inducción de SAHFs, estructuras de hererocromatina asociadas a represión transcripcional de genes relacionados con ciclo celular durante senescencia (Narita et al., 2003). La aparición de SAHFs se refleja en el aumento de zonas más densas en la tinción con DAPI. Como era de esperar, a la vista de los resultados anteriores, tampoco se vieron aumentos en los niveles de SAHFs mediante análisis por inmunofluorescencia (Fig. 16C). Globalmente, estos resultados indican que la expresión de ING4 no está asociada a la aparición de marcadores de senescencia.

La respuesta a daño en ADN provoca parada de ciclo y se ha propuesto que puede contribuir a la entrada en senescencia tras la activación de oncogenes (Bartkova et al., 2005; Hemann and Narita, 2007). Dada la conexión de ING4 con cromatina, quisimos estudiar la posibilidad de que la sobreexpresión de ING4 estuviera asociada a daño en ADN aunque fuera de manera independiente a la inducción de senescencia. Para ello analizamos mediante inmunofluorescencia los niveles de γ-H2AX, marcador

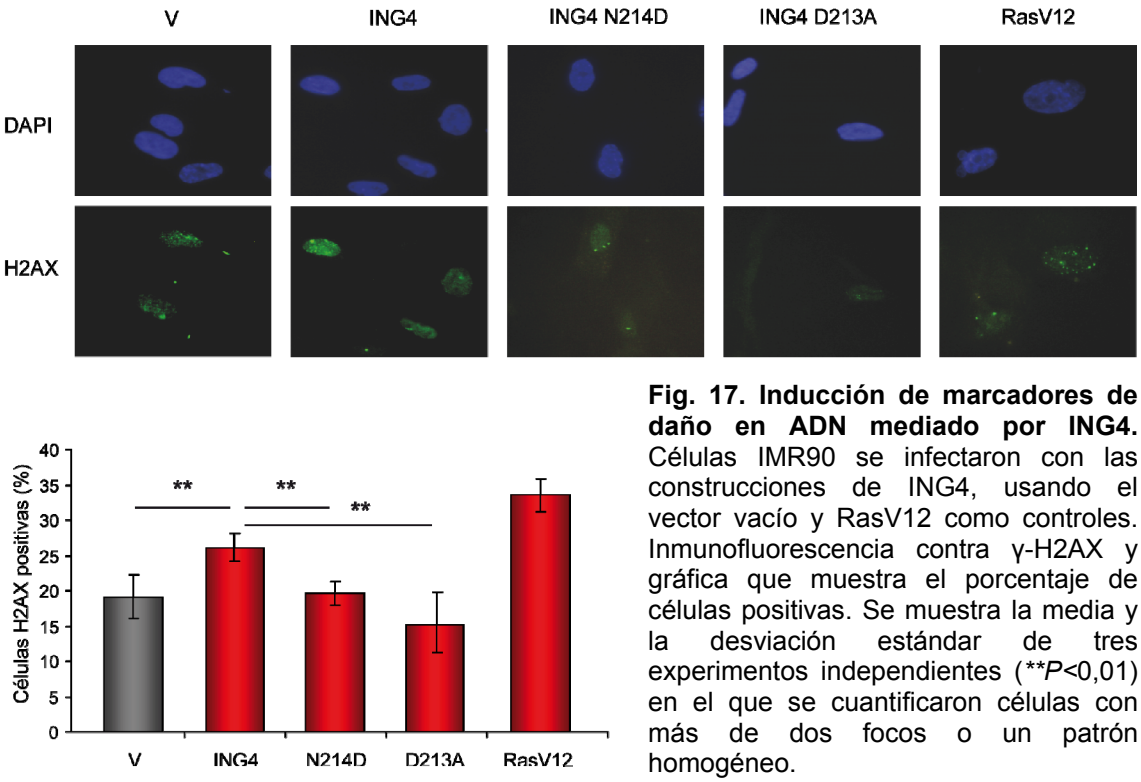

Fig. 17. Inducción de marcadores de daño en ADN mediado por ING4. Células IMR90 se infectaron con las construcciones de ING4, usando el vector vacío y RasV12 como controles. Inmunofluorescencia contra γ-H2AX y gráfica que muestra el porcentaje de células positivas. Se muestra la media y la desviación estándar de tres experimentos independientes (**P<0,01) en el que se cuantificaron células con más de dos focos o un patrón homogéneo.

característico de daño en ADN (Yuan et al., 2010). En células IMR90 infectadas con ING4 y los mutantes puntuales, observamos un ligero aumento de células positivas en las células que expresaban ING4, mientras que este efecto no se veía en el caso de los mutantes (Fig. 17). El patrón de tinción observado en las células con las construcciones de ING4 y en el vector vacío resultó ser diferente al obtenido en células que expresaban RasV12. En estas últimas se obtuvo un patrón de numerosos focos pequeños, mientras que en el resto era de pocos focos de mayor tamaño, siendo incluso homogéneo en todo el núcleo. Esta diferencia en la tinción puede deberse al tipo de daño a ADN al que está asociado ING4. La expresión ectópica de ING4 en las células primarias IMR90 supone por tanto un pequeño aumento en marcadores de daño en ADN que no se da en el caso de los mutantes y que es diferente al producido por oncogenes.

2.3. Conexión de ING4 con las vías de supresión tumoral de p53 y Rb

Las vías de p53 y del retinoblastoma (Rb) constituyen dos de las vías principales de supresión tumoral en mamíferos. Además, en estudios anteriores se ha descrito la conexión de ING4 con p53 (Shiseki et al., 2003; Zhang et al., 2005). Por estos motivos quisimos determinar si la parada de ciclo provocada por ING4 en fibroblastos primarios humanos era dependiente o no de p53 y/o Rb. Para esto, generamos células IMR90 deficientes en estas dos proteínas por infección retroviral con vectores de interferencia de ARN. Las células se volvieron a infectar con vectores para ING4 salvaje, el vector vacío y RasV12. El análisis por inmunoblot demostró la eficiencia de interferencia y la expresión ectópica de ING4 (Fig. 18A).

Para determinar si la inactivación de estas dos vías eliminaba la parada de ciclo inducida por la sobreexpresión de ING4, se llevaron a cabo ensayos de incorporación de BrdU y curvas de crecimiento en las células infectadas. Los resultados obtenidos en los ensayos de incorporación de BrdU indicaron que la pérdida de p53 revertía la parada proliferativa provocada por la sobreexpresión de ING4, mientras que este efecto se mantenía en células que llevaban el interferente de Rb (Fig. 18B y 18C). Resultados similares, aunque no tan claros, se obtuvieron con las curvas de crecimiento (Fig. 18D), lo que indicaba que el efecto de ING4 a nivel proliferativo era dependiente de p53 e independiente de Rb.

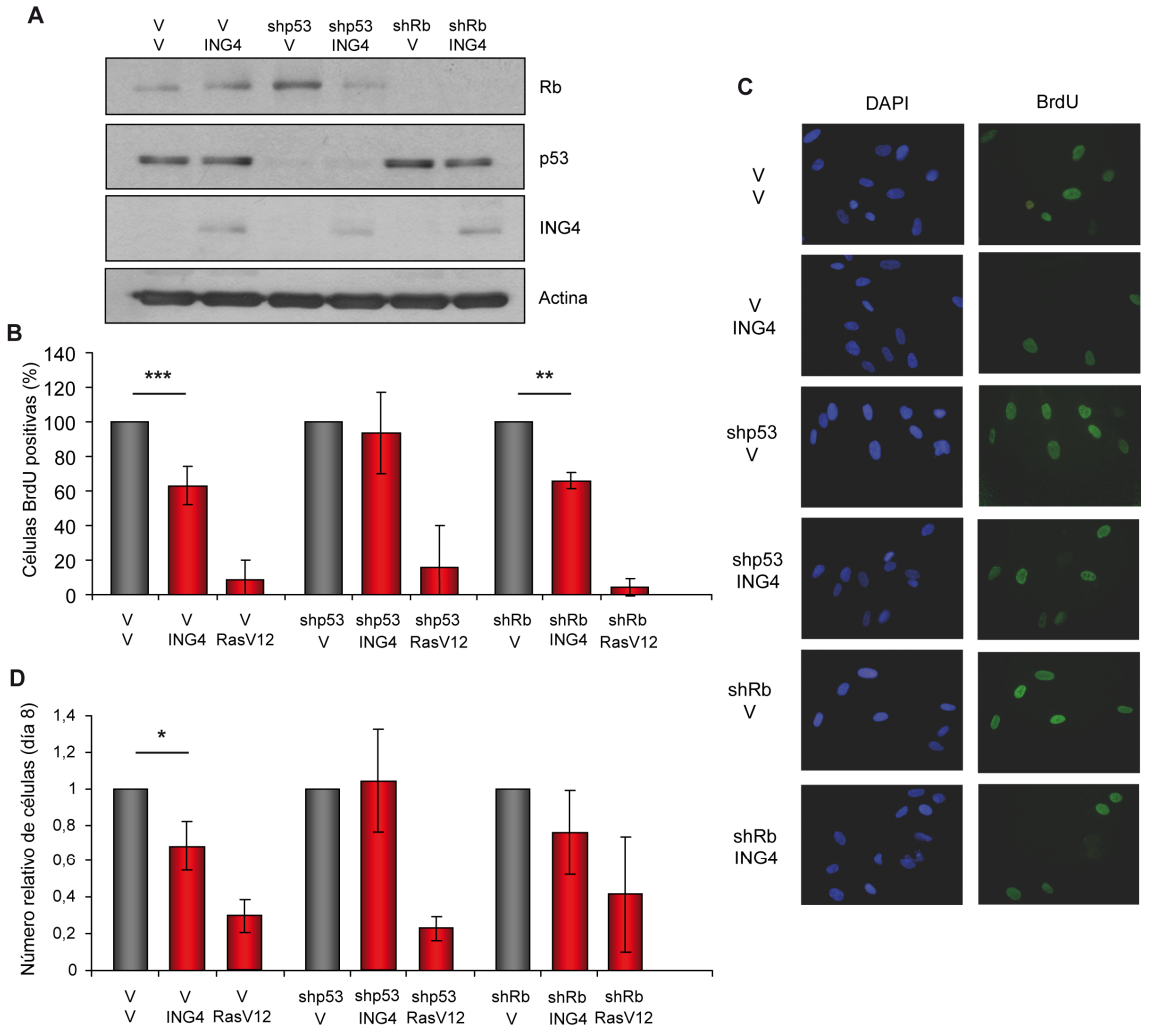

Fig. 18. ING4 provoca parada proliferativa de forma dependiente de p53 e independiente de Rb. A) Análisis por inmunoblot de los niveles de Rb, p53 e ING4 ectópico (usando un anticuerpo anti-HA). **B)** Análisis de incorporación de BrdU. Las células se sometieron a un pulso de BrdU de 4 horas. **C)** Imágenes representativas del ensayo de incorporación de BrdU **D)** Tasa de crecimiento. Las células se tripsinizaron y contaron cada dos días y se determinó su crecimiento relativo al final del experimento. En las gráficas B y D se muestra la media y la desviación estándar de tres experimentos independientes (***P<0,001; **P<0,01; *P<0,05).

A continuación se analizó también si la combinación de interferencia de p53 y Rb con la sobreexpresión de ING4 podría provocar efectos a nivel de inducción de senescencia. Esto se llevó a cabo mediante ensayos de actividad SA-β-Gal y de contaje de SAHFs. Al igual que los resultados obtenidos con las células IMR90 control, las células que expresaban los interferentes de p53 y Rb no mostraron inducción de estos marcadores en ausencia o presencia de ING4 (Fig. 19A y B). Como control, en estos experimentos combinamos la interferencia de p53 y Rb con la expresión de RasV12. Los datos obtenidos mostraron que la interferencia de p53 no era suficiente para el escape de senescencia, mientras que con la interferencia de Rb observamos un efecto diferente en función de los distintos marcadores, al igual que en datos obtenidos en otros grupos (Chicas et al., 2010; Serrano et al., 1997).

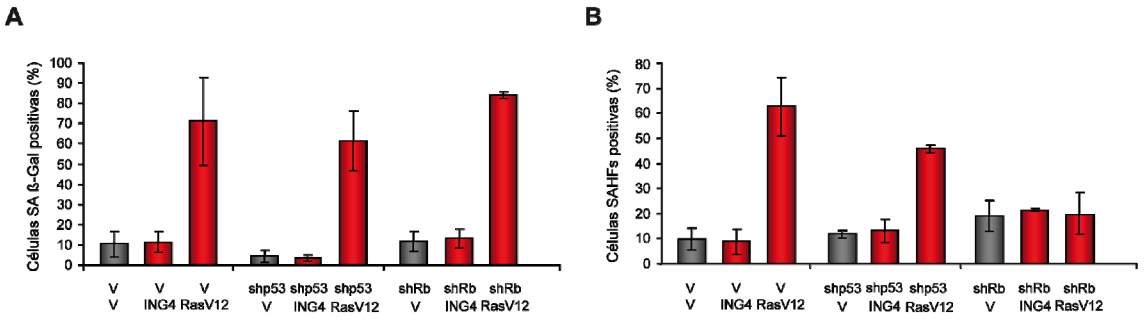

Fig. 19. ING4 no induce senescencia y no depende de p53 o Rb. A) Contaje de la tinción SA β-Gal. **B)** Porcentaje de células que muestran SAHFs. En las gráficas A y B se muestra la media y la desviación estándar de tres experimentos independientes.

2.4. Análisis del perfil de expresión regulado por ING4

La función de ING4 mejor caracterizada es el control de la expresión génica, en conexión con p53, NFκB y con la maquinaria de modificación de cromatina (Hung et al., 2009; Nozell et al., 2008; Shiseki et al., 2003). Esto nos hizo plantearnos el investigar la firma genética asociada a la función de ING4 en células primarias mediante el análisis del perfil de expresión por microarrays. Para ello se utilizaron fibroblastos primarios humanos IMR90 de pase temprano infectados con el vector de ING4 salvaje, el vector vacío y el mutante asociado a tumores N214D. Se obtuvo ARN total el mismo día que se llevaron a cabo los ensayos funcionales (seis días post-selección), que se utilizó para la hibridación de los arrays de expresión (ver métodos). En el análisis se identificaron 87 genes que mostraban expresión diferencial en células IMR90 con ING4 relativo al control de células con vector vacío (81 genes se sobreexpresaban y sólo 6 tenían una expresión reducida) (Fig. 20A y 20B). De este grupo de genes regulados por ING4, 50 genes (aproximadamente un 60%) no estaban regulados en células que expresaban el mutante puntual N214D (Fig. 20B y 20C). A continuación, comparamos estos resultados con los obtenidos en nuestro grupo para ING1b y RasV12 en otro estudio realizado en la misma plataforma con el mismo tipo celular. En ambos casos observamos un nivel de coincidencia limitado: 26 genes con ING1b y 24 genes al compararlo con el perfil de RasV12 (aproximadamente un 30% en ambos) (Fig. 20C, Abad et al., 2011). Estos resultados sugieren un papel diferencial de ING4 dentro de la familia.

A

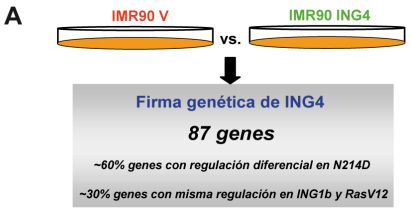

B

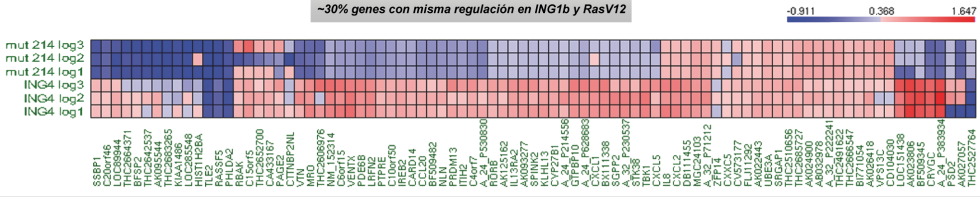

C

Nombre del Gen	ING4	N214D	ING1b	RasV12	Descripción	Función
AK023806	27,35	-1,91	3,05	1,83		Diverso
A_24_P383934	19,29	-1,78	1,12	1,75		Diverso
BF509345	14,94	1,93	1,14	2,64	Transcribed locus	Diverso
CRYGC	12,18	-1,62	1,71	1,22	Crystallin, gamma C	Crecimiento celular y diferenciación
VENTX	9,71	1,19	-1,67	2,98	VENT homeobox homolog (Xenopus)	Transcripción
LOC151438	8,20	-1,92	-1,03	4,16	Hypothetical protein LOC151438	Diverso
C6orf15	7,94	1,20	2,34	-1,30	Chromosome 6 open reading frame 15	Diverso
IL8	7,51	2,99	1,28	3185,88	Interleukin 8	Respuesta inmune
CXCL2	6,94	3,10	3,03	57,01	Chemokine (C-X-C motif) ligand 2	Vía NFKb
TBK1	6,80	1,95	1,33	-1,33	TANK-binding kinase 1	Vía NFKb
MRO	6,80	-1,95	1,02	3,50	Maestro	Crecimiento celular y diferenciación
NM_152314	6,69	1,45	-5,25	24,99		Diverso
A_32_P230537	6,15	2,01	4,03	-1,22		Diverso
SGPP2	6,01	1,90	-1,34	1,71	Sphingosine-1-phosphate phosphotase 2	Metabolismo
BX111338	5,95	2,01	4,25	-1,35	Transcribed locus	Diverso
LRFN2	5,93	-1,09	2,26	-1,12	Leucine rich repeat and fibronectin type III	Función desconocida
CXCL1	5,52	2,02	3,52	3295,41	Chemokine (C-X-C motif) ligand 1	Vía NFKb
PDE6B	5,36	1,02	1,76	-1,18	Phosphodiesterase 6B, cGMP-specific,	Metabolismo
DB111455	5,35	3,01	24,13	-1,78	Transcribed locus	Diverso
A_24_P628683	5,24	1,50	1,81	-1,01		Diverso
GTPBP10	5,24	1,72	-1,67	-1,36	GTP-binding protein 10 (putative)	Transducción de señales
C15orf5	4,98	2,95	8,08	-3,81	Chromosome 15 open reading frame 5	Diverso
STK38	4,97	1,89	1,13	1,80	Serine/threonine kinase 38	Transducción de señales
KLHL13	4,97	2,00	2,06	-14,09	Kelch-like 13 (Drosophila)	Funciones celulares básicas
MGC24103	4,82	3,95	29,61	-43,09	Hypothetical protein MGC24103	Diverso
SPINK2	4,77	1,93	-1,66	-1,06	Serine peptidase inhibitor, Kazal type 2	Metabolismo
THC2606976	4,76	-1,39	-2,22	-1,66		Diverso
AK093277	4,69	1,95	1,59	-1,08	CDNA FLJ35958 fis, clone	Diverso
PRDM13	4,24	1,09	1,35	-1,10	PR domain containing 13	Transcripción
A_32_P71212	4,20	3,68	3,92	-4,82		Diverso
CYP27B1	4,19	1,94	1,46	2,13	Cytochrome P450, family 27, subfamily B,	Metabolismo
IL13RA2	4,19	2,11	-1,43	1279,88	Interleukin 13 receptor, alpha 2	Respuesta inmune
IREB2	4,10	1,29	-1,35	1,17	Iron-responsive element binding protein 2	Transcripción
CXCL5	4,09	1,93	1,21	38,70	Chemokine (C-X-C motif) ligand 5	Vía NFKb
C4orf7	3,99	1,00	8,74	5,35	Chromosome 4 open reading frame 7	Diverso
PTPRE	3,97	1,09	-2,24	28,94	Protein tyrosine phosphatase, receptor	Transducción de señales
THC2685727	3,97	3,89	7,33	1,25		Diverso
AK022443	3,95	2,58	15,36	-1,15	CDNA FLJ12381 fis, clone	Diverso
AK125162	3,95	1,92	-1,66	-1,34	CDNA FLJ43172 fis, clone	Diverso
A_24_P530830	3,90	-1,19	1,11	2,43		Diverso
CARD14	3,82	1,30	1,24	-1,35	Caspase recruitment domain family,	Muerte celular
ITIH2	3,73	1,23	1,09	1,70	Inter-alpha (globulin) inhibitor H2	Respuesta inmune
SRGAP1	3,66	2,97	-1,12	-1,54	SLIT-ROBO Rho GTPase activating	Transducción de señales
UBE3A	3,63	3,35	-1,44	-1,74	Ubiquitin protein ligase E3A (human	Funciones celulares básicas
CCL20	3,52	1,09	-2,25	7,90	Chemokine (C-C motif) ligand 20	Vía NFKb
CA433167	3,49	2,97	95,43	5,28	Transcribed locus	Diverso
C10orf50	3,46	1,20	1,05	-2,10	Chromosome 10 open reading frame 50	Diverso
LOC89944	3,46	-3,95	-1,64	2,73	Hypothetical protein BC008326	Diverso
BF509482	3,38	1,01	1,48	-2,89	Transcribed locus, strongly similar to	Diverso
VTN	3,29	-1,95	-1,71	-2,13	Vitronectin	Adhesión celular
THC2510656	3,27	2,79	4,04	10,55		Diverso
AK095544	3,26	-4,75	-1,83	-1,39	CDNA FLJ38225 fis, clone	Diverso
AK026418	3,25	3,49	4,73	5,96	CDNA: FLJ22765 fis, clone KAIA1180	Diverso
PAGE2	3,24	1,00	-1,16	2,51	P antigen family, member 2 (prostate	Crecimiento celular y diferenciación
RBAK	3,20	2,95	1,95	2,70	RB-associated KRAB zinc finger	Transcripción
A_24_P214556	3,18	2,18	11,69	2,63		Diverso
RORB	3,17	1,98	-1,61	-1,30	RAR-related orphan receptor B	Transducción de señales
THC2491622	3,15	3,93	2,39	-1,40		Diverso
FLJ11292	3,05	2,64	1,03	1,31	Hypothetical protein FLJ11292	Diverso
BI771054	3,01	3,29	1,22	-1,43	Transcribed locus	Diverso
CV573177	2,98	2,97	9,30	-3,07	Transcribed locus	Diverso
THC2652700	2,94	2,96	3,17	1,01		Diverso
THC2664371	2,91	-3,95	-1,05	-1,26		Diverso
SSBP1	2,87	-2,95	-1,08	1,72	Single-stranded DNA binding protein 1	Transcripción
NLN	2,76	1,10	-1,11	1,46	Neurolysin (metallopeptidase M3 family)	Metabolismo
AK024900	2,70	3,96	8,53	1,36	CDNA: FLJ21247 fis, clone COL01205	Diverso
KIAA1486	2,67	-4,39	-1,70	-1,57	KIAA1486 protein	Diverso
A_32_P222241	2,64	3,76	7,42	-246,15		Diverso
C20orf46	2,58	-1,91	1,26	2,70	Chromosome 20 open reading frame 46	Diverso
THC2666547	2,58	3,13	3,85	-1,81		Diverso
AB032978	2,57	3,94	4,56	1,65		Diverso
CD104030	2,50	4,19	-1,08	105,00	Transcribed locus	Diverso
HIST1H2BA	2,46	-4,95	-1,68	-1,34	Histone cluster 1, H2ba	Transcripción
CTTNBP2NL	2,31	2,95	-1,59	-3,09	CTTNBP2 N-terminal like	Función desconocida
CXXC5	2,30	2,19	-1,91	-5,45	CXXC finger 5	Vía NFKb
BFSP2	2,30	-3,81	-1,74	1,25	Beaded filament structural protein 2,	Citoesqueleto
VPS13C	2,30	3,94	-1,62	-1,31	Vacuolar protein sorting 13 homolog C (S.	Función desconocida
LOC285548	2,25	-6,80	-1,70	-1,32	Hypothetical protein LOC285548	Diverso
THC2683265	2,25	-5,02	-1,75	1,47		Diverso
THC2642537	2,18	-3,94	-1,68	-1,37		Diverso
ZFP14	2,00	2,69	1,62	-1,40	Zinc finger protein 14 homolog (mouse)	Transcripción
RASSF5	-2,04	-4,94	-1,49	-1,32	Ras association (RalGDS/AF-6) domain	Transducción de señales
TLE2	-2,95	-6,66	-1,18	-1,08	Transducin-like enhancer of split 2	Transcripción
PHLDA2	-3,20	-2,93	-1,53	7,15	Pleckstrin homology-like domain, family	Crecimiento celular y diferenciación
PSD2	-3,77	1,94	-1,67	-1,34	Pleckstrin and Sec7 domain containing 2	Crecimiento celular y diferenciación
AK027057	-4,69	-1,95	-1,45	-1,32		Diverso
THC2527764	-5,90	1,65	-1,80	1,08		Diverso

Fig. 20. Firma genética asociada a ING4. A) Esquema del protocolo seguido para el análisis y resumen del número de genes regulados. **B)** Representación de los valores de los genes regulados por ING4 y comparación con la regulación con el mutante N214D en los triplicados realizados. **C)** Tabla de genes regulados ≥ 2 veces con ING4 y valores del mutante N214D, ING1b y RasV12 para estos genes.

El análisis de la firma genética de ING4 clasificando los genes por categorías funcionales mostraba un enriquecimiento muy significativo en categorías relacionadas con adhesión, proliferación, migración, actividad inflamatoria y citoquina (Fig. 21A). Un análisis adicional realizado con otra plataforma informática (GSEA; http://www.broadinstitute.org/gsea), confirmó estos resultados y además mostró enriquecimiento en genes relacionados con metástasis (datos no mostrados). A raíz de estos resultados y de nuestros datos previos de ING4 en regulación de la migración mediada por factores liberados al medio extracelular, decidimos centrar nuestro estudio en el análisis de los factores solubles regulados por ING4. Se llevó a cabo un análisis más detallado de categorías relacionadas con los factores solubles, en el que se pudo comprobar un alto grado de representación de categorías relacionadas con actividad citoquina o quimioquina. La comparación de estos datos con la regulación de estas categorías por ING1b mostró que aunque ambas regulan factores solubles, ING1b está más relacionada con la regulación de los receptores de estas moléculas (Fig. 21B). Algunos de los genes con actividad citoquina obtenidos en el array (además de IL-6 por estar relacionada con ING4 en estudios previos, Garkavtsev et al., 2004b) se validaron

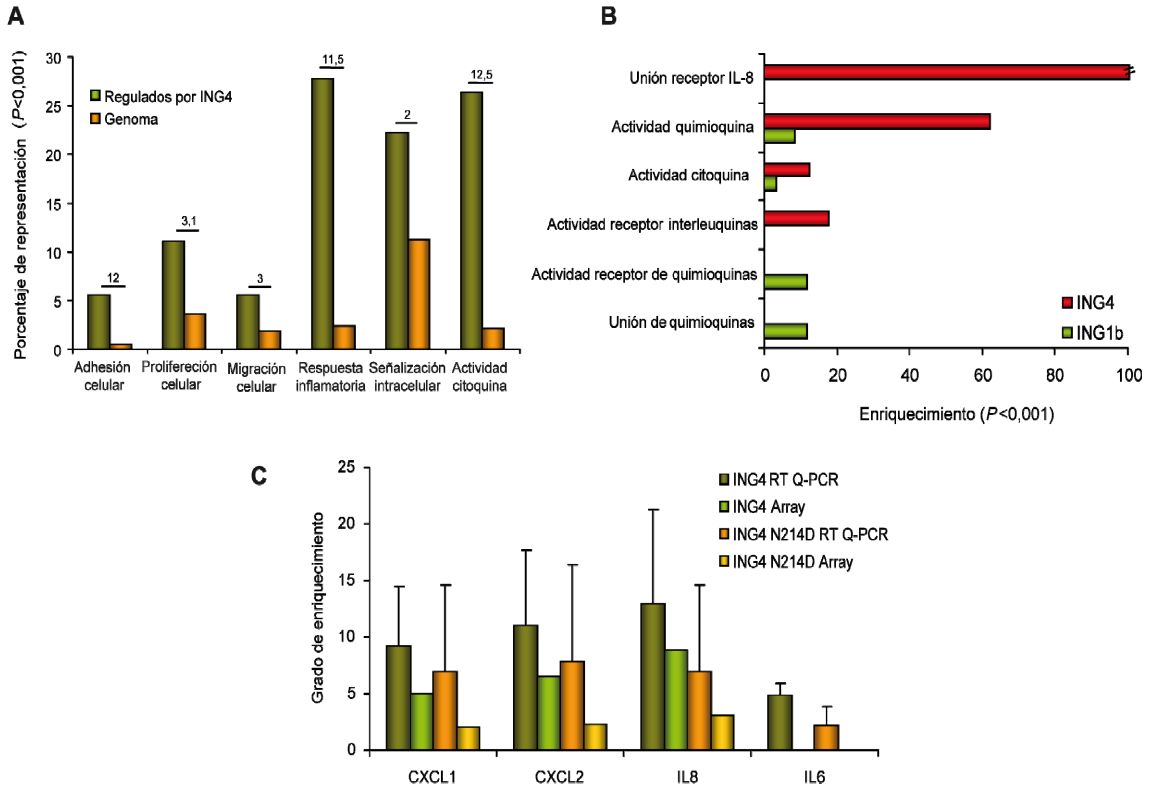

Fig. 21. Categorías funcionales de genes regulados por ING4 y validaciones. A) Análisis del enriquecimiento funcional del grupo de genes regulados por ING4. En cada categoría se representa el grado de enriquecimiento de cada categoría respecto al genoma humano. **B)** Análisis del enriquecimiento funcional en factores solubles de los genes regulados por ING4 e ING1b. En cada categoría se representa el número de veces de enriquecimiento de cada categoría respecto al genoma humano. **C)** Validación por RT-QPCR de una selección de genes identificados en el microarray. Se muestra el grado de expresión relativa en relación al vector vacío. El grado de enriquecimiento obtenido en el array se muestra como referencia. Se muestra la media y la desviación estándar de dos cuantificaciones de ARN diferentes.

por RT-QPCR (Fig. 21C). Para comprobar si los datos obtenidos con el ARN se trasladaban a la producción y liberación de estos factores solubles, llevamos a cabo su análisis en el medio condicionado. Mediante el uso de un array de quimioquinas (ver Materiales y métodos) se comparó el medio condicionado de células IMR90 que expresaban ING4 salvaje con el de células que expresaban el vector vacío. Los resultados mostraron un incremento general de factores solubles de tipo quimioquina en el medio de células con ING4, destacando genes como IL-8, CXCL1, CXCL2 o CXCL5, que también presentaban altos niveles de expresión con ING4 en el array de expresión (Fig. 22A). También se analizaron los niveles de IL-8 mediante ensayos de ELISA utilizando el mismo medio que en el array de quimioquinas pero analizando también los niveles en los mutantes y en el control con RasV12. En estos experimentos se confirmaron de forma general cambios pequeños, aunque reproducibles, en los niveles de IL-8 mediado por ING4 en este tipo celular. En cambio, esta regulación no se daba en el caso de los mutantes (Fig. 22B).

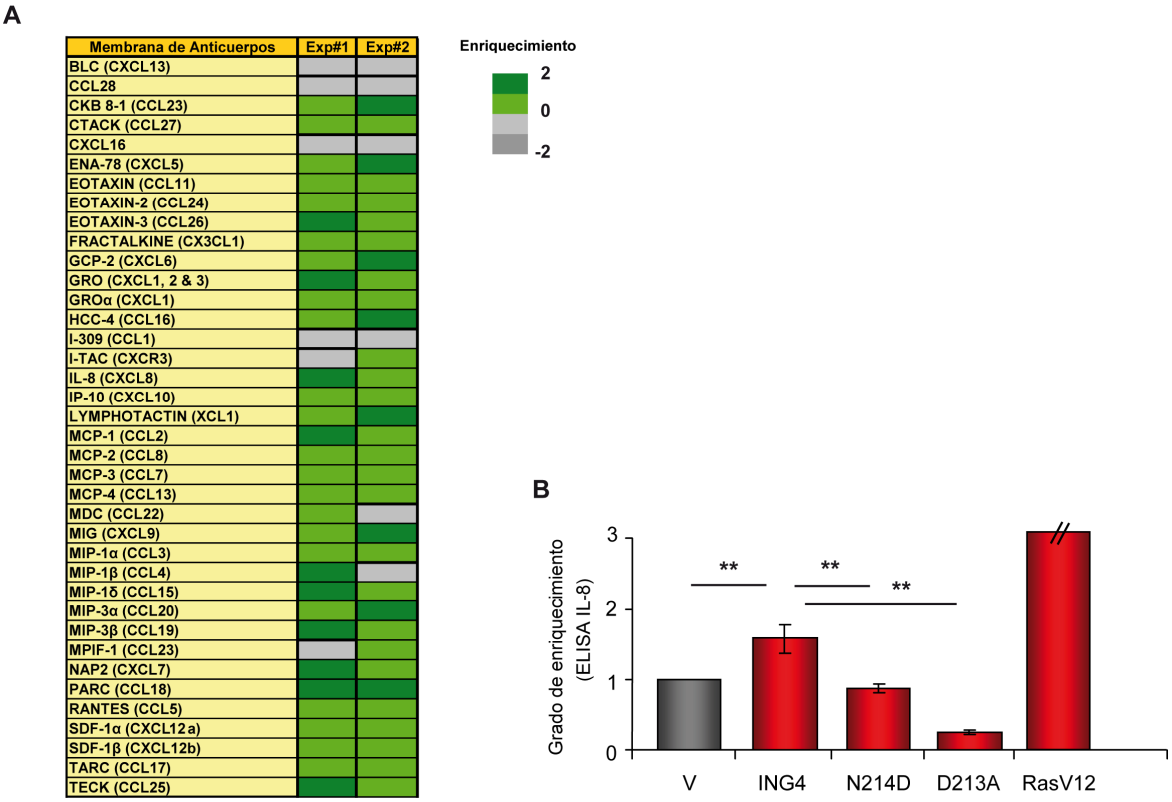

Fig. 22. A) El medio condicionado de células IMR90 que expresaban ING4 o vector vacío se hibridaron en arrays de quimioquinas. Las membranas se revelaron utilizando la actividad peroxidada acoplada a los anticuerpos secundarios. Se muestra la media de dos duplicados técnicos y dos duplicados biológicos, representándose los datos relativizados en función al vector vacío. **B)** Ensayo de ELISA de IL-8. Se muestra la media y la desviación estándar de tres experimentos independientes (***P*<0,01).

2.5. Efectos de ING4 mediados por factores solubles

A partir de los datos obtenidos a nivel de ARN y de producción de quimioquinas, quisimos caracterizar los posibles efectos de la expresión de ING4 en fibroblastos primarios a través de factores solubles. Para ello se analizó el efecto del medio condicionado de células primarias que expresaban ING4 sobre otras células primarias y sobre líneas tumorales. Las células IMR90 infectadas se crecieron y se dejaron llegar a un 90% de confluencia, momento en el que se las privó de suero durante 3 días y se recogió el medio condicionado. Este medio se añadió sobre ambos tipos celulares para determinar los efectos en proliferación celular (Fig. 23A). En primer lugar, se midió la tasa de incorporación de BrdU en la línea tumoral de mama MDA-MB-231 en presencia del medio condicionado de células que expresaban ING4 o los mutantes. Se comprobó que el medio procedente de células infectadas con ING4 salvaje favorecía la proliferación de células MDA-MB-231, mientras que este efecto se perdía con los dos mutantes

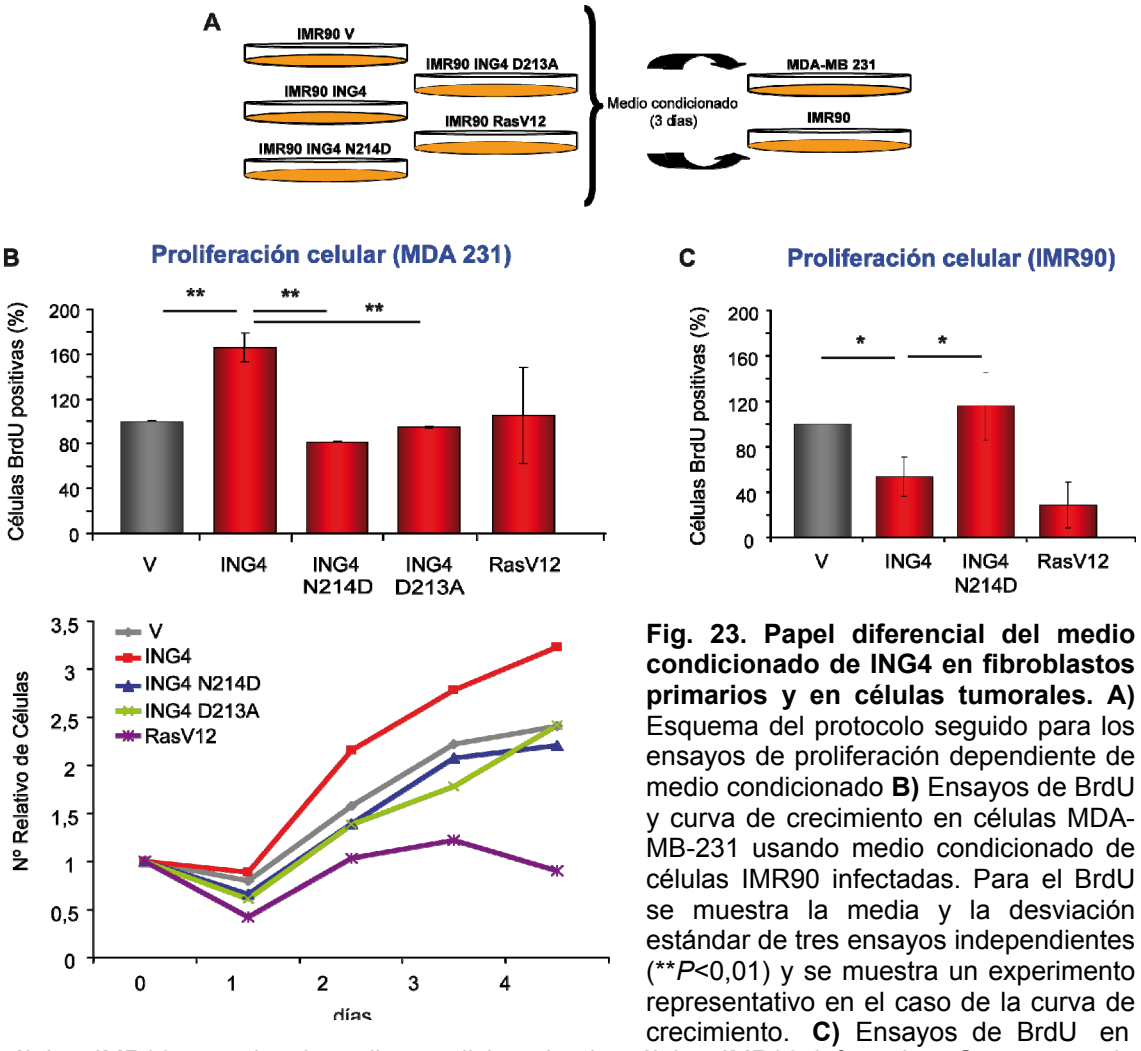

Fig. 23. Papel diferencial del medio condicionado de ING4 en fibroblastos primarios y en células tumorales. A) Esquema del protocolo seguido para los ensayos de proliferación dependiente de medio condicionado **B)** Ensayos de BrdU y curva de crecimiento en células MDA-MB-231 usando medio condicionado de células IMR90 infectadas. Para el BrdU se muestra la media y la desviación estándar de tres ensayos independientes (***P*<0,01) y se muestra un experimento representativo en el caso de la curva de crecimiento. **C)** Ensayos de BrdU en células IMR90 usando el medio condicionado de células IMR90 infectadas. Se muestra la media y la desviación estándar de tres ensayos independientes (**P*<0,05).

puntuales de la proteína. Estos datos se confirmaron mediante curvas de crecimiento (Fig. 23B). En cambio, la adición de los mismos medios condicionados sobre fibroblastos IMR90 no transformados provocó el efecto contrario: inhibición de la proliferación que se perdía en el caso del mutante N214D (Fig. 23C). Estos datos demuestran un papel diferencial de actuación de los factores secretados por ING4 al medio dependiente del contexto celular.

Para profundizar más en los efectos de ING4 a través del medio condicionado, quisimos determinar si IL-8, uno de los factores secretados al medio extracelular en células que expresaban ING4, tenía un papel en proliferación de células tumorales. Para esto se repitieron los ensayos con medio condicionado sobre la línea tumoral MDA-MB-231 utilizando un anticuerpo bloqueante anti-IL-8 a distintas concentraciones. La adición de anticuerpo anti-IL-8 revirtió el efecto proliferativo del medio condicionado de ING4, consistente con un papel importante de IL-8 como factor soluble implicado en la inducción de proliferación en la línea tumoral MDA-MB-231 (Fig. 24A). La efectividad del anticuerpo se midió mediante un ensayo de ELISA utilizando los mismos medios condicionados (Fig. 24B).

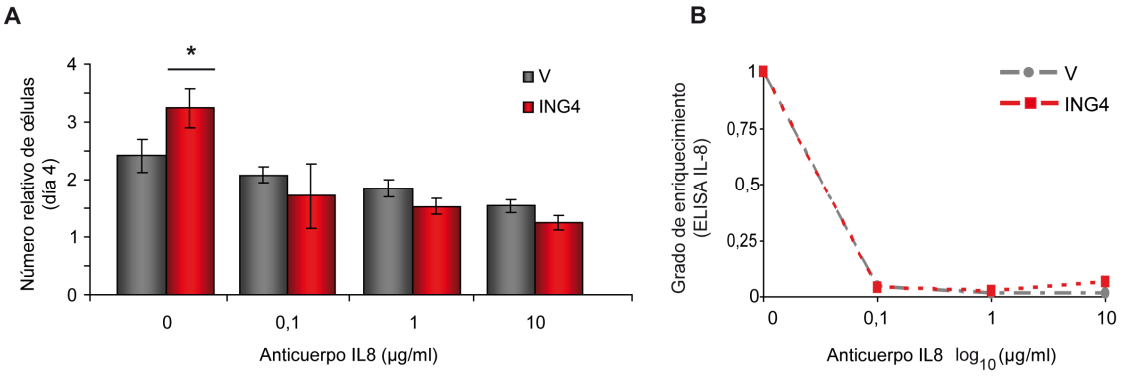

Fig. 24. Papel de IL-8 en el efecto de ING4 en proliferación de células tumorales. A) Tasa de crecimiento. Las células MDA-MB-231 se dejaron crecer durante 4 días a concentraciones crecientes de anticuerpo anti IL-8. Se relativizó el crecimiento celular el último día de la medida. Se muestra la media y la desviación estándar de tres experimentos independientes (**P*<0,05). **B)** Ensayo de ELISA de IL-8 de los medios condicionados utilizados para las curvas de crecimiento.

2.6. Efectos de ING4 en tumorogénesis *in vivo*

Los resultados obtenidos *in vitro* mostraban un papel importante de ING4 en la producción y secreción de factores solubles al medio extracelular en fibroblastos primarios. Para comprobar la hipótesis de que fibroblastos que expresan ING4 son capaces de jugar un papel en el entorno tumoral y promover el crecimiento tumoral, utilizamos un sistema *in vivo*, de forma que pudiéramos recrear un escenario en el que

las células tumorales se vieran rodeadas por un microentorno de fibroblastos que sobreexpresaran ING4. Para estos ensayos, se inyectaron en los flancos de ratones inmunodeficientes nu/nu distintas combinaciones de células IMR90 infectadas, junto con células de la línea MDA-MB-231-TGL. Estas células llevan incorporado un sistema que permite su detección no invasiva mediante bioluminiscencia o fluorescencia (ver materiales y métodos). Se observó la aparición de tumores a lo largo de cinco semanas

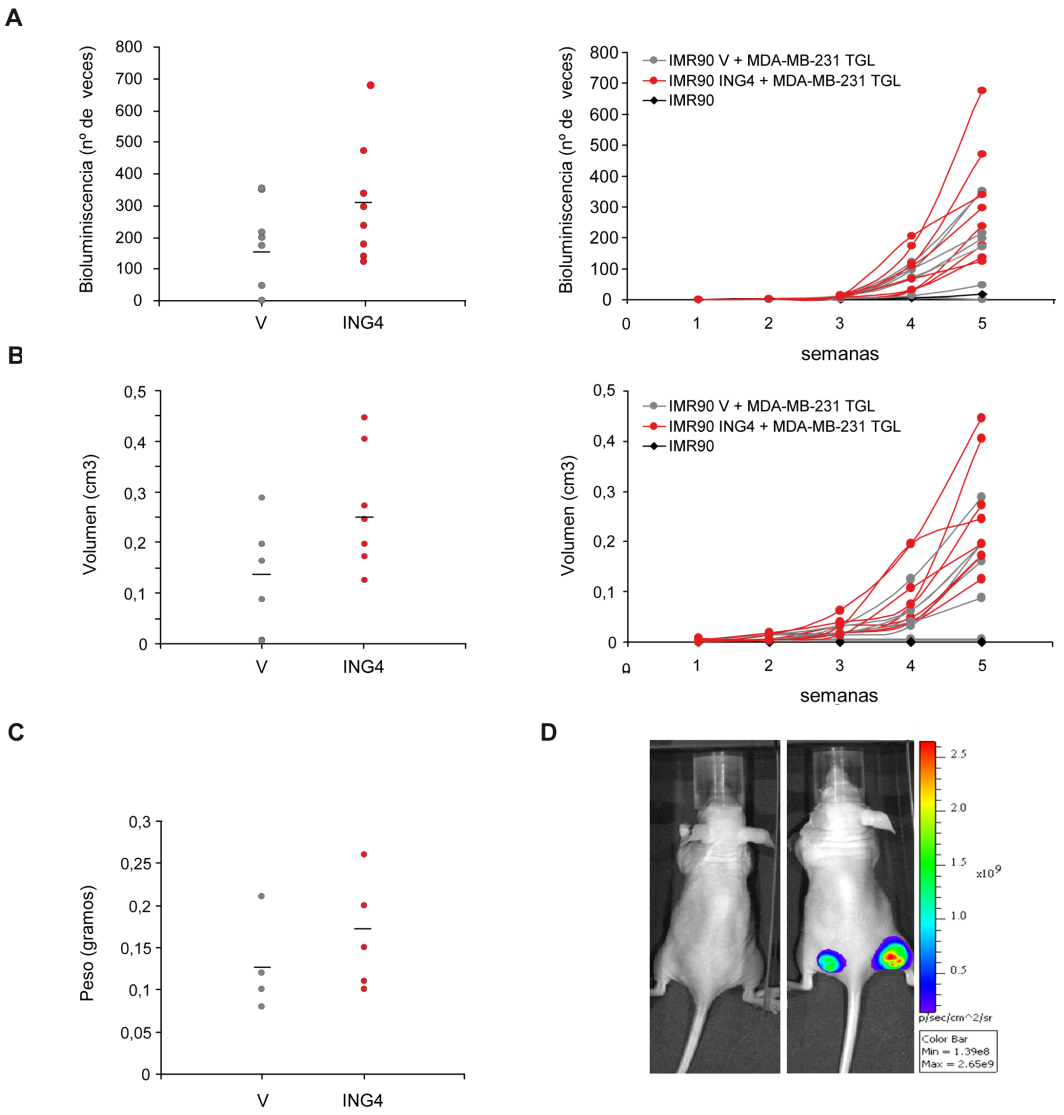

Fig. 25. Fibroblastos que expresan ING4 estimulan el crecimiento tumoral *in vivo*. Los ratones nu/nu fueron inoculados con una mezcla de fibroblastos IMR90 con ING4 o vector vacío junto con células epiteliales de cáncer de mama MDA-MB-231-TGL, 8 flancos de cada, y se midió el crecimiento del tumor durante 5 semanas. **A)** Cuantificación de los datos de bioluminiscencia al final del experimento (izquierda) y a los distintos tiempos (derecha), relativizado la intensidad a la obtenida en la primera medida. **B)** Medición del volumen del tumor al final del experimento (izquierda) y a los distintos tiempos (derecha). **C)** Peso de los tumores al final del experimento. En A) y B) izquierda y C) se representa la media de cada uno de los datos mediante una barra horizontal. **D)** Imagen representativa de la señal de bioluminiscencia. La intensidad de la señal, obtenida como flujo de fotones/segundo se muestra por la escala de colores. Se muestra un ratón control (izquierda) y un ratón con células control en el flanco izquierdo y células con ING4 en el flanco derecho (derecha).

utilizando tanto la emisión de bioluminiscencia como la medición del volumen de los tumores a distintos tiempos. Junto con estas dos medidas, al final del experimento los ratones fueron sacrificados y se les extrajeron los tumores para pesarlos y analizarlos mediante histología. Los flancos de ratones a los que se les había co-inyectado células IMR90 infectadas con ING4 presentaron una mayor actividad luciferasa respecto a los que llevaban células con vector vacío. Este dato de bioluminiscencia correlacionaba con los de volumen y peso del tumor (Fig. 25A, B y C). Por tanto, observamos que la presencia de fibroblastos primarios que expresaban ING4 ectópicamente junto con células tumorales, favorecía la formación de tumores *in vivo*.

3. Efectos de ING4 en inducción de metástasis en pez cebra

La metástasis es un proceso que comprende varias etapas, desde la proliferación hasta la invasión, y es una propiedad de las células tumorales. Recientemente se ha conectado a ING4 con el gen supresor de metástasis BRMS1 (Li and Li, 2010), implicado en la regulación de la angiogénesis. Esta conexión junto con otras que ligan a la proteína con inhibición de migración y angiogénesis y junto a nuestros datos obtenidos en células NIH3T3, nos hicieron plantearnos experimentos de metástasis *in vivo*. Para ello utilizamos células MDA-MB-231-TGL infectadas con ING4, los mutantes D213A y N214D y el vector vacío como control. Evaluamos la formación de metástasis en el sistema de xenógrafos en pez cebra en colaboración con el grupo de la Dra. María Luisa Cayuela (Hospital Universitario Virgen de la Arrixaca). Las células se marcaron con fluorescencia y se transplantaron en el saco vitelino de larvas de pez cebra de dos días de edad para estudiar el comportamiento metastático *in vivo*. Este ensayo permite distinguir larvas sin metástasis, donde las células permanecen en el saco vitelino (Fig. 26A superior), de larvas donde se detectan células marcadas a lo largo del cuerpo del pez, indicativas de metástasis (Fig. 26A inferior). Este ensayo reveló que células que sobreexpresaban ING4 mostraban una menor capacidad metastásica, permaneciendo en el saco vitelino con alta frecuencia, mientras que las larvas a las que se habían inoculado células que sobreexpresaban el vector vacío o los mutantes presentaban un número elevado de metástasis. La cuantificación del porcentaje de larvas con o sin metástasis mostró una disminución de aproximadamente del 60% con ING4 salvaje respecto a las células control, dato que se revertía en el caso de los mutantes puntuales (Fig. 26B).

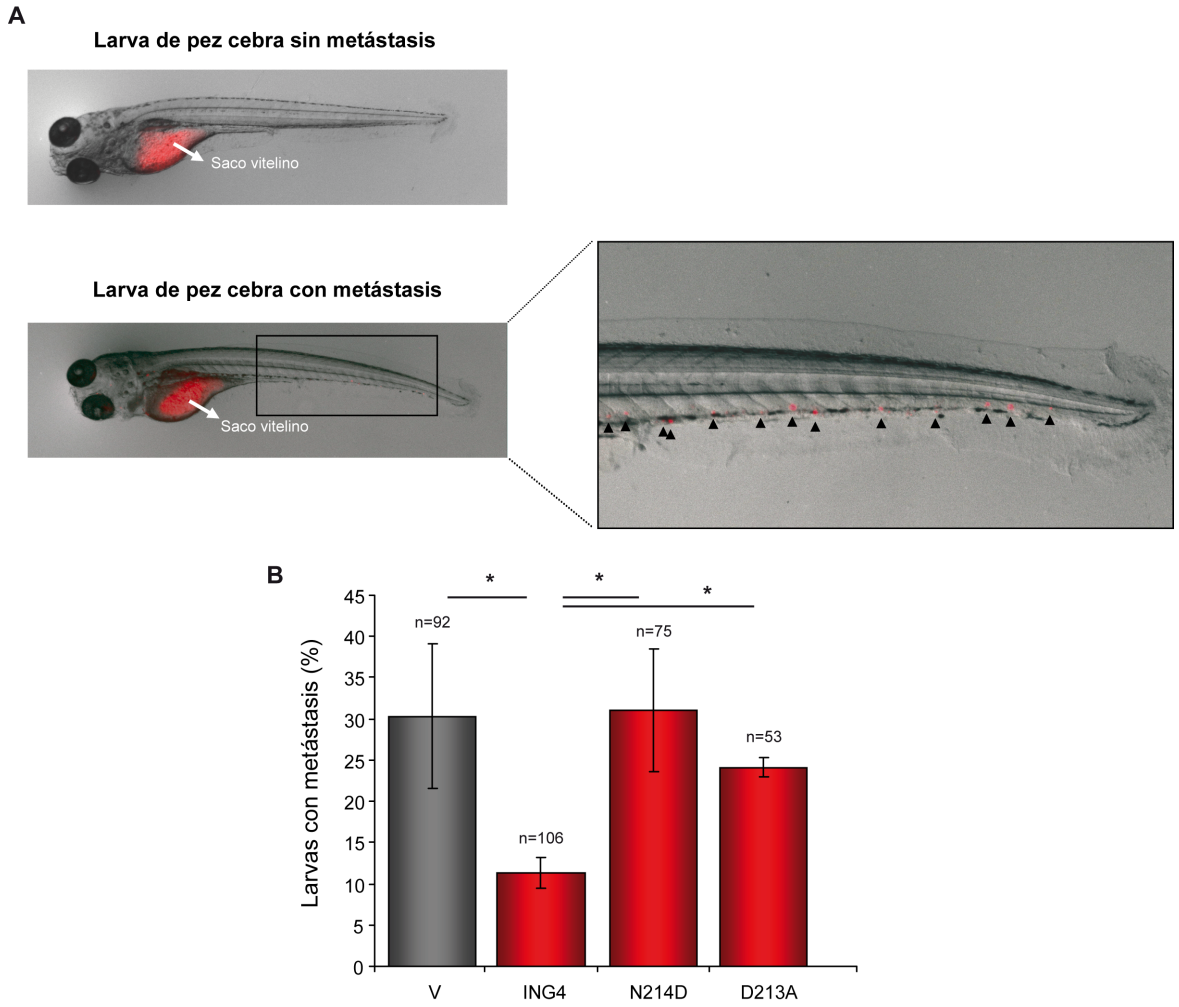

Fig. 26. ING4 reduce el número de metástasis en larvas de pez cebra. A) Imágenes representativas de larvas a 2 días pos-transplante, en el que las células tumorales han invadido el embrión. Las células que no invaden permanecen en el saco vitelino, mientras que las que lo hacen se marcan con flechas. **B)** Representación del porcentaje de larvas con metástasis para cada una de las construcciones utilizadas. Se representa la media y desviación estándar de tres experimentos (*P<0,05), además del número de embriones utilizados en cada caso.

En este trabajo se ha analizado la función de ING4 utilizando distintos sistemas de humano y de ratón. Nuestros datos resaltan la importancia de ING4 en la prevención de tumorogénesis gracias al estudio de mutantes puntuales de la proteína, y muestran un papel importante de acción en el microentorno tumoral mediante la regulación de factores solubles.

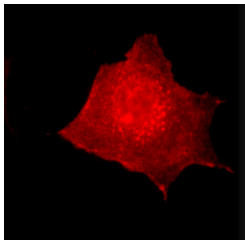

Discusión

Las proteínas de la familia ING ejercen un papel importante como mediadores en los mecanismos de supresión tumoral. Existen numerosas evidencias que las conectan con las vías de p53 y NFκB, y con regulación transcripcional a través del reconocimiento de marcas de histonas y del reclutamiento de complejos modificadores de cromatina. Apoyando el papel de esta familia en la protección frente a tumores, se han descrito distintos tipos de alteraciones para estas proteínas en tumores humanos (Coles and Jones, 2009).

En este trabajo hemos llevado a cabo la caracterización funcional de ING4 mediante el uso de ensayos de ganancia de función *in vitro* e *in vivo.* ING4 está relacionada, al igual que el resto de las proteínas ING, con el control de la proliferación celular, apoptosis y en la regulación de cromatina en conexión con p53 y NFκB. Además, ING4 está relacionada específicamente con una serie de funciones implicadas en progresión tumoral como son la migración, la angiogénesis y la invasión (Garkavtsev et al., 2004; Li and Li, 2010; Shen et al., 2007). El análisis de ING4 en tumores humanos ha identificado distintas alteraciones, entre las que se incluyen expresión reducida de la proteína (Garkavtsev et al., 2004; Gunduz et al., 2005; Li et al., 2008), cambios de localización (Wang et al., 2010) y mutaciones puntuales (Kim et al., 2004). En la mayoría de los casos, los mecanismos que subyacen a estos cambios son aún desconocidos, pero se ha descrito que están asociados con mayor malignidad, en varios estudios. Estos datos sugieren que alteraciones de la proteína ING4 suponen un papel importante en mecanismos de progresión tumoral.

En la primera parte de este estudio hemos analizado el impacto funcional de mutaciones de ING4 identificadas en líneas tumorales de adenocarcinoma de pulmón humano. Mediante la utilización de diferentes técnicas hemos llevado a cabo el análisis funcional de las proteínas mutantes ING4^{Y121N} e ING4^{N214D}, cuyas alteraciones están localizadas en regiones importantes para la función de la proteína. En base a nuestros resultados, concluimos que la mutación Y121N de ING4 no tiene un efecto significativo sobre la funcionalidad de la proteína, mientras que la mutación N214D provoca una disminución en su actividad a distintos niveles como sensibilización a muerte celular, inhibición de la proliferación, migración o crecimiento independiente de anclaje. La mutación N214D está localizada en el dominio PHD, implicado en el reconocimiento de marcas de histonas (H3K4me3). En nuestro estudio analizamos el plegamiento de la proteína mutante ING4^{N214D} y su capacidad de reconocimiento de la marca de histonas mediante ensayos estructurales. Los resultados mostraron que la mutación no afectaba al plegamiento de la proteína ni a la unión a histonas, como ocurre en el caso de otros

miembros de la familia como ING1, en el que mutaciones localizadas en el dominio PHD y asociadas a tumores sí presentan alterados estos parámetros (Pena et al., 2008). A pesar de que no se dan cambios a estos niveles en el mutante N214D, no hemos estudiado si existen variaciones en la capacidad de asociación a complejos acetilasa/deacetilasa o a factores de transcripción que estén implicados en cambios en la regulación génica. La alteración más clara observada para esta forma mutante de ING4 fue el cambio en la estabilidad de la proteína, observándose que la vida media de la proteína era sensiblemente menor a la de ING4 salvaje. Estudios realizados por otros grupos, habían indicado que la degradación de ING4 está mediada por la vía del proteasoma y se había sugerido que esto ocurre mediante su acumulación en el nucleolo y su asociación con la proteína nucleolar ARF (Tsai et al., 2008). En este trabajo, hemos confirmado la participación del proteasoma, comprobando que la degradación tanto de ING4 como del mutante N214D se revierte utilizando inhibidores del proteasoma. En cambio, no hemos observado conexiones con el nucleolo ni colocalización con ARF, ya que el mutante mostró un patrón de localización igual a la proteína salvaje, mayoritariamente nuclear. El mecanismo que explica la menor vida media del mutante N214D se desconoce por el momento. Otras proteínas de la familia ING, también han sido relacionadas con la vía del proteasoma, pero las regiones de ubiquitinación y los mecanismos de degradación difieren. Se ha sugerido que la ubiquitinización de ING4 ocurre en el extremo N terminal, al igual que en ING3 (Chen et al., 2009), mientras que la ubiquitinación de ING1 e ING2 ocurre en el dominio PHD (Nie et al., 2010) . En el caso del mutante N214D de ING4, el efecto en degradación no parece deberse a una interferencia directa con ubiquitinación o citrulinación, ya que las regiones implicadas en estos procesos en el caso de ING4 están localizadas en los primeros 180 aminoácidos de la proteína y en el dominio de localización nuclear respectivamente (Guo and Fast, 2011; Tsai et al., 2008). Pero además de las zonas de ubiquitinación, existen otros residuos que también están implicados en la estabilidad de la proteína y que están alterados en tumores. Por ejemplo, en ING1b la fosforilación de la serina 126 controla la vida media de la proteína (Garate et al., 2007). Esto es interesante ya que este residuo está mutado en algunos tumores (Campos et al., 2004b), en una situación similar a $ING4^{N214D}$. Igualmente, defectos en la estabilidad de ING3 identificados en tumores humanos (Chen et al., 2009), indican que la estabilidad reducida puede ser un mecanismo general de función defectiva de las proteínas ING en tumores. A pesar de esto, no podemos descartar que existan otros efectos funcionales en el mutante N214D que contribuyan a la pérdida de función, además de la deficiencia en la estabilidad de la proteína.

La mutación N214D de ING4 se identificó en una línea celular derivada de adenocarcinoma de pulmón en el que el segundo alelo también estaba inactivado ya que codificaba para una proteína truncada (Kim et al., 2004). Existen distintas variantes de ING4 resultantes del procesamiento alternativo del locus que incluyen proteínas truncadas resultantes de mutaciones de cambio en la pauta de lectura, de función aún desconocida, que se expresan en tejidos normales (Unoki et al., 2006), aunque también han sido identificadas en tumores y en líneas celulares derivadas de ellos (Kim et al., 2004; Li et al., 2009a). La mayoría de estas proteínas truncadas carecen del dominio PHD (Raho et al., 2007), y en estudios recientes realizados en células cancerígenas humanas, se ha caracterizado que una de ellas actúa como dominante negativo de ING4 (Kim et al., 2010). Por tanto, en base a nuestras observaciones y a las de otros grupos, podemos decir que la presencia de distintos tipos de alteraciones hace que las células pierdan la función de ING4. Los ensayos funcionales llevados a cabo en este trabajo caracterizan al mutante N214D como una proteína de pérdida de función, pero que no actúa como dominante negativo ya que no elimina la función de ING4 endógeno. Por lo tanto, existen distintos mecanismos de inactivación de ING4 en tumores humanos, rasgos que han podido ser seleccionados durante la tumorogénesis.

En la segunda parte de este trabajo hemos caracterizado la implicación de ING4 en mecanismos de supresión tumoral en células primarias. Para ello se han utilizado fibroblastos embrionarios humanos de pase temprano (IMR90), que no poseen ninguna mutación y que conservan los mecanismos de supresión tumoral intactos. Este se trata de un sistema no utilizado hasta el momento para el estudio de ING4, por lo que nos ha permitido su análisis desde un punto de vista novedoso, utilizando como herramientas mutantes de pérdida de función de ING4.

En estos estudios, incluimos el mutante D213A, además del mutante N214D usado previamente, como herramienta para estudiar el papel del reconocimiento de marcas de histonas en la función de ING4 en células humanas primarias. Mediante diferentes ensayos de proliferación celular observamos, al igual que en las líneas tumorales, que la expresión ectópica de ING4 tiene un efecto inhibitorio de la proliferación en fibroblastos primarios. Esta capacidad se pierde en las proteínas mutantes ING4^{D213A} e ING4^{N214D}, lo que indica que la regulación de proliferación celular por ING4 requiere del reconocimiento de marcas de histonas, ligando su capacidad como supresor tumoral con mecanismos de regulación epigenética. Este efecto también se pierde en el mutante asociado a tumores humanos.

Otros miembros de la familia ING participan en la regulación de senescencia celular (Abad et al., 2011; Pedeux et al., 2005). Por ello, quisimos estudiar si el efecto

anti-proliferativo de ING4 estaba asociado a senescencia, ya que hasta el momento no existían datos previos que relacionaran a ING4 con esta respuesta. Nuestros datos muestran que la expresión ectópica de ING4 en fibroblastos primarios humanos no está acompañada de la inducción de senescencia ya que no se observan cambios ni para la proteína salvaje ni para los mutantes en marcadores característicos de esta respuesta como morfología, actividad enzimática SA-β-Gal, o formación de SAHFs.

Quisimos estudiar si la inhibición de la proliferación celular provocada por ING4 podría estar relacionada con la activación de la respuesta a daño en ADN. Comprobamos que la expresión ectópica de ING4 induce un ligero aumento del número de células con focos de γ-H2AX, mientras que esto no ocurre en el caso de los mutantes, lo que apoya una conexión con el reconocimiento de marcas de histonas. En cualquier caso, el daño es menor al producido por RasV12. Además, observamos un patrón de tinción con ING4 diferente al provocado por la expresión del oncogén. Se ha descrito que la respuesta antiproliferativa asociada a senescencia inducida por oncogenes está mediada en parte por daño en ADN, provocado por replicación aberrante (Di Micco et al., 2006). En cambio, nunca hemos observado hiperproliferación en el caso de ING4. Igualmente, ING4 ha sido conectada con respuesta a hipoxia (Colla et al., 2007; Ozer et al., 2005), pero no existen evidencias de que aumente los niveles de especies reactivas de oxígeno (ROS), agente genotóxico que provoca la respuesta DDR. Aunque nuestros datos son preliminares y requieren de una mayor profundización en el mecanismo, la acción antiproliferativa de ING4 en conexión con remodelación de cromatina podría estar relacionada con la respuesta DDR.

En trabajos anteriores, se ha descrito la interacción y conexión funcional de ING4 con p53 (Guo and Fast, 2011; Shiseki et al., 2003; Zhang et al., 2005) en otros contextos. Durante el transcurso de este trabajo hemos estudiado la conexión del efecto anti-proliferativo de ING4 en células primarias con dos de las principales vías de supresión tumoral en mamíferos: p53 y Rb. Nuestros resultados indican que los efectos de ING4 en proliferación celular en fibroblastos IMR90 son dependientes de p53, pero independientes de Rb. Datos previos de otros grupos han conectado ING4 con el inhibidor de ciclo p21CIP1, a través de p53 (Zhang et al., 2004). En nuestros experimentos no hemos observado cambios consistentes en los niveles de p21 cuando expresábamos ING4 ectópicamente, aunque sí detectamos en algunos casos un aumento de p27, otro inhibidor de ciclo de la familia Cip/Kip (datos no mostrados).

Con los datos funcionales obtenidos en células primarias, quisimos conocer qué genes estaban mediando estos efectos. La caracterización de perfiles de expresión, nos permitió identificar la firma genética asociada a la parada proliferativa mediada por ING4

en fibroblastos IMR90. Identificamos 87 genes con expresión diferencial en fibroblastos que expresaban ING4 de forma ectópica comparados con fibroblastos control. La mayoría de estos (93%), tenían su expresión aumentada con ING4. Este dato apoya las evidencias de que ING4 forma parte de complejos HAT relacionados con activación transcripcional, mientras que otras proteínas de la familia como ING1b e ING2, están asociadas preferentemente a represión transcripcional vía HDACs (Champagne and Kutateladze, 2009; Doyon et al., 2006). Este es el primer estudio donde se analiza la firma genética asociada a ING4. Hasta el momento, únicamente se ha publicado un análisis mediante inmunoprecipitación de cromatina (ChIP) con ING4 en células tumorales en presencia de daño en ADN (Hung et al., 2009). La comparación de los promotores obtenidos mediante ChIP en dicho estudio con los genes de nuestro array de expresión no muestra coincidencias, aunque esto se puede explicar por tratarse de ensayos diferentes, realizados en otras condiciones y en otro modelo celular.

El análisis con el mutante N214D, mostró que aproximadamente un 60% de los genes regulados por ING4 salvaje no mostraban la misma regulación con el mutante, apoyando la especificidad de la firma genética de ING4. El análisis funcional de los genes regulados por ING4 mostró un enriquecimiento en categorías como adhesión, migración, proliferación celular y en factores solubles de tipo citoquina y quimioquina y genes implicados en respuesta inflamatoria en conexión con la vía de NFκB.

La vía de NFκB está conectada con proliferación, supervivencia y activación de la respuesta inflamatoria e inmune mediante la regulación de factores solubles (Ben-Neriah and Karin, 2011). Nuestro estudio muestra que la expresión de ING4 en células primarias provoca cambios de expresión en dos grupos de genes relacionados con la vía de NFκB. Por una parte, hemos observado cambios en varios reguladores de la vía, como TBK1 y CARD14 (Blonska and Lin, 2011; Shen and Hahn, 2011), aunque no hemos profundizado en esta conexión por el momento. Por otra parte, hemos observado la regulación positiva por ING4 de factores solubles de tipo citoquina y quimioquina, que son genes diana de NFκB, como CXCL1, CXCL2 e IL-8, entre otros.

Hasta el momento, en base a los estudios realizados con sobreexpresión o silenciamiento de ING4 en líneas tumorales y en tumores primarios de glioma y mieloma, se ha sugerido un papel preferente de ING4 como regulador negativo de genes diana de NFκB implicados en inflamación y angiogénesis, como IL-8, IL-6, COX2, o MMP9 (Colla et al., 2007; Garkavtsev et al., 2004; Nozell et al., 2008). Sin embargo, existen datos contradictorios que indican que el efecto de ING4 sobre NFκB es complejo. Resultados con un modelo de ratón deficiente en Ing4, indican que la ausencia de Ing4 se corresponde con hipersensibilidad a lipopolisacárido (LPS), una respuesta mediada por NFκB. Sin embargo, macrófagos deficientes en Ing4, muestran aumentos en los niveles

de algunos genes regulados por NFκB en respuesta a LPS como IL-6, MCP-1 o RANTES, pero también reducción de otros, como TNF-α o IκB, lo que sugiere un papel diferencial de ING4 sobre genes diana de NFκB en este sistema (Coles et al., 2010). Igualmente, no está claro cual sería el mecanismo por el que actuaría. Se ha propuesto que ING4 puede impedir la unión de p65 a cromatina (Garkavtsev et al., 2004), favorecer el reclutamiento de complejos represores HDAC a genes diana (Nozell et al., 2008), o inhibir la acumulación nuclear de NFκB (Coles et al., 2010), pero los datos obtenidos hasta el momento también son contradictorios. Nuestros resultados podrían explicarse por diferencias en el tipo celular usado o por un papel diferente de ING4 en células primarias frente a células inmortalizadas o tumorales. De este modo, en otros trabajos realizados en el mismo sistema de células primarias IMR90 usado en este trabajo, se ha observado que la activación de la vía de NFκB, por ejemplo durante senescencia inducida por oncogenes, está asociada a un efecto antiproliferativo mediado por la regulación de factores solubles (Acosta et al., 2008a; Chien et al., 2011), muchos de los cuales coinciden con los regulados por ING4 en nuestro trabajo. Globalmente, estos datos apoyan la idea de que en un sistema de células primarias, la expresión de ING4 tiene un efecto antiproliferativo, a través de la activación de factores solubles, mediada por la vía de NFκB.

Nuestros resultados apoyan un papel de ING4 en la regulación de factores solubles de tipo citoquina y quimioquina en fibroblastos primarios. Las citoquinas y quimioquinas son moléculas de señalización que además de jugar un papel importante en inflamación y respuesta inmune, también están relacionados con tumorogénesis (Lazennec and Richmond, 2010; Mantovani et al., 2009; Schetter et al., 2010). Se han descrito efectos diversos de estos factores en el contexto de cáncer. La producción y secreción de citoquinas y quimioquinas está asociada a tumorogénesis, favoreciendo el crecimiento tumoral, invasión, inflamación y cambios en el microentorno tumoral (Lazennec and Richmond, 2010; Mantovani et al., 2009), pero también se han asociado con mecanismos opuestos, como la inducción de senescencia celular y regresión tumoral.

Los CAFs, fibroblastos asociados a carcinoma, presentes en el microentorno tumoral presentan un perfil genético especifico que incluye la producción de citoquinas, quimioquinas y componentes de la matriz extracelular que pueden provocar crecimiento tumoral, angiogénesis y metástasis (Grivennikov et al., 2010; Ostman and Augsten, 2009). Los CAFs son diferentes biológicamente a aquellos fibroblastos que se encuentran en tejido normal, ya que potencian el crecimiento tumoral y la

vascularización, mientras que los fibroblastos normales no tienen efecto sobre el crecimiento tumoral (Orimo and Weinberg, 2006).

Curiosamente, la producción de citoquinas y quimioquinas también se ha relacionado con senescencia, un mecanismo de protección antitumoral, formando parte del fenotipo secretor asociado a senescencia (SASP) (Acosta and Gil, 2009; Acosta et al., 2008b; Coppe et al., 2008; Chien et al., 2011; Kuilman and Peeper, 2009; Rodier et al., 2009). Los perfiles de factores solubles asociados a CAFs y a senescencia son similares, pero no del todo coincidentes. Los factores solubles producidos por los CAFs son preferentemente ligandos de CXCR4 (Bieche et al., 2007; Gallagher et al., 2005), mientras que en el SASP son más abundantes los ligandos de CXCR2 (Acosta et al., 2008a). Además en el SASP se regulan tanto factores solubles como receptores, mientras que en el caso de los CAFs lo hacen preferentemente factores solubles. Igualmente, se ha demostrado que el SASP puede tener efectos antagónicos, por un lado promueve senescencia en células no transformadas, pero también puede inducir proliferación de células epiteliales malignas *in vitro* e *in vivo* (Krtolica et al., 2001; Kuilman and Peeper, 2009).

Nuestros resultados con el array de expresión y el array de quimioquinas, indican que la expresión de ING4 en fibroblastos primarios regula la expresión y secreción de factores como CXCL1, CXCL2, CXCL5, CXCL6, IL-8 o CXCL12. El perfil asociado a ING4 solapa parcialmente con los dos fenotipos comentados (SASP y CAFs), pero presenta mayor coincidencia con el de los CAFs (CXCL1, CXCL2, CXCL5, CXCL6, IL-8, CXCL12) (Bieche et al., 2007; Gallagher et al., 2005) que con el del SASP (CXCL1, IL-8, CCL2) (Acosta et al., 2008a; Coppe et al., 2008). Del mismo modo, el perfil global asociado a ING4 no muestra gran similitud al perfil de expresión que se ha asociado a senescencia en nuestro laboratorio y en otros. Al comparar con resultados previos obtenidos en nuestro grupo con el mismo sistema celular y la misma plataforma de microarrays, únicamente un 30% de los genes regulados por ING4 presentan la misma regulación que ING1b o RasV12, dos estímulos de senescencia (Abad et al., 2011; Serrano et al., 1997). Aunque algunas citoquinas como CXCL1 y CXCL2 presentan la misma regulación en ING4 e ING1b, el análisis detallado de categorías funcionales, mostró que ING1b está relacionado tanto con factores solubles como con receptores, mientras que ING4 principalmente regula los propios factores solubles.

Los resultados obtenidos en los ensayos con el medio condicionado mostraron un efecto mitogénico selectivo de ING4, ya que el medio condicionado de células con ING4 provocaba proliferación de células tumorales, mientras que inhibía la proliferación en fibroblastos normales. *In vitro,* este efecto está mediado por la producción de citoquinas y quimioquinas, como lo demuestra la pérdida de efecto al añadir un anticuerpo bloqueante

contra IL-8. Esta quimioquina, entre otras funciones, promueve inflamación e invasividad (Coppe et al., 2008). El bloqueo de su actividad mediante el uso de anticuerpos conlleva una fuerte pérdida de la capacidad proliferativa de las células tumorales. Esto ha sido aplicado recientemente en técnicas de inmunoterapia, en donde se ha comprobado que el bloqueo de la actividad de IL-8 inhibe el crecimiento tumoral, metástasis y angiogénesis (Zigler et al., 2008).

Para extender nuestros resultados de los efectos del medio condicionado sobre células tumorales obtenidos *in vitro,* quisimos estudiar el efecto de ING4 en el crecimiento tumoral *in vivo*. Para ello se inyectaron fibroblastos que expresaban ING4 junto con células tumorales que llevaban un gen reportero de luciferasa (TGL) en los flancos de ratones inmunodeprimidos. Analizamos el crecimiento de tumores mediante bioluminiscencia y volumen a lo largo de cinco semanas. Nuestros resultados mostraron que fibroblastos que expresan ING4 de forma ectópica promueven tumorogénesis *in vivo.*

El fenotipo que hemos observado asociado a ING4 *in vitro* e *in vivo* solapa parcialmente con el de los CAFs y con el de células senescentes. La falta de inducción de senescencia *in vitro* sugiere que el efecto de ING4 sería independiente de senescencia y apoyaría más un papel de ING4 en relación con los CAFs. Aunque la

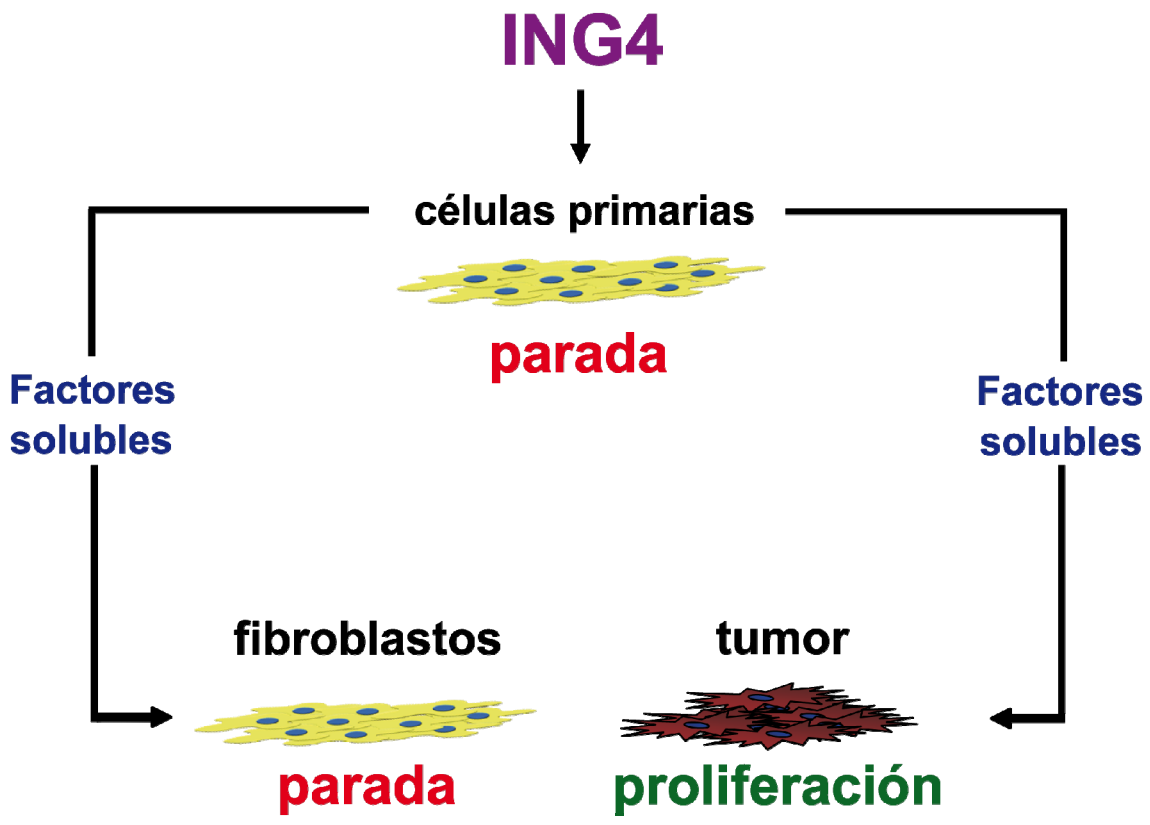

Fig. 27. Mecanismo de acción de ING4 en células primarias.

expresión ectópica de ING4 no es un potente inductor de senescencia por si mismo, no podemos descartar totalmente un papel en senescencia, y cabe la posibilidad de que contribuya de algún modo a esta respuesta. Hemos intentado abordar esta cuestión mediante la utilización de ARNs de interferencia para ING4 en las células primarias, pero hasta el momento no hemos conseguido un silenciamiento efectivo de ING4.

En cualquier caso, nuestros resultados indican que ING4 regula en fibroblastos primarios un fenotipo secretor con efectos diferenciales en proliferación de células tumorales o no-tumorales, que según el contexto puede estar asociado a uno u otro proceso. Nuestros datos sugieren que el nivel de expresión de ING4 en células del microentorno de un tumor podría ser relevante para su crecimiento y progresión. Para poner a prueba esta hipótesis en el contexto tumoral, tenemos previsto extender nuestros experimentos mediante análisis de muestras de carcinomas, analizando los niveles de ING4 endógeno tanto en las células tumorales como en las células del microentorno. Asimismo, el análisis histológico de los tumores inducidos en los ensayos de tumorogénesis nos proporcionará información acerca del nivel de vascularización y malignidad de los tumores.

En un estudio complementario, hemos investigado también el papel de ING4 en migración y metástasis en un modelo animal. Nuestros resultados y los de otros grupos indican que ING4 tiene capacidad de inhibir migración e invasión *in vitro* (Li and Li, 2010; Li et al., 2008; Shen et al., 2007). Recientemente se ha demostrado también que reduce metástasis en un modelo animal de cáncer de mama (Kim et al., 2010), pero hasta la fecha no se ha analizado directamente su papel en las distintas etapas de diseminación tumoral, como la capacidad de invasión local, circular por la sangre y colonizar otros órganos (Valastyan and Weinberg, 2011). Para abordar el papel de ING4 en metástasis *in vivo* y correlacionarlo con funciones de ING4, hemos llevado a cabo un ensayo de metástasis en pez cebra. En este modelo, la transparencia de las larvas permite un seguimiento preciso de las células tumorales marcadas con fluorescencia (Marques et al., 2009). Nuestros resultados mostraron que la expresión ectópica de ING4 en células tumorales tiene un efecto inhibitorio de migración y metástasis en este sistema, que se pierde con los mutantes de unión a cromatina y asociado a tumores. Estos resultados indican que, de forma similar a otras funciones esenciales de ING4, su papel en metástasis requiere su capacidad de regular expresión génica y se pierde en mutantes asociados a tumores. Actualmente estamos extendiendo estos estudios, con ensayos de metástasis en ratón, mediante inyección en la vena caudal en ratones inmunodeprimidos, de manera que podamos determinar el efecto de ING4 en metástasis en distintos modelos animales.

En resumen, el trabajo realizado en esta tesis aporta nuevos datos acerca del papel de ING4 en supresión tumoral, los efectos de mutaciones de ING4 en tumores humanos y la importancia funcional del reconocimiento de marcas de histonas. Mediante el uso de modelos de ganancia de función en distintos modelos celulares, primarios y tumorales, hemos demostrado que ING4 regula proliferación celular, migración y metástasis. Además, hemos demostrado que los efectos en proliferación no están relacionados con un fenotipo senescente y que son dependientes de p53 e independientes de Rb. A través del estudio de la firma genética asociada a ING4 y ensayos *in vitro* e *in vivo,* hemos demostrado un efecto diferencial de ING4 en proliferación, mediado por factores solubles: inhibiendo la proliferación en células primarias y favoreciéndola en células tumorales. Nuestros resultados indican que ING4 juega un importante papel en la liberación de factores solubles de tipo citoquina y quimioquina que podría influir en el crecimiento y la progresión tumoral, a través de la conexión del tumor con su entorno.

Conclusiones

1. El mutante N214D de ING4, asociado a tumores, presenta una menor estabilidad de la proteína, que se traduce en funcionalidad deficiente, indicando que la pérdida de función de ING4 puede contribuir a la formación de tumores.

2. La expresión de ING4 en células primarias provoca inhibición de la proliferación celular que requiere del reconocimiento de marcas de histonas. Este efecto es dependiente de p53 e independiente de Rb.

3. El efecto antiproliferativo de ING4 en fibroblastos primarios está acompañado de un aumento en daño en ADN, pero no está asociado a senescencia celular.

4. La firma genética asociada a la sobreexpresión de ING4 en fibroblastos primarios muestra una elevada representación de factores solubles de tipo citoquina y quimioquina y de genes de la vía de NFκB.

5. El medio condicionado de células primarias que sobreexpresan ING4 tiene un efecto diferencial en proliferación celular, favoreciendo la proliferación de células tumorales e inhibiendo el crecimiento de fibroblastos primarios.

6. Los fibroblastos con expresión ectópica de ING4 promueven tumorogénesis *in vivo*, apoyando un papel de ING4 en la conexión del tumor con su microentorno.

7. La expresión de ING4 en células tumorales tiene un efecto inhibitorio de la migración y metástasis en pez cebra. Este efecto se pierde en mutantes de ING4.

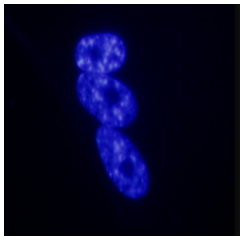

Bibliografía

Abad, M., Moreno, A., Palacios, A., Narita, M., Blanco, F., Moreno-Bueno, G., and Palmero, I. (2011). The tumor suppressor ING1 contributes to epigenetic control of cellular senescence. Aging Cell *10*, 158-171.

Acosta, J.C., and Gil, J. (2009). A role for CXCR2 in senescence, but what about in cancer? Cancer Res *69*, 2167-2170.

Acosta, J.C., O'Loghlen, A., Banito, A., Guijarro, M.V., Augert, A., Raguz, S., Fumagalli, M., Da Costa, M., Brown, C., Popov, N.*, et al.* (2008a). Chemokine signaling via the CXCR2 receptor reinforces senescence. Cell *133*, 1006-1018.

Acosta, J.C., O'Loghlen, A., Banito, A., Raguz, S., and Gil, J. (2008b). Control of senescence by CXCR2 and its ligands. Cell Cycle *7*, 2956-2959.

Aguissa-Toure, A.H., Wong, R.P., and Li, G. (2011). The ING family tumor suppressors: from structure to function. Cell Mol Life Sci *68*, 45-54.

Baker, L.A., Allis, C.D., and Wang, G.G. (2008). PHD fingers in human diseases: Disorders arising from misinterpreting epigenetic marks. Mutat Res *647*, 3-12.

Bartkova, J., Horejsi, Z., Koed, K., Kramer, A., Tort, F., Zieger, K., Guldberg, P., Sehested, M., Nesland, J.M., Lukas, C.*, et al.* (2005). DNA damage response as a candidate anti-cancer barrier in early human tumorigenesis. Nature *434*, 864-870.

Bates, S., Ryan, K.M., Phillips, A.C., and Vousden, K.H. (1998). Cell cycle arrest and DNA endoreduplication following p21Waf1/Cip1 expression. Oncogene *17*, 1691-1703.

Ben-Neriah, Y., and Karin, M. (2011). Inflammation meets cancer, with NF-kappaB as the matchmaker. Nat Immunol *12*, 715-723.

Berdasco, M., and Esteller, M. (2010). Aberrant epigenetic landscape in cancer: how cellular identity goes awry. Dev Cell *19*, 698-711.

Bieche, I., Chavey, C., Andrieu, C., Busson, M., Vacher, S., Le Corre, L., Guinebretiere, J.M., Burlinchon, S., Lidereau, R., and Lazennec, G. (2007). CXC chemokines located in the 4q21 region are up-regulated in breast cancer. Endocr Relat Cancer *14*, 1039-1052.

Blonska, M., and Lin, X. (2011). NF-kappaB signaling pathways regulated by CARMA family of scaffold proteins. Cell Res *21*, 55-70.

Cai, L., Li, X., Zheng, S., Wang, Y., Li, H., Yang, J., and Sun, J. (2009). Inhibitor of growth 4 is involved in melanomagenesis and induces growth suppression and apoptosis in melanoma cell line M14. Melanoma Res *19*, 1-7.

Campos, E.I., Chin, M.Y., Kuo, W.H., and Li, G. (2004a). Biological functions of the ING family tumor suppressors. Cell Mol Life Sci *61*, 2597-2613.

Campos, E.I., Martinka, M., Mitchell, D.L., Dai, D.L., and Li, G. (2004b). Mutations of the ING1 tumor suppressor gene detected in human melanoma abrogate nucleotide excision repair. Int J Oncol *25*, 73-80.

Carmeliet, P., and Jain, R.K. (2000). Angiogenesis in cancer and other diseases. Nature *407*, 249-257.

Coles, A.H., Gannon, H., Cerny, A., Kurt-Jones, E., and Jones, S.N. (2010). Inhibitor of growth-4 promotes IkappaB promoter activation to suppress NF-kappaB signaling and innate immunity. Proc Natl Acad Sci U S A *107*, 11423-11428.

Coles, A.H., and Jones, S.N. (2009). The ING gene family in the regulation of cell growth and tumorigenesis. J Cell Physiol *218*, 45-57.

Colla, S., Tagliaferri, S., Morandi, F., Lunghi, P., Donofrio, G., Martorana, D., Mancini, C., Lazzaretti, M., Mazzera, L., Ravanetti, L*., et al.* (2007). The new tumor-suppressor gene inhibitor of growth family member 4 (ING4) regulates the production of proangiogenic molecules by myeloma cells and suppresses hypoxia-inducible factor-1 alpha (HIF-1alpha) activity: involvement in myeloma-induced angiogenesis. Blood *110*, 4464-4475.

Collado, M., and Serrano, M. (2006). The power and the promise of oncogene-induced senescence markers. Nat Rev Cancer *6*, 472-476.

Coppe, J.P., Patil, C.K., Rodier, F., Sun, Y., Munoz, D.P., Goldstein, J., Nelson, P.S., Desprez, P.Y., and Campisi, J. (2008). Senescence-associated secretory phenotypes reveal cell-nonautonomous functions of oncogenic RAS and the p53 tumor suppressor. PLoS Biol *6*, 2853-2868.

Champagne, K.S., and Kutateladze, T.G. (2009). Structural insight into histone recognition by the ING PHD fingers. Curr Drug Targets *10*, 432-441.

Chen, G., Wang, Y., Garate, M., Zhou, J., and Li, G. (2009). The tumor suppressor ING3 is degraded by SCF(Skp2)-mediated ubiquitin-proteasome system. Oncogene *29*, 1498-1508.

Chicas, A., Wang, X., Zhang, C., McCurrach, M., Zhao, Z., Mert, O., Dickins, R.A., Narita, M., Zhang, M., and Lowe, S.W. (2010). Dissecting the unique role of the retinoblastoma tumor suppressor during cellular senescence. Cancer Cell *17*, 376-387.

Chien, Y., Scuoppo, C., Wang, X., Fang, X., Balgley, B., Bolden, J.E., Premsrirut, P., Luo, W., Chicas, A., Lee, C.S*., et al.* (2011). Control of the senescence-associated secretory phenotype by NF-{kappa}B promotes senescence and enhances chemosensitivity. Genes Dev *25*, 2125-2136.

Dejana, E., Orsenigo, F., Molendini, C., Baluk, P., and McDonald, D.M. (2009). Organization and signaling of endothelial cell-to-cell junctions in various regions of the blood and lymphatic vascular trees. Cell Tissue Res *335*, 17-25.

Di Micco, R., Fumagalli, M., Cicalese, A., Piccinin, S., Gasparini, P., Luise, C., Schurra, C., Garre, M., Nuciforo, P.G., Bensimon, A*., et al.* (2006). Oncogene-induced senescence is a DNA damage response triggered by DNA hyper-replication. Nature *444*, 638-642.

Dimri, G.P., Lee, X., Basile, G., Acosta, M., Scott, G., Roskelley, C., Medrano, E.E., Linskens, M., Rubelj, I., Pereira-Smith, O*., et al.* (1995). A biomarker that identifies senescent human cells in culture and in aging skin in vivo. Proc Natl Acad Sci U S A *92*, 9363-9367.

Doyon, Y., Cayrou, C., Ullah, M., Landry, A.J., Cote, V., Selleck, W., Lane, W.S., Tan, S., Yang, X.J., and Cote, J. (2006). ING tumor suppressor proteins are critical regulators of chromatin acetylation required for genome expression and perpetuation. Mol Cell *21*, 51-64.

Egeblad, M., Nakasone, E.S., and Werb, Z. (2010). Tumors as organs: complex tissues that interface with the entire organism. Dev Cell *18*, 884-901.

Gaengel, K., Genove, G., Armulik, A., and Betsholtz, C. (2009). Endothelial-mural cell signaling in vascular development and angiogenesis. Arterioscler Thromb Vasc Biol *29*, 630-638.

Gallagher, P.G., Bao, Y., Prorock, A., Zigrino, P., Nischt, R., Politi, V., Mauch, C., Dragulev, B., and Fox, J.W. (2005). Gene expression profiling reveals cross-talk between melanoma and fibroblasts: implications for host-tumor interactions in metastasis. Cancer Res *65*, 4134-4146.

Garate, M., Campos, E.I., Bush, J.A., Xiao, H., and Li, G. (2007). Phosphorylation of the tumor suppressor p33(ING1b) at Ser-126 influences its protein stability and proliferation of melanoma cells. FASEB J *21*, 3705-3716.

Garkavtsev, I., Kazarov, A., Gudkov, A., and Riabowol, K. (1996). Suppression of the novel growth inhibitor p33ING1 promotes neoplastic transformation. Nat Genet *14*, 415-420.

Garkavtsev, I., Kozin, S.V., Chernova, O., Xu, L., Winkler, F., Brown, E., Barnett, G.H., and Jain, R.K. (2004). The candidate tumour suppressor protein ING4 regulates brain tumour growth and angiogenesis. Nature *428*, 328-332.

Goeman, F., Thormeyer, D., Abad, M., Serrano, M., Schmidt, O., Palmero, I., and Baniahmad, A. (2005). Growth inhibition by the tumor suppressor p33ING1 in immortalized and primary cells: involvement of two silencing domains and effect of Ras. Mol Cell Biol *25*, 422-431.

Gomez-Cabello, D., Callejas, S., Benguria, A., Moreno, A., Alonso, J., and Palmero, I. (2010). Regulation of the microRNA processor DGCR8 by the tumor suppressor ING1. Cancer Res *70*, 1866-1874.

Gong, W., Suzuki, K., Russell, M., and Riabowol, K. (2005). Function of the ING family of PHD proteins in cancer. Int J Biochem Cell Biol *37*, 1054-1065.

Gonzalez, L., Freije, J.M., Cal, S., Lopez-Otin, C., Serrano, M., and Palmero, I. (2006). A functional link between the tumour suppressors ARF and p33ING1. Oncogene *25*, 5173-5179.

Grivennikov, S.I., Greten, F.R., and Karin, M. (2010). Immunity, inflammation, and cancer. Cell *140*, 883-899.

Gunduz, M., Nagatsuka, H., Demircan, K., Gunduz, E., Cengiz, B., Ouchida, M., Tsujigiwa, H., Yamachika, E., Fukushima, K., Beder, L*., et al.* (2005). Frequent deletion and down-regulation of ING4, a candidate tumor suppressor gene at 12p13, in head and neck squamous cell carcinomas. Gene *356*, 109-117.

Guo, Q., and Fast, W. (2011). Citrullination of inhibitor of growth 4 (ING4) by peptidylarginine deminase 4 (PAD4) disrupts the interaction between ING4 and p53. J Biol Chem *286*, 17069-17078.

Han, X., Feng, X., Rattner, J.B., Smith, H., Bose, P., Suzuki, K., Soliman, M.A., Scott, M.S., Burke, B.E., and Riabowol, K. (2008). Tethering by lamin A stabilizes and targets the ING1 tumour suppressor. Nat Cell Biol *10*, 1333-1340.

Hanahan, D., and Weinberg, R.A. (2000). The hallmarks of cancer. Cell *100*, 57-70.

Hanahan, D., and Weinberg, R.A. (2011). Hallmarks of cancer: the next generation. Cell *144*, 646-674.

Haviv, I., Polyak, K., Qiu, W., Hu, M., and Campbell, I. (2009). Origin of carcinoma associated fibroblasts. Cell Cycle *8*, 589-595.

Hayden, M.S., and Ghosh, S. (2008). Shared principles in NF-kappaB signaling. Cell *132*, 344-362.

He, G.H., Helbing, C.C., Wagner, M.J., Sensen, C.W., and Riabowol, K. (2005). Phylogenetic analysis of the ING family of PHD finger proteins. Mol Biol Evol *22*, 104-116.

Hemann, M.T., and Narita, M. (2007). Oncogenes and senescence: breaking down in the fast lane. Genes Dev *21*, 1-5.

Hung, T., Binda, O., Champagne, K.S., Kuo, A.J., Johnson, K., Chang, H.Y., Simon, M.D., Kutateladze, T.G., and Gozani, O. (2009). ING4 mediates crosstalk between histone H3 K4 trimethylation and H3 acetylation to attenuate cellular transformation. Mol Cell *33*, 248-256.

Joyce, J.A., and Pollard, J.W. (2009). Microenvironmental regulation of metastasis. Nat Rev Cancer *9*, 239-252.

Kalluri, R., and Zeisberg, M. (2006). Fibroblasts in cancer. Nat Rev Cancer *6*, 392-401.

Karin, M., Cao, Y., Greten, F.R., and Li, Z.W. (2002). NF-kappaB in cancer: from innocent bystander to major culprit. Nat Rev Cancer *2*, 301-310.

Kerbel, R., and Folkman, J. (2002). Clinical translation of angiogenesis inhibitors. Nat Rev Cancer *2*, 727-739.

Kim, S., Chin, K., Gray, J.W., and Bishop, J.M. (2004). A screen for genes that suppress loss of contact inhibition: identification of ING4 as a candidate tumor suppressor gene in human cancer. Proc Natl Acad Sci U S A *101*, 16251-16256.

Kim, S., Welm, A.L., and Bishop, J.M. (2010). A dominant mutant allele of the ING4 tumor suppressor found in human cancer cells exacerbates MYC-initiated mouse mammary tumorigenesis. Cancer Res *70*, 5155-5162.

Krtolica, A., Parrinello, S., Lockett, S., Desprez, P.Y., and Campisi, J. (2001). Senescent fibroblasts promote epithelial cell growth and tumorigenesis: a link between cancer and aging. Proc Natl Acad Sci U S A *98*, 12072-12077.

Kuilman, T., and Peeper, D.S. (2009). Senescence-messaging secretome: SMS-ing cellular stress. Nat Rev Cancer.

Kumamoto, K., Spillare, E.A., Fujita, K., Horikawa, I., Yamashita, T., Appella, E., Nagashima, M., Takenoshita, S., Yokota, J., and Harris, C.C. (2008). Nutlin-3a activates p53 to both down-regulate inhibitor of growth 2 and up-regulate mir-34a, mir-34b, and mir-34c expression, and induce senescence. Cancer Res *68*, 3193-3203.

Lazennec, G., and Richmond, A. (2010). Chemokines and chemokine receptors: new insights into cancer-related inflammation. Trends Mol Med *16*, 133-144.

Li, H., Ilin, S., Wang, W., Duncan, E.M., Wysocka, J., Allis, C.D., and Patel, D.J. (2006). Molecular basis for site-specific read-out of histone H3K4me3 by the BPTF PHD finger of NURF. Nature *442*, 91-95.

Li, J., and Li, G. (2010). Cell Cycle Regulator ING4 Is a Suppressor of Melanoma Angiogenesis That Is Regulated by the Metastasis Suppressor BRMS1. Cancer Res *70*, 10445-10453.

Li, J., Martinka, M., and Li, G. (2008). Role of ING4 in human melanoma cell migration, invasion, and patient survival. Carcinogenesis *29*, 1373-1379.

Li, M., Jin, Y., Sun, W.J., Yu, Y., Bai, J., Tong, D.D., Qi, J.P., Du, J.R., Geng, J.S., Huang, Q.*, et al.* (2009a). Reduced expression and novel splice variants of ING4 in human gastric adenocarcinoma. J Pathol *219*, 87-95.

Li, X., Zhang, Q., Cai, L., Wang, Y., Wang, Q., Huang, X., Fu, S., Bai, J., Liu, J., Zhang, G.*, et al.* (2009b). Inhibitor of growth 4 induces apoptosis in human lung adenocarcinoma cell line A549 via Bcl-2 family proteins and mitochondria apoptosis pathway. J Cancer Res Clin Oncol *135*, 829-835.

Li, Z., Xie, Y., Sheng, W., Miao, J., Xiang, J., and Yang, J. (2010). Tumor-suppressive effect of adenovirus-mediated inhibitor of growth 4 gene transfer in breast carcinoma cells in vitro and in vivo. Cancer Biother Radiopharm *25*, 427-437.

Liu, E., Wu, J., Cao, W., Zhang, J., Liu, W., Jiang, X., and Zhang, X. (2007). Curcumin induces G2/M cell cycle arrest in a p53-dependent manner and upregulates ING4 expression in human glioma. J Neurooncol *85*, 263-270.

Loewith, R., Meijer, M., Lees-Miller, S.P., Riabowol, K., and Young, D. (2000). Three yeast proteins related to the human candidate tumor suppressor p33(ING1) are associated with histone acetyltransferase activities. Mol Cell Biol *20*, 3807-3816.

Lowe, S.W., Cepero, E., and Evan, G. (2004). Intrinsic tumour suppression. Nature *432*, 307-315.

Mantovani, A., Allavena, P., Sica, A., and Balkwill, F. (2008). Cancer-related inflammation. Nature *454*, 436-444.

Mantovani, A., Savino, B., Locati, M., Zammataro, L., Allavena, P., and Bonecchi, R. (2009). The chemokine system in cancer biology and therapy. Cytokine Growth Factor Rev *21*, 27-39.

Marques, I.J., Weiss, F.U., Vlecken, D.H., Nitsche, C., Bakkers, J., Lagendijk, A.K., Partecke, L.I., Heidecke, C.D., Lerch, M.M., and Bagowski, C.P. (2009). Metastatic behaviour of primary human tumours in a zebrafish xenotransplantation model. BMC Cancer *9*, 128.

Matthews, A.G., Kuo, A.J., Ramon-Maiques, S., Han, S., Champagne, K.S., Ivanov, D., Gallardo, M., Carney, D., Cheung, P., Ciccone, D.N.*, et al.* (2007). RAG2 PHD finger couples histone H3 lysine 4 trimethylation with V(D)J recombination. Nature *450*, 1106-1110.

Medema, R.H., Klompmaker, R., Smits, V.A., and Rijksen, G. (1998). p21waf1 can block cells at two points in the cell cycle, but does not interfere with processive DNA-replication or stress-activated kinases. Oncogene *16*, 431-441.

Menendez, C., Abad, M., Gomez-Cabello, D., Moreno, A., and Palmero, I. (2009). ING proteins in cellular senescence. Curr Drug Targets *10*, 406-417.

Millau, J.F., Bastien, N., and Drouin, R. (2009). P53 transcriptional activities: a general overview and some thoughts. Mutat Res *681*, 118-133.

Minn, A.J., Gupta, G.P., Siegel, P.M., Bos, P.D., Shu, W., Giri, D.D., Viale, A., Olshen, A.B., Gerald, W.L., and Massague, J. (2005). Genes that mediate breast cancer metastasis to lung. Nature *436*, 518-524.

Mishra, P.J., Humeniuk, R., Medina, D.J., Alexe, G., Mesirov, J.P., Ganesan, S., Glod, J.W., and Banerjee, D. (2008). Carcinoma-associated fibroblast-like differentiation of human mesenchymal stem cells. Cancer Res *68*, 4331-4339.

Moreno-Bueno, G., Peinado, H., Molina, P., Olmeda, D., Cubillo, E., Santos, V., Palacios, J., Portillo, F., and Cano, A. (2009). The morphological and molecular features of the epithelial-to-mesenchymal transition. Nat Protoc *4*, 1591-1613.

Narita, M., Nunez, S., Heard, E., Narita, M., Lin, A.W., Hearn, S.A., Spector, D.L., Hannon, G.J., and Lowe, S.W. (2003). Rb-mediated heterochromatin formation and silencing of E2F target genes during cellular senescence. Cell *113*, 703-716.

Naviaux, R.K., Costanzi, E., Haas, M., and Verma, I.M. (1996). The pCL vector system: rapid production of helper-free, high-titer, recombinant retroviruses. J Virol *70*, 5701-5705.

Nie, J., Liu, L., Wu, M., Xing, G., He, S., Yin, Y., Tian, C., He, F., and Zhang, L. (2010). HECT ubiquitin ligase Smurf1 targets the tumor suppressor ING2 for ubiquitination and degradation. FEBS Lett *584*, 3005-3012.

Nouman, G.S., Anderson, J.J., Lunec, J., and Angus, B. (2003). The role of the tumour suppressor p33 ING1b in human neoplasia. J Clin Pathol *56*, 491-496.

Nozell, S., Laver, T., Moseley, D., Nowoslawski, L., De Vos, M., Atkinson, G.P., Harrison, K., Nabors, L.B., and Benveniste, E.N. (2008). The ING4 tumor suppressor attenuates NF-kappaB activity at the promoters of target genes. Mol Cell Biol *28*, 6632-6645.

Orimo, A., and Weinberg, R.A. (2006). Stromal fibroblasts in cancer: a novel tumor-promoting cell type. Cell Cycle *5*, 1597-1601.

Ostman, A., and Augsten, M. (2009). Cancer-associated fibroblasts and tumor growth--bystanders turning into key players. Curr Opin Genet Dev *19*, 67-73.

Ozer, A., and Bruick, R.K. (2005). Regulation of HIF by prolyl hydroxylases: recruitment of the candidate tumor suppressor protein ING4. Cell Cycle *4*, 1153-1156.

Ozer, A., Wu, L.C., and Bruick, R.K. (2005). The candidate tumor suppressor ING4 represses activation of the hypoxia inducible factor (HIF). Proc Natl Acad Sci U S A *102*, 7481-7486.

Palacios, A., Garcia, P., Padro, D., Lopez-Hernandez, E., Martin, I., and Blanco, F.J. (2006). Solution structure and NMR characterization of the binding to methylated histone tails of the plant homeodomain finger of the tumour suppressor ING4. FEBS Lett *580*, 6903-6908.

Palacios, A., Moreno, A., Oliveira, B.L., Rivera, T., Prieto, J., Garcia, P., Fernandez-Fernandez, M.R., Bernado, P., Palmero, I., and Blanco, F.J. (2010). The dimeric structure and the bivalent recognition of H3K4me3 by the tumor suppressor ING4 suggests a mechanism for enhanced targeting of the HBO1 complex to chromatin. J Mol Biol *396*, 1117-1127.

Palacios, A., Munoz, I.G., Pantoja-Uceda, D., Marcaida, M.J., Torres, D., Martin-Garcia, J.M., Luque, I., Montoya, G., and Blanco, F.J. (2008). Molecular basis of histone H3K4me3 recognition by ING4. J Biol Chem *283*, 15956-15964.

Palmero, I., Murga, M., Zubiaga, A., and Serrano, M. (2002). Activation of ARF by oncogenic stress in mouse fibroblasts is independent of E2F1 and E2F2. Oncogene *21*, 2939-2947.

Palmero, I., and Serrano, M. (2001). Induction of senescence by oncogenic Ras. Methods Enzymol *333*, 247-256.

Pasquale, E.B. (2010). Eph receptors and ephrins in cancer: bidirectional signalling and beyond. Nat Rev Cancer *10*, 165-180.

Pedeux, R., Sengupta, S., Shen, J.C., Demidov, O.N., Saito, S., Onogi, H., Kumamoto, K., Wincovitch, S., Garfield, S.H., McMenamin, M.*, et al.* (2005). ING2 regulates the onset of replicative senescence by induction of p300-dependent p53 acetylation. Mol Cell Biol *25*, 6639-6648.

Pena, P.V., Davrazou, F., Shi, X., Walter, K.L., Verkhusha, V.V., Gozani, O., Zhao, R., and Kutateladze, T.G. (2006). Molecular mechanism of histone H3K4me3 recognition by plant homeodomain of ING2. Nature *442*, 100-103.

Pena, P.V., Hom, R.A., Hung, T., Lin, H., Kuo, A.J., Wong, R.P., Subach, O.M., Champagne, K.S., Zhao, R., Verkhusha, V.V.*, et al.* (2008). Histone H3K4me3 binding is required for the DNA repair and apoptotic activities of ING1 tumor suppressor. J Mol Biol *380*, 303-312.

Pietras, K., and Ostman, A. (2010). Hallmarks of cancer: interactions with the tumor stroma. Exp Cell Res *316*, 1324-1331.

Polager, S., and Ginsberg, D. (2009). p53 and E2f: partners in life and death. Nat Rev Cancer *9*, 738-748.

Prieur, A., and Peeper, D.S. (2008). Cellular senescence in vivo: a barrier to tumorigenesis. Curr Opin Cell Biol *20*, 150-155.

Raho, G., Miranda, C., Tamborini, E., Pierotti, M.A., and Greco, A. (2007). Detection of novel mRNA splice variants of human ING4 tumor suppressor gene. Oncogene *26*, 5247-5257.

Rasanen, K., and Vaheri, A. (2010). Activation of fibroblasts in cancer stroma. Exp Cell Res *316*, 2713-2722.

Raza, A., Franklin, M.J., and Dudek, A.Z. (2010). Pericytes and vessel maturation during tumor angiogenesis and metastasis. Am J Hematol *85*, 593-598.

Rodier, F., and Campisi, J. (2011). Four faces of cellular senescence. J Cell Biol *192*, 547-556.

Rodier, F., Coppe, J.P., Patil, C.K., Hoeijmakers, W.A., Munoz, D.P., Raza, S.R., Freund, A., Campeau, E., Davalos, A.R., and Campisi, J. (2009). Persistent DNA damage signalling triggers senescence-associated inflammatory cytokine secretion. Nat Cell Biol *11*, 973-979.

Ruland, J. (2011). Return to homeostasis: downregulation of NF-kappaB responses. Nat Immunol *12*, 709-714.

Saha, A., Bamidele, A., Murakami, M., and Robertson, E.S. (2010). EBNA3C attenuates the function of p53 through interaction with inhibitor of growth family proteins 4 and 5. J Virol *85*, 2079-2088.

Scott, M., Bonnefin, P., Vieyra, D., Boisvert, F.M., Young, D., Bazett-Jones, D.P., and Riabowol, K. (2001). UV-induced binding of ING1 to PCNA regulates the induction of apoptosis. J Cell Sci *114*, 3455-3462.

Schetter, A.J., Heegaard, N.H., and Harris, C.C. (2010). Inflammation and cancer: interweaving microRNA, free radical, cytokine and p53 pathways. Carcinogenesis *31*, 37-49.

Serrano, M., Lin, A.W., McCurrach, M.E., Beach, D., and Lowe, S.W. (1997). Oncogenic ras provokes premature cell senescence associated with accumulation of p53 and p16INK4a. Cell *88*, 593-602.

Shen, J.C., Unoki, M., Ythier, D., Duperray, A., Varticovski, L., Kumamoto, K., Pedeux, R., and Harris, C.C. (2007). Inhibitor of growth 4 suppresses cell spreading and cell migration by interacting with a novel binding partner, liprin alpha1. Cancer Res *67*, 2552-2558.

Shen, R.R., and Hahn, W.C. (2011). Emerging roles for the non-canonical IKKs in cancer. Oncogene *30*, 631-641.

Shi, X., and Gozani, O. (2005). The fellowships of the INGs. J Cell Biochem *96*, 1127-1136.

Shi, X., Hong, T., Walter, K.L., Ewalt, M., Michishita, E., Hung, T., Carney, D., Pena, P., Lan, F., Kaadige, M.R.*, et al.* (2006). ING2 PHD domain links histone H3 lysine 4 methylation to active gene repression. Nature *442*, 96-99.

Shimoda, M., Mellody, K.T., and Orimo, A. (2010). Carcinoma-associated fibroblasts are a rate-limiting determinant for tumour progression. Semin Cell Dev Biol *21*, 19-25.

Shiseki, M., Nagashima, M., Pedeux, R.M., Kitahama-Shiseki, M., Miura, K., Okamura, S., Onogi, H., Higashimoto, Y., Appella, E., Yokota, J.*, et al.* (2003). p29ING4 and p28ING5 bind to p53 and p300, and enhance p53 activity. Cancer Res *63*, 2373-2378.

Smith, T.G., Robbins, P.A., and Ratcliffe, P.J. (2008). The human side of hypoxia-inducible factor. Br J Haematol *141*, 325-334.

Soliman, M.A., and Riabowol, K. (2007). After a decade of study-ING, a PHD for a versatile family of proteins. Trends Biochem Sci *32*, 509-519.

Stott, F.J., Bates, S., James, M.C., McConnell, B.B., Starborg, M., Brookes, S., Palmero, I., Ryan, K., Hara, E., Vousden, K.H.*, et al.* (1998). The alternative product from the

human CDKN2A locus, p14(ARF), participates in a regulatory feedback loop with p53 and MDM2. EMBO J *17*, 5001-5014.

Tallen, G., Farhangi, S., Tamannai, M., Holtkamp, N., Mangoldt, D., Shah, S., Suzuki, K., Truss, M., Henze, G., Riabowol, K.*, et al.* (2009). The inhibitor of growth 1 (ING1) proteins suppress angiogenesis and differentially regulate angiopoietin expression in glioblastoma cells. Oncol Res *18*, 95-105.

Tsai, K.W., Tseng, H.C., and Lin, W.C. (2008). Two wobble-splicing events affect ING4 protein subnuclear localization and degradation. Exp Cell Res *314*, 3130-3141.

Unoki, M., Shen, J.C., Zheng, Z.M., and Harris, C.C. (2006). Novel splice variants of ING4 and their possible roles in the regulation of cell growth and motility. J Biol Chem *281*, 34677-34686.

Valastyan, S., and Weinberg, R.A. (2011). Tumor metastasis: molecular insights and evolving paradigms. Cell *147*, 275-292.

Vousden, K.H., and Prives, C. (2009). Blinded by the Light: The Growing Complexity of p53. Cell *137*, 413-431.

Walzak, A.A., Veldhoen, N., Feng, X., Riabowol, K., and Helbing, C.C. (2008). Expression profiles of mRNA transcript variants encoding the human inhibitor of growth tumor suppressor gene family in normal and neoplastic tissues. Exp Cell Res *314*, 273-285.

Wang, Q.S., Li, M., Zhang, L.Y., Jin, Y., Tong, D.D., Yu, Y., Bai, J., Huang, Q., Liu, F.L., Liu, A.*, et al.* (2010). Down-regulation of ING4 is associated with initiation and progression of lung cancer. Histopathology *57*, 271-281.

Xie, Y., Zhang, H., Sheng, W., Xiang, J., Ye, Z., and Yang, J. (2008). Adenovirus-mediated ING4 expression suppresses lung carcinoma cell growth via induction of cell cycle alteration and apoptosis and inhibition of tumor invasion and angiogenesis. Cancer Letters *271*, 105-116.

Xing, F., Saidou, J., and Watabe, K. (2010). Cancer associated fibroblasts (CAFs) in tumor microenvironment. Front Biosci *15*, 166-179.

Ythier, D., Larrieu, D., Brambilla, C., Brambilla, E., and Pedeux, R. (2008). The new tumor suppressor genes ING: genomic structure and status in cancer. Int J Cancer *123*, 1483-1490.

Yuan, J., Adamski, R., and Chen, J. (2010). Focus on histone variant H2AX: to be or not to be. FEBS Lett *584*, 3717-3724.

Zhang, X., Wang, K.S., Wang, Z.Q., Xu, L.S., Wang, Q.W., Chen, F., Wei, D.Z., and Han, Z.G. (2005). Nuclear localization signal of ING4 plays a key role in its binding to p53. Biochem Biophys Res Commun *331*, 1032-1038.

Zhang, X., Xu, L.S., Wang, Z.Q., Wang, K.S., Li, N., Cheng, Z.H., Huang, S.Z., Wei, D.Z., and Han, Z.G. (2004). ING4 induces G2/M cell cycle arrest and enhances the chemosensitivity to DNA-damage agents in HepG2 cells. FEBS Lett *570*, 7-12.

Zhang, X., Zhu, W., Zhang, J., Huo, S., Zhou, L., Gu, Z., and Zhang, M. (2010a). MicroRNA-650 targets ING4 to promote gastric cancer tumorigenicity. Biochem Biophys Res Commun *395*, 275-280.

Zhang, X.J., Ye, H., Zeng, C.W., He, B., Zhang, H., and Chen, Y.Q. (2010b). Dysregulation of miR-15a and miR-214 in human pancreatic cancer. J Hematol Oncol *3*, 46.

Zhou, L., Picard, D., Ra, Y.S., Li, M., Northcott, P.A., Hu, Y., Stearns, D., Hawkins, C., Taylor, M.D., Rutka, J.*, et al.* (2010). Silencing of thrombospondin-1 is critical for myc-induced metastatic phenotypes in medulloblastoma. Cancer Res *70*, 8199-8210.

Zigler, M., Villares, G.J., Lev, D.C., Melnikova, V.O., and Bar-Eli, M. (2008). Tumor immunotherapy in melanoma: strategies for overcoming mechanisms of resistance and escape. Am J Clin Dermatol *9*, 307-311.

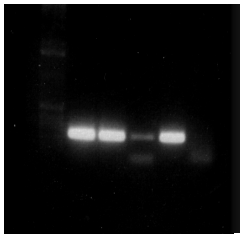

Anexo

El trabajo realizado durante el desarrollo de la tesis ha dado lugar a las siguientes publicaciones, que se adjuntan como anexo:

Publicaciones que forman parte de la Tesis Doctoral:

Moreno, A., Palacios, A., Orgaz, J., Jimenez, B., Blanco, F., Palmero, I. (2010). Functional impact of cancer-associated mutations in the tumour suppressor protein ING4. Carcinogenesis, *31*, 1932-8

Otras publicaciones:

Abad, M., **Moreno, A.**, Palacios, A., Narita, M., Blanco, F., Moreno-Bueno, G., Narita, M., Palmero, I. (2011). The tumor suppressor ING1 contributes to epigenetic control of cellular senescence. Aging Cell, *10*, 158,71

Palacios, A., **Moreno, A.**, Oliveira, B., Rivera, T., Prieto, J., García, P., Bernadó, P., Palmero, I., Blanco, F. (2010). The dimeric structure and the bivalent recognition of H3K4me3 by the tumor suppressor ING4 suggest a mechanism for enhanced targeting of HBO1 complex to chromatin. J Mol Biol, *396*, 1117-27

Gómez Cabello, D., Callejas, S., Benguria, A., **Moreno, A.**, Alonso, J., Palmero, I. (2010). Regulation of the microRNA processor DGCR8 by the tumor suppressor ING1. Cancer Res, *70*, 1866-74

Menéndez, C., Abad, M., Gómez-Cabello, D., **Moreno, A.**, Palmero I. (2009). ING proteins in cellular senescence. Curr Drug Targets, *10*, 406-17

Carcinogenesis vol.31 no.11 pp.1932–1938, 2010
doi:10.1093/carcin/bgq171
Advance Access publication August 12, 2010

Functional impact of cancer-associated mutations in the tumor suppressor protein ING4

Alberto Moreno, Alicia Palacios[1], Jose Luis Orgaz, Benilde Jimenez, Francisco J.Blanco[1,2] and Ignacio Palmero*

Instituto de Investigaciones Biomédicas "Alberto Sols", Consejo Superior de Investigaciones Científicas-Universidad Autónoma de Madrid, Arturo Duperier 4, E-28029 Madrid, Spain, [1]Structural Biology Unit, CIC bioGUNE, E-48160 Derio, Spain and [2]Ikerbasque Science Foundation, Bilbao, Spain

*To whom correspondence should be addressed. Tel: +34 915854491; Fax: +34 915854401;
Email: ipalmero@iib.uam.es

Inhibitor of growth 4 (ING4) is a member of the ING family of tumor suppressor proteins. In this study, we have analyzed the impact of two mutations in ING4 associated with human tumors (Y121N and N214D), testing their behavior in a series of functional, biochemical and structural analyses. We report that the N214D mutation dramatically dampened the ability of ING4 to inhibit proliferation, anchorage-independent growth or cell migration or to sensitize to cell death. In turn, the Y121N mutant did not differ significantly from wild-type ING4 in our assays. Neither of the mutations altered the normal subcellular localization of ING4, showing predominantly nuclear accumulation. We investigated the molecular basis of the defect in the activity of the N214D mutant. The folding and ability to bind histone marks of ING4 was not significantly altered by this mutation. Instead, we found that the functional impairment of the N214D mutant correlates with reduced protein stability due to increased proteasome-mediated degradation. In summary, our data demonstrates that a point mutation of ING4 associated to human tumors leads to the loss of several essential functions of ING4 pertinent to tumor protection and highlight the importance of ING4 function to prevent tumorigenesis.

Introduction

Mammalian cells possess protective mechanisms that prevent tumor initiation and progression (1,2). The ING proteins constitute a family of evolutionary conserved proteins with important roles in different responses associated with tumor protection, such as apoptosis, DNA repair or cellular senescence (3). In mammals, the ING family includes five loci (ING1–ING5), some of which produce several protein variants by alternative splicing. Inhibitor of growth 4 (ING4) is a member of the ING family with a role in cellular processes critical for tumor initiation and progression. ING4 can regulate apoptosis (4) and proliferation, in common with other ING proteins, but also has a specific role in anchorage-independent growth (5), angiogenesis (6,7), cell migration (8,9) or response to hypoxia (6,10,11). Like other ING proteins, ING4 exerts its function mainly as a chromatin regulator, linking histone marks to complexes with histone-modifying activities. ING4 specifically binds H3K4me3 (histone H3 trimethylated at lysine 4, a distinctive mark of euchromatin) through its plant homeodomain (PHD) domain (12–15), and it is also a component of complexes with histone acetyltransferase activity, in connection with HBO1 (7,16,17). ING4 can also cooperate with p53 and nuclear factor-kappaB in transcriptional control, contributing to p53 posttranslational modifications or as a cofactor for both (18–20). Alterations in the ING4 locus have been described in diverse human tumors, including glioma, myeloma, breast carcinoma or head and neck squamous cell carcinoma (3,5,17,21). Reduced levels of ING4 messenger RNA or protein are the most prevalent alterations of ING4 in tumors. In addition, there are also examples of short deletions and insertions or point mutations that result in truncations or amino acid changes in the ING4 protein sequence (5,22,23). Given the proposed role of ING4 in preventing tumor initiation and progression, here we sought to study the functional impact of point mutations in ING4 associated with human tumors, with the aim to obtain insights on the role of this protein in tumor suppression.

Abbreviations: ARF, alternative reading frame; BrdU, bromodeoxyuridine; H3K4me3, histone H3 trimethylated at lysine 4; HMVEC, human microvascular endothelial cells; ING4, inhibitor of growth 4; NMR, Nuclear magnetic resonance; PHD, plant homeodomain.

Materials and methods

Mutagenesis

Mutant versions of ING4 were generated with the Quick Change Site-Directed Mutagenesis Kit (Stratagene, La Jolla, CA), using the complementary DNA of the human ING4 protein cloned in the retroviral vector pLPC as a template (variant v1; 24) cloned in the retroviral vector pLPC. Specific mutations were incorporated by polymerase chain reaction using *Pfu* Turbo DNA Polymerase (Stratagene), and subsequent digestion with DpnI, to eliminate the methylated parental band. They were confirmed by sequencing.

Cell culture

Immortalized mouse fibroblasts (NIH3T3) and the human cell lines U2OS (osteosarcoma), HT1080 (fibrosarcoma) H23 and H82 (lung carcinoma), and 293T (embryonic kidney epithelium) were cultured in Dulbecco's modified Eagle's medium (Gibco, Grand Island, NY), containing 10% fetal calf serum, in the presence of penicillin–streptomycin, at 37°C and 5% CO_2. Human microvascular endothelial cells (HMVEC) were grown in MCDB 131 medium (Sigma, St Louis, MO), supplemented with 10% fetal calf serum, 2 mM L-glutamine, 10 ng/ml epidermal growth factor, 10 ng/ml hydrocortisone and 16.32 μg/ml bovine pituitary extract (Invitrogen, Carlsbad, CA).

Transfections

Transient transfection of 293T cells was performed using the calcium phosphate method, as described previously (25,26). Transient transfection of U2OS cells was carried out with FuGENE (Roche, Manheim, Germany), following the manufacturer's protocol.

Retroviral infection

Retroviral infection of NIH3T3 cells was performed essentially as described previously (26). The following vectors were used: pLPC, pLPC-AU5-ING4, pLPC-AU5-ING4^{Y121N}, pLPC-AU5-ING4^{N214D}, pLPC-HA-ING4, pLPC-HA-ING4^{N214D}, pWZLHygro and pWZL Hygro-RasV12.

Immunoblot

The preparation of total cell lysates, electrophoresis and western blot analysis was carried out as described in ref. 27. The antibodies used were anti-ING4 (ab3714, 1:500 dilution; AbCam, Cambridge, UK), anti-AU5 (MMS-135R, 1:500 dilution; Covance, Princeton, NJ) and anti-hemmaglutinin (Hybridoma clone 12CA5, 1:500 dilution). We used an anti-actin antibody (AC-15, 1:10 000 dilution; Sigma) as a loading control.

Reverse transcription–polymerase chain reaction

Total RNA was prepared using Tri Reagent (Sigma) from cells growing asynchronously. Five micrograms of total RNA was used for complementary DNA synthesis using M-MLV reverse transcriptase (Promega, Madison, WI). One microliter of the reaction was used to perform polymerase chain reactions. The oligos used were as follows: ING4 forward, 5′-ATTGCCTTTGTCACCAGGTC-3′ and ING4 reverse, 5′-GGAACCACTCGATGGAACAA-3′. Quantitative polymerase chain reaction was performed using Universal Probe Library probes in an ABI 9700 machine.

DNA synthesis rate

To measure the incorporation of bromodeoxyuridine (BrdU), NIH3T3 cells were plated on LabTek (Nunc, Rochester, NY) chamber slides (∼20 000 cells per well in eight-well chambers) and 24 h later incubated for 6 h with BrdU, at a final concentration of 10 μM. BrdU-positive cells were detected by immunofluorescence using an anti-BrdU antibody (BP40250, 1:1000 dilution; Megabase Research Products, Lincoln, NE). The samples were counterstained with 4′,6-diamidino-2-phenylindole to visualize the nucleus. At least 200 cells were counted for each condition.

Immunofluorescence

U2OS cells seeded in glass chamber slides (20 000 cells per well in eight-well LabTek Chambers) were transfected with the ING4 constructs and the following day, they were processed for immunofluorescence as described in ref. 28. The samples were analyzed in a fluorescence microscope Leica Leitz DM RB or in a Leica TCSSP2 DMIRE 2 confocal microscope. An antibody against the AU5 tag was used (MMS-135R, 1:500 dilution; Covance). As secondary antibodies, we used goat-anti-rabbit Alexa 488 or goat-anti-mouse Alexa 488 both from Molecular Probes, Invitrogen (dilution 1:500).

Cell migration assays

The assays were conducted using modified Boyden chambers with 0.5% gelatin-coated polycarbonate membranes (6.5 mm diameter, 8.0 μm pore size; Corning Incorporated, Corning, NY). To obtain the conditioned medium, retrovirally infected NIH3T3 cells were grown until 80% confluence and, after extensive washing with phosphate-buffered saline, were maintained in serum-free medium for 48 h. Subsequently, the collected media were concentrated 60-fold using Ultra-15 concentrators (Millipore Corporation, Billerica, MA). HMVEC, serum-starved for 16 h, were plated in serum-free MCDB 131 medium on the upper chamber of the Transwell (1.2×10^5 cells), whereas conditioned medium (15 μg/ml in serum-free medium) was placed in the lower chamber. Cells were allowed to migrate for 18 h at 37°C and non-migrated cells were removed from the top chamber with a cotton swab. Migrated cells were fixed and stained with Diff-Quik (Dade Behring, Newark, NJ) and counted at 20 fields of maximum migration under a light microscope at ×40 magnification.

Cell viability assays

NIH3T3 cells (1.5×10^5) infected with ING4 vectors were plated and treated with increasing concentrations of doxorubicin. After 24 h, cells were collected and stained with Trypan blue for direct counting of viable cells under the microscope.

Anchorage-independent growth

NIH3T3 cells infected with $ING4^{N214D}$ mutant and wild-type ING4 were re-infected with a vector carrying the oncogenic version of Ha-Ras (pWZLHygro-RasV12) or empty vector as a control. Infected cells were resuspended in a pre-warmed solution of 0.3% agarose in complete medium and plated on 60 mm plates with a bottom layer of 0.5% agarose, at a density of 10^5 cells per plate. Colonies were visually counted after 15 days.

Nuclear magnetic resonance spectroscopy and structure determination

Nuclear magnetic resonance (NMR) experiments were recorded on Bruker AVANCEII 600 MHz (with cryoprobe) and 700 MHz spectrometers at 25°C in 20 mM sodium phosphate pH 6.5, 50 mM NaCl, 1 mM perdeuterated dithiothreitol and 9% (vol/vol) $2H_2O$. Backbone and side chain resonance assignment were obtained using a set of 2D and 3D NMR spectra recorded on a 0.5 mM PHD^{N214D} sample uniformly enriched in ^{15}N. Distance restraints collected from NOESY spectra were used to calculate an ensemble of models using torsion angle dynamics. Further details are given as supplementary data, available at *Carcinogenesis* Online.

Binding to histone marks

Synthetic lyophilized peptides were purchased from PolyPeptide, Strasbourg, France. They contained the sequences ARTKQTARKSTGGKAY, histone H3 residues 1–15 and GGAKRHKVLRDNIQY, histone H4 residues 14–27, with an extra Tyr residue at the C-termini to measure the peptide concentration by absorbance. Peptides with trimethylated lysine at positions 4 or 9 of histone H3 or position 20 of histone H4 were tested for binding to ING4-PHD^{N214D}. The binding and dissociation constant were measured by NMR spectroscopy as described above.

Protein half-life assays

The 293T cells were transiently transfected with ING4 constructions, using calcium phosphate. At 36 h post-transfection, cycloheximide was added to the medium at a final concentration of 50 μg/ml to inhibit protein synthesis. The proteasome inhibitors MG132 (Sigma) or lactacystin (Calbiochem, San Diego, CA) were added 1 h before the start of treatment with cycloheximide at a final concentration of 20 or 10 μM, respectively. The lysates were analyzed by immunoblot using an anti-hemmaglutinin antibody.

Results

Cell proliferation

We generated mutant versions of the human ING4 protein, which included two missense point mutations detected in lung carcinoma cell lines (29). The Y121N mutation is located close to the nuclear localization signal , whereas the N214D mutation is within the conserved PHD domain, next to a residue involved in the interaction with

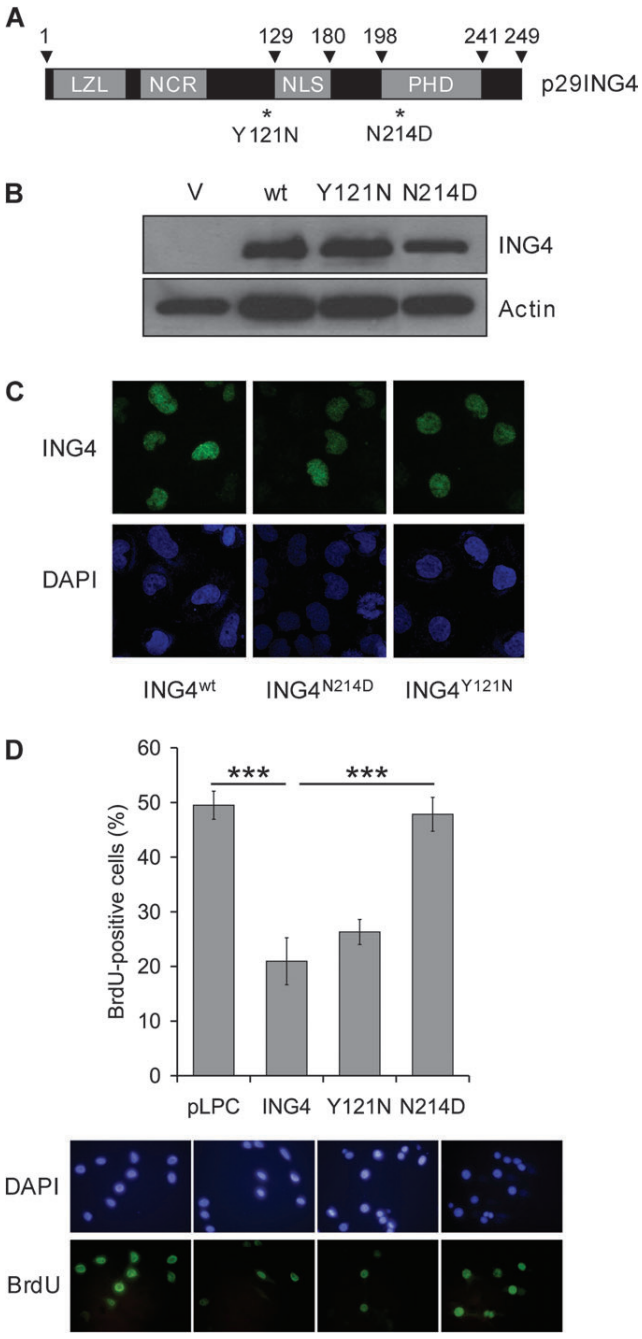

Fig. 1. (**A**) Schematic diagram of the human ING4 protein. The position of the point mutations used is indicated with asterisks. Functional domains are represented by gray boxes. Arrowheads indicate the residues that delimitate the domains relevant for the mutants. (**B**) Western blot showing expression of ectopic wild-type ($ING4^{wt}$) or mutant ($ING4^{N214D}$ or $ING4^{Y121N}$) in transiently transfected U2OS cells, using an anti-ING4 antibody. (**C**) Immunofluorescence analysis of the location of the indicated versions of ING4 in transiently transfected U2OS cells. An antibody against the AU5 tag was used to visualize ectopic ING4. (**D**) Percentage of BrdU-positive cells in NIH3T3 fibroblasts infected with the indicated vectors, using immunofluorescence against BrdU (see Materials and Methods, $^{***}P < 0.001$). The graph (top) represents the average and standard deviation of three independent experiments. Immunofluorescence images from a representative experiment are shown (bottom).

methylated histone (D213; 12) and near two cysteine residues (C212 and C217), responsible for the maintenance of the PHD domain structure (Figure 1A). We confirmed that all the ING4 variants were efficiently expressed (Figure 1B). Using immunofluorescence, we observed that both mutant forms of ING4 displayed a subcellular distribution indistinguishable from the wild-type version, with predominantly nuclear localization and limited cytoplasmic expression (Figure 1C). ING4 overexpression has a clear antiproliferative effect zin several different cell types (4,24). This is one of the best-characterized phenotypes for ING4, so we decided to start our study by testing the behavior of cancer-associated ING4 mutants in this context. The rate of DNA synthesis was estimated by BrdU incorporation in asynchronous populations of NIH3T3 cells infected with empty vector or vectors encoding wild-type ING4 and both mutants, $ING4^{N214D}$ and $ING4^{Y121N}$ (Figure 1D). As expected, the ectopic expression of $ING4^{wt}$ significantly decreased the number of BrdU-positive cells compared with the control with empty vector (49.5% of BrdU-positive cells in the control versus 20.9% in ING4-expressing cells, $P < 0.001$). The Y121N mutant caused a reduction in division rate similar to wild-type ING4 (26.3% of positive cells), whereas cells expressing the N214D mutant showed a rate of BrdU incorporation similar to control cells infected with empty vector (47.8%), indicating that the antiproliferative effect of the ING4 protein was impaired by this mutation. Similar results were obtained with the human tumor cell line HT1080 (supplementary Figure 2 is available at *Carcinogenesis* Online).

Cell migration

Increased cell migration, invasion and angiogenic potential are distinctive features of tumor cells, associated with their metastatic capacity. ING4 is unique among ING proteins in that it can inhibit the angiogenic potential of tumor cells and represses migration and invasion in these cells (9,24,30). Thus, we decided to determine whether these properties were altered in the ING4 cancer mutants. The anti-migratory function of ING4 is exerted mainly in a non-cell-autonomous fashion, through the repression of promigratory-secreted factors (6,7,17,31). For this reason, conditioned medium of cells expressing different versions of ING4 were used in migration assays, to test their ability as a chemotactic substrate for human microvascular endothelial cells, HMVEC (Figure 2). Consistent with the role of ING4 as a negative regulator of cell migration and angiogenesis, the medium from cells expressing wild-type ING4 was less efficient in induction of migration (~60% of the control cells). In contrast, the effect on cell migration of conditioned medium from cells expressing the N214D mutant was undistinguishable from that of control vector-infected cells. In this assay, the mutant $ING4^{Y121N}$ had no significant functional impact, leading to levels of migration similar to those obtained for wild-type ING4, in line with the results obtained in the proliferation assay. Similar results were obtained in migration assays of HMVEC with independent constructs of ING4 that contained a different tag (supplementary Figure 1A is available at *Carcinogenesis* Online). The impact of cancer mutations in the cell-autonomous anti-migratory action of ING4 was also determined in wound healing assays with NIH3T3 cells expressing wild-type or mutant ING4, leading to similar conclusions (supplementary Figure 1B is available at *Carcinogenesis* Online).

Anchorage-independent growth

ING4 was isolated in a screening for proteins with the ability to revert the loss of anchorage dependence, a hallmark of transformed cells (12). To analyze the impact of ING4 cancer mutations in this context, NIH3T3 cells infected with ING4 constructs or empty vector were oncogenically transformed with an activated Ha-Ras oncogene (RasV12). Cells were then allowed to grow in soft agar for 15 days and the number of colonies at the end of the experiment was counted (Figure 3). The $ING4^{Y121N}$ protein was not further analyzed because it displayed wild-type activity in the assays described above. The ability

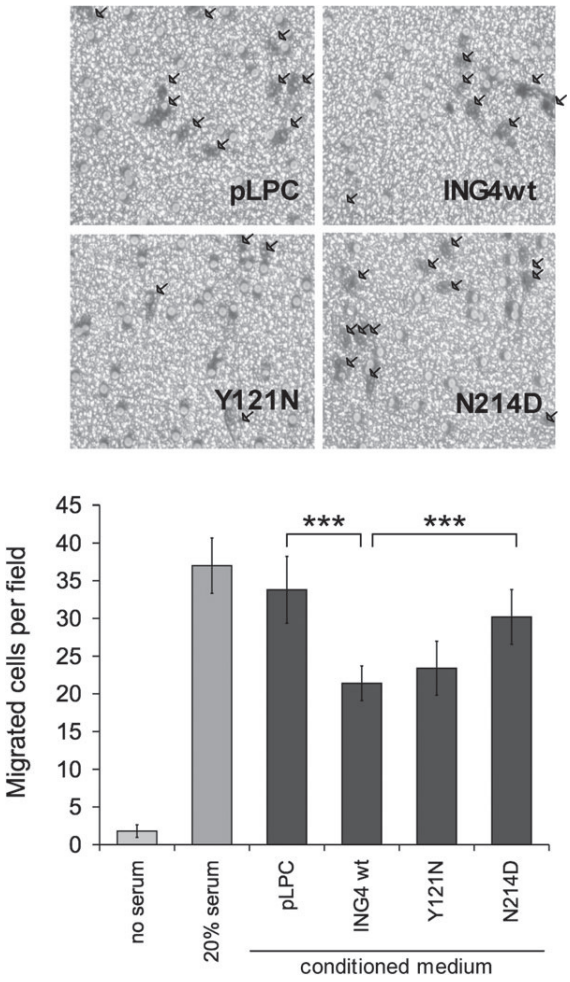

Fig. 2. Effects on migration of mutant versions of ING4. Conditioned medium from NIH3T3 mouse fibroblasts infected with vectors for wild-type or mutant ING4 or empty vector was used in a Transwell migration assay of HMVEC cells (see Materials and Methods). Medium with either 20% or no fetal calf serum was used as positive and negative controls, respectively. Images of representative fields are shown. Arrows indicate migrated cells. Average and standard deviation values shown are representative of three independent experiments ($^{***}P < 0.001$).

of Ras-expressing NIH3T3 cells to form colonies in soft agar was significantly reduced by the concomitant overexpression of the wild-type form of ING4, when compared with control cells expressing Ras and an empty vector (30% reduction). However, this inhibitory effect was lost in Ras-NIH3T3 fibroblasts co-expressing the mutant N214D, which displayed an ability to form colonies not significantly different to control cells.

Impact on cell viability

Overexpression of ING4 can lead to increased cell death, either alone or in synergy with DNA damaging agents (12). To test the impact of cancer-associated mutations in this function of ING4, we performed a cell viability assay in NIH3T3 fibroblasts infected with $ING4^{wt}$ and $ING4^{N214D}$. Cells were treated with doxorubicin, an agent that causes DNA damage, and we scored the ability of the different ING4 versions to sensitize this agent. As expected, wild-type ING4 expression caused a dramatic increase in doxorubicin-triggered cell death (~3-fold), but this effect was almost completely abolished in fibroblasts expressing the mutant version $ING4^{N214D}$ (Figure 4). Similar results were obtained with the human tumor cell line HT1080 (supplementary Figure 2 is available at *Carcinogenesis* Online).

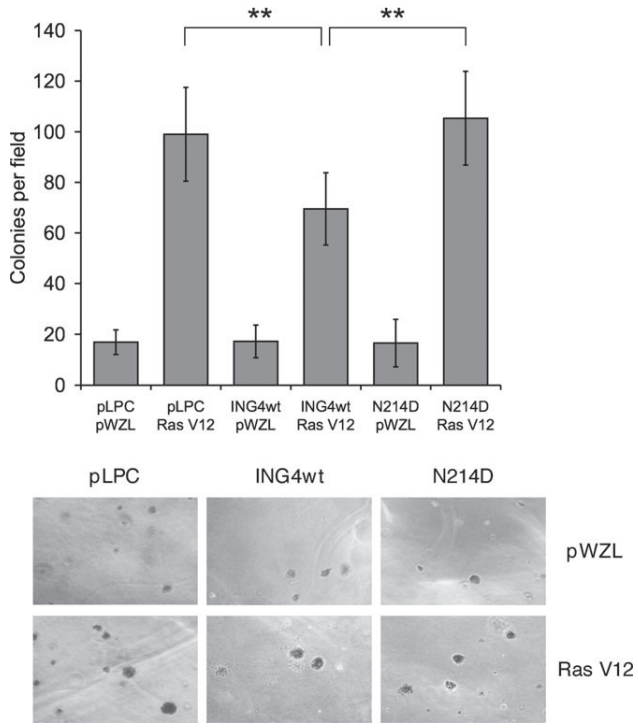

Fig. 3. Anchorage-independent growth. NIH3T3 cells were serially infected with vectors expressing mutant or wild-type ING4 or empty vector followed by a vector expressing RasV12 or its empty vector. After selection, cells were grown in soft agar for 15 days and the number of colonies was determined. The average and standard deviation of two experiments are shown ($^{**}P < 0.01$). Representative bright field images (×200 magnification) are also shown.

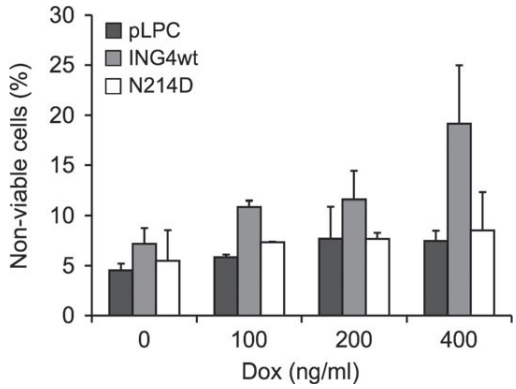

Fig. 4. Sensitization to cell death. NIH3T3 fibroblasts stably expressing wild-type ING4, the N214D mutant or empty vector were treated with doxorubicin at the indicated doses and the percentage of non-viable cells was measured 24 h later by Trypan blue exclusion. The graph shows averages and standard deviations from two independent experiments.

Impact on protein structure and binding to histone marks

Since the presence of the N214D mutation consistently led to the reduced activity of ING4 in several functional assays, we set to establish the molecular mechanism underlying this apparent loss of function. First, we investigated the effects of the N214D mutation in the folding of the ING4 molecule and in recognition of histone marks. To study the impact in protein structure, the N214D mutant PHD domain was analyzed in solution by NMR. Full structure determination and refinement (supplementary Table 1 is available at *Carcinogenesis* Online) showed that the three-dimensional structure for residues 195–244 is essentially the same as for wild-type ING4, whereas the NMR signals of the chain termini are highly flexible in the two molecules. [Figure 5A, see also (13)]. The pattern of backbone ^{1}H-^{15}N signals in the heteronuclear single quantium correlation spectrum displayed significant differences between mutant and wild-type PHDs (supplementary Figure 3A and B is available at *Carcinogenesis* Online), caused by the local change in the chemical environment due to the addition of a negative charge at the end of a short side chain in the N214D mutant, which affects the nearby residues on the structured protein. We also used NMR to test the ability of mutant ING4 to bind histone marks. Wild-type ING4, like other ING proteins, can specifically recognize the histone mark H3K4me3 through its PHD domain (12,13,32). We observed that the ING4-PHD^{N214D} mutant also binds preferentially to the H3K4me3 mark, using the same site as the wild-type PHD (Figure 5B), with very similar affinity and specificity. The K_d for H3K4me3 and N214D was 3 ± 1 μM compared with 4 ± 1 μM for wild-type ING4 [Figure 5C, see also (32)]. The PHD fingers of ING1 and ING2 have been shown to act as phosphoinositide receptors through their C-terminal basic regions, which are much shorter in ING3-5 (33). As previously found for the wild-type ING4 molecule (32), the ING4-PHD^{N214D} mutant showed no detectable binding to a panel of different phosphoinositides (data not shown). Collectively, this set of biophysical assays indicates that the N214D mutation does not have a significant impact in the folding or ability to recognize histone marks of ING4.

Impact on protein stability

During the course of our experiments, we consistently observed reduced levels of the ING4^{N214D} protein, relative to the wild-type form, in fibroblasts stably expressing the different forms of ING4 (Figure 6A, left, see also Figure 1B). However, wild-type and mutant ING4 constructs were expressed similarly at RNA level, with slightly elevated RNA expression for ING4^{N214D} (Figure 6A, right). These results suggested that the N214D mutation could cause a defect in ING4 protein stability. To investigate the effects of this mutation on the turnover of the ING4 protein, we performed half-life experiments in 293T cells transiently transfected with vectors expressing hemmaglutinin-tagged ING4^{wt} and ING4^{N214D} and subsequently treated with cycloheximide (Figure 6B and C). The decline of the amount of the N214D protein was considerably faster than for wild-type ING4 (Figure 6B, left, and Figure 6C). It has been recently reported that ING4 protein levels are controlled by proteasome-mediated degradation (34). To evaluate the link of the reduced protein stability of the N214D mutant to the proteasome pathway, half-life experiments were performed in the presence of the proteasome inhibitor MG132. MG132 reversed the reduced stability of the N214D mutant, leading to increased half-lives of both mutant and wild-type proteins (Figure 6B, right, and Figure 6C). Similar results were obtained with lactacystin, another proteasome inhibitor (supplementary Figure 4 is available at *Carcinogenesis* Online). It has been suggested that the stability of ING4 depends on its accumulation in the nucleolus and its association to the tumor suppressor protein alternative reading frame (ARF) (34). In contrast, our immunofluorescence analyses consistently showed a predominantly nuclear localization for wild-type or mutant ING4, without accumulation in the nucleolus, even with nucleolar exclusion in some instances. Accordingly, no colocalization with the nucleolar protein ARF was observed for any of the ING4 versions analyzed (Figure 1C; supplementary Figure 5 is available at *Carcinogenesis* Online). Of note, our results could be confirmed with cell lines expressing endogenous mutant ING4. We observed reduced levels of endogenous ING4 protein in the small-cell lung carcinoma cell line H82, which harbors the mutant allele N214D, relative to H23, a lung adenocarcinoma line with the Y121N mutation (5; Figure 6D). The reduced levels of endogenous ING4 in this cell line could be reverted after proteasome inhibition (supplementary Figure 6 is available at *Carcinogenesis* Online). Thus, this set of experiments show that the N214D mutation leads to reduced ING4 protein stability.

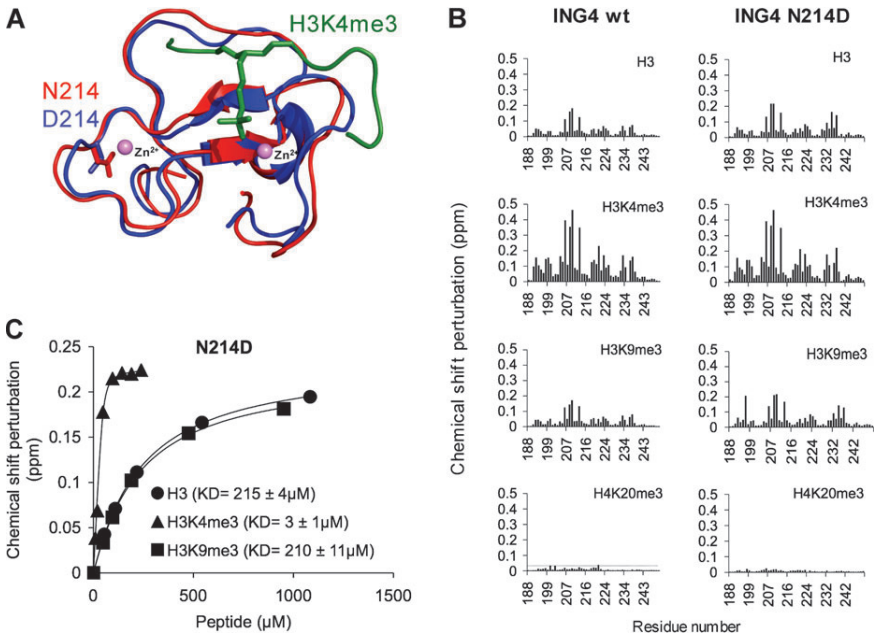

Fig. 5. Protein folding and binding to histone marks. (**A**) Superimposition of the mean solution structures of the wild-type (red) and N214D mutant (blue) ING4-PHD fingers. The backbones of residues 195–244 (excluding the flexible chain termini) are shown as ribbons (secondary structure elements) or coils (other non-regular structures). The side chains of residue 214 (N or D) are shown in sticks. Depicted in green is the backbone structure of the H3K4me3 peptide, with the trimethylated lysine residue shown in sticks, as seen in the crystal structure of its complex with the wild-type ING4-PHD. The two Zn^{2+} cations bound to the mutant PHD are shown as violet spheres. (**B**) Bar plots of the chemical shift perturbations observed for each residue in the ^{1}H-^{15}N heteronuclear single quantium correlation spectra of the wild-type or N214D mutant PHD domains in the presence of a 4-fold molar excess of the indicated histone peptides. The estimated experimental error (±0.012 p.p.m.) is indicated by the dotted line in the plot corresponding to peptide H4K20me3. (**C**) Plots of the chemical shift perturbation of the W237 amide resonance of PHD (50 μM) as a function of the concentration of the different peptides. The symbol's height indicates the experimental error.

Discussion

ING proteins are increasingly regarded as important mediators in tumor suppression. Supporting the relevance of these proteins in tumor protection, different types of inactivating alterations of ING proteins have been observed in human tumors, and mouse models with deficiency in ING1 are tumor-prone (reviewed in ref. 3). ING4, like other ING proteins, is involved in control of proliferation and apoptosis, but it also has a specific role in restraining additional responses relevant in tumor progression, such as angiogenesis and invasion (4,5). In this study, we have examined the functional impact of two point mutations in ING4 found in lung tumor cell lines, in order to understand the contribution of alterations in ING proteins to tumorigenesis (5). Based on our results, using a range of functional assays, we conclude that the N214D mutation markedly dampens ING4 activity. In turn, the Y121N mutation had no significant impact in the normal function of the ING4 protein. In particular, the N214D mutant version of ING4 was less efficient in sensitization to cell death and inhibition of proliferation, cell migration or anchorage-independent growth. The N214 residue is located in the conserved PHD domain, which acts as recognition module for H3K4me3. Therefore, we investigated possible effects of the mutation in several structural and binding parameters of ING4. Our results rule out a significant impact of this mutation in the correct folding of the ING4 PHD domain or in the binding to histone marks, unlike cancer-associated mutations in the same domain of the ING1 protein (35). While these structural parameters are normal in the N214D mutant, we have not investigated other functions of ING4 in transcription control, such as the association to histone acetyltransferase–histone deacetylase complexes or transcription factors, therefore we cannot at this point rule out alterations in gene regulation associated to the N214D mutant. The most significant alteration observed for the N214D mutant was its reduced protein stability relative of wild-type ING4. A recent report has showed that ING4 protein degradation is mediated by proteasome-mediated proteolysis and might be mediated by its accumulation in the nucleolus and its association with the tumor suppressor nucleolar protein ARF (34). We have confirmed that the degradation of wild-type or mutant ING4 proteins can be reverted with proteasome inhibitors. However, we found that ING4 protein stability could not be correlated with accumulation in nucleolus or colocalization with ARF because wild-type and mutant ING4 consistently showed a uniform nuclear localization pattern. The precise mechanism responsible for the altered protein stability of the N214D mutant is currently not known. Direct inhibition of ubiquitination is unlikely. Although the specific residues that are ubquitinated in ING4 have not been identified, ubiquitination is supposed to occur in the first 180 residues of the protein, distant from the N214 residue (34). Instead, the N214D mutation might have some effect in the fine tuning of the process, in a similar situation to ING1, where phosphorylation of S126 influences proteasome-mediated protein turnover (36). Of note, mutations in S126 of ING1 have been found in human tumors (37), as is the case for N214 of ING4. Interestingly, two very recent reports show that ING2 and ING3, other members of the ING family, are also regulated by proteasome-mediated degradation. In the case of ING3, this control was found altered in melanoma, leading to diminished ING3 protein levels (38,39). Therefore, it appears that abnormally decreased protein stability, albeit by different ways of action, might be a general mechanism responsible for defective ING protein function in tumors. It should be noted that, although reduced stability clearly correlates with defective function of N214D mutant, we cannot formally rule out the existence of additional functional defects that could synergize with the aberrant stability to account for the defective tumor suppressive functions of the N214D version. Different types of ING4 alterations have been reported in human tumors. Reduced levels of ING4 RNA and protein are frequently found in many types of tumors, including glioma (7,17), myeloma (6), melanoma (30,40), breast carcinoma (5), head and neck squamous cell carcinoma (21) or gastric cancer (23). In some instances, tumors with ING4 downregulation

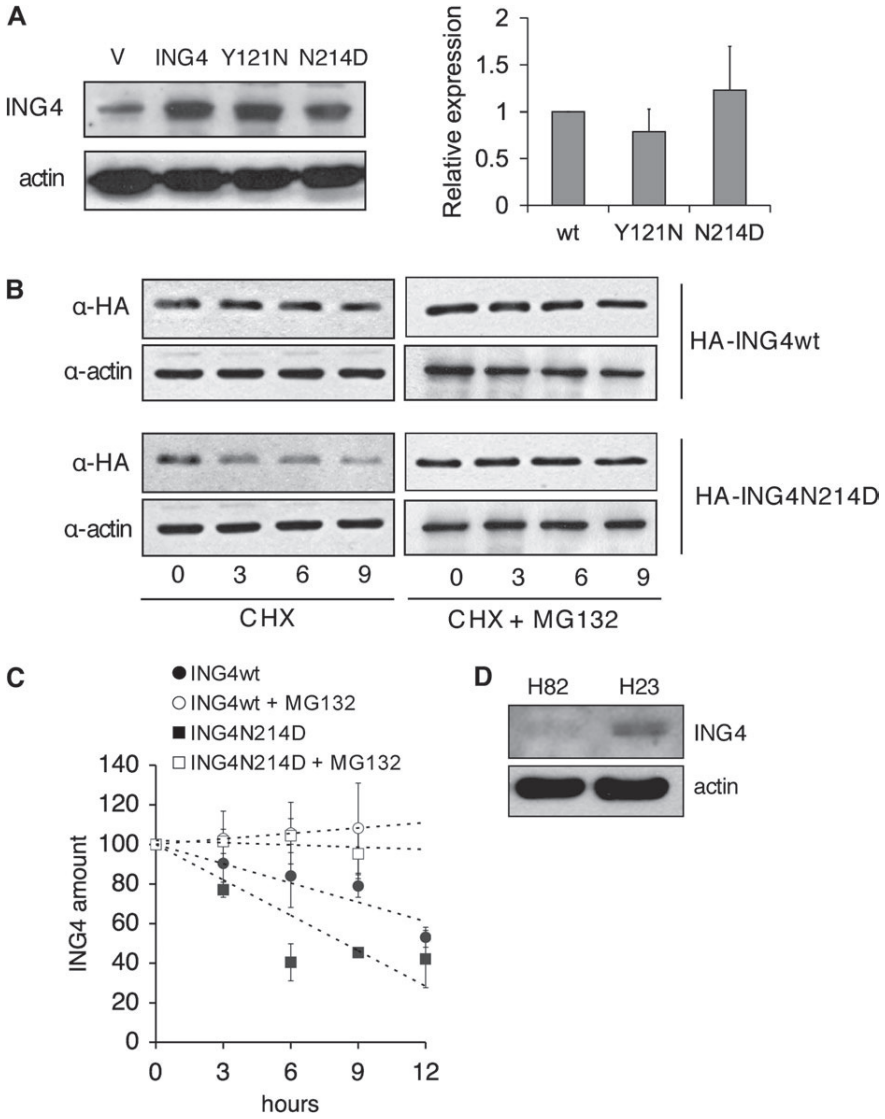

Fig. 6. Protein half-life. (**A**) Western blot analysis (left) of protein levels for the indicated versions of ING4 in infected NIH3T3 cells, detected with an antibody against ING4. Quantitative reverse transcription–polymerase chain reaction analysis (right) showing the amount of vector-derived transcripts for the indicated forms of ING4 in NIH3T3. The average and standard deviation of three independent assays is shown. The value for wild-type ING4 was used as a reference. (**B**) 293T cells were transiently transfected with the vectors shown and treated with cycloheximide (CHX) alone or combined with MG132, as indicated. Samples were taken at the time points shown and analyzed by western blot with an antibody against the hemmaglutinin (HA) tag, using actin as a loading control. (**C**) Quantitation of half-life experiments. At each time point, the signal for ectopic ING4 was quantitated and normalized relative to the actin signal. The graph shows the average and standard deviations from three independent experiments. (**D**) Western blot analysis of endogenous ING4 in the human lung cancer cell lines H23 and H82.

also showed loss-of-heterozygosity at the chromosomal region encompassing the ING4 locus (5,21). The molecular mechanism responsible for downregulation of ING4 in those tumors retaining normal ING4 alleles is currently unclear. In many cases, ING4 underexpression is associated with increased angiogenesis, advanced tumor grade and poor prognosis (6,7,23,30,41). Truncated forms of the ING4 protein, originating from alternative splicing or frameshift mutations have also been found in primary tumors and tumor cell lines (5,22,23). However, different ING4 splice variants are normally expressed in non-tumor tissue (24) and it is currently unclear whether any of these truncated forms of ING4 are bona fide tumor-specific versions. Interestingly, most of the truncated proteins lack the conserved C-terminal PHD domain and therefore they might act as dominant negatives (7). The remaining class of ING4 alterations in cancer, which we have studied in our report, are missense mutations found in tumor cell lines (5). Our functional assays indicate that the N214D mutation results in a hypomorphic phenotype, and it does not seem to act as a dominant-negative form because it did not abolish endogenous ING4 function. Interestingly, the N214D mutation was found in a lung carcinoma cell line where the second ING4 allele was also inactivated by a frameshift mutation leading to a truncated ING4 protein (5). We predict that the presence of these two independent alterations in the ING4 locus renders these cells defective for ING4 function, and this trait has been selected during tumorigenesis. After submission of this manuscript, Kim *et al.* (42) have reported that a truncated version of ING4 found in human cancer acts as a dominant mutant to promote tumorigenesis. Taken together with our results, these findings highlight the existence of diverse mechanisms for ING4 inactivation in human tumors.

In summary, the current study has revealed that a cancer-associated mutation in ING4 results in abnormally reduced protein stability, which in turn causes defects in several functions of ING4 relevant

as barriers to tumor initiation and/or progression. These results indicate that the loss of ING4 function confers a selective advantage in tumor formation, and highlight the importance of ING4 in tumor protection.

Supplementary material

Supplementary data, Figures 1–6 and Table 1 can be found at http://carcin.oxfordjournals.org/

Funding

Spanish Ministry of Science and Innovation (BFU2006-10882 and SAF2009-09031 to I.P., CTQ2008-03115/BQU to F.J.B. and SAF2007-62292 to B.J.).

Acknowledgements

F.B. is an Ikerbasque Research Professor. We thank D.Pantoja-Uceda and P.Garcia for help with NMR structure calculations and R.Perona for sharing reagents.

Conflict of Interest Statement: None declared.

References

1. Hahn,W.C. *et al*. (2002) Modelling the molecular circuitry of cancer. *Nat. Rev. Cancer*, **2**, 331–341.
2. Hanahan,D. *et al*. (2000) The hallmarks of cancer. *Cell*, **100**, 57–70.
3. Coles,A.H. *et al*. (2009) The ING gene family in the regulation of cell growth and tumorigenesis. *J. Cell. Physiol.*, **218**, 45–57.
4. Zhang,X. (2004) ING4 induces G2/M cell cycle arrest and enhances the chemosensitivity to DNA-damage agents in HepG2 cells. *FEBS Lett.*, **570**, 7–12.
5. Kim,S. *et al*. (2004) A screen for genes that suppress loss of contact inhibition: identification of ING4 as a candidate tumor suppressor gene in human cancer. *Proc. Natl Acad. Sci. USA*, **101**, 16251–16256.
6. Colla,S. *et al*. (2007) The new tumor-suppressor gene inhibitor of growth family member 4 (ING4) regulates the production of proangiogenic molecules by myeloma cells and suppresses hypoxia-inducible factor-1 alpha (HIF-1alpha) activity: involvement in myeloma-induced angiogenesis. *Blood*, **110**, 4464–4475.
7. Garkavtsev,I. *et al*. (2004) The candidate tumour suppressor protein ING4 regulates brain tumour growth and angiogenesis. *Nature*, **428**, 328–332.
8. Li,X. *et al*. (2008) ING4 induces cell growth inhibition in human lung adenocarcinoma A549 cells by means of Wnt-1/B-catenin signaling pathway. *Anat. Rec.*, **291**, 593–600.
9. Shen,J.C. *et al*. (2007) Inhibitor of growth 4 suppresses cell spreading and cell migration by interacting with a novel binding partner, liprin alpha1. *Cancer Res.*, **67**, 2552–2558.
10. Ozer,A. *et al*. (2005) Regulation of HIF by prolyl hydroxylases: recruitment of the candidate tumor suppressor protein ING4. *Cell Cycle*, **4**, 1153–1156.
11. Ozer,A. *et al*. (2005) The candidate tumor suppressor ING4 represses activation of the hypoxia inducible factor (HIF). *Proc. Natl Acad. Sci. USA*, **102**, 7481–7486.
12. Hung,T. *et al*. (2009) ING4 mediates crosstalk between histone H3 K4 trimethylation and H3 acetylation to attenuate cellular transformation. *Mol. Cell*, **33**, 248–256.
13. Palacios,A. *et al*. (2008) Molecular basis of histone H3K4me3 recognition by ING4. *J. Biol. Chem.*, **283**, 15956–15964.
14. Pena,P.V. *et al*. (2006) Molecular mechanism of histone H3K4me3 recognition by plant homeodomain of ING2. *Nature*, **442**, 100–103.
15. Shi,X. *et al*. (2006) ING2 PHD domain links histone H3 lysine 4 methylation to active gene repression. *Nature*, **442**, 96–99.
16. Doyon,Y. *et al*. (2006) ING tumor suppressor proteins are critical regulators of chromatin acetylation required for genome expression and perpetuation. *Mol. Cell*, **21**, 51–64.
17. Nozell,S. *et al*. (2008) The ING4 tumor suppressor attenuates NF-kappaB activity at the promoters of target genes. *Mol. Cell. Biol.*, **28**, 6632–6645.
18. Iizuka,M. *et al*. (2008) Hbo1 Links p53-dependent stress signaling to DNA replication licensing. *Mol. Cell. Biol.*, **28**, 140–153.
19. Shiseki,M. *et al*. (2003) p29ING4 and p28ING5 bind to p53 and p300, and enhance p53 activity. *Cancer Res.*, **63**, 2373–2378.
20. Zhang,X. (2005) Nuclear localization signal of ING4 plays a key role in its binding to p53. *Biochem. Biophys. Res. Commun.*, **331**, 1032–1038.
21. Gunduz,M. *et al*. (2005) Frequent deletion and down-regulation of ING4, a candidate tumor suppresor gene at 12p13, in head and neck squamous cell carcinomas. *Gene*, **356**, 109–117.
22. Raho,G. *et al*. (2007) Detection of novel mRNA splice variants of human ING4 tumor suppressor gene. *Oncogene*, **26**, 5247–5257.
23. Li,M. *et al*. (2009) Reduced expression and novel splice variants of ING4 in human gastric adenocarcinoma. *J. Pathol.*, **219**, 87–95.
24. Unoki,M. *et al*. (2006) Novel splice variants of ING4 and their possible roles in the regulation of cell growth and motility. *J. Biol. Chem.*, **281**, 34677–34686.
25. Palmero,I. *et al*. (2001) Induction of senescence by oncogenic Ras. *Methods Enzymol.*, **333**, 247–256.
26. Goeman,F. *et al*. (2005) Growth inhibition by the tumor suppressor p33ING1 in immortalized and primary cells: involvement of two silencing domains and effect of Ras. *Mol. Cell. Biol.*, **25**, 422–431.
27. Palmero,I. *et al*. (2002) Activation of ARF by oncogenic stress in mouse fibroblasts is independent of E2F1 and E2F2. *Oncogene*, **21**, 2939–2947.
28. Gonzalez,L. *et al*. (2006) A functional link between the tumour suppressors ARF and p33ING1. *Oncogene*, **25**, 5173–5179.
29. Kim,S. (2005) HuntING4 new tumor suppressors. *Cell Cycle*, **4**, 516–517.
30. Li,J. *et al*. (2008) Role of ING4 in human melanoma cell migration, invasion, and patient survival. *Carcinogenesis*, **29**, 1373–1379.
31. Xie,Y. *et al*. (2008) Adenovirus-mediated ING4 expression suppresses lung carcinoma cell growth via induction of cell cycle alteration and apoptosis and inhibition of tumor invasion and angiogenesis. *Cancer Lett.*, **271**, 105–116.
32. Palacios,A. *et al*. (2006) Solution structure and NMR characterization of the binding to methylated histone tails of the plant homeodomain finger of the tumour suppressor ING4. *FEBS Lett.*, **580**, 6903–6908.
33. Gozani,O. *et al*. (2003) The PHD finger of the chromatin-associated protein ING2 functions as a nuclear phosphoinositide receptor. *Cell*, **114**, 99–111.
34. Tsai,K. *et al*. (2008) Two wobble splicing events affect ING4 protein subnuclear localization and degradation. *Exp. Cell Res.*, **314**, 3130–3141.
35. Pena,P.V. *et al*. (2008) Histone H3K4me3 binding is required for the DNA repair and apoptotic activities of ING1 tumor suppressor. *J. Mol. Biol.*, **380**, 303–312.
36. Garate,M. *et al*. (2007) Phosphorylation of the tumor suppressor p33(ING1b) at Ser-126 influences its protein stability and proliferation of melanoma cells. *FASEB J.*, **21**, 3705–3716.
37. Campos,E.I. *et al*. (2004) Mutations of the ING1 tumor suppressor gene detected in human melanoma abrogate nucleotide excision repair. *Int. J. Oncol.*, **25**, 73–80.
38. Chen,G. *et al*. (2010) The tumor suppressor ING3 is degraded by SCF(Skp2)-mediated ubiquitin-proteasome system. *Oncogene*, **29**, 1498–1508.
39. Nie,J. *et al*. (2010) HECT ubiquitin ligase Smurf1 targets the tumor suppressor ING2 for ubiquitination and degradation. *FEBS Lett.*, **584**, 3005–3012.
40. Cai,L. *et al*. (2009) Inhibitor of growth 4 is involved in melanomagenesis and induces growth suppression and apoptosis in melanoma cell line M14. *Melanoma Res.*, **19**, 1–7.
41. Fang,F. *et al*. (2009) Decreased expression of inhibitor of growth 4 correlated with poor prognosis of hepatocellular carcinoma. *Cancer Epidemiol. Biomarkers Prev.*, **18**, 409–416.
42. Kim,S. *et al*. (2010) A dominant mutant allele of the ING4 tumor suppressor found in human cancer cells exacerbates MYC-initiated mouse mammary tumorigenesis. *Cancer Res.*, **70**, 5155–5162.

Received March 26, 2010; revised July 28, 2010; accepted August 8, 2010

SUPPLEMENTARY MATERIAL

1. SUPPLEMENTARY FIGURES

Supplementary Figure 1. Effect of cancer-associated mutations of ING4 in cell migration. (**A**) Conditioned medium from NIH3T3 cells retrovirally infected with the indicated vectors were used to assess their effect in migration of vascular endothelial cells as described in Material and Methods (***, $P<0.001$). (**B**) NIH3T3 cells infected with the indicated vectors were analyzed in a "wound-healing" assay. The gap distance was measured at the indicated time points and it is represented relative to the distance at time 0. The average and standard deviation from two experiments are shown.

Supplementary Figure 2. Functional impact of ING4 mutations in the HT1080 cell line. (**A**) Western Blot analysis of the ectopic expression of wild-type ING4 and the N214D mutant after retroviral infection, using an antibody against the HA tag. (**B**) Percentage of BrdU-positive cells. The graph shows the average and standard deviation of two independent experiments. (**C**) Cell viability. HT1080 cells expressing wild-type or mutant ING4 were treated with different doses of doxorubycin and the percentage of non-viable cells was measured 24 hours later using Trypan blue. The graph shows the average and standard deviation from two independent experiments.

Supplementary Figure 3. (**A**) Overlay of ^{1}H-^{15}N-HSQC spectra of ING4-PHD fingers (188-249) corresponding to the wild-type sequence (black) or the N214D mutant (red). Peaks from amide side chains are connected by straight lines and those of N214 are labeled. Also labeled are the backbone amide signals of N214 (wild-type) and D214 (mutant). (**B**) Bar plot of the differences in the measured CSP for each ING4 PHD residue in the WT and N214D molecule (except for the mutated residue). The experimental error (± 0.012 ppm) is indicated by the dotted line.

Supplementary Figure 4. Protein half-life. 293T cells were transiently transfected with the vectors shown and treated with cycloheximide (CHX) alone or together with the proteasome inhibitor Lactacystin. Samples were taken at the indicated time points (hours) and analyzed by Western Blot with an antibody against the HA tag, using actin as a loading control.

Supplementary Figure 5. Immunofluorescence analysis of NARF2 cells (a derivative of U2OS cells with inducible expression of p14ARF; Stott et al., 1998) transiently transfected with vectors for AU5-tagged wild type or mutant ING4 were treated with IPTG (1 mM, 24 hours) to induce p14ARF expression. An antibody against the AU5 tag was used to detect ectopic ING4, p14ARF was detected with the 54-75 polyclonal rabbit antibody (a gift from David Parry, DNAX). Nuclei were counterstained with DAPI. Right panel shows a larger magnification of representative cells.

Supplementary Figure 6. Western Blot analysis of the endogenous levels of ING4 in the H82 cell line, after addition of the proteasome inhibitor MG132.

2. SUPPLEMENTARY METHODS

Wound healing assay. NIH3T3 fibroblasts infected with retroviruses for the different constructs of ING4 were plated in 6-well plates and left to reach confluence. An incision was made in the cell lawn with a pipette tip and closure of the gap was followed with micro-photographs taken at different times.

NMR spectroscopy and structure determination. NMR experiments were recorded on Bruker AVANCEII 600 MHz (with cryoprobe) and 700 MHz spectrometers at 25 ºC in 20mM sodium phosphate pH 6.5, 50 mM NaCl, 1mM perdeuterated dithiothreitol (DTT) and 9% (v/v) $^{2}H_2O$. Backbone and side chain resonance assignment were obtained using a set of 2D

and 3D NMR spectra recorded on a 0.5 mM PHD^{N214D} sample uniformly enriched in ^{15}N. Chemical shifts were measured relative to internal 2,2-dimethyl-2-silapentane-5-sulfonate sodium salt (DSS) for ^{1}H and calculated for ^{15}N (Wishart et al., 1995). Spectra were processed and analyzed with XWINMR (Bruker), NMRPipe (Delaglio et al., 1995) and NMRView (Johnson, 2004). Distance restraints were obtained from 2D-NOESY and 3D-^{15}N-NOESY spectra (with 120 ms and 80 ms mixing times respectively). Structures were calculated with CYANA and used for NOE assignment in an iterative manner. The structures were refined by energy minimization with AMBER 7.0 (Case et al., 2002). The RMSD between the wild type and mutant proteins was calculated for the ordered region of the chain (195-244) using the mean structures calculated with MolMol (Koradi et al., 1996).

Phosphoinositide binding assay. GST fusion proteins of wild-type and mutant PHD domains (cloned in the plasmid pGEX-6P-2) were purified by affinity GST chromatography (GE Healthcare GST-Trap columns) and gel filtration (Superdex 75, GE Healthcare). PIP strips and soluble D-myo-Phosphatidylinositol 5-phosphate (PI5P) were purchased from Echelon Biosciences. Incubation of PIP strips with GST-PHD molecules at 0.5 μg/ml was performed following the manufacturer's protocol. Binding was detected using an in-house anti-GST monoclonal antibody and a secondary anti mouse IgG-HRP antibody (Sigma) followed by ECL (GE Healthcare) detection.

3. REFERENCES FOR SUPPLEMENTARY MATERIAL

D.A. Case, D.A. Pearlman, J.W. Caldwell, T.E. Cheatham III, J. Wang, W.S. Ross, C.L. Simmerling, T.A. Darden, K.M. Merz, R.V. Stanton, A.L. Cheng, J.J. Vincent, M. Crowley, V. Tsui, H. Gohlke, R.J. Radmer, Y. Duan, J. Pitera, I. Massova, G.L. Seibel, U.C. Singh, P.K. Weiner and P.A. Kollman (2002), AMBER 7, University of California, San Francisco.

Delaglio, F., Grzesiek, S., Vuister, G. W., Zhu, G., Pfeifer, J., and Bax, A. (1995) *J Biomol NMR,* **6**, 277-293.

Johnson, B.A. (2004). *Meth. Mol. Biol,* **278**, 313-352.

Koradi R, Billeter M, Wüthrich K. (1996). *J Mol Graph*, **14**, 29-32.

Laskowski R A, Rullmann J A C, MacArthur M W, Kaptein R, Thornton J M (1996). *Journal of Biomolecular NMR*, **8**, 477-486.

Stott FJ, Bates S, James MC, McConnell BB, Starborg M, Brookes S, Palmero I, Ryan K, Hara E, Vousden KH, Peters G. (1998). *EMBO J*, **17**, 5001-5014.

Wishart, D. S., Bigam, C. G., Yao, J., Abildgaard, F., Dyson, H. J., Oldfield, E., Markley, J. L.,and Sykes, B. D. (1995). *J Biomol NMR,* **6**, 135-140.

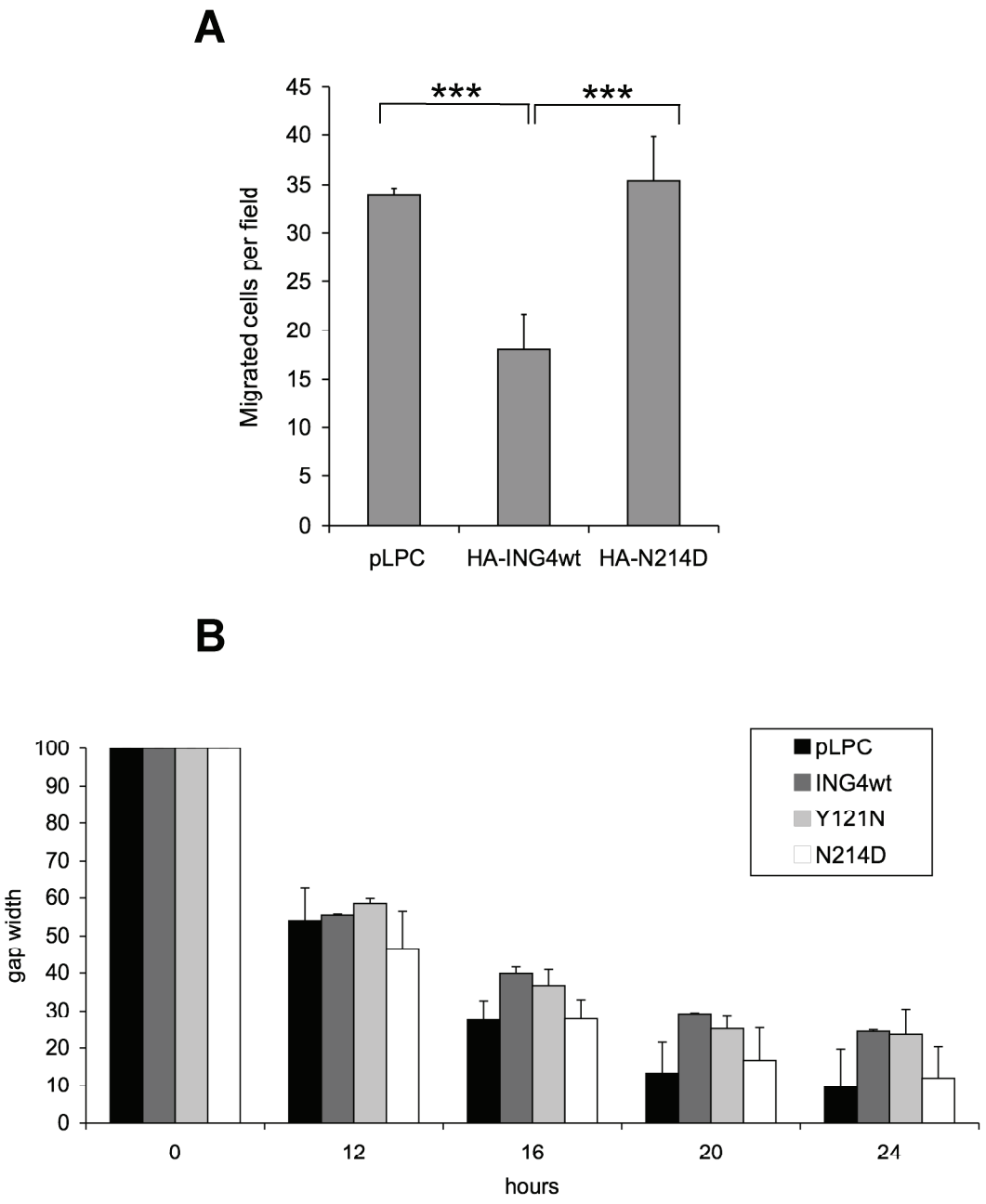

Moreno, Supp Fig. 1

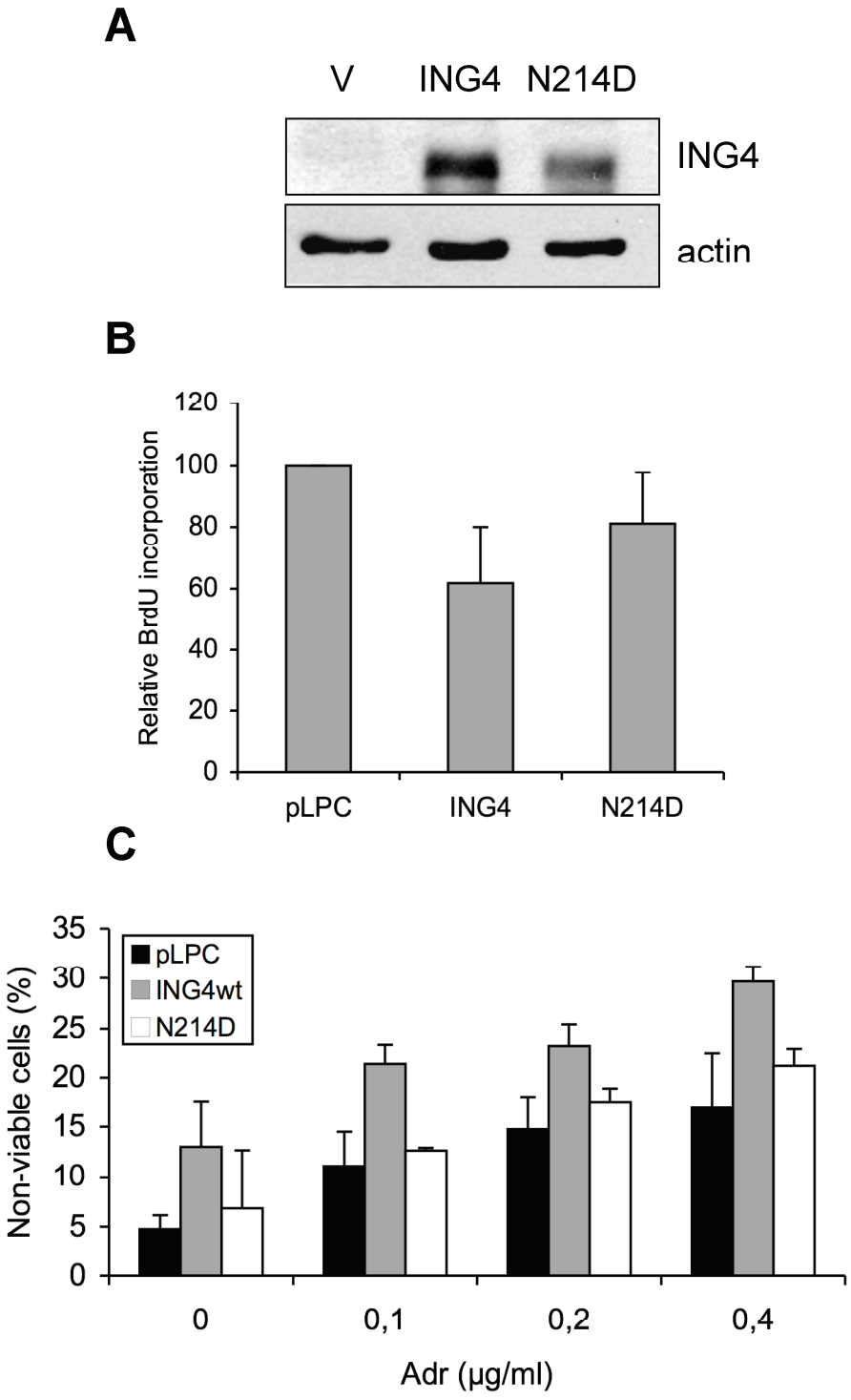

Moreno, Supp Fig. 2

A

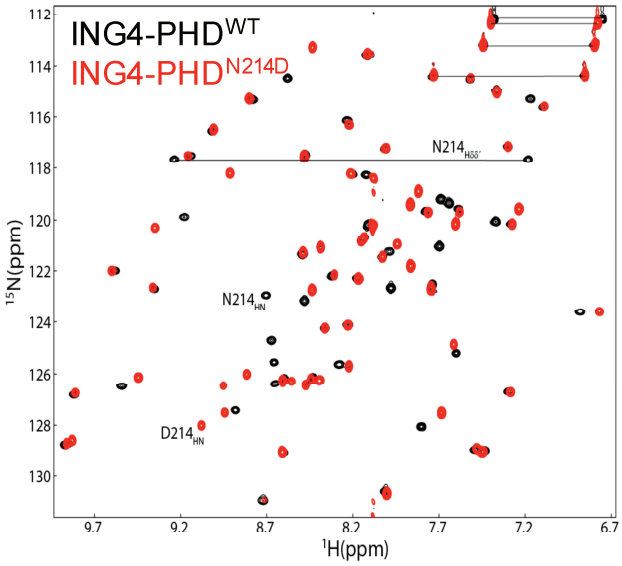

B

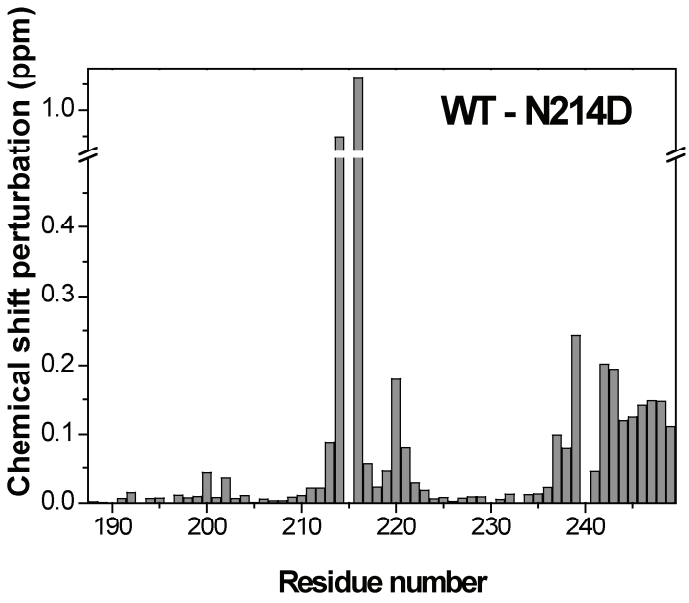

Moreno, Supp Fig 3

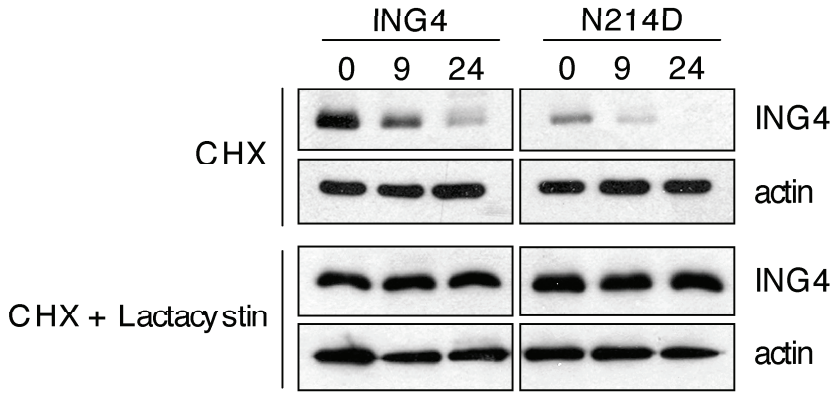

Moreno, Supp Fig. 4

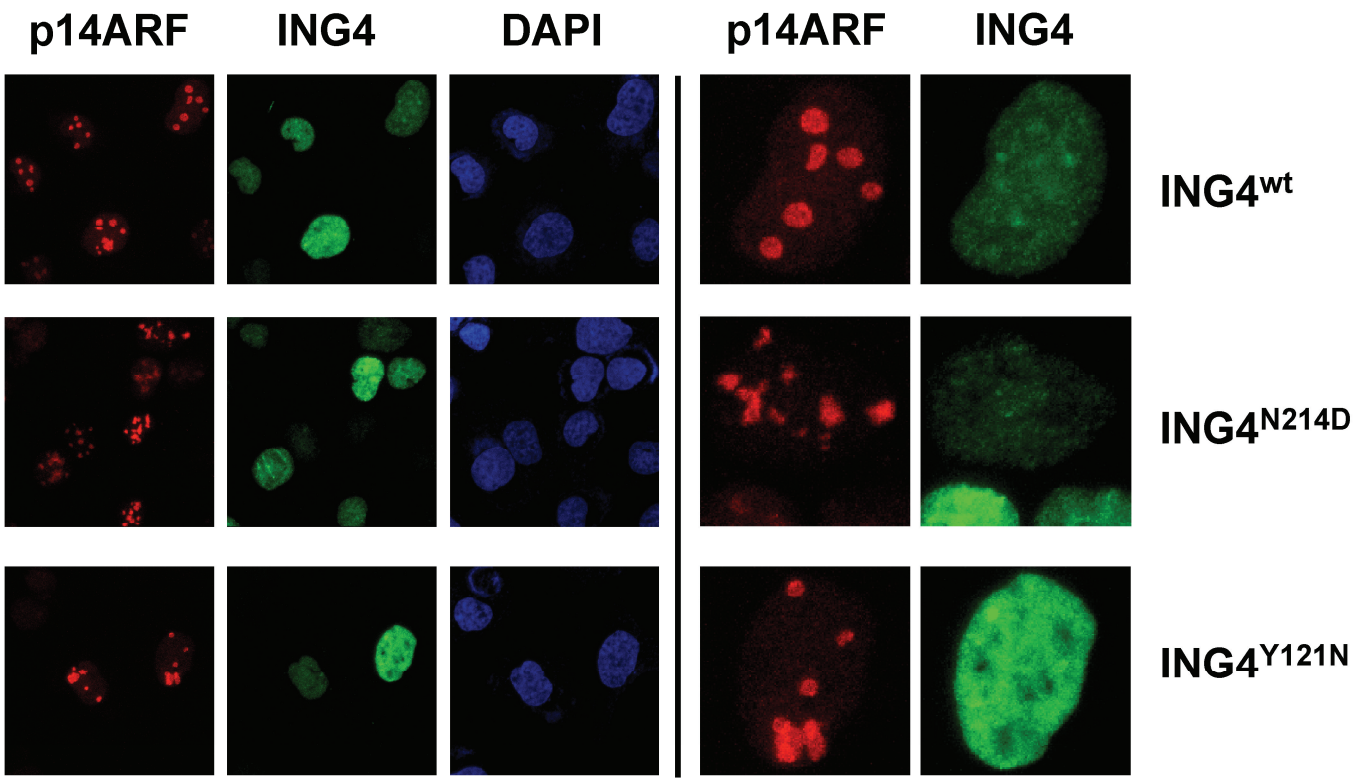

Moreno, Supp Fig. 5

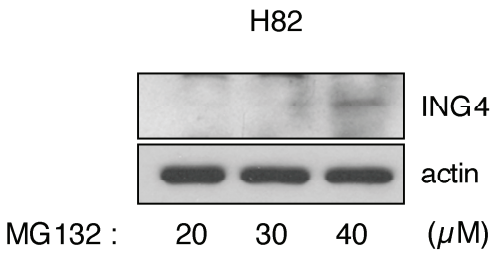

Moreno, Supp Fig. 6

Supplementary Table1. Structural statistics of the 25 best NMR structures of the mutant PHD^{N214D} of ING4 (residues 188-249).

NOE distance constraints	
Intra-residual distances	258
Sequential distances	255
Medium-range distances (i-j) < 5	189
Long-range distances (i-j) ≥ 5	382
Total	1084
Compliance with restraints and force fields	
Final CYANA target function value [a] ($Å^2$)	1.76
Maximum distance restraint violation (Å)	0.35
Number of violations >0.3 Å	4
AMBER energy[b] (kcal/mol)	440
RMS deviations from ideal geometry	
Bond lengths (Å)	0.01
Bond angles (º)	2.35
RMSD to mean coordinates (Å) (195-244)	
Backbone N,C^{α},C'	0.58
All heavy atoms	1.4
Ramachandran plot statistics[c]	
Most favorable regions (%)	56.2
Additional allowed regions (%)	34.2
Generously allowed regions (%)	6.8
Disallowed regions (%)	2.8

[a]The final CYANA target function value was computed for the structure before energy minimization with AMBER.

[b]Average values over the 25 final energy-minimized CYANA conformers.

[c]Calculated with PROCHECK-NMR (Laskowski et al., 1996).

Aging Cell (2011) **10,** pp158–171 Doi: 10.1111/j.1474-9726.2010.00651.x

The tumor suppressor ING1 contributes to epigenetic control of cellular senescence

María Abad,[1,*] Alberto Moreno,[1] Alicia Palacios,[2] Masako Narita,[4] Francisco Blanco,[2,3] Gema Moreno-Bueno,[1] Masashi Narita[4] and Ignacio Palmero[1]

[1]Instituto de Investigaciones Biomédicas ''Alberto Sols'' CSIC-UAM, E-28029 Madrid, Spain
[2]CIC bioGUNE, E-48160 Derio, Spain
[3]IKERBASQUE, Basque Foundation for Science, Bilbao, Spain
[4]Cancer Research UK Cambridge Research Institute, Li Ka Shing Centre, CB2 0RE Cambridge, UK

Summary

Cellular senescence is an effective tumor-suppressive mechanism that causes a stable proliferative arrest in cells with potentially oncogenic alterations. Here, we have investigated the role of the p33ING1 tumor suppressor in the regulation of cellular senescence in human primary fibroblasts. We show that p33ING1 triggers a senescent phenotype in a p53-dependent fashion. Also, endogenous p33ING1 protein accumulates in chromatin in oncogene-senescent fibroblasts and its silencing by RNA interference impairs senescence triggered by oncogenes. Notably, the ability to induce senescence is lost in a mutant version of p33ING1 present in human tumors. Using specific point mutants, we further show that recognition of the chromatin mark H3K4me3 is essential for induction of senescence by p33ING1. Finally, we demonstrate that ING1-induced senescence is associated to a specific genetic signature with a strong representation of chemokine and cytokine signaling factors, which significantly overlaps with that of oncogene-induced senescence. In summary, our results identify ING1 as a critical epigenetic regulator of cellular senescence in human fibroblasts and highlight its role in control of gene expression in the context of this tumor-protective response.
Key words: cellular senescence; chromatin; ING1; p53; histone marks.

Introduction

Higher organisms possess defense mechanisms that restrain the ability of cells with potentially oncogenic alterations to progress to form tumors (Lowe *et al.*, 2004). In this context, cellular senescence has emerged recently as an antiproliferative tumor-suppressive mechanism, at a similar level with apoptosis (Prieur & Peeper, 2008; Collado & Serrano, 2010). Cellular senescence can be elicited by a series of alterations in normal cellular homeostasis, including telomere dysfunction, DNA damage, oxidative stress, or aberrant promitogenic signals (Campisi & d'Adda di Fagagna, 2007; Courtois-Cox *et al.*, 2008). The senescent phenotype is defined by several cellular and molecular markers, best characterized in fibroblasts, including flat extended morphology, increased heterochromatinization, and a pH-specific Beta-Galactosidase activity (Senescence-Associated Beta Galactosidase, SA-BetaGal; Dimri *et al.*, 1995; Collado & Serrano, 2006). Senescence is characterized by a specific gene expression program, where epigenetic regulation plays an essential role (Adams, 2007; Funayama & Ishikawa, 2007; Narita, 2007). The relevance of oncogene-induced senescence as a tumor-protective barrier *in vivo* is now firmly established (Braig *et al.*, 2005; Chen *et al.*, 2005; Collado *et al.*, 2005; Michaloglou *et al.*, 2005; Courtois-Cox *et al.*, 2006; Dankort *et al.*, 2007). Senescence is activated in premalignant lesions, as a result of aberrant mitogenic signals caused by activated oncogenes, blocking progression to malignant lesions (reviewed in Mooi & Peeper, 2006; Collado *et al.*, 2007; Courtois-Cox *et al.*, 2008; Prieur & Peeper, 2008). Given the importance of senescence as an effective tumor-suppressive mechanism, there is an obvious interest in elucidating the regulatory mechanisms of senescence. The ING proteins are a family of sequence-conserved proteins, frequently inactivated in human tumors, which control vital cellular processes such as apoptosis, proliferation, or cell migration (reviewed in Soliman & Riabowol, 2007; Ythier *et al.*, 2008; Coles & Jones, 2009). ING proteins participate in transcriptional control via the reading and establishment of chromatin marks (Champagne & Kutateladze, 2009). In particular, ING proteins act as specific readers of trimethylated Lysine 4 in histone H3 (H3K4me3), a distinctive mark of active promoters and also take part in complexes with histone acetyl-transferase (HAT) or deacetylase (HDAC) activities (Soliman & Riabowol, 2007). ING proteins have also been connected to the p53 pathway, as regulators of p53 protein stability and posttranslational modification, or as transcriptional cofactors, although there is also evidence for p53-independent functions (Coles & Jones, 2009). Given the relevance of cellular senescence as an antitumor barrier, we sought to dissect the mechanisms whereby ING1, the founding member of the ING family, regulates senescence. Our

Correspondence
Ignacio Palmero, Instituto de Investigaciones Biomédicas ''Alberto Sols'' CSIC-UAM, Arturo Duperier 4, E-28029 Madrid, Spain. Tel.: +34 915854491; fax: +34 915854401; e-mail: ipalmero@iib.uam.es
*Present address: Spanish National Cancer Research Center, CNIO, Madrid, Spain.

Accepted for publication *5 November 2010*

Aging Cell

data support a critical role for this protein in the circuitry responsible for implementation of senescence, in a p53-dependent manner, and highlight its role in chromatin control and regulation of gene expression in this context.

Results

p33ING1 induces senescence in human fibroblasts in a p53-dependent manner

To investigate the role of the ING1 locus in cellular senescence, we ectopically expressed p33ING1, the major product of the human ING1 locus (also known as ING1b), in early passage IMR-90 human fibroblasts. Retroviral transduction was used to achieve moderate stable expression, to avoid nonphysiological overexpression. As a control, we used the activated form of the human Ha-Ras oncogene (RasV12), an extensively characterized trigger of oncogene-induced senescence in these cells (Serrano *et al.*, 1997). Enforced expression of ING1 caused a dramatic reduction in proliferation, as shown by a decrease in thymidine incorporation or in the number of BrdU-positive cells (Fig. 1A,D). The inverse correlation between ING1 expression and BrdU incorporation could also be observed in individual cells by immunofluorescence. Eighty-five percent of AU5-positive cells were BrdU-negative, while 65% of AU5-negative cells or vector-infected cells were BrdU-negative, confirming the antiproliferative effect of ectopic ING1 (Fig. 1B). ING1-expressing fibroblasts also displayed distinctive markers of cellular senescence, such as SA-BetaGal activity (Fig. 1C,E), and flat enlarged morphology (Fig. 1C). Thus, ectopic expression of p33ING1 in normal human

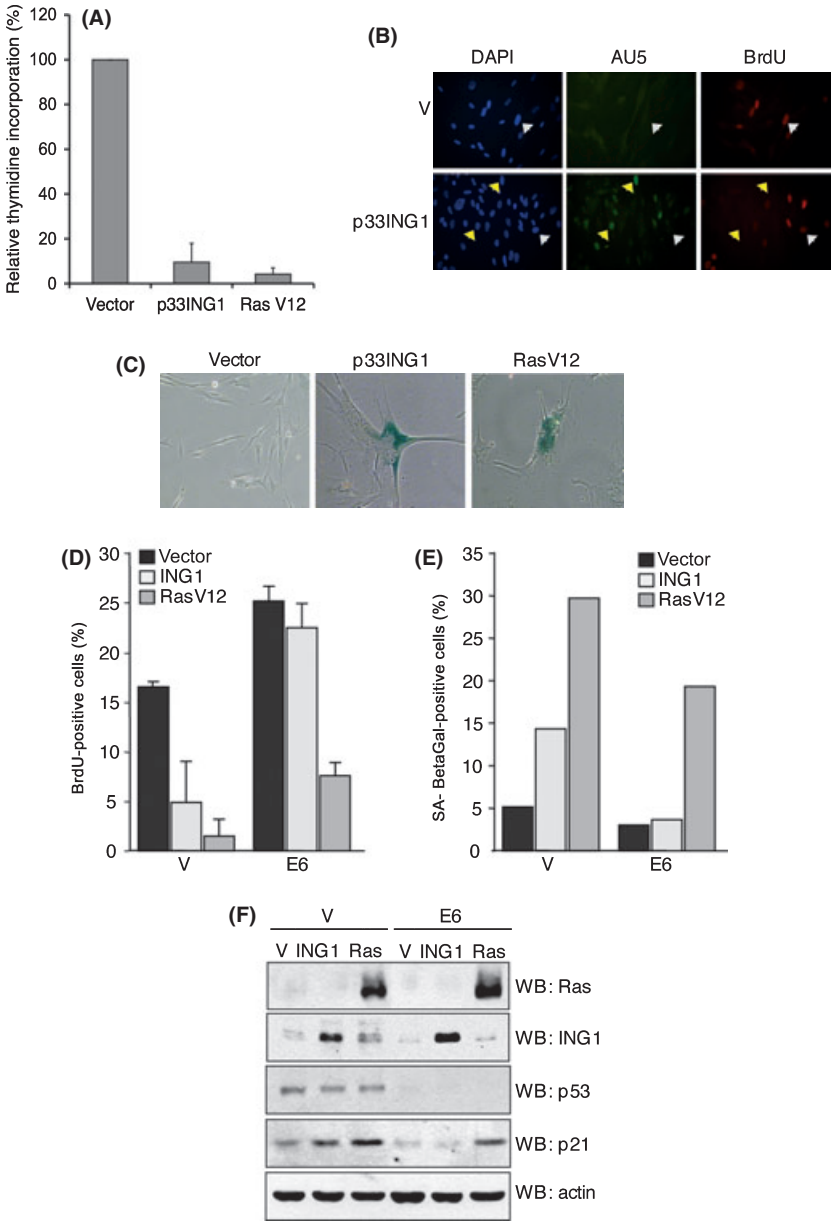

Fig. 1 p53-dependent induction of senescence by ING1. (A) Incorporation of tritiated thymidine in early passage IMR-90 fibroblasts after retroviral transduction with vectors expressing p33ING1, RasV12, or empty vector. The values shown are relative to vector-infected cells. The average and SD from three experiments are shown. (B) Immunofluorescence microscopy showing expression of AU5-tagged ectopic p33ING1 (AU5) and BrdU incorporation (BrdU) in IMR-90 fibroblasts infected with the indicated vectors. Nuclei were counterstained with DAPI. White arrowheads indicate BrdU-positive, ING1-negative cells, and yellow arrowheads indicate BrdU-negative, ING1-positive cells. (C) Representative micrographs of fibroblasts infected with the indicated vectors, after detection of SA-BetaGal activity. (D) Rate of BrdU incorporation of IMR-90 fibroblasts serially infected with the HPV16 E6 oncoprotein (E6) or empty vector, followed by infection with p33ING1, RasV12, or empty vector, at day 6 postselection. The average and SD from three experiments is shown. (E) Percentage of SA-BetaGal-positive cells, as in panel D. A representative experiment at day 6 postselection is shown. (F) Western blot analysis of the indicated proteins in cells serially infected with E6 and p33ING1 (ING1) or RasV12 (Ras).

fibroblasts provokes a cell-cycle arrest with features of cellular senescence, supporting a causal role for ING1 in the implementation of this response (see also Goeman *et al.*, 2005). p33ING1, like other ING proteins, has been functionally linked to the p53 pathway (Coles & Jones, 2009) via mechanisms including control of p53 protein stability, posttranslational modifications or as transcriptional cofactors. In human fibroblasts, both the p53 and the p16INK4A-Rb pathway need to be inactivated to bypass oncogene-induced senescence (Collado *et al.*, 2007). To investigate the functional connection between p33ING1 and p53 in the context of senescence, we inactivated the p53 pathway in these cells, using the E6 oncoprotein from human papilloma virus (Fig. 1F). Ectopic expression of p33ING1 failed to induce a significant cell-cycle arrest in fibroblasts expressing E6 (Fig. 1D). Similarly, the induction of the senescence marker SA-BetaGal by p33ING1 was largely abolished in E6-expressing cells (Fig. 1E). In agreement with previous reports, inactivation of the p53 pathway was not sufficient to bypass senescence by RasV12 in these cells (Fig. 1E), which requires additional inactivation of the Rb pathway (Collado *et al.*, 2007). Interestingly, ING1 increased the level of p21CIP1, a p53 target associated with senescence. The induction of p21CIP1 by ING1 was lost in E6-expressing cells (Fig. 1F), in contrast to the effect of Ras on p21, which is known to be p53-independent (Kivinen *et al.*, 1999). Thus, p33ING1 induces senescence in human fibroblasts through a p53-dependent mechanism.

ING1 is essential for oncogene-induced senescence

To gain insights into the involvement of the endogenous p33ING1 protein in senescence, we analyzed the expression of ING1 in senescent fibroblasts. We observed a clear increase in p33ING1 total protein levels in Ras-senescent fibroblasts, relative to nonsenescent vector-infected fibroblasts (Fig. 2A). The induction of p33ING1 by oncogenic stress was confirmed using an inducible system for oncogene-induced senescence, where the activity of a fusion of the Ras effector MEK with the estrogen receptor (MEK-ER) can be controlled by addition of 4-hydroxy-tamoxifen (4-OHT). The levels of p33ING1 increased in 4-OHT-treated MEK-ER fibroblasts, in parallel with the onset of a

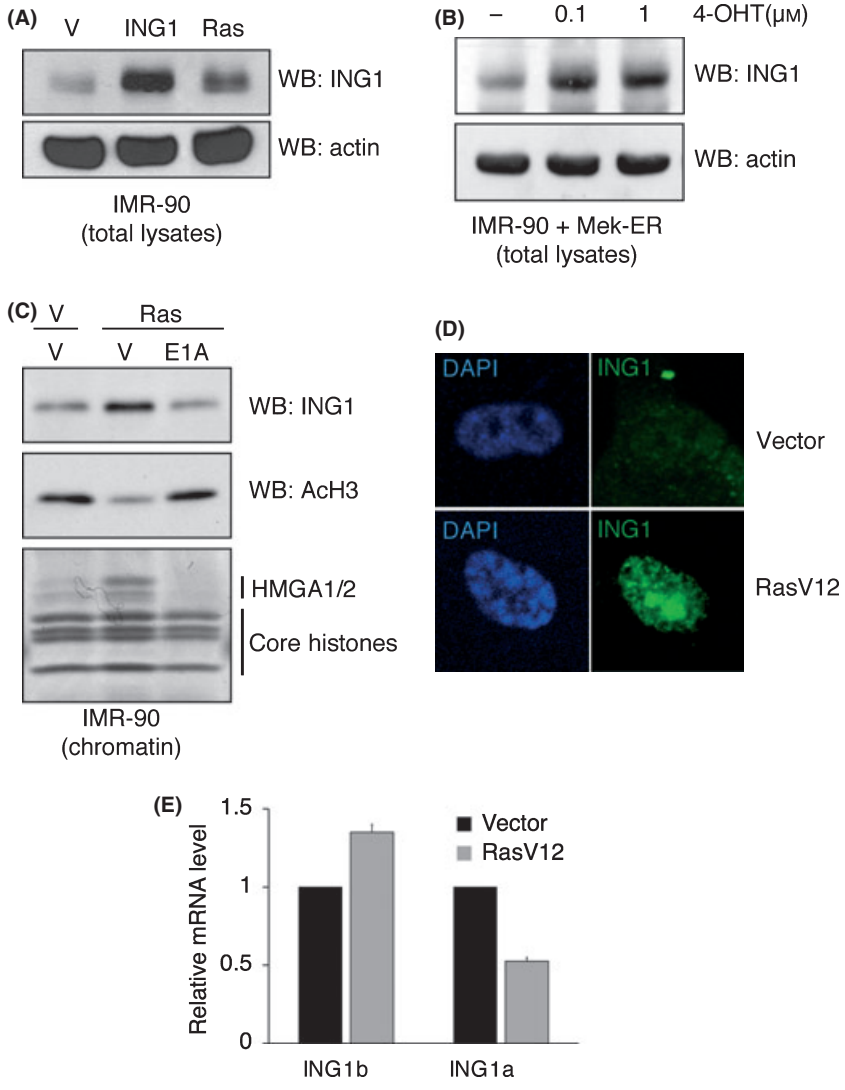

Fig. 2 Regulation of ING1 during senescence. (A) Western blot analysis of the p33ING1 protein in total cell lysates from early passage IMR-90 fibroblasts infected with vectors expressing p33ING1 (ING1) or RasV12 (Ras), at day 6 postselection. (B) Western blot analysis of the p33ING1 protein in IMR-90 fibroblasts expressing MEK with the estrogen receptor 3 days after addition of 4-hydroxy-tamoxifen (4-OHT). (C) Western blot analysis of the indicated proteins in chromatin fractions of IMR-90 cells serially infected with vectors for E1A and Ras, and the corresponding empty vectors. Core histones were detected with Coomassie blue. (D) Immunofluorescence microscopy of Ras-senescent or control IMR-90 fibroblasts with an antibody against ING1. DAPI was used to stain the nuclei. (E) Quantitative PCR analysis of the expression of the ING1a and ING1b transcripts in fibroblasts expressing RasV12 or controls with empty vector. The average and SD from two experiments is shown.

cell-cycle arrest in these cells (data not shown). p33ING1 is a predominantly nuclear protein that participates in transcriptional control. Consistent with the results with total lysates, we observed a clear increase in p33ING1 in the chromatin fraction of Ras-senescent IMR-90 fibroblasts, in parallel with known markers of senescent chromatin, like reduced acetylated histone H3 or increased HMGA histone–like proteins (Narita *et al.*, 2003, 2006) (Fig. 2C; Fig. S1). Significantly, the accumulation of p33ING1 was abolished in fibroblasts co-expressing RasV12 and E1A, an adenoviral oncoprotein that allows bypass of oncogene-induced senescence in these cells by inactivating essential tumor-suppressive pathways (Serrano *et al.*, 1997). This observation clearly establishes a link between ING1 accumulation in chromatin and Ras-induced senescence, and not only Ras signaling. The accumulation of ING1 in nuclei during oncogene-induced senescence was further confirmed in immunofluorescence experiments, using an anti-ING1 antibody (Fig. 2D). We analyzed if the increase in p33ING1 protein levels in senescence could also be observed at the level of RNA. The human *ING1* locus encodes two protein products, p33ING1 (encoded by transcript ING1b) and p47ING1A (transcript ING1a). Quantitative PCR analysis did not show a robust increase in the transcript encoding p33ING1 (transcript ING1b) in Ras-senescent cells (< 2-fold; Fig. 2E), suggesting that the accumulation of p33ING1 is mediated by posttranscriptional mechanisms. It has been reported that p47ING1A RNA and protein increase during replicative senescence in human fibroblasts (Soliman *et al.*, 2008). In contrast to this finding, we observed a decrease in the ING1a-specific transcript in Ras-senescent human fibroblasts (Fig. 2E). We could not study the p47ING1A protein in this setting, because a specific band corresponding to p47ING1A was not detectable in our Western blot experiments (data not shown). Next, we wished to determine whether p33ING1 is a physiological mediator of oncogene-induced senescence. With this purpose, we used stable expression of a miR30-based short hairpin RNA specific for the transcript encoding p33ING1 (transcript ING1b), which led to a clear reduction in p33ING1 protein (Fig. 3A). Vectors encoding sh-ING1b or the empty miR30 backbone were introduced into IMR-90 fibroblasts, previously infected with a MEK-ER vector. Addition of 4-OHT to MEK-ER fibroblasts resulted in a dramatic reduction in their growth rate, indicative of induction of senescence (Fig. 3B). In contrast, the growth of MEK-ER fibroblasts expressing sh-RNA against p33ING1 was not significantly inhibited by 4-OHT, in comparison with control vehicle, although the shRNA itself inhibited growth to some degree. Therefore, p33ING1 accumulates in oncogene-senescent chromatin, and its suppression by RNA interference impairs oncogene-triggered senescence, supporting a critical role for this protein in the implementation of this response.

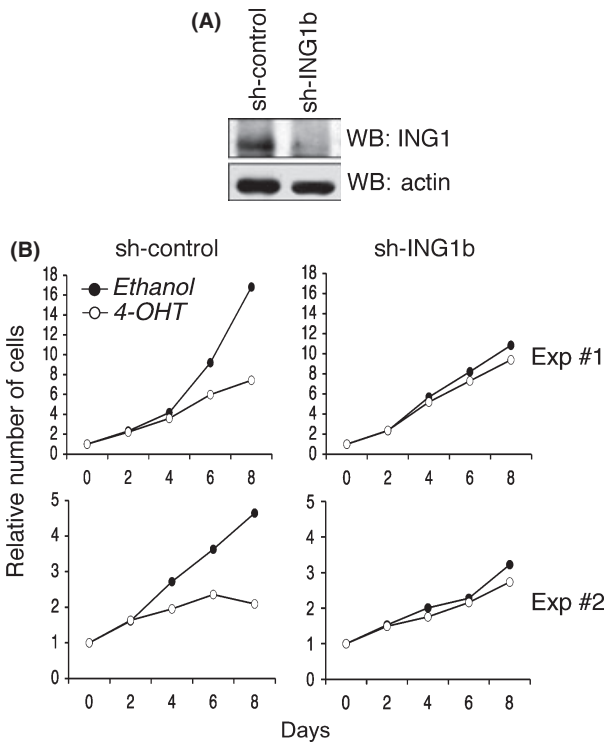

Fig. 3 Bypass of oncogene-induced senescence by RNA interference against p33ING1. (A) Western analysis of p33ING1 protein in IMR-90 fibroblasts infected with the empty shRNAmir vector LMP (sh-control) or a vector expression shRNAmir against p33ING1 (sh-ING1b). (B) Growth curves of IMR90- MEK with the estrogen receptor fibroblasts retrovirally infected with the indicated shRNAmir vectors, treated with 1 μM 4-hydroxytamoxifen or ethanol. The number of cells at each time point is represented relative to the number of cells at day 1. Two independent experiments are shown.

Recognition of chromatin marks is essential for the induction of senescence by ING1

ING proteins participate in the recognition of the histone mark H3K4me3 (histone H3 trimethylated in Lysine 4), a feature of transcriptionally active promoters (Shi *et al.*, 2006; Hung *et al.*, 2009; Palacios *et al.*, 2008; Pena *et al.*, 2006, 2008; reviewed in Champagne & Kutateladze, 2009). Structural studies have identified several residues in the conserved plant homeo domain (PHD) domain essential for the binding of ING proteins to H3K4me3 (Pena *et al.*, 2006; Shi *et al.*, 2006). Given the relevance of epigenetic control in gene regulation during senescence (Adams, 2007; Narita, 2007), we decided to investigate the impact of this feature of ING1 in regulation of senescence. To this end, we designed mutations in two ING1 residues equivalent to those essential for H3K4me3 binding in ING2 and ING4 (Palacios *et al.*, 2006, 2008; Pena *et al.*, 2006; Shi *et al.*, 2006), specifically Tyrosine 212 and Tryptophan 235, which were replaced with Alanines (designated Y212A and W235A, respectively, Fig. 4A). Both mutant p33ING1 proteins were easily detected after retroviral transduction of IMR-90 fibroblasts, reaching levels significantly higher than the wild-type form (Fig. 4B). Immunofluorescence studies also revealed a normal pattern of subcellular localization, showing nuclear staining with no obvious differences in the distribution within the nucleus (Fig. 4C). We investigated the ability of both histone-binding mutants to induce senescence. In contrast to the reduced proliferation observed in cells with wild-type ING1, fibroblasts

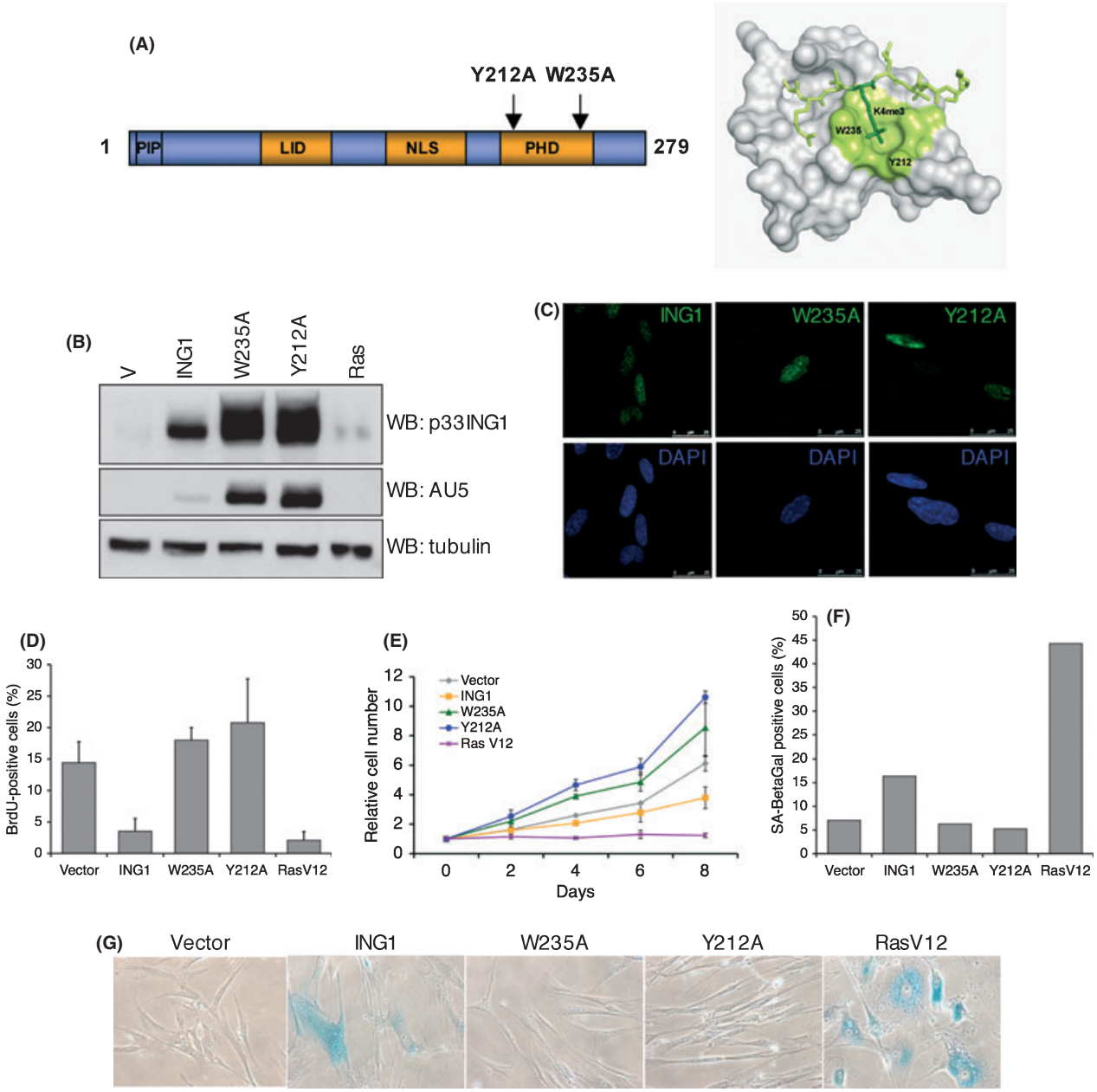

Fig. 4 Recognition of histone marks is essential for ING1-induced senescence. (A) *Left*, Schematic representation of the p33ING1 protein, indicating the position of the residues mutated in this work. PIP, PCNA-interacting protein motif; LID, Lamin Interacting Domain; NLS, nuclear localization signal; PHD, plant homeo domain. *Right*, Three-dimensional model of the complex of ING1-PHD bound to H3K4me3. ING1 is shown in gray, with the hydrophobic pocket involved in the binding highlighted in green. The position of the two mutated residues, Y212 and W235, is shown. The N-terminus of H3K4me3 is shown in green in stick representation. (B) Western blot showing expression of ectopic AU5-p33ING1 (AU5) or total p33ING1 in IMR-90 cells expressing the indicated versions of p33ING1 or RasV12. Tubulin was used as a loading control. (C) Confocal fluorescence images showing subcellular localization of wild-type ING1 (ING1) and the Y212A and W235A mutants in retrovirally infected IMR-90 cells. Nuclei were stained with DAPI. (D) Rate of BrdU incorporation in IMR-90 cells expressing the indicated vectors, at day 6 postselection. The average and SD of three independent experiments is shown. (E) Growth curve of IMR-90 cells as in D. The average and SD of two independent experiments is shown. (F) Percentage of SA-BetaGal-postive cells at day 6 postselection, as in D. A representative experiment is shown. (G) Micrographs showing the morphology and SA-BetaGal staining in cells infected with the indicated vectors.

expressing either of the mutants showed proliferation rates similar or higher than controls, as measured by BrdU incorporation or cumulative growth over an 8-day period (Fig. 4D,E). Consistently, expression of the W235A or Y212A mutants did not cause an increase in the number of SA-BetaGal-positive cells, or provoked a change in cell morphology, in contrast to wild-type ING1 (Fig. 4F,G). Oncogenic Ras was used in these assays as a positive control for senescence induction. These results clearly indicate that the recognition of histone marks is essential for the induction of senescence by p33ING1 in human fibroblasts.

A tumor-associated mutation in ING1 abolishes its ability to trigger senescence

The ING1 locus is inactivated in a large number of human tumors, including squamous cell carcinoma, breast cancer, and melanoma (Nouman *et al.*, 2003; Ythier *et al.*, 2008). The most frequent alteration of ING1 in tumors is its reduced expression and/or aberrant localization. However, a small number of point missense mutations in ING1 have also been found in human tumors. To test the impact of cancer-associated mutations in ING1's ability to trigger senescence, we focused on the C215S mutation found in primary head and neck squamous cell carcinomas (HNSCC) and hepatocellular carcinomas (HCC; Gunduz *et al.*, 2000). The mutated residue (Cys 215) is predicted to play an essential role in stabilizing the structure of the conserved PHD domain. We confirmed that an ING1 PHD domain containing the C215S mutation is essentially unfolded in solution (Fig. S2; see Data S1 for Methods). To test whether this cancer-associated mutation in ING1 could impinge in its ability to trigger senescence, we infected IMR-90 early passage fibroblasts with a retrovirus expressing the C215S mutant. As with the other mutants used in this study, the C215S version was easily detected, reaching levels higher than the wild-type protein (Fig. 5A) and showed normal nuclear localization (data not shown). Ectopic expression of this mutant version of ING1 failed to trigger an antiproliferative response in human fibroblasts (Fig. 5B). Also, no obvious induction of senescence markers, such as flat morphology or SA-BetaGal activity, was observed (Fig. 5C and 5D). Thus, a mutation in ING1 present in human tumors abolishes ING1-induced senescence. This observation further strengthens the link between regulation of senescence by ING1 and its tumor-protective action.

Connection of ING1 with SAHFs

In human fibroblasts, and some other cell types, senescence is accompanied by the appearance of macroscopic regions of facultative heterochromatin, known as senescence-associated heterochromatin foci, or SAHFs (Narita *et al.*, 2003, 2006). The SAHFs are identified as spots with intense DAPI staining, they are enriched in heterochromatin markers, such as heterochromatin protein1 (HP1) and H3K9me3, and exclude euchromatic markers, like acetylated histones and H3K4me3 (Narita *et al.*, 2003, 2006). As the link to transcriptional repression and chromatin control appears to be essential for senescence induction by ING1 (Fig. 4, see also Goeman *et al.*, 2005), we set to investigate the connection between ING1 and the SAHFs. Consistent with their relative ability to trigger senescence, ectopic expression of wild-type ING1 led to an increase in SAHF-positive cells, a robust senescence marker in this cell type, but no increase was observed after expression of either histone-binding mutant (Fig. 6A). However, we did not observe a significant accumulation of ectopic or endogenous ING1 in the SAHFs, in immunofluorescence experiments. Consistent with our data showing that the pro-senescence activity of p33ING1 requires H3K4me3 association, ING1, like H3K4me3, was found excluded from SAHFs (Figs 6B and S3). Thus, these data reinforce the critical role of the association between ING1 and H3K4me3 for senescence induction.

ING1-induced senescence is defined by a specific genetic signature

Our results with histone-binding mutants of p33ING1 strongly support the notion that induction of senescence by p33ING1

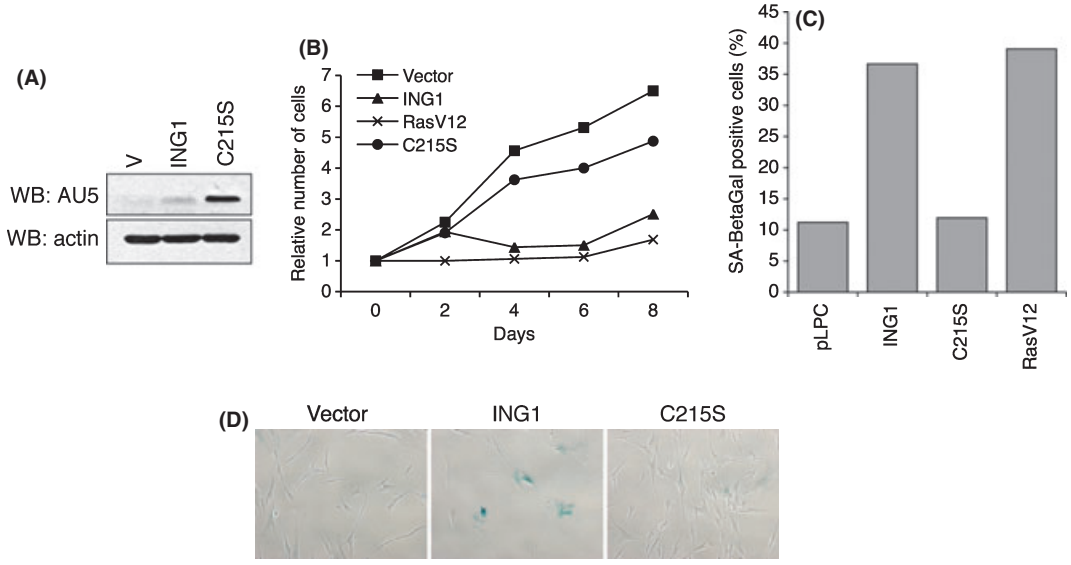

Fig. 5 Lack of senescence induction in a cancer-associated ING1 mutant. (A) Western blot showing the expression of ectopic AU5-tagged wild-type p33ING1 (ING1) or the C215S mutant. Actin was used as a loading control. (B) Growth curves of IMR-90 fibroblasts expressing the indicated vectors. (C) Percentage of SA-BetaGal-positive cells after infection of IMR-90 fibroblasts with the indicated vectors, at day 6 postselection. A representative experiment is shown. (D) Micrographs showing the morphology and SA-BetaGal staining in IMR-90 fibroblasts infected with the indicated vectors.

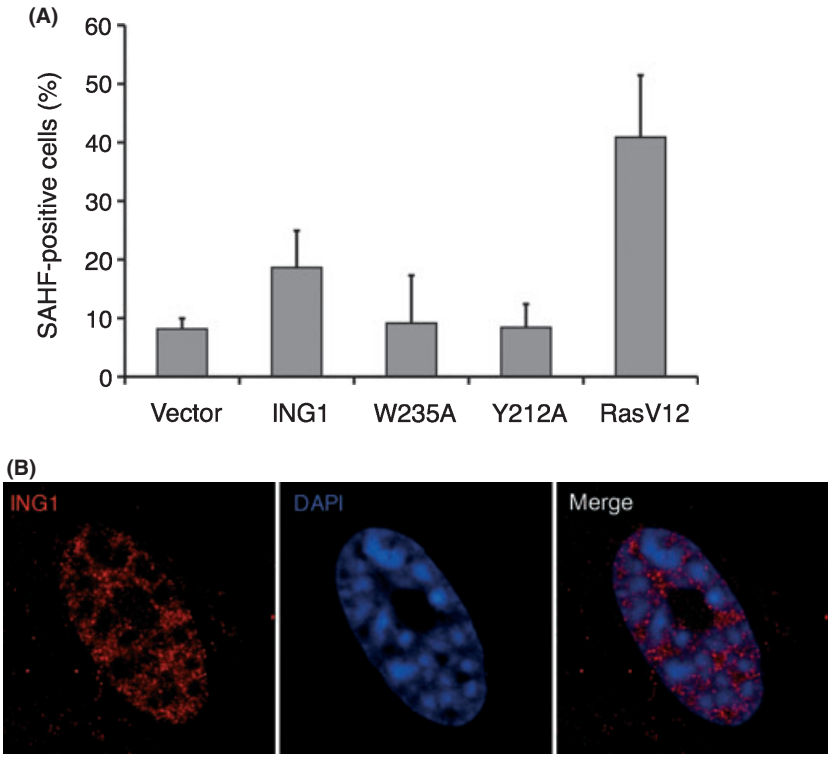

Fig. 6 Connection of ING1 with SAHFs. (A) Percentage of SAHF-positive cells in IMR-90 fibroblasts infected with the indicated vectors. The average and SD from three experiments is shown. (B) Confocal fluorescence images showing subcellular localization of endogenous ING1 in Ras-senescent IMR-90 fibroblasts. SAHFs are visualized as hyperchromatic foci in the DAPI staining.

depends on its ability to regulate gene expression through recognition and establishment of chromatin marks. To investigate the transcriptional signature associated with the induction of senescence by p33ING1, we performed a genome-wide expression profile analysis. To this end, early passage IMR-90 fibroblasts were infected with vectors encoding wild-type p33ING1 or the Y212A and W235A mutants. Ras-senescent fibroblasts were also analyzed, as a control for oncogene-induced senescence. Total RNA was prepared at a time postselection where the differential effects of each ING1 protein were evident (Fig. S4A) and used to interrogate whole genome expression arrays. A subset of 286 genes was differentially expressed at least twofold in IMR-90 fibroblasts arrested by wild-type ING1 expression, with respect to vector-infected fibroblasts (Table S1). Within this group, 200 genes (70%) were upregulated in ING1-expressing cells, while 86 genes (30%) were downregulated. Next, we compared the expression profiles caused by wild-type or histone-binding-mutant versions of p33ING1. Of note, the expression profiles caused by the two mutants were highly similar (over 69% coincidence). This pattern is in keeping with the expected structural consequences of the mutations and their impact in senescence. Most importantly, the expression patterns associated with wild-type or mutant ING1 could be easily discriminated. For 72% of the genes associated with wild-type ING1, the expression in both mutants was different to wild type, raising to 94% in at least one of the mutants (Fig. 7D, Table S1). In most cases, genes regulated with wild-type ING1 were unchanged with the mutants (151 genes, 53%), but we also found some examples (31 genes, 11%) of opposite regulation in wild type and mutants that might reflect dominant-negative effects (see for example CXCR7, upregulated by ING1 and downregulated by the mutants; or HHIP1, with the reverse pattern (Table S1, Fig. 7C). Interestingly, although both histone-binding mutants behaved very similarly in this assay, there were statistically significant differences between them, with a higher similarity between the Y212A mutant and wild-type ING1. These results closely correlate with the binding affinities for H3K4me3 of each mutant (Pena *et al.*, 2008). The functional category analysis of ING1-regulated genes identified a significant enrichment for genes involved in chemokine and cytokine signaling. Notably, these factors have recently been identified as important regulators of senescence, as part of the senescence associated secretory phenotype (SASP) (Acosta *et al.*, 2008; Kuilman *et al.*, 2008) (Fig. S4B). Next, we compared the set of ING1-specific genes with those modified in Ras-senescent fibroblasts to identify common signatures between Ras- and ING1-induced senescence. We found a significant overlap between both signatures (24% of genes with statistically significant differential expression, with a FDR of 0.10) and selected a group of 45 genes coregulated in Ras-senescent and ING1-senescent cells (Fig. 7A). Interestingly, although p33ING1 caused both up- and downregulation, the similarity between p33ING1 and Ras was higher within the set of genes downregulated by ING1 (Fig. 7D). As for the complete set of ING1-regulated genes, the subset overlapping with Ras also showed a significant enrichment for genes involved in chemokine and cytokine signaling (Fig. 7B; Acosta *et al.*, 2008; Kuilman *et al.*, 2008). The differential expression

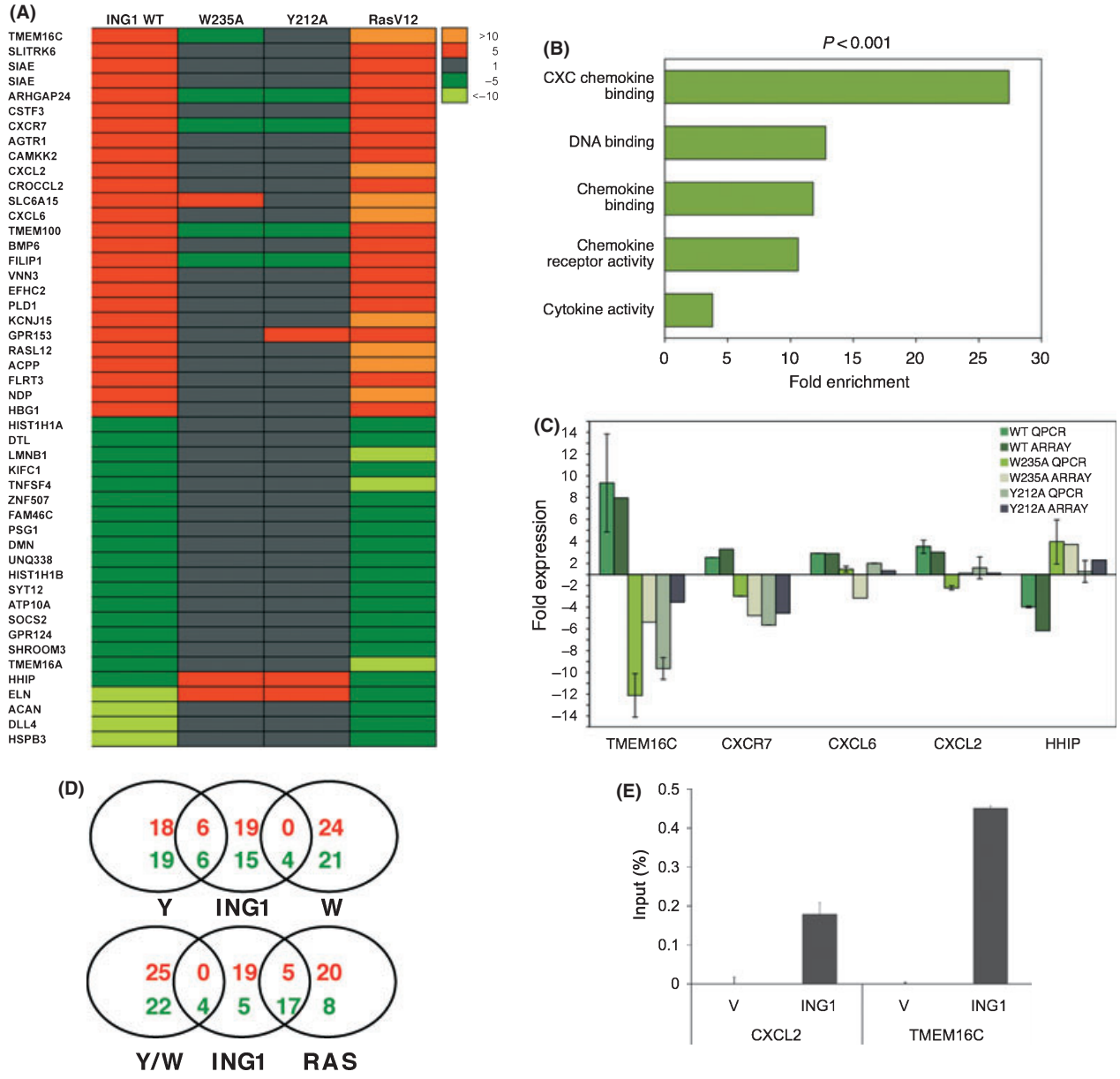

Fig. 7 Genetic signature of ING1-induced senescence. (A) Heat-map representation of gene expression profiles of genes with differential expression in ING1-infected fibroblasts, no regulation with ING1 mutants and overlapping expression with Ras-infected fibroblasts (see text for details). (B) Functional enrichment analysis of the subset of genes represented in A. The fold enrichment of the indicated set relative to total genome is represented for each category. Statistical significance was determined with a Fisher's exact test using the FatiGO application (C). Validation by real-time quantitative PCR of a selection of genes identified in the microarray analysis. The expression relative to vector-infected controls is shown. In each case, the relative expression data obtained from the array is shown for reference. The average and SD from three independent QPCR assays is shown. (D) Venn diagram of genes with differential expression in IMR-90 with wild-type p33ING1 (ING1), relative to the Y212A mutant (Y), the W235A mutant (W), both mutants together (Y/W) or RasV12 (RAS). The data corresponds to the 50 genes most up- or downregulated in each set. Red numbers indicate upregulated genes and green numbers, downregulated genes. (E) Chromatin immunoprecipitation showing binding of ectopic p33ING1 to promoter regions of CXCL2 and TMEM16C. The graph shows the percentage of input immunoprecipitated with the AU5 antibody for each locus in vector (V) or AU5-p33ING1 (ING1) infected fibroblasts, after substraction of background (nonspecific antibody precipitation). The average and SD from triplicates are shown.

results from the microarray analysis were successfully validated for a selection of genes, using real-time quantitative PCR (Fig. 7C). To test the direct involvement of ING1 in the transcriptional regulation of these genes, we performed chromatin immunoprecipitation (ChIP) assays for two of the genes of the ING1 signature, CXCL2 and TMEM16C. ChIP assays showed specific binding of ectopic p33ING1 to chromatin in promoter regions of both genes in ING1-senescent fibroblasts (Fig. 7E). Of note, in both cases, ING1 binding was detected within a genomic region enriched in H3K4me3 marks in IMR90 cells (http://neomorph.salk.edu/human_methylome/browser.html). Thus, induction of senescence by p33ING1 is characterized by a

specific genetic signature, which partially overlaps with that of Ras-induced senescence, with a strong presence of genes of the senescent secretory phenotype.

Discussion

The products of the *ING1* locus participate in the control of cellular processes relevant to tumor protection, such as apoptosis, cell-cycle arrest, or DNA repair (Soliman & Riabowol, 2007; Coles & Jones, 2009; Menendez *et al.*, 2009). Alterations of the *ING1* locus are frequent in different types of human tumors (Nouman *et al.*, 2003; Ythier *et al.*, 2008), indicating an important role in tumor suppression. Likewise, mice genetically deficient in the *Ing1* locus show increased predisposition to lymphoma formation (Kichina *et al.*, 2006; Coles *et al.*, 2007). Senescence is increasingly recognized as an essential tumor-suppressive mechanism (Campisi & d'Adda di Fagagna, 2007; Prieur & Peeper, 2008; Collado & Serrano, 2010). Therefore, identifying the mechanism by which tumor suppressors engage the senescent response is highly relevant to understand how they prevent tumor formation, and the impact of their alterations in human tumors. The link between ING proteins and cellular senescence has been previously investigated (Garkavtsev & Riabowol, 1997; Goeman *et al.*, 2005; Pedeux *et al.*, 2005; Abad *et al.*, 2007; Soliman *et al.*, 2008; reviewed in Menendez *et al.*, 2009). However, these studies have frequently led to conflicting results, and the role of specific ING isoforms or the precise mechanisms involved have remained unclear. Here, we have used cell-based gain and loss of function approaches, combined with expression profiling to dissect the role of p33ING1 in senescence. Collectively, our results identify ING1 as a critical epigenetic regulator of oncogene-induced senescence in human fibroblasts. We show that p33ING1 accumulates in chromatin during oncogene-driven senescence, ectopic p33ING1 triggers a senescent phenotype, and RNA interference against p33ING1 impairs growth inhibition by the MEK oncogene. From a mechanistic point of view, one of the major conclusions of our work is that chromatin-mediated gene regulation has an essential role in senescence control by ING1. ING1 participates in gene regulation via the recognition of the chromatin mark H3K4me3 and recruitment of histone-modifying complexes (Champagne & Kutateladze, 2009). We show here that the independent mutation of two residues essential for H3K4me3 binding abolishes ING1's ability to induce senescence. Biophysical and biochemical studies with ING1 and the close homolog ING2 indicate that the Y212 and W235A mutations used in this study specifically impair binding to H3K4me3, but they do not disrupt folding or interaction with partners (Pena *et al.*, 2006, Pena *et al.*, 2008; Shi *et al.*, 2006). Supporting this notion, we find that all the ING1 mutants used in our study (Y212A, W235A, C215S) retain the ability to coprecipitate with p53, an interaction critical for ING1 tumor-suppressive action (Fig. S5). Thus, our data establish a clear correlation between H3K4me3 recognition and senescence induction by ING1. Previous reports have revealed an important role in senescence for a number of proteins involved in the establishment or recognition of chromatin marks, like BMI (Jacobs *et al.*, 1999), CBX7 and 8 (Gil *et al.*, 2004; Dietrich *et al.*, 2007), JMJD3 (Barradas *et al.*, 2009), or Suv39H (Braig *et al.*, 2005). ING proteins are highly specific readers of H3K4me3 marks. Genetic alterations that result in aberrant addition, removal, or reading of this chromatin mark are frequent in leukemias and solid tumors (Chi *et al.*, 2010). However, evidence of direct involvement of H3K4me3 regulators in senescence is scarce. The MLL1 methylase (Kotake *et al.*, 2009) and the dual H3K4me3/H3K36me de-methylases JHDM1A and JHDM1B (He *et al.*, 2008; Pfau *et al.*, 2008) are mediators of oncogene and replicative senescence, via the regulation of the Ink4a/Arf locus. To our knowledge, ING proteins (this report and Pedeux *et al.*, 2005) are the only examples of specific H3K4me3 readers involved in senescence, further underlying the importance of proper regulation of this mark in the context of chromatin dynamics in senescence.

Transcriptional repression of some loci during senescence occurs in heterochromatin domains known as SAHFs (Narita *et al.*, 2003, 2006). ING1 has been linked to transcriptional repression (Kuzmichev *et al.*, 2002; Goeman *et al.*, 2005), and we show here that it accumulates in senescent chromatin. However, ING1 does not appear to be a stable component of the SAHFs. Rather, it was found consistently excluded from the SAHFs and frequently enriched in its periphery. Of note, H3K4me3 is also excluded from the SAHFs (Narita *et al.*, 2003). Two hypothesis consistent with ING1's bivalent role as reader of active chromatin marks and component of repressor complexes (Champagne & Kutateladze, 2009) could be considered. p33ING1 might contribute to define the boundaries between SAHFs and active chromatin. Alternatively, it might participate in the dynamic switch between transcriptional activation and repression in euchromatin of senescent nuclei. Further experiments are needed to identify the precise mechanism linking ING1 to chromatin domains in senescent cells.

Our expression analysis has allowed us to define a distinct genetic signature for ING1-induced senescence of human fibroblasts, which partially overlaps with that associated to Ras-induced senescence. Interestingly, this common signature is enriched in mediators of cytokine and chemokine signaling. Cytokines and chemokines play critical roles in different aspects of normal physiology and pathology, including inflammation, immune response, or tumor growth and metastasis (Mantovani *et al.*, 2008; Lazennec & Richmond, 2010; Schetter *et al.*, 2010). Cytokines and chemokines can induce proliferation of tumor or normal cells (Mantovani *et al.*, 2008), but they can also promote senescence (Acosta *et al.*, 2008; Coppe *et al.*, 2008; Kuilman *et al.*, 2008; Wajapeyee *et al.*, 2008; Rodier *et al.*, 2009) defining the so-called SASP or senescence-messaging secretome (SMS) (Kuilman & Peeper, 2009). Our data suggest that the pro-senescence action of ING1 in primary fibroblasts is largely mediated by the activation of a secretory response, similarly to other senescence triggers. ING1, like

other ING proteins, can cooperate with NF-kappaB in transcriptional control (Garkavtsev *et al.*, 2004; Gomez-Cabello *et al.*, 2010), and putative NF-kappaB sites are present in many genes of the ING1 signature (data not shown). Interestingly, NF-kappaB is an important player in gene regulation during senescence, in part as a regulator of SASP/SMS genes (Bernard *et al.*, 2004; Acosta *et al.*, 2008; Wang *et al.*, 2009). Collectively, our results are consistent with a model where ING1 contributes to SASP/SMS gene expression during senescence, in cooperation with NF-kappaB.

The ING protein ING2 has also been implicated in cellular senescence. Similarly to p33ING1, ING2 can trigger senescence in a p53-dependent manner (Pedeux *et al.*, 2005), but conflicting results have been described for the silencing of ING2 (Pedeux *et al.*, 2005; Kumamoto *et al.*, 2008). Interestingly, ING2 is the ING protein most closely related to p33ING1, and they are associated to similar transcriptional repressor complexes (Doyon *et al.*, 2006). It is feasible that regulation of senescence is a common feature of this subclass of 'repressor INGs', and it would be interesting to determine whether the role of ING2 in senescence involves a chromatin-related mechanism, as with ING1.

While chromatin-mediated regulation appears to be the essential feature for induction of senescence by ING1, other mechanisms might also play a role. DNA damage caused by hyperproliferation, telomere dysfunction, or other stimuli can activate senescence (Campisi & d'Adda di Fagagna, 2007; Collado *et al.*, 2007). We have found evidence of a DNA damage response in ING1-expressing cells but this response was very limited and, more importantly, did not correlate with the ability to induce senescence of the different ING1 versions tested (Fig. S6).

Our results also show that the implementation of senescence by p33ING1 requires an intact p53 pathway. The p53 pathway plays an essential role in senescence control in different settings. In the case of the human fibroblasts, the Rb pathway plays a similar role and concomitant inactivation of both pathways is required to bypass senescence (Campisi & d'Adda di Fagagna, 2007; Collado *et al.*, 2007). There are conflicting results about the dependence on p53 of the biologic functions of ING1 *in vivo* or *in vitro* (Coles & Jones, 2009). Most likely, the link between ING1 and p53 is context dependent. In this respect, our data clearly indicate that implementation of senescence by ING1 in this cell type is fully dependent on p53, and therefore represents an example of a p53-dependent function of ING1 linked to tumor protection.

ING1 can be altered by different mechanisms in human cancer, including missense point mutations in a subset of tumors (Ythier *et al.*, 2008). We find that a version of p33ING1 carrying a cancer-associated mutation was ineffective in induction of senescence. This is the first direct evidence of the association between senescence and tumor-specific alterations in ING1. Taken together with the independent observation of defective apoptosis in other tumor-associated ING1 mutants (Pena *et al.*, 2008), our results strongly indicate that the ability to implement cellular senescence is a requisite for an effective tumor-protective action by ING1, further supporting the notion that apoptosis and senescence play equivalent roles as protective barriers against tumorigenesis.

Experimental procedures

Cell culture

IMR-90 primary human diploid fibroblasts were obtained from the American Type Culture Collection (ATCC; Manassas, VA, USA) and grown in Dulbecco's modified Eagle's medium (GIBCO, Grand Island, NY, USA) supplemented with 10% fetal calf serum and containing antibiotics, at 37 °C in 5% CO_2. As exceptions, IMR-90 cells infected with the E6 oncoprotein were grown in medium with 20% fetal bovine serum, and IMR-90 expressing an inducible form of MEK1 (MEK1:ER) were cultured in DMEM without Phenol Red (GIBCO).

Mutagenesis

Mutant versions of p33ING1 were generated using the Quick Change Site-Directed Mutagenesis Kit (Stratagene, La Jolla, CA, USA), using as a template the ORF of the human p33ING1 protein cloned in the retroviral vector pLPC (Goeman *et al.*, 2005). Specific mutations were incorporated by PCR using Pfu Turbo DNA Polymerase (Stratagene), and they were confirmed by sequencing.

RNA interference vectors

For the generation of shRNAmirs, we used the LMP vector (Dickins *et al.*, 2005, a gift from S. Lowe, CSHL, USA) that allows the production of specific shRNAs using a miR30 microRNA backbone. The cloning of the ING1b-specific sequence into the LMP vector was performed following the recommended protocols (http://www.openbiosystems.com). The ING1b sequence targeted was ACCTTTCGACTTGCAGAGAAAT (nucleotides 77–99, relative to the AUG).

Retroviral transduction

We used early passage IMR-90 with < 30 PDL (*Population Doubling Level*) in all our experiments. We performed retroviral transduction with amphotropic and ecotropic viruses. In the latter case, IMR-90 cells were previously infected with a virus driving the expression of the ecotropic receptor. Retroviral infection was performed essentially as described in Goeman *et al.*, 2005, with minor modifications. In brief, for the production of virus, 293T cells were transiently transfected with 10 μg of pCLEco or pCLAmpho vector (which express the viral genes *gag, pol* and *envEco or envAmpho*) and 10 μg of the vector of interest. Forty-eight hours later, the supernatant containing the viral particles was diluted 1 in 2 with fresh medium, filtered, and polybrene was added to a final concentration of

8 μg mL^{-1}. This supernatant was added to IMR-90 cells, seeded the previous day at a concentration of 8×10^5 cells per 10-cm dish. This procedure was repeated 12 h later using 4 μg mL^{-1} of polybrene and 24 h later using 8 μg mL^{-1}. After 24 h of recovery with fresh medium, cells were subjected to antibiotic selection (2 μg mL^{-1} of Puromycin or 400 mg mL^{-1} of G418) for a period of 3–6 days.

Growth curves

Infected cells were seeded in duplicate a day after the end of selection at a density of 20 000 cells per well in 24-well plates. At the indicated time points, cells were trypsinized and counted. In the case of MEK1-inducible IMR-90 cells, following infection with the shRNA-mir vectors and selection, cells were treated with 1mM of 4-OHT (Sigma, St Louis, MO, USA), or with an equivalent amount of ethanol. Cells were trypsinized and counted at the indicated time points, after beginning of treatment.

Senescence-associated Beta-Galactosidase activity assay

Infected and selected IMR-90 cells were seeded in 6-well plates at a density of 40 000 cells per well. The day after, cells were fixed and stained for SA-BetaGal activity as previously described (Dimri *et al.*, 1995). At least 200 cells were counted to measure the percentage of SA-BetaGal-positive cells.

BrdU incorporation assay

IMR-90 cells were plated in 8-well glass chamber slides (LabTek, Rochester, NY, USA), at 30 000 cells per chamber). Twenty-four hours later, cells were incubated for 6 h with 10 μM BrdU. BrdU-positive cells were detected by immunofluorescence using an anti-BrdU antibody (1:1000 dilution; Megabase Research Products, Lincoln, NE, USA). Cells were costained with DAPI to visualize nuclei. To determine the percentage of BrdU-positive cells, at least 200 nuclei were counted.

Immunofluorescence

Cells were seeded in chamber slides as above-mentioned at a density of 30 000 cells per chamber. Twenty-four hours later, they were processed essentially as described in (Gonzalez *et al.*, 2006). We used the following antibodies: AU5 (1:500, MMS-135R Covance, Princeton, NJ, USA), ING1 (LG1, a rabbit polyclonal against the C-terminus of the human p33ING1 protein; 1:500), gamma-H2AX (1:500, JBW301; Upstate, Billerica, MA, USA).

Western blot

Preparation of total lysates and Western blot analysis was carried out as previously described (Palmero *et al.*, 2002). Chromatin was isolated as described (Narita *et al.*, 2006). The antibodies used were p53 (1:500, DO-1; Santa Cruz, Santa Cruz, CA, USA), ING1 (LG1, 1:1000), p21CIP1 (1:500, C19, Santa Cruz), Ras (1:2000, OP-40; Calbiochem, Darmstadt, Germany), and AU5 (1:500, MMS-135R: Covance), Acetylated histone H3 (1:1000; Upstate), Phospho-ATM (1:1000, 05-740; Upstate).

Quantitative PCR

Total RNA was isolated from asynchronously growing IMR-90 cells using Tri Reagent (Sigma). Two micrograms of total RNA was used to synthesize cDNA using M-MLV reverse transcriptase (Promega, Madison, WI, USA). One microgram of reaction was used to perform standard PCR or quantitative PCRs. For quantitative PCR of ING1 transcripts, the following primers were used: *ING1exon1b Forward,* GGACTACCTGGACTCCAT; *ING1exon1a Forward,* TCGGAGACAGTTTCAGGC; *ING1exon2 Reverse,* CGACTGAAGCGCTCGTA; *GAPDH Forward*, CAGAAGACTGTGGATGG; *GAPDH Reverse*, GCTTCACCACCTTCTTG. For validation of microarray results, the following primers were used, for each gene forward primer followed by reverse primer: *TMEM16C*; TCAGAGCAGAAGGCTTGATG, AAACATGATATCGGGGCTTG; *CXCL2*; CATCGAAAAGATGCTGAAAAATG, TTCAGGAACAGCCACCAATA; *CXCL6*, GTCCTTCGGGCTCCTTGT, CAGCACAGCAGAGACAGGAC; *CXCR7*, CGATGCCTCCAGAGTCTCA, GGCAGATCATTTGGTGCTCT; *HHIP*, TTCACAAACTTGTTCAAAGTGGA, ATGCGAGGCTTAGCAGTCC. The 18S ribosomal RNA was used as internal reference. For quantitation of ChIP, the following primers were used: *CXCL2*, CAGGCGGTTATCTCGGTATCTC, CTTTTATGCATGGTTGGGGC; *TMEM16C*, TCACTTCTTTGGGTATCGGGT, CACAGGGGCTGAAAAAACAC.

Microarray gene expression profiles

Microarray experiments were performed using Human Whole Genome 4X44K array G4112F (Agilent Technologies, Santa Clara, CA, USA). Two independent retroviral infections were performed in early passage IMR-90 fibroblasts with wild-type p33ING1, W235A and Y212A ING1 mutants, RasV12 and empty vector. Total RNA from the different cell populations was extracted as previously described (Moreno-Bueno *et al.*, 2009). RNA was labeled and hybridized to arrays using the Low RNA Linear Amplification Kit and the In Situ Hybridization Kit Plus (Agilent Technologies), respectively. Competitive hybridization was performed for each sample, using as a reference a reverse-labeled sample from vector-infected cells. After hybridization and washing, the slides were scanned in an Axon GenePix Scanner (Axon Instruments Inc., Union City, CA, USA) and analyzed using Feature Extraction Software 10.0 (Agilent Technologies). Two different RNA samples obtained from each condition were labeled with Cy5-dUTP. The RNA samples from control, vector-infected cells were labeled with Cy3-dUTP (Agilent Technologies). Two additional hybridizations were performed using the reciprocal fluorochrome labeling. For the identification of genes with differential expression in IMR90 cells expressing p33ING1 with respect to control cells, we used the GEPAS gene expression

analysis package (http://gepas3.bioinfo.cipf.es) and selected those genes whose signal differed by a factor of at least twofold in all of the samples with a standard deviation lower than 0.5. This subset was further analyzed with respect to their expression in the rest of samples. Functional enrichment analysis was performed using the FatiGO application (http://babelomics.bioinfo.cipf.es/).

Chromatin immunoprecipitation

Chromatin immunoprecipitation assays were performed essentially as described in Gomez-Cabello *et al.*, 2010. from IMR-90 fibroblast infected with AU5-tagged p33ING1 or empty vector. Immunoprecipitation was carried out with an anti-AU5 antibody or an isotype-matched nonspecific mouse IgG.

Acknowledgments

We thank Manuel Serrano for valuable assistance with experiments in the final phase of the project and critical reading of the manuscript, Scott Lowe for reagents, Manuel Collado for comments on the manuscript, Adrián Martín and Weronika Kucharewicz for help with immunoprecipitation experiments, and Carmen L Pereira for help with the structural analysis. This work is supported by grants from the Spanish Ministry of Science and Innovation to IP (BFU2006-10882, SAF2009-09031) and FJB (CTQ2008-03115/BQU).

References

Abad M, Menendez C, Fuchtbauer A, Serrano M, Fuchtbauer EM, Palmero I (2007) Ing1 mediates p53 accumulation and chromatin modification in response to oncogenic stress. *J. Biol. Chem.* **282**, 31060–31067.

Acosta JC, O'Loghlen A, Banito A, Guijarro MV, Augert A, Raguz S, Fumagalli M, Da Costa M, Brown C, Popov N, Takatsu Y, Melamed J, d'Adda di Fagagna F, Bernard D, Hernando E, Gil J (2008) Chemokine signaling via the CXCR2 receptor reinforces senescence. *Cell* **133**, 1006–1018.

Adams PD (2007) Remodeling chromatin for senescence. *Aging Cell* **6**, 425–427.

Barradas M, Anderton E, Acosta JC, Li S, Banito A, Rodriguez-Niedenfuhr M, Maertens G, Banck M, Zhou MM, Walsh MJ, Peters G, Gil J (2009) Histone demethylase JMJD3 contributes to epigenetic control of INK4a/ARF by oncogenic RAS. *Genes Dev.* **23**, 1177–1182.

Bernard D, Gosselin K, Monte D, Vercamer C, Bouali F, Pourtier A, Vandenbunder B, Abbadie C (2004) Involvement of Rel/nuclear factor-kappaB transcription factors in keratinocyte senescence. *Cancer Res.* **64**, 472–481.

Braig M, Lee S, Loddenkemper C, Rudolph C, Peters AH, Schlegelberger B, Stein H, Dorken B, Jenuwein T, Schmitt CA (2005) Oncogene-induced senescence as an initial barrier in lymphoma development. *Nature* **436**, 660–665.

Campisi J, d'Adda di Fagagna F (2007) Cellular senescence: when bad things happen to good cells. *Nat. Rev. Mol. Cell Biol.* **8**, 729–740.

Champagne KS, Kutateladze TG (2009) Structural insight into histone recognition by the ING PHD fingers. *Curr. Drug Targets* **10**, 432–441.

Chen Z, Trotman LC, Shaffer D, Lin HK, Dotan ZA, Niki M, Koutcher JA, Scher HI, Ludwig T, Gerald W, Cordon-Cardo C, Pandolfi PP (2005) Crucial role of p53-dependent cellular senescence in suppression of Pten-deficient tumorigenesis. *Nature* **436**, 725–730.

Chi P, Allis CD, Wang GG (2010) Covalent histone modifications-miswritten, misinterpreted and mis-erased in human cancers. *Nat. Rev. Cancer* **10**, 457–469.

Coles AH, Jones SN (2009) The ING gene family in the regulation of cell growth and tumorigenesis. *J. Cell. Physiol.* **218**, 45–57.

Coles AH, Liang H, Zhu Z, Marfella CG, Kang J, Imbalzano AN, Jones SN (2007) Deletion of p37Ing1 in mice reveals a p53-independent role for Ing1 in the suppression of cell proliferation, apoptosis, and tumorigenesis. *Cancer Res.* **67**, 2054–2061.

Collado M, Serrano M (2006) The power and the promise of oncogene-induced senescence markers. *Nat. Rev. Cancer* **6**, 472–476.

Collado M, Serrano M (2010) Senescence in tumours: evidence from mice and humans. *Nat. Rev. Cancer* **10**, 51–57.

Collado M, Gil J, Efeyan A, Guerra C, Schuhmacher AJ, Barradas M, Benguria A, Zaballos A, Flores JM, Barbacid M, Beach D, Serrano M (2005) Tumour biology: senescence in premalignant tumours. *Nature* **436**, 642.

Collado M, Blasco MA, Serrano M (2007) Cellular senescence in cancer and aging. *Cell* **130**, 223–233.

Coppe JP, Patil CK, Rodier F, Sun Y, Munoz DP, Goldstein J, Nelson PS, Desprez PY, Campisi J (2008) Senescence-associated secretory phenotypes reveal cell-nonautonomous functions of oncogenic RAS and the p53 tumor suppressor. *PLoS Biol.* **6**, 2853–2868.

Courtois-Cox S, Genther Williams SM, Reczek EE, Johnson BW, McGillicuddy LT, Johannessen CM, Hollstein PE, MacCollin M, Cichowski K (2006) A negative feedback signaling network underlies oncogene-induced senescence. *Cancer Cell* **10**, 459–472.

Courtois-Cox S, Jones SL, Cichowski K (2008) Many roads lead to oncogene-induced senescence. *Oncogene* **27**, 2801–2809.

Dankort D, Filenova E, Collado M, Serrano M, Jones K, McMahon M (2007) A new mouse model to explore the initiation, progression, and therapy of BRAFV600E-induced lung tumors. *Genes Dev.* **21**, 379–384.

Dickins RA, Hemann MT, Zilfou JT, Simpson DR, Ibarra I, Hannon GJ, Lowe SW (2005) Probing tumor phenotypes using stable and regulated synthetic microRNA precursors. *Nat. Genet.* **37**, 1289–1295.

Dietrich N, Bracken AP, Trinh E, Schjerling CK, Koseki H, Rappsilber J, Helin K, Hansen KH (2007) Bypass of senescence by the polycomb group protein CBX8 through direct binding to the INK4A-ARF locus. *EMBO J.* **26**, 1637–1648.

Dimri GP, Lee X, Basile G, Acosta M, Scott G, Roskelley C, Medrano EE, Linskens M, Rubelj I, Pereira-Smith O, Peacocket M, Campisi J (1995) A biomarker that identifies senescent human cells in culture and in aging skin in vivo. *Proc. Natl. Acad. Sci. USA* **92**, 9363–9367.

Doyon Y, Cayrou C, Ullah M, Landry AJ, Cote V, Selleck W, Lane WS, Tan S, Yang XJ, Cote J (2006) ING tumor suppressor proteins are critical regulators of chromatin acetylation required for genome expression and perpetuation. *Mol. Cell* **21**, 51–64.

Funayama R, Ishikawa F (2007) Cellular senescence and chromatin structure. *Chromosoma* **116**, 431–440.

Garkavtsev I, Riabowol K (1997) Extension of the replicative life span of human diploid fibroblasts by inhibition of the p33ING1 candidate tumor suppressor. *Mol. Cell. Biol.* **17**, 2014–2019.

Garkavtsev I, Kozin SV, Chernova O, Xu L, Winkler F, Brown E, Barnett GH, Jain RK (2004) The candidate tumour suppressor protein ING4 regulates brain tumour growth and angiogenesis. *Nature* **428**, 328–332.

Gil J, Bernard D, Martinez D, Beach D (2004) Polycomb CBX7 has a unifying role in cellular lifespan. *Nat. Cell Biol.* **6**, 67–72.

Goeman F, Thormeyer D, Abad M, Serrano M, Schmidt O, Palmero I, Baniahmad A (2005) Growth inhibition by the tumor suppressor p33ING1 in immortalized and primary cells: involvement of two silencing domains and effect of Ras. *Mol. Cell. Biol.* **25**, 422–431.

Gomez-Cabello D, Callejas S, Benguria A, Moreno A, Alonso J, Palmero I (2010) Regulation of the microRNA processor DGCR8 by the tumor suppressor ING1. *Cancer Res.* **70**, 1866–1874.

Gonzalez L, Freije JM, Cal S, Lopez-Otin C, Serrano M, Palmero I (2006) A functional link between the tumour suppressors ARF and p33ING1. *Oncogene* **25**, 5173–5179.

Gunduz M, Ouchida M, Fukushima K, Hanafusa H, Etani T, Nishioka S, Nishizaki K, Shimizu K (2000) Genomic structure of the human ING1 gene and tumor-specific mutations detected in head and neck squamous cell carcinomas. *Cancer Res.* **60**, 3143–3146.

He J, Kallin EM, Tsukada YI, Zhang Y (2008) The H3K36 demethylase Jhdm1b/Kdm2b regulates cell proliferation and senescence through p15(Ink4b). *Nat. Struct. Mol. Biol.* **15**, 1133–1134.

Hung T, Binda O, Champagne KS, Kuo AJ, Johnson K, Chang HY, Simon MD, Kutateladze TG, Gozani O (2009) ING4 mediates crosstalk between histone H3 K4 trimethylation and H3 acetylation to attenuate cellular transformation. *Mol. Cell* **33**, 248–256.

Jacobs JJ, Scheijen B, Voncken JW, Kieboom K, Berns A, van Lohuizen M (1999) Bmi-1 collaborates with c-Myc in tumorigenesis by inhibiting c-Myc- induced apoptosis via INK4a/ARF. *Genes Dev.* **13**, 2678–2690.

Kichina JV, Zeremski M, Aris L, Gurova KV, Walker E, Franks R, Nikitin AY, Kiyokawa H, Gudkov AV (2006) Targeted disruption of the mouse ing1 locus results in reduced body size, hypersensitivity to radiation and elevated incidence of lymphomas. *Oncogene* **25**, 857–866.

Kivinen L, Tsubari M, Haapajarvi T, Datto MB, Wang XF, Laiho M (1999) Ras induces p21Cip1/Waf1 cyclin kinase inhibitor transcriptionally through Sp1-binding sites. *Oncogene* **18**, 6252–6261.

Kotake Y, Zeng Y, Xiong Y (2009) DDB1-CUL4 and MLL1 mediate oncogene-induced p16INK4a activation. *Cancer Res.* **69**, 1809–1814.

Kuilman T, Peeper DS (2009) Senescence-messaging secretome: SMSing cellular stress. *Nat. Rev. Cancer* **9**, 81–94.

Kuilman T, Michaloglou C, Vredeveld LC, Douma S, van Doorn R, Desmet CJ, Aarden LA, Mooi WJ, Peeper DS (2008) Oncogene-induced senescence relayed by an interleukin-dependent inflammatory network. *Cell* **133**, 1019–1031.

Kumamoto K, Spillare EA, Fujita K, Horikawa I, Yamashita T, Appella E, Nagashima M, Takenoshita S, Yokota J, Harris CC (2008) Nutlin-3a activates p53 to both down-regulate inhibitor of growth 2 and up-regulate mir-34a, mir-34b, and mir-34c expression, and induce senescence. *Cancer Res.* **68**, 3193–3203.

Kuzmichev A, Zhang Y, Erdjument-Bromage H, Tempst P, Reinberg D (2002) Role of the Sin3-histone deacetylase complex in growth regulation by the candidate tumor suppressor p33(ING1). *Mol. Cell. Biol.* **22**, 835–848.

Lazennec G, Richmond A (2010) Chemokines and chemokine receptors: new insights into cancer-related inflammation. *Trends Mol. Med.* **16**, 133–144.

Lowe SW, Cepero E, Evan G (2004) Intrinsic tumour suppression. *Nature* **432**, 307–315.

Mantovani A, Allavena P, Sica A, Balkwill F (2008) Cancer-related inflammation. *Nature* **454**, 436–444.

Menendez C, Abad M, Gomez-Cabello D, Moreno A, Palmero I (2009) ING proteins in cellular senescence. *Curr. Drug Targets* **10**, 406–417.

Michaloglou C, Vredeveld LC, Soengas MS, Denoyelle C, Kuilman T, van der Horst CM, Majoor DM, Shay JW, Mooi WJ, Peeper DS (2005) BRAFE600-associated senescence-like cell cycle arrest of human naevi. *Nature* **436**, 720–724.

Mooi WJ, Peeper DS (2006) Oncogene-induced cell senescence – halting on the road to cancer. *N. Engl. J. Med.* **355**, 1037–1046.

Moreno-Bueno G, Peinado H, Molina P, Olmeda D, Cubillo E, Santos V, Palacios J, Portillo F, Cano A (2009) The morphological and molecular features of the epithelial-to-mesenchymal transition. *Nat. Protoc.* **4**, 1591–1613.

Narita M (2007) Cellular senescence and chromatin organisation. *Br. J. Cancer* **96**, 686–691.

Narita M, Nunez S, Heard E, Narita M, Lin AW, Hearn SA, Spector DL, Hannon GJ, Lowe SW (2003) Rb-mediated heterochromatin formation and silencing of E2F target genes during cellular senescence. *Cell* **113**, 703–716.

Narita M, Narita M, Krizhanovsky V, Nunez S, Chicas A, Hearn SA, Myers MP, Lowe SW (2006) A novel role for high-mobility group a proteins in cellular senescence and heterochromatin formation. *Cell* **126**, 503–514.

Nouman GS, Anderson JJ, Lunec J, Angus B (2003) The role of the tumour suppressor p33 ING1b in human neoplasia. *J. Clin. Pathol.* **56**, 491–496.

Palacios A, Garcia P, Padro D, Lopez-Hernandez E, Martin I, Blanco FJ (2006) Solution structure and NMR characterization of the binding to methylated histone tails of the plant homeodomain finger of the tumour suppressor ING4. *FEBS Lett.* **580**, 6903–6908.

Palacios A, Munoz IG, Pantoja-Uceda D, Marcaida MJ, Torres D, Martin-Garcia JM, Luque I, Montoya G, Blanco FJ (2008) Molecular basis of histone H3K4me3 recognition by ING4. *J. Biol. Chem.* **283**, 15956–15964.

Palmero I, Murga M, Zubiaga A, Serrano M (2002) Activation of ARF by oncogenic stress in mouse fibroblasts is independent of E2F1 and E2F2. *Oncogene* **21**, 2939–2947.

Pedeux R, Sengupta S, Shen JC, Demidov ON, Saito S, Onogi H, Kumamoto K, Wincovitch S, Garfield SH, McMenamin M, Nagashima M, Grossman SR, Appella E, Harris CC (2005) ING2 regulates the onset of replicative senescence by induction of p300-dependent p53 acetylation. *Mol. Cell. Biol.* **25**, 6639–6648.

Pena PV, Davrazou F, Shi X, Walter KL, Verkhusha VV, Gozani O, Zhao R, Kutateladze TG (2006) Molecular mechanism of histone H3K4me3 recognition by plant homeodomain of ING2. *Nature* **442**, 100–103.

Pena PV, Hom RA, Hung T, Lin H, Kuo AJ, Wong RP, Subach OM, Champagne KS, Zhao R, Verkhusha VV, Li G, Gozani O, Kutateladze TG (2008) Histone H3K4me3 binding is required for the DNA repair and apoptotic activities of ING1 tumor suppressor. *J. Mol. Biol.* **380**, 303–312.

Pfau R, Tzatsos A, Kampranis SC, Serebrennikova OB, Bear SE, Tsichlis PN (2008) Members of a family of JmjC domain-containing oncoproteins immortalize embryonic fibroblasts via a JmjC domain-dependent process. *Proc. Natl. Acad. Sci. USA* **105**, 1907–1912.

Prieur A, Peeper DS (2008) Cellular senescence in vivo: a barrier to tumorigenesis. *Curr. Opin. Cell Biol.* **20**, 150–155.

Rodier F, Coppe JP, Patil CK, Hoeijmakers WA, Munoz DP, Raza SR, Freund A, Campeau E, Davalos AR, Campisi J (2009) Persistent DNA damage signalling triggers senescence-associated inflammatory cytokine secretion. *Nat. Cell Biol.* **11**, 973–979.

Schetter AJ, Heegaard NH, Harris CC (2010) Inflammation and cancer: interweaving microRNA, free radical, cytokine and p53 pathways. *Carcinogenesis* **31**, 37–49.

Serrano M, Lin AW, McCurrach ME, Beach D, Lowe SW (1997) Oncogenic ras provokes premature cell senescence associated with accumulation of p53 and p16INK4a. *Cell* **88**, 593–602.

Shi X, Hong T, Walter KL, Ewalt M, Michishita E, Hung T, Carney D, Pena P, Lan F, Kaadige MR, Lacoste N, Cayrou C, Davrazou F, Saha A, Cairns BR, Ayer DE, Kutateladze TG, Shi Y, Cote J, Chua KF, Gozani O (2006) ING2 PHD domain links histone H3 lysine 4 methylation to active gene repression. *Nature* **442**, 96–99.

Soliman MA, Riabowol K (2007) After a decade of study-ING, a PHD for a versatile family of proteins. *Trends Biochem. Sci.* **32**, 509–519.

Soliman MA, Berardi P, Pastyryeva S, Bonnefin P, Feng X, Colina A, Young D, Riabowol K (2008) ING1a expression increases during replicative senescence and induces a senescent phenotype. *Aging Cell* **7**, 783–794.

Wajapeyee N, Serra RW, Zhu X, Mahalingam M, Green MR (2008) Oncogenic BRAF induces senescence and apoptosis through pathways mediated by the secreted protein IGFBP7. *Cell* **132**, 363–374.

Wang J, Jacob NK, Ladner KJ, Beg A, Perko JD, Tanner SM, Liyanarachchi S, Fishel R, Guttridge DC (2009) RelA/p65 functions to maintain cellular senescence by regulating genomic stability and DNA repair. *EMBO Rep.* **10**, 1272–1278.

Ythier D, Larrieu D, Brambilla C, Brambilla E, Pedeux R (2008) The new tumor suppressor genes ING: genomic structure and status in cancer. *Int. J. Cancer* **123**, 1483–1490.

Supporting Information

Additional supporting information may be found in the online version of this article:

Data S1 Methods.

Fig. S1 Subcellular distribution of p33ING1.

Fig. S2 Effect of the C215S mutation on protein folding.

Fig. S3 Connection of ING1 with SAHFs.

Fig. S4 Expression profiling.

Fig. S5 Association to p53.

Fig. S6 DNA damage response in ING1-expressing fibroblasts.

Table S1 Genes with differential expression in p33ING1-infected IMR-90 fibroblasts, relative to vector-infected cells.

As a service to our authors and readers, this journal provides supporting information supplied by the authors. Such materials are peer-reviewed and may be re-organized for online delivery, but are not copy-edited or typeset. Technical support issues arising from supporting information (other than missing files) should be addressed to the authors.

doi:10.1016/j.jmb.2009.12.049 *J. Mol. Biol.* (2010) **xx**, xxx–xxx

JMB

Available online at www.sciencedirect.com

ScienceDirect

ELSEVIER

The Dimeric Structure and the Bivalent Recognition of H3K4me3 by the Tumor Suppressor ING4 Suggests a Mechanism for Enhanced Targeting of the HBO1 Complex to Chromatin

Alicia Palacios[1], Alberto Moreno[2], Bruno L. Oliveira[3], Teresa Rivera[3], Jesús Prieto[3], Pascal García[3], M. Rosario Fernández-Fernández[4], Pau Bernadó[5], Ignacio Palmero[2] and Francisco J. Blanco[1,6]*

[1]*CIC bioGUNE, Structural Biology Unit, Parque Tecnológico de Bizkaia, 48160 Derio, Spain*

[2]*Instituto de Investigaciones Biomédicas "Alberto Sols", CSIC-UAM, Arturo Duperier 4, 28029 Madrid, Spain*

[3]*Structural Biology and Biocomputing Programme, Centro Nacional de Investigaciones Oncológicas (CNIO), Melchor Fernández Almagro 3, 28029 Madrid, Spain*

[4]*Center for Protein Engineering, MRC, Cambridge, UK*

[5]*Institute for Research in Biomedicine, Baldiri Reixac 10-12, 08028 Barcelona, Spain*

[6]*IKERBASQUE, Basque Foundation for Science, 48011 Bilbao, Spain*

Received 1 October 2009; received in revised form 23 December 2009; accepted 23 December 2009

Edited by P. Wright

The INhibitor of Growth (ING) family of tumor suppressors regulates the transcriptional state of chromatin by recruiting remodeling complexes to sites with histone H3 trimethylated at position K4 (H3K4me3). This modification is recognized by the plant homeodomain (PHD) present at the C-terminus in the five members of the ING family. ING4 facilitates histone H3 acetylation by the HBO1 complex. Here, we show that ING4 forms homodimers through its N-terminal domain, which folds independently into an elongated coiled-coil structure. The central region of ING4, which contains the nuclear localization sequence, is disordered and flexible and does not directly interact with p53, or does it with very low affinity, in contrast to previous findings. The NMR analysis of the full-length protein reveals that the two PHD fingers of the dimer are chemically equivalent and independent of the rest of the molecule. The detailed NMR analysis of the full-length dimeric protein binding to histone H3K4me3 shows essentially the same binding site and affinity as the isolated PHD finger. Therefore, the ING4 dimer has two identical and independent binding sites for H3K4me3 tails, which, in the context of the chromatin, could belong to the same or to different nucleosomes. These results show that ING4 is a bivalent reader of the chromatin H3K4me3 modification and suggest a mechanism for enhanced targeting of the HBO1 complex to specific chromatin sites. This mechanism could be common to other ING-containing remodeling complexes.

Keywords: ING4 structure; histone tail; chromatin; NMR; SAXS

**Corresponding author.* E-mail address: fblanco@cicbiogune.es.

Present addresses: B. L. Oliveira, Instituto Tecnológico e Nuclear, Estrada Nacional 10, 2686-953 Sacavém, Portugal; P. Garcia, Oncura, Orense 85, 28020 Madrid, Spain; M. R. Fernandez-Fernandez, Centro de Biología Molecular Severo Ochoa, CSIC-UAM, Nicolás Cabrera 1, 28049 Cantoblanco, Spain.

Abbreviations used: ING, inhibitor of growth; HSQC, heteronuclear single quantum coherence; SAXS, small-angle X-ray scattering; NLS, nuclear localization signal; PHD, plant homeodomain; GTA, glutaraldehyde ; OD, optical density.

0022-2836/$ - see front matter

Please cite this article as: Palacios, A., *et al.*, The Dimeric Structure and the Bivalent Recognition of H3K4me3 by the Tumor Suppressor ING4 Suggests a Mechanism for Enhanced Targeting of the HBO1..., *J. Mol. Biol.* (2010), doi:10.1016/j.jmb.2009.12.049

Introduction

The nuclear DNA of eukaryotic cells is packed with proteins into chromatin, the nucleosome being its fundamental unit. Two superhelical turns of DNA wind around an octamer of the four core histones. The flexible N-terminal tails of histones provide internucleosomal linkages and, together with other proteins, allow for higher levels of compaction.[1] The structure of chromatin is highly dynamic and has a strong impact in DNA replication, repair, and transcription.[2,3] Its regulation is largely based on posttranslational covalent modifications of certain residues at the N-terminal histone tails, which directly affect the level of chromatin condensation and/or recruit specific chromatin remodeling complexes to their location. The combinatorial nature of these histone modifications, as well as their correlation with many chromatin-template processes, has led to the proposal of the existence of a "histone code" as the basis for a fundamental regulatory mechanism that extends the information potential of the genetic code.[4] Histone tails are modified by specific enzymatic complexes of proteins, some of them with domains that recognize one or more of the possible modifications.[5]

The INhibitor of Growth (ING) family of tumor suppressors consists of five homologous proteins[6] that regulate the transcriptional state of chromatin by recruiting remodeling complexes to sites with histone H3 trimethylated at position K4 (H3K4me3). This histone post translation modification is recognized by their C-terminal plant homeodomains (PHDs).[7] ING1 and ING2 form part of histone deacetylase complexes, while ING3, ING4, and ING5 do so with histone acetyl transferase complexes.[8] The amino acid sequences of the ING proteins indicate that they have a conserved N-terminal region, a central non-conserved region containing the nuclear localization signal (NLS), and a conserved C-terminal PHD.[9] The structures of the PHD fingers of ING1,[10] ING2,[11] ING4,[12] and ING5[13] bound to H3K4me3 fragments have been determined, displaying very similar structures, with some differences in the conformation of the bound histone peptide.[12] However, the structure of the full-length ING proteins is still unknown.

We set out to experimentally study the structural and functional organization of ING4, which facilitates H3 acetylation by the histone acetyl transferase–HBO1 complex.[14] With this aim, we have produced the full-length ING4 protein and four fragments spanning the N-terminal domain, the central NLS region, the PHD finger, or combinations of them (Fig. 1). Their structures have then been analyzed by different techniques. We show that ING4 dimerizes through its N-terminal domain with a coiled-coil structure and results in a molecule with two PHD fingers that independently bind to H3K4me3 histone marks.

Fig. 1. Domain organization of ING4 and the boundaries of the designed constructs. The predicted helices and coiled-coil structures in the N-terminal domain are indicated with curvy black lines and dark green boxes, respectively.

Results and Discussion

Strategy and definition of the domain boundaries

To explore the domain organization of ING4, we defined several constructs, considering the preservation of both the conserved sequence stretches and the predicted secondary-structure elements, as well as the particular residues found at the borders of the putative domains that may facilitate solubility and analysis of the expressed proteins (Fig. 1). Secondary-structure predictions suggest the presence of two long helices (residues 4–52 and 57–107) in the N-terminal conserved domain, no secondary structure in the non-conserved central region, and three short β-strands in the PHD finger. The predicted helices partially overlap with two segments (21–55 and 90–117) predicted to form coiled-coil structures. The first predicted helix overlaps with the postulated leucine zipper-like motif (1–65) and the second one overlaps with the potential chromatin regulatory domain.[9] The boundaries of the N-terminal domain (Nt) were thus defined as residues 1–118, which are followed by a long stretch of predominantly polar amino acids with high potential to be disordered. The C-terminal construct (residues 188–249, PHD) has been described previously[15] and consists of the canonical PHD, with its characteristic C_4HC_3 zinc finger motif, plus short chain extensions at the N- and C-termini, which are not strictly part of the PHD finger and have been found to be flexible and disordered.[12] The central region, rich in positively charged amino acids, contains the nuclear localization sequence[9] and is named hereafter NLS (residues 119–188). Although no such isolated NLS construct was studied, its conformational behavior was explored as part of the other constructs containing it.

ING4 is a dimer in solution and inside living cells

The mass gradients measured in sedimentation equilibrium experiments of ING4 correspond to a dimeric molecule (Fig. 2). Sedimentation velocity measurements show that those molecules containing the Nt domain are dimers, while those lacking it are monomers (Fig. 2 and Table 1). Cross-linking experiments with glutaraldehyde (GTA) confirm that the Nt region contains the dimerization site of ING4. In experiments in mammalian cells with transient expression of ING4 with N-terminal tags AU5 or HA, we found that AU5-ING4 can be

Please cite this article as: Palacios, A., *et al.*, The Dimeric Structure and the Bivalent Recognition of H3K4me3 by the Tumor Suppressor ING4 Suggests a Mechanism for Enhanced Targeting of the HBO1..., *J. Mol. Biol.* (2010), doi:10.1016/j.jmb.2009.12.049

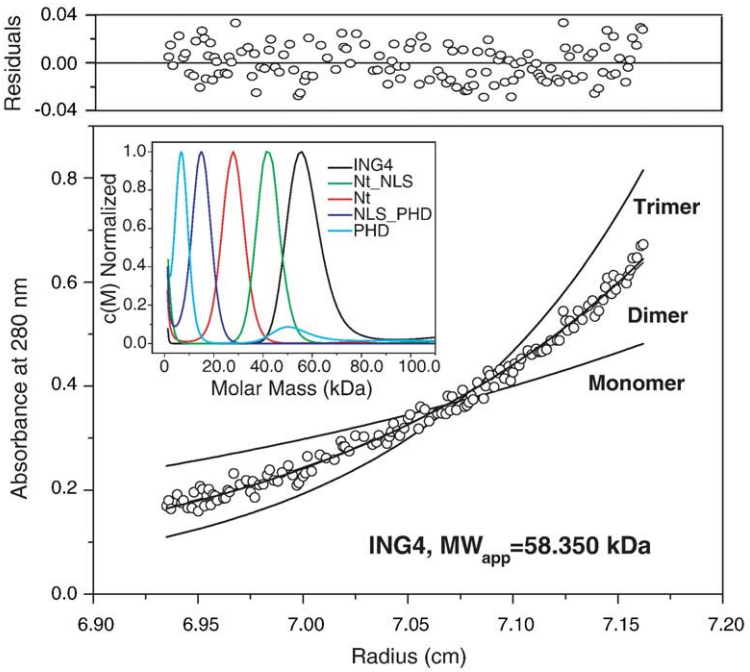

Fig. 2. Analytical ultracentrifugation analysis of the ING4 and its fragments. The experimental sedimentation equilibrium gradient of ING4 at 11,000 rpm is shown (circles) together with the calculated gradients (lines) for a monomeric, dimeric, and trimeric molecule. The upper panel shows the best-fit residuals (dimer gradient). Inset: sedimentation velocity data of ING4 protein and the four different fragments.

specifically co-precipitated with an antibody against the HA tag and can only be achieved in cells expressing both tagged molecules (Fig. 3). These results indicate that at least two ING4 molecules interact inside living cells.

Structure of the ING4 dimeric molecule

ING4 sediments with a coefficient of 2.9 S, while for a 57-kDa spherical molecule, a value of 5.1 S would be expected, indicating that the shape of the ING4 molecule differs substantially from a sphere. If ING4 were an oblate ellipsoid, an axial ratio of 8 would be required to reproduce the observed sedimentation coefficient. The molecular parameters derived from small-angle X-ray scattering (SAXS) measurements also show that ING4 does not have a globular structure (Table 1).

ING4 has a high content of helical structure, as indicated by the two minima at 208 and 222 nm and maximum at around 190 nm in its circular dichroism (CD) spectrum (Fig. 4). Nevertheless, the absolute ellipticity indicates that a large part of the chain is not helical. This pattern is more pronounced for Nt_NLS, and even more for the Nt region, with an ellipticity ratio ($[\Theta]_{222\ nm}/[\Theta]_{208\ nm}>1$) typical of coiled-coil structures.[17] The spectrum of PHD has a minimum at 202 nm and a small negative ellipticity in the range 230–210 nm, as expected from the low content of canonical α-helix and β-sheet secondary structure in the PHD finger, which consists mainly of loops stabilized by the two Zn^{2+} clusters.[15] The shape of the spectra of Nt_NLS and NLS_PHD can be explained by the combination of the spectra of Nt or PHD, respectively, and the spectrum of a random-coil chain: less negative ellipticity at 222 nm, less positive ellipticity at 190 nm, and a shift to lower wavelengths of the Nt minimum at 208 nm and the PHD minimum at 202 nm. These results suggest that NLS behaves as a disordered random coil. Furthermore, the spectrum of ING4 indicates that the secondary structure of ING4 is essentially the same

Table 1. Molecular weights obtained from sedimentation velocity experiments and global molecular dimensions derived from SAXS measurements for the different constructs of ING4

Molecule	Theoretical MW (Da)[a]	Observed MW (Da)[b]	R_g (Å)[c]	R_g (Å)[d]	D_{max} (Å)[e]
ING4	28,530	55,500	62.7±1.0	64.5	220±10
Nt	13,857	27,400	26.4±0.3	27.8	104±5
Nt_NLS	21,479	39,500	41.5±0.3	44.9	168±5
NLS_PHD	14,692	14,600	n.d.	n.d.	n.d.
PHD	7315	6800	n.d.	n.d.	n.d.

n.d., not determined.
[a] Calculated from the amino acid sequence.
[b] Derived from the sedimentation velocity measurements.
[c] Radius of gyration determined from the small-angle region ($s\times R_g<1.3$) forward scattering using the Guinier approximation.
[d] Radius of gyration derived from the distance distribution functions computed with the program GNOM.[16]
[e] Maximum particle dimension derived from the distance distribution functions computed with the program GNOM.[16]

Please cite this article as: Palacios, A., *et al.*, The Dimeric Structure and the Bivalent Recognition of H3K4me3 by the Tumor Suppressor ING4 Suggests a Mechanism for Enhanced Targeting of the HBO1..., *J. Mol. Biol.* (2010), doi:10.1016/j.jmb.2009.12.049

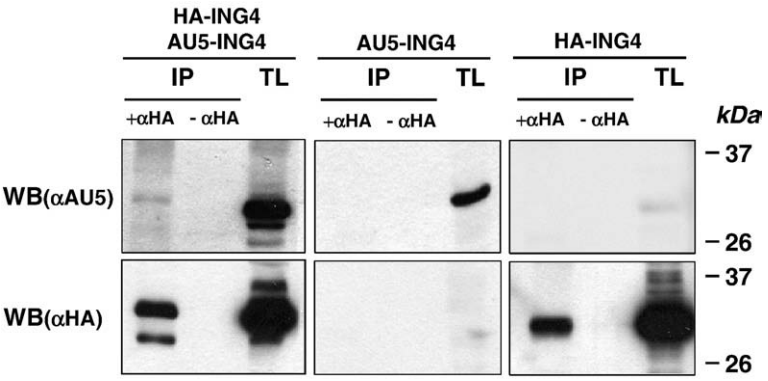

Fig. 3. Analysis of ING4 association inside living cells by immunoprecipitation. Lysates from cells transiently transfected with vectors expressing HA-ING4 (right-hand panels), AU5-ING4 (middle panels), or both (left-hand panels) were immunoprecipitated (IP) with (αHA) or without (−αHA) an antibody against the HA tag. The presence of each protein in the immunocomplexes was analyzed by Western blotting (WB) with antibodies against AU5 (αAU5, upper panels) or against HA (αHA, lower panels) tag. TL is the total lysate.

as the sum of the secondary structures of its three regions, suggesting that each domain is structurally independent from the rest of the chain. The thermal denaturation curves show cooperative unfolding transitions for the full-length ING4 protein and Nt and Nt_NLS constructs (with an apparent melting temperature of 56 °C), as well as for NLS_PHD and PHD (with a midpoint denaturation temperature around 86 °C). Helical structures have the strongest signal in protein CD spectra; therefore, the signal from Nt dominates the transition in those constructs containing this domain, while the random-coil NLS region contributes a nearly invariant molar ellipticity that flattens the curves of the corresponding constructs, especially that of NLS_PHD (still, when expanded in the vertical scale, a transition with the same midpoint temperature as the PHD is observed). Altogether, the CD data indicate that Nt and PHD are domains with well-defined tertiary structures, while the NLS is a random coil, and that the three regions are independent with weak interactions among them, if any (Fig. 4).

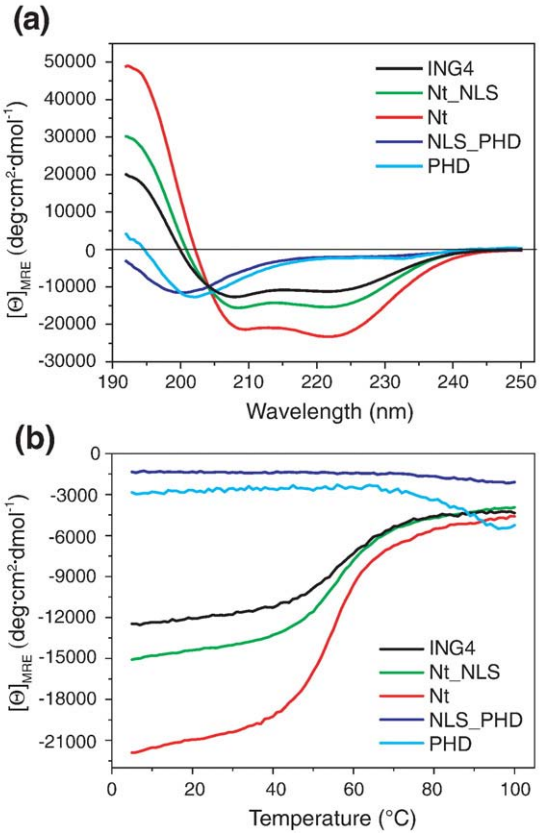

Fig. 4. Structure and stability of ING4 proteins analyzed by CD. (a) Far-UV spectra of the five constructs recorded at 25 °C in 20 mM sodium phosphate buffer, pH 6.5, 200 mM NaCl, and 1 mM DTT. (b) Thermal denaturation curves of the same molecules and in the same buffer as before followed by the change in their molar residue ellipticity at 222 nm.

The ^{1}H–^{15}N-heteronuclear single quantum coherence (HSQC) NMR spectrum of the 57-kDa ING4 dimer (Fig. 5a) displays distinct sets of peaks that can be recognized in the spectra of the individual fragments (Fig. 5b and c). A detailed analysis shows that for 83% of the backbone amide signals of the PHD, the ^{1}H and ^{15}N resonance frequencies closely match those of a corresponding signal in the spectrum of full-length ING4 (chemical shift perturbations <0.065 ppm). For the other residues, signal overlap or a larger unknown shift precludes a reliable assessment of the actual displacement. This result demonstrates that the Nt and PHD domains are independent non-interacting domains linked by a flexible NLS segment. In the spectrum of the Nt domain, the number of observed peaks is smaller than expected from its amino acid sequence, and most of them are narrow and non-dispersed. This result is consistent with a 28-kDa elongated coiled-coil molecule as this molecular size, shape, and structure (with the ^{1}H–^{15}N bonds aligned with the longitudinal helical axis) result in unfavorable NMR relaxation properties and thus in poor sensitivity. Most likely, the observed signals correspond to residues in the most flexible parts (mostly in the loops and chain ends). At higher temperatures, the increased overall molecular tumbling slows the relaxation of the NMR signals favoring their measurement, and a larger number of dispersed peaks is observed in the spectra. Although there is still substantial signal overlap, the number of signals in the ^{1}H–^{15}N-HSQC NMR spectra of the Nt domain suggests that it forms symmetric dimers.

Please cite this article as: Palacios, A., *et al.*, The Dimeric Structure and the Bivalent Recognition of H3K4me3 by the Tumor Suppressor ING4 Suggests a Mechanism for Enhanced Targeting of the HBO1..., *J. Mol. Biol.* (2010), doi:10.1016/j.jmb.2009.12.049

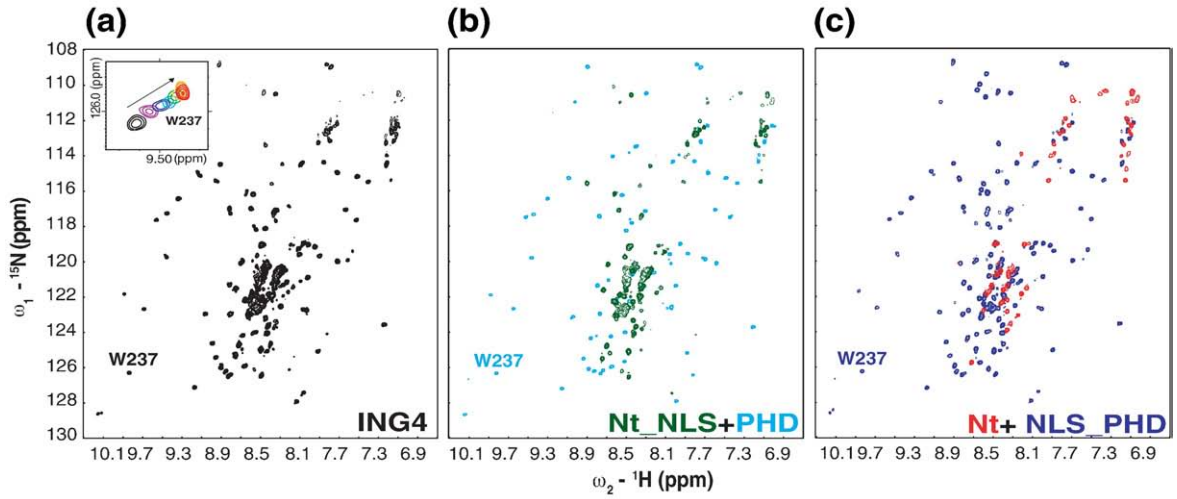

Fig. 5. NMR analysis of ING4 proteins and binding of ING4 to H3K4me3. ^{1}H–^{15}N-HSQC NMR spectra of ING4 (a), Nt_NLS (green) overlaid with that of PHD (light blue) (b), and of Nt (red) overlaid with that of NLS_PHD (dark blue) (c). The NMR data were acquired and processed in the same way and plotted to show the signals above the noise level. The signal of W237 is indicated in the spectra of the fragments containing it. The inset in (a) is a zoom of the region with the W237 signal in the ING4 spectra measured at different ING4:H3K4me3-peptide ratios. Each point of the titration is shown with a different color, from 1:0 (in black) to 1:4 (in red).

The SAXS measurements show that the Nt domain has a defined structure, but ING4 and Nt_NLS have a dual behavior, with folded and random components. The Kratky representation of the scattering profiles has been used previously to discriminate between folded and unfolded proteins.[18] The Kratky plot of Nt displays a pronounced peak that indicates that it is a folded protein. In contrast, the Kratky plot Nt_NLS shows a less pronounced peak added to the continuous increase of the $I(s)s^2$ values with s, a typical observation in unstructured molecules. The SAXS measurements on Nt_NLS yield values of R_g and D_{max} (Table 1) that are in agreement with this semiquantitative interpretation of the Kratky representation. For Nt, the distance distribution function $p(r)$ was calculated using a maximum dimension of 104 Å. It peaks at approximately $r=20$ Å and decreases linearly towards D_{max}, although the slope smoothes at the largest distances. In a first approximation, these features are characteristic of a $p(r)$ belonging to an elongated cylinder with an approximate diameter of 40 Å.[19,20] With an axial rise of 1.5 Å/residue, the length is slightly larger than expected for a 50-residue-long helix (75 Å) but smaller than calculated for a 100-residue-long one (150 Å). The radius of the cylinder, around 40 Å, is slightly larger than expected for an assembly of four helices.[21] Considering the coiled-coil structure and dimeric nature of Nt, these data indicate that the Nt domain of ING4 folds into a helix–loop–helix structure, which dimerizes as a four-helix coiled coil. Alternative model structures would not be consistent with the three independent experimental measurements. The value of D_{max} could be explained by the flexibility of the chain ends (as suggested by its NMR spectrum) or by a dimerization that is not in register but shifted so that the overall length of the coiled coil is larger than the length of the individually packed helices. A slightly curved assembly could be the reason for the larger apparent diameter.[22]

A low-resolution *ab initio* structural model of the Nt domain based on the SAXS data shows an elongated molecule (Fig. 6). Together with the CD and NMR spectra, and the secondary-structure predictions, we interpret this model as a helix–loop–helix structure that dimerizes into a four-helix coiled-coil. However, it is not possible to derive from the SAXS whether the helical monomers interact in a parallel or antiparallel way. The maximum distance derived from the SAXS measurements on ING4 might indicate an antiparallel dimer assembly since this would result in an average longer molecule. Helical wheel analysis of the different four-helix coiled-coil arrangements did not show a clear preference for any of them based on the pattern of buried and exposed amino acids (data not shown). The presence of long disordered regions in ING4 and Nt_NLS precluded a similar structural modeling for these molecules.

The NLS region contains the sequence that directs ING4 to the nucleus and could also contain sites for binding to other proteins such as p53. The ING proteins cooperate with the p53 signaling pathway and, with the exception of ING3, have been reported to co-immunoprecipitate with p53 after ectopic co-expression.[23] Co-immunoprecipitation of ING4 and p53[24] suggests that they physically interact, and the p53 binding site on ING4 has been mapped to the NLS region by pull-down experiments.[25] We have tried to characterize in detail this interaction by NMR but it has not been possible to confirm the binding, indicating that the interaction is at most very weak. In the presence of p53, the signals of

Please cite this article as: Palacios, A., *et al.*, The Dimeric Structure and the Bivalent Recognition of H3K4me3 by the Tumor Suppressor ING4 Suggests a Mechanism for Enhanced Targeting of the HBO1..., *J. Mol. Biol.* (2010), doi:10.1016/j.jmb.2009.12.049

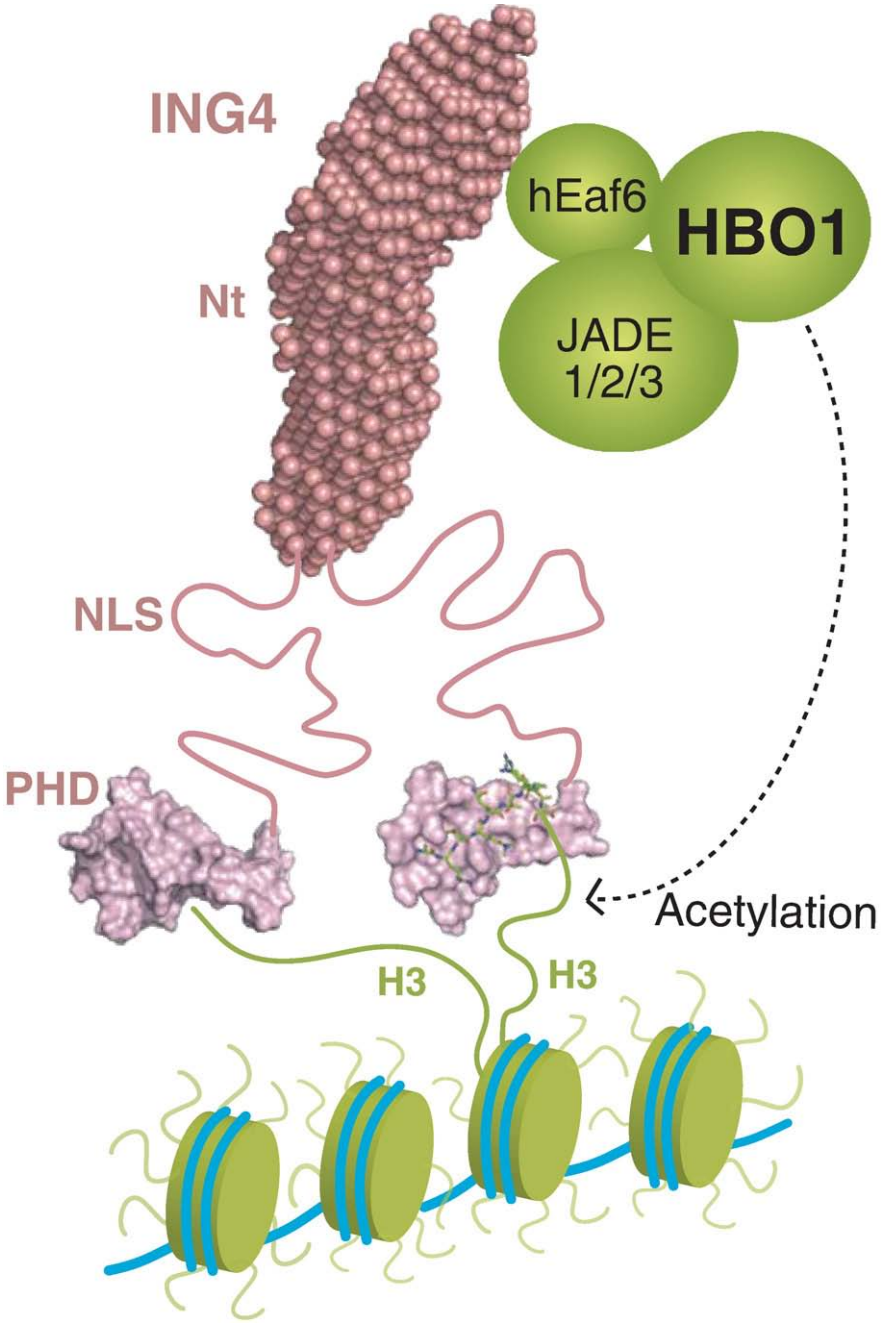

Fig. 6. Model of ING4 engaging nucleosomes with H3K4me3 marks and facilitating histone H3 acetylation by the HBO1 complex. The dimeric Nt domain is shown as the SAXS-derived model, the NLS as lines, and the PHD fingers as the surfaces of its NMR structure (left one) and of its crystal structure bound to the H3K4me3 peptide (right-hand one). The representations of the Nt dimer and the PHD fingers are done approximately at the same scale, but those of the HBO1 complex and the nucleosomes are not.

NLS_PHD do not appreciably change in frequency, line width, or intensity (Fig. 7), and the same occurs when the signals of p53 (uniformly deuterated in the non-labile protons) are observed in the presence or absence of NLS_PHD. The NLS_PHD fragment of ING4 used here (residues 119–249) is almost identical with one of the glutathione *S*-transferase-fused fragments of ING4 (the one spanning residues 120–248) used in pull-down experiments that were positive for p53 binding.[25] As no significant chemical shift perturbations (above the experimental error) were observed, it is not possible to confirm the interaction, but a lower limit for the dissociation constant (K_d) of the putative complex can be estimated. Assuming an equimolar complex, and that we should be able to detect significant perturbations in the chemical shifts when at least 20% of the ^{15}N-labeled protein is bound to the unlabeled one,[26,27] the dissociation constant would be larger than 320 μM (estimated from the absence

Please cite this article as: Palacios, A., *et al.*, The Dimeric Structure and the Bivalent Recognition of H3K4me3 by the Tumor Suppressor ING4 Suggests a Mechanism for Enhanced Targeting of the HBO1..., *J. Mol. Biol.* (2010), doi:10.1016/j.jmb.2009.12.049

of changes in the p53 spectra, recorded at a protein concentration of 100 μM).

ING4 is a bivalent reader of H3K4me3

The long and disordered NLS tethers the PHD to the Nt domain, but its length and flexibility confer a high degree of mobility to the PHD finger with respect to the Nt. As a result, the assignment of many of the previously assigned backbone NMR signals of the PHD[15] can be transferred to the well-resolved regions of the ING4 spectrum (Fig. 5a) by matching the chemical shifts of the corresponding signals. The presence of a single set of signals for all the identified amino acids indicates that the two PHD fingers of the dimer are chemically equivalent. The assignment allows for the detailed NMR analysis of the binding of the full-length dimeric protein to histone H3K4me3. The chemical shift perturbations of ING4 signals upon the addition of a 15-residue-long H3K4me3 peptide shows essentially the same binding site, affinity (K_d=1.3±0.5 μM), and discrimination between the different methylated forms of histone H3 at K4 (Fig. 8) as the isolated PHD finger.[12,14] Therefore, the ING4 dimer has two identical and independent binding sites for H3K4me3 tails, which, in the context of the chromatin, could belong to the same or to different nucleosomes.

Our results could have important implications for the mechanism of action of ING4 in chromatin regulation. The bivalency of ING4 would enhance HBO1 targeting to chromatin sites enriched in H3K4me3 marks, because when two such modifications are within the reach of the complex, binding to the first site will reduce the entropic cost of the second site binding.[28,29] The resulting higher affinity[16] would favor HBO1 binding over other monovalent complexes. Analogously, two nearby H3K4me3 chromatin sites would compete favorably for HBO1 binding over distant ones and also with peptides from clipped histones.[30] Further robustness of HBO1 complex recruitment to the chromatin would be provided by the PHD fingers of its JADE components, which differ in their specificity for histone H3 tails.[31]

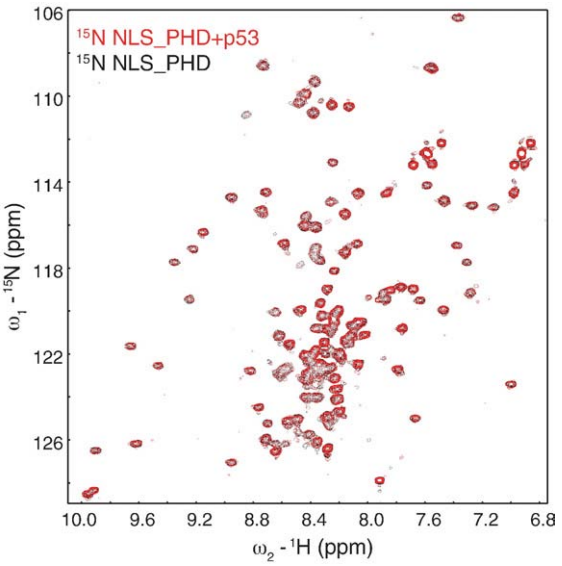

Fig. 7. NMR analysis of the interaction of ING4 with p53. The ^{1}H–^{15}N-HSQC NMR spectrum of the 1:1 (monomer molar ratio) mixture of 50 μM ^{15}N-NLS_PHD and unlabeled p53 (in red) is overlaid on the spectrum of ^{15}N-NLS_PHD alone (in black). The spectra were recorded at 20 °C and 600 MHz under identical conditions.

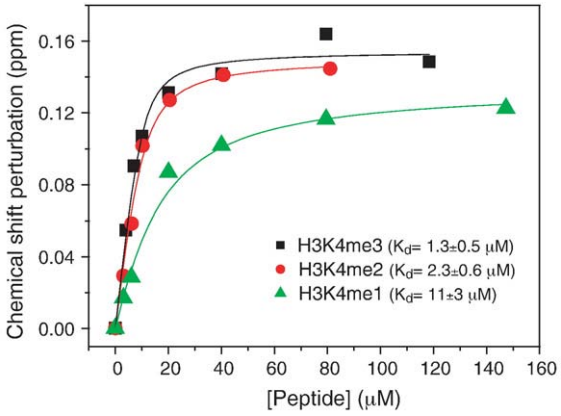

Fig. 8. ING4 binding to histone-H3 methylated peptides by NMR. The chemical shift perturbation experienced by the signal of W237 in the ^{1}H–^{15}N HSQC spectrum of ING4 is represented as a function of peptide concentration. The signal of W237 was assigned based on the similarity of its resonance frequencies with the corresponding signal assigned in the spectrum of the isolated PHD. The height of the symbols represents the experimental error in the measured chemical shift perturbation. We have previously reported that the PHD finger of ING4 (PHD) binds to the methylated H3K4meX peptides with dissociation constants (K_d) of 3.9±0.7, 2±1, and 6±2 μM for X=3, 2, and 1, respectively.[12,15]

Conclusions

The dimerization of ING4 and the flexibility of its NLS region result in a bivalent recognition of H3K4me3 and suggest a mechanism for enhanced targeting of HBO1 complex to the chromatin. All the ING proteins (except ING1) have a leucine zipper-like sequence at their N-terminal domains, suggesting that they could also form coiled-coil homodimers,[9] and thus enhance the targeting of their corresponding complexes to the chromatin. Furthermore, the existence of ING heterodimers is an intriguing possibility that would increase the functional diversity of these proteins.

Materials and Methods

Sequence analysis and structure prediction

The sequence alignment of the five ING protein sequences (as obtained from the Swissprot database)

Please cite this article as: Palacios, A., *et al.*, The Dimeric Structure and the Bivalent Recognition of H3K4me3 by the Tumor Suppressor ING4 Suggests a Mechanism for Enhanced Targeting of the HBO1..., *J. Mol. Biol.* (2010), doi:10.1016/j.jmb.2009.12.049

was performed with Clustal-X.[32] For ING1, the predominant isoform in healthy tissues (p33ING1b) was used.[33] Secondary-structure prediction was performed using JPred,[34] which uses the Lupas algorithm to predict coiled-coil structures.[35] Disordered regions were predicted with PONDR.[36]

Cloning and mutagenesis

A synthetic gene of the full-length ING4 (isoform v1[37]) with codons optimized for expression in *Escherichia coli* (Entelechon GmbH) was used to subclone five different ING4 constructs into the expression vector pET11d by PCR using the appropriate forward and backward oligonucleotides. The full-length ING4 (residues 1–249) and four fragments designed to encompass one or two of its three regions or domains were cloned: Nt (1–118), Nt_NLS (1–188), NLS_PHD (119–249), and PHD (189–249). For overexpression of ING4 in 293T cells, the ING4 human gene was amplified by PCR with N-terminal AU5 or HA tags and cloned into the retroviral expression vector pLPC.

Protein expression and purification

All the proteins were overexpressed in *E. coli* BL21(DE3) cells grown in LB medium supplemented before induction with 50 μM $ZnCl_2$. Isotope-enriched proteins were produced in minimal medium with $^{15}NH_4Cl$. Expression was induced with 0.5 mM IPTG at an OD_{600} (optical density at 600 nm) of 0.6 and the cells were harvested by centrifugation after 4 h of induction at 37 °C. After sonication and ultracentrifugation, proteins were found in the soluble fraction (Nt), in the insoluble fraction (ING4, NLS_PHD and PHD), or in both (Nt_NLS). Insoluble proteins were recovered from the pellets by solubilization in 6 M urea, refolded by a 1:10 dilution into cold 20 mM Tris, pH 8.0, 1 mM DTT, and 50 μM $ZnCl_2$ (for constructs containing the PHD) and purified by anion-exchange chromatography (Q-Sepharose column, GE Healthcare), followed by gel-filtration separation (Superdex 75, GE Healthcare). The purification of insoluble protein NLS_PHD was facilitated by decreasing the pH of the soluble fraction in 6.0 M urea to 3.0 to precipitate acid proteins and DNA. After ultracentrifugation, the pH was changed back to 8.0 and purified by anion-exchange chromatography (the protein comes in the flow-through) followed by cation-exchange chromatography (SP-Sepharose column, using a NaCl gradient for protein elution). After refolding by dilution into cold buffer, the protein was concentrated and polished by gel filtration. Soluble Nt and Nt_NLS proteins were purified by anion-exchange chromatography followed by several steps of gel-filtration separation. A small amount of PHD was purified directly from the soluble fraction of the lysed cells by anion-exchange and gel-filtration chromatography yielding an identical 1D NMR spectrum as the refolded molecule. Pure proteins were concentrated and dialyzed against 20 mM phosphate buffer, pH 6.5, and 50 mM NaCl, and its identity was verified by mass spectrometry.

Analytical ultracentrifugation

Experiments were performed at 20 °C in an Optima XL-A (Beckman Coulter Inc.) analytical ultracentrifuge equipped with UV-visible optics, using an An50Ti rotor, with 3-mm double sector centerpieces of Epon charcoal. The sedimentation velocity experiments were carried out at 42,000 rpm, and absorbance scans were taken at 280 nm. The protein samples had ODs between 0.5 and 0.7 (concentrations in the range 30–100 μM). These measurements were performed in the following buffers: 20 mM sodium phosphate buffer, pH 6.5, 200 mM NaCl, and 1 mM DTT (Nt, Nt_NLS, NLS_PHD); 20 mM Tris, pH 8.0, 300 mM NaCl, and 1 mM DTT (ING4); and 20 mM sodium phosphate buffer, pH 6.5, 50 mM NaCl, and 1 mM DTT (PHD). The concentrations of the samples were at OD values between 0.5 and 0.7 at 280 nm. The sedimentation coefficients were calculated by continuous distribution $c(s)$ Lamm equation model as implemented in the SEDFIT program. These experimental values were corrected to standard conditions to get the corresponding $s_{20,w}$ values using the SEDNTERP program.[38] Further hydrodynamic analysis (i.e., calculation of frictional coefficient ratio) was performed with the SEDFIT program to obtain de c(M) distribution.[39] Sedimentation equilibrium measurements on ING4 were performed in the same buffer as the sedimentation velocity experiment. Short-column (23 μl volume), low-speed sedimentation equilibrium experiments were performed at three successive speeds (5000, 7000, and 11,000 rpm). The system was assumed to be at equilibrium when successive absorbance scans (at 280 nm) did not change. The baseline signal was measured after high-speed centrifugation (5 h at 42,000 rpm). The apparent average molecular weight of the protein was obtained using the program EQASSOC.[40]

Chemical cross-linking

GTA at 25% was purchased from Sigma. Experiments were performed at room temperature with Nt and PHD molecules at 25 μM in phosphate buffer saline (PBS, 10 mM sodium phosphate, 2 mM potassium phosphate, 2.7 mM potassium chloride, 137 mM sodium chloride, pH 7.2) in the presence of 1 mM DTT and supplemented with NaCl to a total concentration of 300 mM. Proteins were incubated with three different protein:GTA molar ratios (1:20, 1:50, and 1:80) for 1 h, and reactions were stopped with 2 M $NaBH_4$ for 15 min. Cross-linked proteins were separated by SDS-PAGE and stained with Coomassie.

Immunoprecipitation

293T cells were transiently transfected with vectors expressing AU5-tagged and HA-tagged versions of full-length human ING4, using a standard calcium phosphate protocol. Total protein lysates were prepared 48 h after transfection with RIPA lysis buffer (10 mM $NaPO_4$, pH 7.2, 300 mM NaCl, 0.1% SDS, 1% NP40, 1% deoxycholate, and 2 mM ethylenediaminetetraacetic acid) as previously described.[41,42] For immunoprecipitation, lysates containing 1 mg of total protein were incubated overnight at 4 °C, with constant rotation with 1 μl of an anti-HA tag antibody (clone 12CA2, Roche) or anti-AU5 tag antibody (MMS135R, Covance) or without antibody as a negative control. Thirty microliters of a slurry containing protein-A agarose beads (GE Healthcare) was added to the mix and incubated for 1 h in the same conditions. Beads were washed four times with ice-cold RIPA buffer and proteins in the immunoprecipitate were recovered by incubation with 2× SDS loading buffer (40 μl per immunoprecipitation) for 5 min at 90 °C. The presence of each protein in the immunocomplex was

Please cite this article as: Palacios, A., *et al.*, The Dimeric Structure and the Bivalent Recognition of H3K4me3 by the Tumor Suppressor ING4 Suggests a Mechanism for Enhanced Targeting of the HBO1..., *J. Mol. Biol.* (2010), doi:10.1016/j.jmb.2009.12.049

analyzed by Western blotting with antibodies against AU5 tag (1/500) and HA tag (1/500). The immunoprecipitation was repeated several times to confirm its reproducibility.

Circular dichroism

The spectra were performed in a Jasco J-810 spectropolarimeter at 25 °C. The spectra were the average of 15 scans, recorded using a 0.1-mm path-length quartz cuvette on 50-μM protein samples in 20 mM sodium phosphate, pH 6.5, 200 mM NaCl, and 1 mM DTT. The average helical content calculated from the molar residue ellipticity at 222 nm assuming 50-residue-long helices (as predicted by JPred) is 30%, 41%, and 63% for ING4, Nt_NLS, and Nt, respectively.[43] Thermal denaturation curves were measured in 2-mm path-length cuvettes closed with a Teflon cap on 25-μM protein solutions. Protein unfolding was induced by increasing temperature at a rate of 1 °C/min from 5 to 100 °C, and the ellipticity at 222 nm was recorded at intervals of 1 °C.

Small-angle X-ray scattering

Data were collected at X33 beamline at the European Molecular Biology Laboratory in the storage ring DORIS III of the Deutsches Elektronen Synchrotron, Hamburg.[44] Scattering curves of ING4, Nt, and Nt_NLS constructs were measured at 10 °C at protein concentrations of 327 μM (ING4), 500 and 260 μM (Nt), and 251 and 186 μM (Nt_NLS). An exposure time of 2 min was used for the measurements. The scattering profiles covered a range of momentum transfer of $0.02 < s < 0.5$ Å^{-1}. Radiation damage was minimal or absent since no significant changes were observed after repetitive exposures of the protein solutions. Buffer scattering profiles were measured before and after the sample measurements, averaged, and subtracted from the scattering profiles of the protein solutions. Resulting profiles were merged to avoid inter-particle interactions. All data manipulations were done using standard procedures with the software PRIMUS.[45] The forward scattering, $I(0)$ and the radius of gyration, R_g, were evaluated using the Guinier approximation, assuming that at very small angles ($s < 1.3/R_g$), the intensity can be well represented by $I(s) = I(0)\exp(-(sR_g)^2/3)$. The distance distribution function, $p(r)$, was computed from the entire curve with the program GNOM[46] by optimizing the maximum particle dimension, D_{max}. Low-resolution *ab initio* model structures of the Nt domain were built from the SAXS measurements using the program GASBOR.[47] The protein was represented by an assembly of 236 dummy residues inside a search volume. Starting from a random distribution, 10 assemblies that fit the experimental scattering profile were generated using a simulated annealing protocol. These 10 independent GASBOR models were averaged with the program package DAMAVER[48] to yield the most probable shape of the molecule.

NMR spectroscopy

NMR spectra of ING4 proteins were recorded at 25 °C on samples with a protein concentration of approximately 130 μM in 20 mM sodium phosphate, pH 6.5, 200 mM NaCl, 1 mM perdeuterated DTT, 5% ^2H_2O, and 0.01% NaN_3. Chemical shifts were measured relative to internal 2,2-dimethyl-2-silapentane-5-sulfonate sodium salt for ^1H and calculated for ^{15}N.[49] Spectra were processed with XWINMR, TOPSpin (Bruker), and/or NMRPipe.[50] The titration of ING4 with the peptides and the NMR binding analysis were performed as described previously.[15] The interaction of NLS_PHD with p53 was examined by NMR at 20 °C on samples prepared at 1:1 monomer molar ratios.

Peptide binding analysis by NMR

The synthetic peptides H3K4meX correspond to residues 1–15 of histone H3 plus an extra tyrosine residue at the C-terminus (ARTKQTARKSTGGKAY) to facilitate the quantification of peptide concentration by UV absorbance. Three peptides named with X = 1, 2, or 3 (mono-, di-, and trimethylated, respectively) differ in the number of methyls bound to the amino group of Lys4. These peptides have free N- and C-termini and were purchased from NeoMPS (Strasbourg). The titration of ING4 with the peptides and the NMR binding analysis were performed as previously described.[15] To measure the interaction of NLS_PHD with p53 by NMR, we prepared mixed samples at 1:1 monomer molar ratio, and NMR experiments were registered at 20 °C. For p53 observation, U-^{15}N-^2H-p53 (with protonated amides) was used, and transverse relaxation optimized spectroscopy ^1H–^{15}N-correlation spectra were recorded at 900 MHz. For NLS_PHD observation, U-^{15}N-NLS_PHD was used, and ^1H–^{15}N HSQC spectra were recorded at 600 MHz. The control samples (the isotope-labeled proteins alone) and the test samples (labeled-p53/NLS_PHD and labeled-NLS_PHD/unlabeled-p53) were simultaneously dialyzed against the same buffer (25 mM sodium phosphate, pH 7.2, 150 mM NaCl, and 5 mM perdeuterated DTT). The protein concentration was 100 μM in the labeled-p53-containing samples and 50 μM in the labeled-NLS_PHD-containing samples (monomer protein concentration).

Acknowledgements

We thank Prof. A. R. Fersht for support and helpful discussions; C. González, L. Cheng, and C. M. Blair for help with protein purification; D. Padró and S. M. V. Freund for help with NMR; and G. Montoya for critical manuscript reading. This work was supported by grants from Ministerio de Ciencia e Innovación (CTQ2008-03115/BQU), European Union (3D-REPERTOIRE, contract no. LSHG-CT-2005-512028), Fundación Mutua Madrileña to F.J.B., and ETORTEK-2008 grant to CIC bioGUNE. We also acknowledge the support to European Molecular Biology Laboratory Hamburg by European Commission–Research Infrastructure Action contract no. RII/2004/5060008. P.B. holds a Ramón y Cajal contract, and M.R.F.-F. was a Career Development Fellow of the MRC-UK.

Supplementary Data

Supplementary data associated with this article can be found, in the online version, at doi:10.1016/j.jmb.2009.12.049

Please cite this article as: Palacios, A., *et al.*, The Dimeric Structure and the Bivalent Recognition of H3K4me3 by the Tumor Suppressor ING4 Suggests a Mechanism for Enhanced Targeting of the HBO1..., *J. Mol. Biol.* (2010), doi:10.1016/j.jmb.2009.12.049

References

1. Kan, P. Y., Caterino, T. L. & Hayes, J. J. (2009). The H4 tail domain participates in intra- and internucleosome interactions with protein and DNA during folding and oligomerization of nucleosome arrays. *Mol. Cell. Biol.* **29**, 538–546.
2. Groth, A., Rocha, W., Verreault, A. & Almouzni, G. (2007). Chromatin challenges during DNA replication and repair. *Cell*, **128**, 721–733.
3. Li, B., Carey, M. & Workman, J. L. (2007). The role of chromatin during transcription. *Cell*, **128**, 707–719.
4. Jenuwein, T. & Allis, C. D. (2001). Translating the histone code. *Science*, **293**, 1074–1080.
5. Taverna, S. D., Li, H., Ruthenburg, A. J., Allis, C. D. & Patel, D. J. (2007). How chromatin-binding modules interpret histone modifications: lessons from professional pocket pickers. *Nat. Struct. Mol. Biol.* **14**, 1025–1040.
6. Russell, M., Berardi, P., Gong, W. & Riabowol, K. (2006). Grow-ING, Age-ING and Die-ING: ING proteins link cancer, senescence and apoptosis. *Exp. Cell Res.* **312**, 951–961.
7. Shi, X., Hong, T., Walter, K. L., Ewalt, M., Michishita, E., Hung, T. *et al.* (2006). ING2 PHD domain links histone H3 lysine 4 methylation to active gene repression. *Nature*, **442**, 96–99.
8. Doyon, Y., Cayrou, C., Ullah, M., Landry, A. J., Cote, V., Selleck, W. *et al.* (2006). ING tumor suppressor proteins are critical regulators of chromatin acetylation required for genome expression and perpetuation. *Mol. Cell*, **21**, 51–64.
9. He, G. H., Helbing, C. C., Wagner, M. J., Sensen, C. W. & Riabowol, K. (2005). Phylogenetic analysis of the ING family of PHD finger proteins. *Mol. Biol. Evol.* **22**, 104–116.
10. Pena, P. V., Hom, R. A., Hung, T., Lin, H., Kuo, A. J., Wong, R. P. *et al.* (2008). Histone H3K4me3 binding is required for the DNA repair and apoptotic activities of ING1 tumor suppressor. *J. Mol. Biol.* **380**, 303–312.
11. Pena, P. V., Davrazou, F., Shi, X., Walter, K. L., Verkhusha, V. V., Gozani, O. *et al.* (2006). Molecular mechanism of histone H3K4me3 recognition by plant homeodomain of ING2. *Nature*, **442**, 100–103.
12. Palacios, A., Munoz, I. G., Pantoja-Uceda, D., Marcaida, M. J., Torres, D., Martin-Garcia, J. M. *et al.* (2008). Molecular basis of histone H3K4me3 recognition by ING4. *J. Biol. Chem.* **283**, 15956–15964.
13. Champagne, K. S., Saksouk, N., Pena, P. V., Johnson, K., Ullah, M., Yang, X. J. *et al.* (2008). The crystal structure of the ING5 PHD finger in complex with an H3K4me3 histone peptide. *Proteins*, **72**, 1371–1376.
14. Hung, T., Binda, O., Champagne, K. S., Kuo, A. J., Johnson, K., Chang, H. Y. *et al.* (2009). ING4 mediates crosstalk between histone H3 K4 trimethylation and H3 acetylation to attenuate cellular transformation. *Mol. Cell*, **33**, 248–256.
15. Palacios, A., Garcia, P., Padro, D., Lopez-Hernandez, E., Martin, I. & Blanco, F. J. (2006). Solution structure and NMR characterization of the binding to methylated histone tails of the plant homeodomain finger of the tumour suppressor ING4. *FEBS Lett.* **580**, 6903–6908.
16. Ruthenburg, A. J., Li, H., Patel, D. J. & Allis, C. D. (2007). Multivalent engagement of chromatin modifications by linked binding modules. *Nat. Rev., Mol. Cell Biol.* **8**, 983–994.
17. Dutta, K., Alexandrov, A., Huang, H. & Pascal, S. M. (2001). pH-induced folding of an apoptotic coiled coil. *Protein Sci.* **10**, 2531–2540.
18. Doniach, S. (2001). Changes in biomolecular conformation seen by small angle X-ray scattering. *Chem. Rev.* **101**, 1763–1778.
19. Glatter, O. K. & Kratky, O. (1982). *Small Angle X-ray Scattering*. Academic Press, New York, NY.
20. Svergun, D. I. & Koch, M. H. J. (2003). Small-angle scattering studies of biological macromolecules in solution. *Rep. Prog. Phys.* **66**, 1735–1782.
21. Tarbouriech, N., Curran, J., Ruigrok, R. W. & Burmeister, W. P. (2000). Tetrameric coiled coil domain of Sendai virus phosphoprotein. *Nat. Struct. Biol.* **7**, 777–781.
22. Yousef, M. S., Kamikubo, H., Kataoka, M., Kato, R. & Wakatsuki, S. (2008). Miranda cargo-binding domain forms an elongated coiled-coil homodimer in solution: implications for asymmetric cell division in *Drosophila*. *Protein Sci.* **17**, 908–917.
23. Coles, A. H. & Jones, S. N. (2009). The ING gene family in the regulation of cell growth and tumorigenesis. *J. Cell. Physiol.* **218**, 45–57.
24. Shiseki, M., Nagashima, M., Pedeux, R. M., Kitahama-Shiseki, M., Miura, K., Okamura, S. *et al.* (2003). p29ING4 and p28ING5 bind to p53 and p300, and enhance p53 activity. *Cancer Res.* **63**, 2373–2378.
25. Zhang, X., Wang, K. S., Wang, Z. Q., Xu, L. S., Wang, Q. W., Chen, F. *et al.* (2005). Nuclear localization signal of ING4 plays a key role in its binding to p53. *Biochem. Biophys. Res. Commun.* **331**, 1032–1038.
26. Hajduk, P. J., Gerfin, T., Boehlen, J. M., Haberli, M., Marek, D. & Fesik, S. W. (1999). High-throughput nuclear magnetic resonance-based screening. *J. Med. Chem.* **42**, 2315–2317.
27. Meyer, B. & Peters, T. (2003). NMR spectroscopy techniques for screening and identifying ligand binding to protein receptors. *Angew. Chem., Int. Ed. Engl.* **42**, 864–890.
28. Jencks, W. P. (1981). On the attribution and additivity of binding energies. *Proc. Natl Acad. Sci. USA*, **78**, 4046–4050.
29. Ruthenburg, A. J., Wang, W., Graybosch, D. M., Li, H., Allis, C. D., Patel, D. J. & Verdine, G. L. (2006). Histone H3 recognition and presentation by the WDR5 module of the MLL1 complex. *Nat. Struct. Mol. Biol.* **13**, 704–712.
30. Santos-Rosa, H., Kirmizis, A., Nelson, C., Bartke, T., Saksouk, N., Cote, J. & Kouzarides, T. (2009). Histone H3 tail clipping regulates gene expression. *Nat. Struct. Mol. Biol.* **16**, 17–22.
31. Saksouk, N., Avvakumov, N., Champagne, K. S., Hung, T., Doyon, Y., Cayrou, C. *et al.* (2009). HBO1 HAT complexes target chromatin throughout gene coding regions via multiple PHD finger interactions with histone H3 tail. *Mol. Cell*, **33**, 257–265.
32. Thompson, J. D., Gibson, T. J., Plewniak, F., Jeanmougin, F. & Higgins, D. G. (1997). The CLUSTAL_X windows interface: flexible strategies for multiple sequence alignment aided by quality analysis tools. *Nucleic Acids Res.* **25**, 4876–4882.
33. Feng, X., Hara, Y. & Riabowol, K. (2002). Different HATS of the ING1 gene family. *Trends Cell Biol.* **12**, 532–538.
34. Cuff, J. A., Clamp, M. E., Siddiqui, A. S., Finlay, M. & Barton, G. J. (1998). JPred: a consensus secondary structure prediction server. *Bioinformatics*, **14**, 892–893.
35. Lupas, A., Van Dyke, M. & Stock, J. (1991). Predicting coiled coils from protein sequences. *Science*, **252**, 1162–1164.
36. Li, X., Romero, P., Rani, M., Dunker, A. K. & Obradovic, Z. (1999). Predicting protein disorder for

Please cite this article as: Palacios, A., *et al.*, The Dimeric Structure and the Bivalent Recognition of H3K4me3 by the Tumor Suppressor ING4 Suggests a Mechanism for Enhanced Targeting of the HBO1..., *J. Mol. Biol.* (2010), doi:10.1016/j.jmb.2009.12.049

N-, C-, and internal regions. *Genome Inform. Ser. Workshop Genome Inform.* **10**, 30–40.
37. Unoki, M., Shen, J. C., Zheng, Z. M. & Harris, C. C. (2006). Novel splice variants of ING4 and their possible roles in the regulation of cell growth and motility. *J. Biol. Chem.* **281**, 34677–34686.
38. Laue, T. M. S., Shah, B. D., Ridgeway, T. M. & Pelletier, S. L. (1992). *Computer-Aided Interpretation of Analytical Sedimentation Data for Proteins.* Royal Society of Chemistry, Cambridge, UK.
39. Schuck, P. & Rossmanith, P. (2000). Determination of the sedimentation coefficient distribution by least-squares boundary modeling. *Biopolymers*, **54**, 328–341.
40. Minton, A. P. (1994). *Modern Analytical Ultracentrifugation.* Birkhauser Boston, Inc., Cambridge, MA.
41. Palmero, I., Murga, M., Zubiaga, A. & Serrano, M. (2002). Activation of ARF by oncogenic stress in mouse fibroblasts is independent of E2F1 and E2F2. *Oncogene*, **21**, 2939–2947.
42. Gonzalez, L., Freije, J. M., Cal, S., Lopez-Otin, C., Serrano, M. & Palmero, I. (2006). A functional link between the tumour suppressors ARF and p33ING1. *Oncogene*, **25**, 5173–5179.
43. Chen, Y. H., Yang, J. T. & Chau, K. H. (1974). Determination of the helix and beta form of proteins in aqueous solution by circular dichroism. *Biochemistry*, **13**, 3350–3359.
44. Roessle, M. W., Klaering, R., Ristau, U., Robrahn, B., Jahn, D., Gehrmann, T. *et al.* (2007). Upgrade of the small-angle X-ray scattering beamline X33 at the European Molecular Biology Laboratory, Hamburg. *J. Appl. Crystallogr.* **40**, 190–194.
45. Konarev, P. V., Volkov, V. V., Sokolova, A. V., Koch, M. H. J. & Svergun, D. I. (2003). PRIMUS: a Windows PC-based system for small-angle scattering data analysis. *J. Appl. Crystallogr.* **36**, 1277–1282.
46. Svergun, D. I. (1992). Determination of the regularization parameter in indirect-transform methods using perceptual criteria. *J. Appl. Crystallogr.* **25**, 495–503.
47. Svergun, D. I., Petoukhov, M. V. & Koch, M. H. (2001). Determination of domain structure of proteins from X-ray solution scattering. *Biophys. J.* **80**, 2946–2953.
48. Volkov, V. V. & Svergun, D. I. (2003). Uniqueness of ab initio shape determination in small-angle scattering. *Appl. Crystallogr.* **36**, 860–864.
49. Wishart, D. S., Bigam, C. G., Yao, J., Abildgaard, F., Dyson, H. J., Oldfield, E. *et al.* (1995). ^{1}H, ^{13}C and ^{15}N chemical shift referencing in biomolecular NMR. *J. Biomol. NMR*, **6**, 135–140.
50. Delaglio, F., Grzesiek, S., Vuister, G. W., Zhu, G., Pfeifer, J. & Bax, A. (1995). NMRPipe: a multidimensional spectral processing system based on UNIX pipes. *J. Biomol. NMR*, **6**, 277–293.

Please cite this article as: Palacios, A., *et al.*, The Dimeric Structure and the Bivalent Recognition of H3K4me3 by the Tumor Suppressor ING4 Suggests a Mechanism for Enhanced Targeting of the HBO1..., *J. Mol. Biol.* (2010), doi:10.1016/j.jmb.2009.12.049

Published Online First on February 23, 2010 as 10.1158/0008-5472.CAN-09-2088

Molecular and Cellular Pathobiology

Cancer Research

Regulation of the MicroRNA Processor DGCR8 by the Tumor Suppressor ING1

Daniel Gómez-Cabello[1], Sergio Callejas[2], Alberto Benguría[2], Alberto Moreno[1], Javier Alonso[3], and Ignacio Palmero[1]

Abstract

The ING family of tumor suppressor proteins controls several cellular functions relevant to antitumor protection, such as cell cycle control, apoptosis, senescence, or migration. ING proteins are functionally linked to the p53 pathway, and they participate in transcriptional control via the recognition of histone marks and recruitment of protein complexes with chromatin-modifying activity to specific promoters. Here, we have investigated the global effect of ING1 in gene regulation through genome-wide analysis of expression profiles in primary embryonic fibroblasts deficient for the *Ing1* locus. We find that Ing1 has a predominant role as transcriptional repressor in this setting, affecting the expression of genes involved in a variety of cellular functions. Within the subset of genes showing differential expression, we have identified DGCR8, a protein involved in the early steps of microRNA biogenesis. We show that ING1 binds to the DGCR8 promoter and controls its transcription through chromatin regulation. We also find that ING1 and DGCR8 can cooperate in restraining proliferation. In summary, this study reveals a novel connection between ING1 and a regulator of microRNA biogenesis and identifies new links between tumor suppressor proteins and the microRNA machinery. *Cancer Res; 70(5); 1866–74. ©2010 AACR.*

Introduction

The ING proteins constitute a family of sequence-related, evolutionary conserved proteins, with tumor suppressor activity in mammals (reviewed in refs. 1, 2). p33ING1 (also known as ING1b) is encoded in the ING1 locus together with two other alternative products: p47ING1a (in humans) and p24ING1c (in humans and mice). Alterations in the *ING1* locus have been reported in different types of human tumors, most frequently the reduced expression or mislocalization of ING1 and fewer cases of point missense mutations (reviewed in ref. 3). Furthermore, the inactivation of the *Ing1* locus in mice results in an increased incidence of lymphomas (4–6). p33ING1 has been functionally linked to the p53 tumor suppressor pathway and to chromatin regulation. Different activities of p33ING1, such as induction of cell cycle arrest, apoptosis, or DNA repair, require a functional p53 pathway *in vitro* (7), although p53-independent functions have also been described (8). It has been suggested that ING1 can influence p53 protein stabilization, and/or its posttranslational modification (9), or act as a cofactor in the regulation of target genes (10). On the other hand, p33ING1, in common with other ING proteins, has a general role in transcriptional regulation. ING proteins recognize specific histone methyl marks [preferentially histone H3 trimethylated in Lys4 (H3K4me3)] through their conserved PHD domain (11–15) and allow the recruitment of complexes with histone deacetylase (HDAC) or histone acetyltransferase activity to target genes (16–19). Despite the advances in identifying cellular functions controlled by ING1 or the mechanistic basis for its control of gene expression, the downstream targets of ING1 are largely unknown. Here, we have used primary embryonic fibroblasts derived from mice deficient for the *Ing1* locus to investigate the global effect of Ing1 in gene expression and identify genes and processes regulated by Ing1 that may account for its tumor-suppressive action. Among the genes with differential expression, we have identified the microRNA regulator protein Dgcr8, a protein involved in the early steps of microRNA biogenesis. These findings reveal a novel link between tumor suppressor proteins and microRNA biogenesis.

Materials and Methods

Cell culture. Preparation and culture of mouse embryo fibroblasts (MEF) and retroviral infection experiments were carried out as previously described (20). Early-passage MEFs (with less than four population doublings) were used for all the experiments. For lentiviral infections, 293T cells were transiently transfected with the appropriate lentiviral expression vector and the vectors pMD2-G, pMDLg/pRRE, and pRSV-Rev, which encode lentiviral proteins. The medium

Authors' Affiliations: [1]Instituto de Investigaciones Biomédicas CSIC-UAM; [2]Centro Nacional de Investigaciones Cardiovasculares; [3]Unidad de Tumores Sólidos Infantiles, Instituto de Salud Carlos III, Madrid, Spain

Note: Supplementary data for this article are available at Cancer Research Online (http://cancerres.aacrjournals.org/).

Current address for D. Gómez-Cabello: M.D. Anderson International España, Madrid, Spain.

Corresponding Author: Ignacio Palmero, Instituto de Investigaciones Biomédicas CSIC-UAM, Arturo Duperier, 4, 28029 Madrid, Spain. Phone: 34-915854491; Fax: 34-915854401; E-mail: ipalmero@iib.uam.es.

doi: 10.1158/0008-5472.CAN-09-2088

containing lentiviruses was recovered, filtered through a 0.45-μm filter, diluted 1 in 2 with fresh medium, and added to the recipient cells. The same procedure was repeated 12 h later. The following vectors were used for retroviral or lentiviral transduction: pLPC-AU5ING1 (10), pSuper-DGCR8, pSicoR-DGCR8 (21), and the relevant empty vectors. The inducible line EMG was generated by stable transfection with the vectors pWZL-Blast-rtTA and pHRS-AU5-ING1 of the ARF-inducible NARF2 cell line (a kind gift of Gordon Peters, Cancer Research UK; ref. 22). All cells were grown in DMEM containing 10% fetal bovine serum. Bromodeoxyuridine (BrdUrd) incorporation was measured as described (10) using a 6-h pulse. For chromatin immunoprecipitation (ChIP) assays, trichostatin A (TSA) was added at a final concentration of 32 nmol/L 1 h before harvesting the cells. For colony formation assays, cells were seeded at a density of 800 or 8000 per well in six-well plates. After 10 d, cells were fixed with formaldehyde and stained with Giemsa stain solution, and the colonies were counted. For growth curves, cells were seeded in 24-well plates, at 2×10^4 per well, in triplicate. At different time points, cells were trypsinized and counted with a Neubauer chamber.

Analysis of gene expression profiles. CodeLink mouse whole-genome microarrays (Applied Microarrays, Inc.) were used to analyze gene expression profiles. Total RNA was isolated with TriReagent (Sigma), and its integrity was assessed using an Agilent 2100 Bioanalyzer (Agilent Technologies). Labeling and hybridization were performed using the CodeLink iExpress assay reagent kit according to the manufacturer's instructions. After hybridization and washing, slides were scanned in an Axon GenePix scanner and analyzed using CodeLink Expression Analysis software. Data were median normalized, $\log_2$ transformed, and exported to the MeV software (TIGR) for additional statistical analysis and graphical visualization. We analyzed three independent preparations of early-passage MEF for each genotype, each derived from an individual embryo. Genes with ratios between *Ing1*-deficient and wild-type higher than 2 or lower than 0.5, with statistical significance ($P < 0.05$, Student's t test), were selected for further analysis. Functional genomics analysis of differentially expressed genes was carried out with the Fatigo suite.[4] Statistical differences between the percentages of Gene Ontology (GO) terms were calculated by Fisher's exact test.

Chromatin immunoprecipitation. ChIP analysis was performed essentially as described by Weinmann and Farnham (23) with some modifications. For immunoprecipitation, the following antibodies were used: 1 μg of anti-AU5 (Covance Research Products, Inc.), 2 μg of anti-H3K4me3 (Abcam), 1 μg of anti-p53 (DO-1, Santa Cruz Biotechnology), 2 μg of anti–acetylated histone H3 (Upstate Millipore), and 2 μg of anti–acetylated histone H4 (Millipore). The precipitated DNA was analyzed by PCR with the appropriate primers (see Supplementary Data).

Quantitative real-time PCR. Total RNA was isolated with TriReagent, as recommended by the manufacturer. cDNA was generated using reverse transcriptase Moloney murine leukemia virus (Promega), and the real-time PCR was performed in ABI 7900HT or ABI 9700 machines (Applied Biosystems) using SYBR Green for labeling and ribosomal 18S RNA or glyceraldehyde-3-phosphate dehydrogenase (GAPDH) as standards.

Western blot. Western blot analysis was carried out as previously described (10) using the following antibodies: anti-DGCR8 (1:300 dilution; PTG-Lab), anti-human p53 (DO-1; 1:500 dilution), anti-AU5 (1:500 dilution), anti-actin (1:10,000 dilution; Sigma), anti-p33ING1 (LG1, 1:1,000 dilution; ref. 10).

Immunofluorescence. Exponentially growing, low-passage MEFs were fixed with 4% paraformaldehyde in PBS, permeabilized with 0.1% Triton X-100 in PBS, and incubated in blocking solution (PBS containing 2% bovine serum albumin) overnight at 4°C. The primary antibody (anti-Dgcr8, 1:100 dilution; PTG-Lab) was added in blocking solution, left for 60 min at room temperature, and washed with PBS containing 0.1% Triton X-100 (three to four washes, 15 min each) followed by incubation with a fluorochrome-conjugated secondary antibody (donkey anti-rabbit Alexa Fluor 488, 1:500 dilution) and washing in the same conditions used with the primary antibodies. Cells were mounted with Vectashield mounting medium with 4′,6-diamidino-2-phenylindole (DAPI; Vector Laboratories) and analyzed using a Zeiss Axiophot microscope.

Results

Identification of genes regulated by Ing1 in mouse fibroblasts. To investigate the general effect of Ing1 on gene expression, we carried out a genome-wide expression profiling analysis using CodeLink mouse whole-genome expression arrays. We chose for this study primary MEFs of very early passage (see Materials and Methods) to avoid effects of unknown genetic makeup associated with tumor-derived or immortalized cell lines or changes due to the accumulation of divisions in culture. The *Ing1*-deficient MEFs we have used in this study display a dramatic reduction (>90%) in the expression of all the transcripts of the locus, as a consequence of the insertion of a BetaGeo genetrap cassette. The levels of the p33ING1 protein (the only ING1 peptide detectable in MEFs) are also reduced to the same extent (24). Of the 37,898 probes, representing >30,000 genes, present in the array, we found a significantly differential expression associated to Ing1 status (at least 2-fold change, see Materials and Methods) for 466 of them (~1.2% of the total). This indicates that Ing1 controls the expression of a very specific subset of genes in our system. Of the group of genes showing differential expression, the majority (70%, 328 of 466) were upregulated in *Ing1*-deficient fibroblasts relative to wild-type counterparts (Fig. 1A). This finding indicates a predominant role for Ing1 as a transcriptional repressor, in agreement with previous biochemical studies (16, 18). As an internal validation of the experiment, we found that the signal for the Ing1 probe was reduced ~10-fold in the *Ing1*-mutant fibroblasts (*Ing1*-mutant/wild-type ratio, 0.11; $P = 0.0004$), consistent with our previous characterization of the expression of the *Ing1* locus in this cell type (24). In addition, we found that the expression of the other *Ing*

[4] http://www.fatigo.org

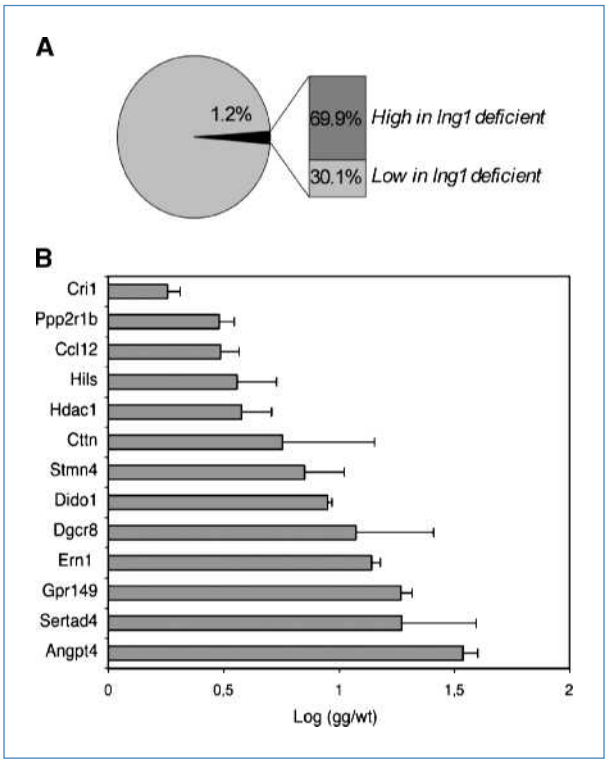

Figure 1. A, schematic depiction of the global analysis of gene expression in *Ing1*-deficient mouse fibroblasts. The percentage of probes showing differential expression is indicated, and the percentage of probes within this group with increased or reduced expression in *Ing1*-deficient cells is shown. B, expression analysis of a subset of genes differentially expressed in *Ing1*-deficient fibroblasts. RNA levels in wild-type or *Ing1*-deficient fibroblasts were calculated using quantitative real-time RT-PCR. The ratio between *Ing1*-deficient and wild-type cells is shown using a logarithmic scale. Error bars indicate SDs from three independent assays.

loci is not significantly altered in *Ing1*-mutant cells, with the possible exception of Ing5 (Supplementary Table S1). These results further validate the usefulness of this cellular system to identify genes specifically regulated by Ing1.

Functional enrichment analysis showed that Ing1 status alters the expression of proteins involved in a variety of cellular processes (Supplementary Table S2). Interestingly, the most significant enrichments correspond to the categories of response to stress (13.16% of differentially expressed genes versus 6.76% of total, 7.2-fold enrichment) and transcriptional repression (4.79% of differentially expressed genes versus 1.48% of total, 3.2-fold enrichment). Within the former group, a significant enrichment was detected for G protein–related factors (4.69% versus 0.65%, 7.2-fold enrichment) and chemokine-related factors (15.38% versus 1.01%, 15.3-fold enrichment). To validate the data obtained with the array, we selected a set of genes based on their score in the array and their functional importance (Table 1) and quantified the levels of their transcripts by real-time quantitative reverse transcription-PCR (RT-PCR; Fig. 1B). This analysis showed a good correlation between the signals from the array and RNA levels for the majority of genes studied, validating the data from the array.

Ing1 regulates Dgcr8. From the subset of genes with validated differential expression, we chose to analyze in detail Dgcr8, one of the genes with increased expression in Ing1-deficient fibroblasts. Dgcr8 (DiGeorge syndrome critical region 8, also known as Pasha) encodes an RNA-binding protein involved in the early steps of processing of microRNAs (25). Given the growing evidence of the importance of the microRNA machinery in the context of cancer, we wished to know if Dgcr8 could be a direct transcriptional target of Ing1, providing a link between this tumor suppressor protein and the microRNA machinery.

First, we used Western blot and immunofluorescence to investigate the levels and localization of the Dgcr8 protein in normal and *Ing1*-mutant MEFs (Fig. 2). The amount of Dgcr8 protein was modestly increased in the *Ing1*-mutant cells (~2-fold), consistent with the data from the array and quantitative RT-PCR (Fig. 2A). Expression of ectopic p33ING1 in *Ing1*-deficient fibroblasts dramatically reduced Dgcr8 protein levels, further supporting the correlation between Ing1 and Dgcr8 protein levels (Fig. 2B). In accordance with previous reports (26), we found that Dgcr8 shows a predominantly nuclear staining in both wild-type and *Ing1*-mutant fibroblasts. Dgcr8 showed an even distribution through the nucleoplasm, with some degree of accumulation in speckles in both genotypes (Fig. 2C).

Ing1 is a direct transcriptional regulator of Dgcr8. To test whether Ing1 participates directly in the transcriptional control of the Dgcr8 locus, we performed ChIP experiments. Attempts to detect the endogenous p33ING1 protein on the Dgcr8 promoter in mouse fibroblasts were unsuccessful because of the failure of the anti-ING1 antibody to work in this assay (data not shown). To circumvent this problem, we used a tagged version of p33ING1 in two different experimental settings. First, we used a cell line (EMG) generated in our laboratory from the U2OS-derived, p14ARF-inducible, NARF2 line (22). EMG cells have been engineered to allow doxycycline-inducible expression of AU5 tagged-p33ING1 and independent isopropyl-L-thio-B-D-galactopyranoside (IPTG)–inducible expression of the p53 activator p14ARF (see Materials and Methods). When ING1 expression was induced on addition of doxycycline (Fig. 3A, left), we could easily detect the binding of the ING1 protein to the promoter region of the DGCR8 locus by ChIP using an antibody against the AU5 tag (Fig. 3A, right, and D). As a control of the specificity of the assay, binding of p33ING1 to the housekeeping GAPDH locus was not detected. These results were confirmed in HCT116 colon carcinoma cells transiently transfected with a vector expressing AU5-tagged p33ING1 (Fig. 3B, left). ChIP analysis with the anti-AU5 antibody again showed binding of ectopic ING1 to the DGCR8 promoter in ING1-transfected cells and not in vector-transfected controls (Fig. 3B, right, and D).

It has been suggested that ING1 can cooperate with p53 in transcriptional regulation (7). To test whether the presence of ING1 in the DGCR8 promoter was affected by p53, we increased endogenous p53 levels in the EMG cells by means of the inducible expression of p14ARF (Fig. 3C, left). ChIP

Table 1. Selected genes with differential expression in *Ing1*-deficient fibroblasts

Accession number	Gene symbol	Gene name	Ratio gg/wt	*t* test
NM_177346	*Gpr149*	G protein–coupled receptor 149	11.24	0.0209
NM_007803	*Cttn (EMS1)*	Cortactin	10.65	0.002
NM_023913	*Ern1*	Endoplasmic reticulum to nucleus signaling 1	9.82	0.0009
NM_025613	*Cri1 (Eid1)*	EP300 interacting inhibitor of differentiation 1	9.56	0.0157
NM_020581	*Angptl4*	Angiopoietin-like 4	9.32	0.019
NM_175551	*Dido1*	Death inducer-obliterator 1	5.17	0.042
NM_018792	*Hils1*	Histone linker H1 domain, spermatid-specific 1	3.80	0.02
NM_198247	*Sertad4*	SERTA domain containing 4	3.39	0.02
NM_019675	*Stmn4*	Stathmin-like 4	3.04	0.06
NM_011331	*Ccl12 (MCP5)*	Chemokine (C-C motif) ligand 12	2.75	0.04
NM_033324	*Dgcr8*	DiGeorge syndrome critical region gene 8	2.69	0.04
NM_008228	*Hdac1*	Histone deacetylase 1	2.63	0.0159
NM_028614	*Ppp2r1b*	Protein phosphatase 2 regulatory subunit A, β isoform	2.58	0.0068
NM_010545	*Rps14*	Ribosomal protein S14	0.19	0.003
NM_013653	*Ccl5*	Chemokine (C-C motif) ligand 5	0.17	0.026
NM_009628	*Adnp*	Activity-dependent neuroprotective protein	0.13	0.03
NM_011919	*Ing1*	Inhibitor of growth 1	0.11	0.0004

Abbreviations: wt, wild-type; g/g, *Ing1*-deficient.

experiments with the anti-AU5 antibody showed undistinguishable results with or without p53 accumulation (compare Fig. 3C with Fig. 3A), suggesting that the binding of p33ING1 to the DGCR8 promoter region is not affected by p53 levels (Fig. 3C). As a control for the specificity of the detection of ING1 in the DGCR8 promoter, we carried out additional ChIP experiments with an anti-p53 antibody in EMG cells after induction of p14ARF by IPTG (22). We could not detect specific

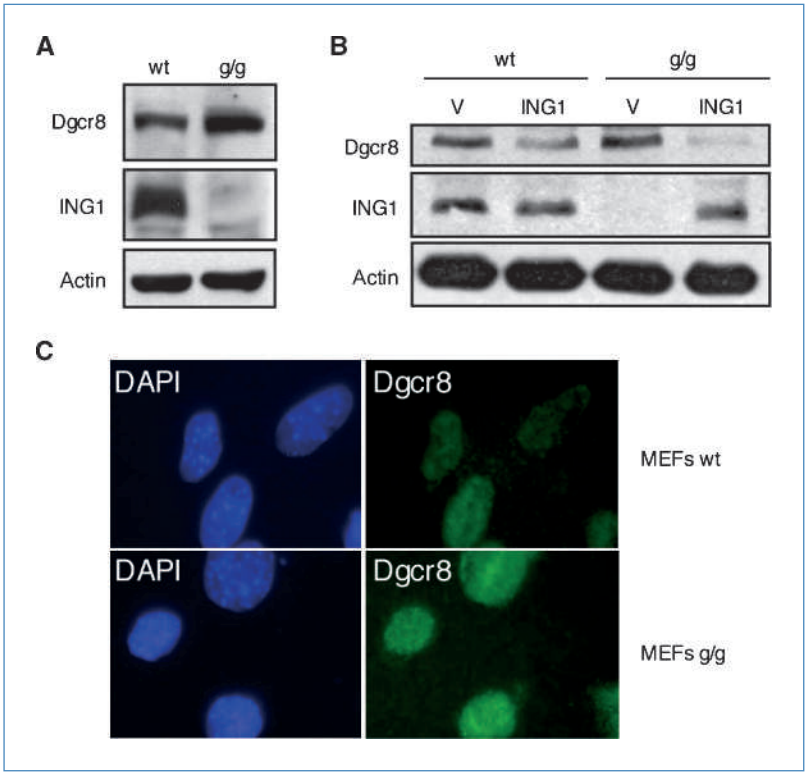

Figure 2. Protein levels and subcellular localization of Dgcr8. A, Western blot analysis of Dgcr8 protein levels in early-passage wild-type (wt) or *Ing1*-deficient (g/g) MEFs. A blot for p33ING1 is shown as a genotype control. Actin was used as a loading control. B, Western blot analysis, as in A, in early-passage MEFs retrovirally infected with p33ING1. C, immunofluorescence images obtained with an antibody against Dgcr8 in exponentially growing early-passage MEFs of the indicated genotypes. DAPI counterstaining is shown to identify nuclei.

binding of p53 to the DGCR8 promoter under conditions where the promoter of the p53 target p21CIP1 could be recovered in chromatin precipitated with the p53 antibody (Supplementary Fig. S1). Note than binding of p53 to the p21 promoter is independent of p53 levels in this cell line (27).

Mechanism of regulation of Dgcr8 by Ing1. To determine the mechanism underlying the regulation of Dgcr8 by ING1, we investigated the status of several histone modifications in the Dgcr8 promoter in wild-type or *Ing1*-mutant fibroblasts using ChIP. We found that the acetylation of histone H3 and histone H4 in the Dgcr8 promoter was significantly increased in *Ing1*-mutant cells (Fig. 4A). H3K4me3 is considered a mark of transcriptionally active chromatin and is specifically recognized by ING1 and other ING proteins. The amount of H3K4me3 recovered in chromatin for the Dgcr8 promoter was not grossly altered in *Ing1*-deficient cells, consistent with the notion that ING1 acts primarily as a reader of this mark but does not influence its methylation (Fig. 4A). Collectively, these results suggest that ING1 contributes to the transcriptional repression of Dgcr8 by the inhibition of histone acetylation through active recruitment of deacetylation complexes. To confirm the involvement of HDACs in the repression of Dgcr8 by Ing1, we treated fibroblasts of both genotypes with TSA, an inhibitor of class I and class II HDACs. Treatment with TSA resulted in an increase of Dgcr8 RNA and protein in wild-type MEFs (Fig. 4B and C), which correlated with increased presence of acetylated histones in ChIP experiments (Supplementary Fig. S2). *Ing1*-deficient cells retained a limited response to TSA, which could be due to residual Ing1 expression in *Ing1*-mutant MEFs or to Ing1-independent HDAC activity.

MicroRNA expression in Ing1-deficient fibroblasts. To test whether the altered levels of Dgcr8 observed in

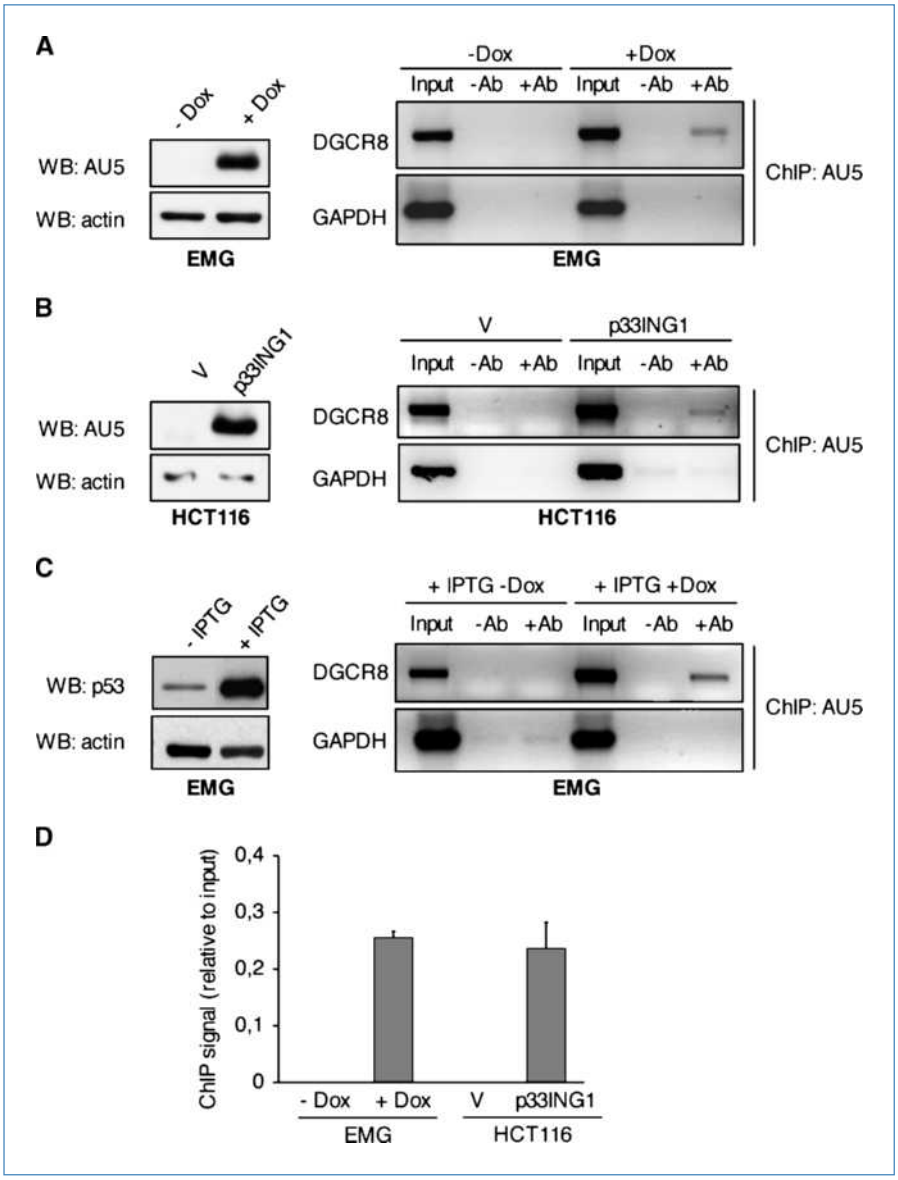

Figure 3. ChIP analysis of the presence of ING1 at the DGCR8 promoter. A, ChIP in the inducible line EMG. Left, cells were treated with doxycycline (Dox) for 24 h to induce AU5-p33ING1 expression; right, immunoprecipitation of chromatin was performed with an antibody against the AU5 tag followed by PCR for the DGCR8 promoter. PCR for GAPDH is shown as a negative control. B, left, ChIP in HCT116 cells transiently transfected with a vector expressing AU5-p33ING1 or an empty vector; right, immunoprecipitation of chromatin was performed as described in A 48 h after transfection. C, ChIP in the inducible line EMG. Left, cells were treated with IPTG for 24 h to induce p14ARF (data not shown) and p53 protein levels; right, immunoprecipitation of chromatin was performed with an antibody against the AU5 tag as described in A. WB, Western blot; –Ab, control without antibody; +Ab, sample with the indicated specific antibody. D, quantitation of ChIP signals from experiments shown in A and B. Error bars indicate SD from two experiments.

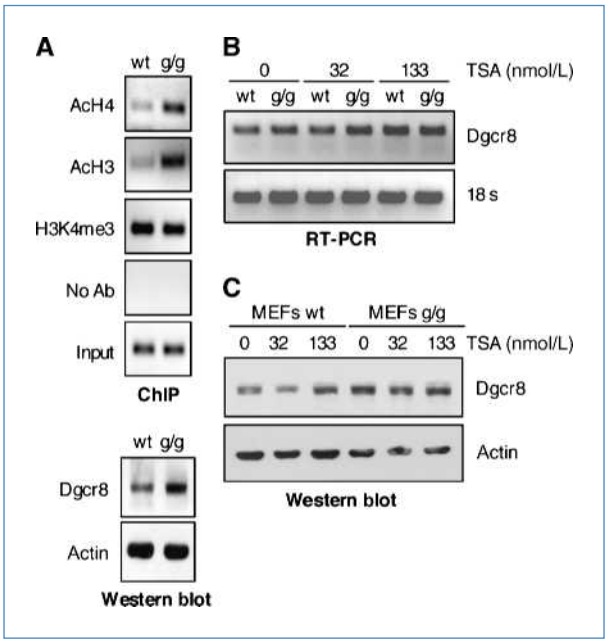

Figure 4. Role of histone acetylation in the regulation of Dgcr8 by Ing1. A, top, ChIP was performed in wild-type or *Ing1*-deficient MEFs with antibodies against the indicated histone marks followed by PCR amplification of the Dgcr8 promoter; bottom, Western blot analysis of Dgcr8 protein level in the MEFs used in the ChIP assay. B, levels of the Dgcr8 transcript were analyzed by RT-PCR in MEFs of the indicated genotypes 12 h after treatment with different concentrations of TSA. The rRNA 18S is used as a control for template amount and integrity. C, Western blot analysis of Dgcr8 protein in the same conditions as in B. Actin is used as a loading control. AcH3, acetylated histone H3; AcH4, acetylated histone H4.

Ing1-deficient cells had an effect in the normal expression of microRNAs in mouse fibroblasts, we analyzed the expression profile of mature microRNAs in wild-type or *Ing1*-mutant early-passage fibroblasts using a miRNA microarray from Agilent Technologies. We identified a small subset of mature miRNAs that displayed statistically significant differences in *Ing1*-deficient cells relative to wild-type controls. Interestingly, all the miRNAs in this subset were upregulated in *Ing1*-deficient fibroblasts relative to the wild-type controls (Supplementary Fig. S3A). Additional microRNA expression analysis in the inducible EMG cell line showed that the set of miRNAs upregulated in *Ing1*-deficient MEFs was also downregulated on ING1 induction in this cell line, further supporting the link between ING1 levels and the expression of these miRNAs (Supplementary Fig. S3B). The differential expression of mature miR-192 (the miRNA with the highest upregulation) was validated by quantitative PCR (Supplementary Fig. S3C). Some of the miRNAs with highest scores in this analysis showed sequence similarity between them, and they were predicted to share potential target transcripts using the miRanda algorithm, suggesting that the group of miRNAs deregulated in *Ing1*-deficient fibroblasts might control a common set of targets (Supplementary Fig. S3D).

Functional link between ING1 and DGCR8. We explored whether the link between ING1 and DGCR8 expression could have a functional implication. To this end, we stably expressed a short hairpin RNA (shRNA) against DGCR8 in the inducible EMG line, which resulted in a highly efficient reduction of endogenous DGCR8 levels (Fig. 5A, left). As previously described, induction of ING1 expression had a clear antiproliferative effect in these cells, which could be measured in growth curves or in colony formation assays ($P = 0.019$ in colony formation assays; Fig. 5A, right, and B). Unexpectedly, the independent suppression of DGCR8 by itself also resulted in reduced proliferation ($P = 0.01$ in colony formation assays). Concomitant induction of ING1 expression and silencing of DGCR8 led to enhanced antiproliferative effect in both assays (compare pSi-DGCR8 + Dox versus pSicoR + Dox; $P = 0.12$; Fig. 5A and B). The functional connection between both proteins was also investigated in primary MEFs (Fig. 5C). Silencing of endogenous Dgcr8 expression with an RNA interference retroviral vector also reduced the proliferation rate in MEFs, either wild-type or *Ing1*-mutant, but the reduction in BrdUrd-positive cells was slightly higher in MEFs with functional Ing1 (25.09% versus 18.85%).

Discussion

The products of the Ing1 locus participate in several cellular functions with important implications in tumor suppression, such as cell cycle control, apoptosis, DNA repair, or senescence (1, 2). Here, we have taken an unbiased approach to identify Ing1 targets responsible for its cellular functions, namely, the comparison by microarray analysis of the expression profiles of MEFs with the *Ing1* locus inactivated with a gene trap cassette, relative to their wild-type littermates. With this experimental setup, we aimed to avoid the possible effects of passage in culture, unknown genetic changes of immortalized or transformed cell lines, or possible nonphysiologic effects due to the use of ectopic gene delivery. The inspection of the global effect of Ing1 status in gene expression revealed that the majority of differentially expressed genes were upregulated in *Ing1*-mutant cells. These genes are potential targets of Ing1-dependent repression. Our results agree with previous biochemical data showing that the mammalian p33ING1 protein is predominantly associated to repressor complexes with HDAC activity (18, 19). Collectively, these results support the notion that Ing1 has a predominant role as a mediator of transcriptional repression.

GO analysis revealed a very significant enrichment in *Ing1*-mutant cells of proteins involved in different aspects of chemokine signaling. Interleukin-8, a soluble cytokine, is a well-known target of the related protein ING4 (28, 29). Our results with Ing1 open the possibility that regulation of chemokine or cytokine signaling could be a shared feature of ING proteins. Furthermore, bioinformatic analysis also shows that a large proportion of Ing1-regulated genes contain consensus binding sequences for NF-κB. ING4 can interact with and regulate the activity of NF-κB (28–30). Therefore, our unbiased analysis also supports the existence of cooperation between Ing1 and NF-κB in transcriptional control and indicates that Ing1 and Ing4 might participate in similar signaling pathways. Additional studies aimed to identify Ing1-regulated genes have been reported by other groups using either antisense against

Ing1 in a mouse mammary epithelial cell line (31) or overexpression of ING1 or ING2 in human primary fibroblasts (32). Interestingly, there is very limited overlap between our results and those of these studies. The use of different cell types and/or microarray platforms could account for some of these differences. More importantly, unlike the previous studies, we have not used ectopic expression, and instead, we have analyzed genetically defined primary cells differing in their Ing1 status. Therefore, we are confident that our results reflect faithfully the role of endogenous Ing1 in gene regulation. One of the genes with increased expression in *Ing1*-mutant cells is DGCR8 (also known as Pasha in some species). The DGCR8 protein plays an essential role in the processing of canonical microRNAs in the nucleus (33, 34). DGCR8 and the RNase Drosha form a nuclear complex known as the Microprocessor, which catalyzes the cleavage of the primary miRNA transcripts (pri-miRNA) to yield ~70-nucleotide-long stem-loop intermediates (pre-miRNAs) that are subsequently exported to the cytoplasm, where they are substrates of Dicer to produce mature miRNAs (35). The increasing evidence of the relevance of alterations in the microRNA machinery in cancer (36) prompted us to investigate further the connection between ING1 and DGCR8 expression. Our data clearly identify Dgcr8 as a novel direct target of transcriptional repression by ING1, which adjusts to the canonical model for ING action, via the direct binding to histone marks and recruitment of

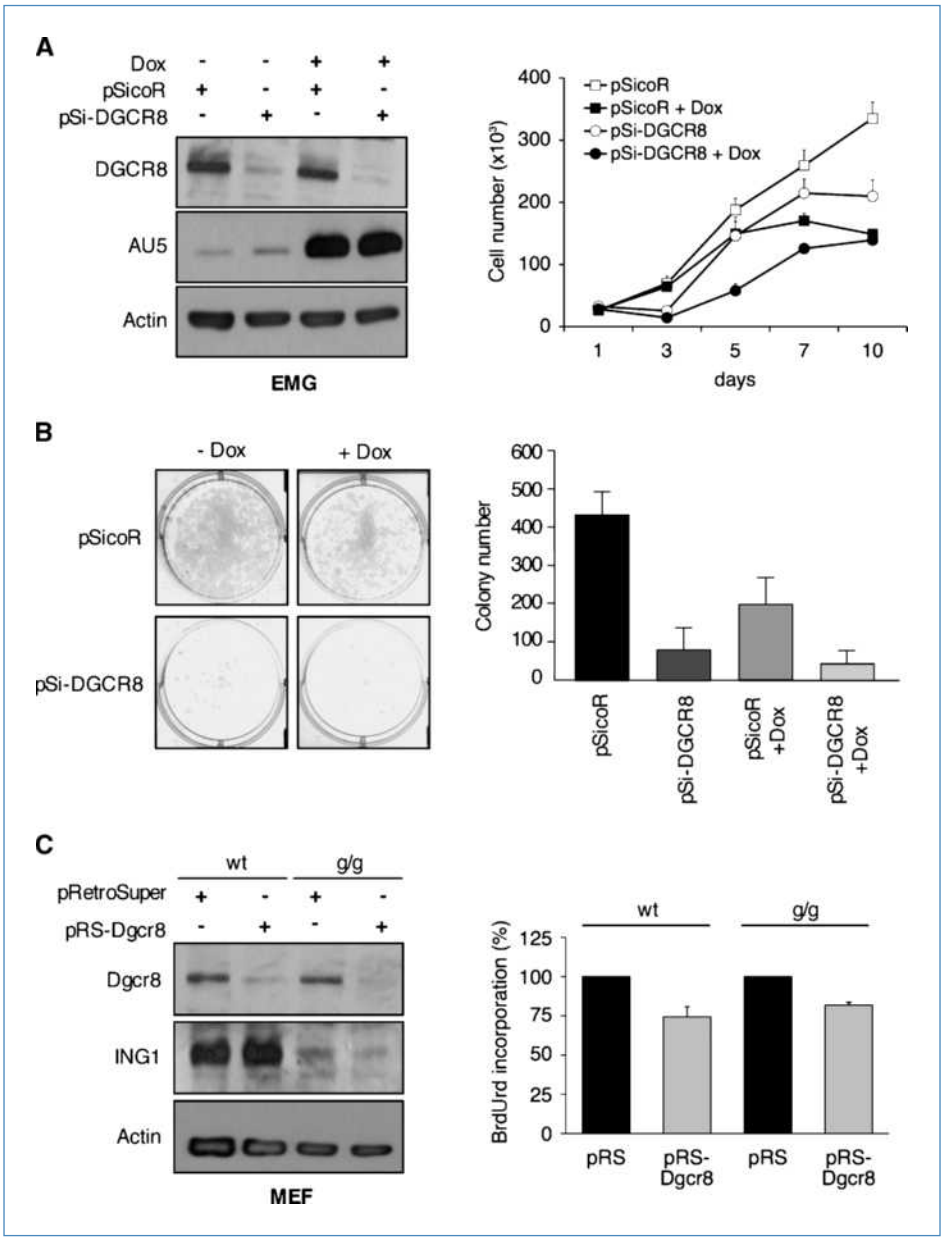

Figure 5. Functional link between DGCR8 and ING1. A, left, Western blot of EMG cells infected with a lentiviral vector expressing a shRNA against DGCR8 (pSi-DGCR8) or empty vector (pSicoR) combined with the induction of AU5-ING1 with doxycycline. A, right, growth curves of EMG cells expressing DGCR8 shRNA and/or with induction of AU5-ING1. A representative experiment is shown. Error bars represent SD of triplicates. B, growth of EMG cells expressing DGCR8 shRNA and/or with induction of AU5-ING1. Cells were seeded at 8,000 per well and stained with Giemsa 10 d later. Right, number of colonies from two independent experiments. Error bars indicate SDs. C, left, Western blot analysis of wild-type or *Ing1*-deficient fibroblasts retrovirally infected with a vector expressing a shRNA against Dgcr8 (pRS-Dgcr8) or empty vector (pRetroSuper). C, right, BrdUrd-positive cells, relative to vector-infected cells, measured by immunofluorescence against BrdUrd (see Materials and Methods). The average and SDs from two experiments are shown.

HDAC complexes to its promoter. To our knowledge, this is the first characterization of the mechanism of transcriptional regulation by ING1 at a specific target gene, and it validates the general model for gene regulation by ING1 and other ING proteins. Alteration in miRNA expression is now recognized as a common feature of human cancers (36). Deregulation of microRNA activity in tumors can occur at different steps of the microRNA biogenesis machinery, with transcriptional regulation of primary miRNA being the best characterized. Our results provide a novel link, acting at the step of miRNA nuclear processing. We show that the tumor suppressor ING1 contributes to the transcriptional regulation of DGCR8 expression, a critical mediator of miRNA biogenesis. The deregulation of Dgcr8 is paralleled by the increased expression of a small subset of mature miRNAs in *Ing1*-mutant fibroblasts. As ING1 is frequently inactivated in tumors, these observations potentially identify a novel mechanism for altered miRNA function in cancer (i.e., the transcriptional control by tumor suppressors of proteins involved in the processing of miRNAs). The functional effect of altered DGCR8 levels is not unambiguously established. Kumar and colleagues (21) have reported increased proliferation and transformation in tumor cell lines where DGCR8 has been suppressed by RNA interference. On the other hand, mice deficient for the Dgcr8 locus show embryonic lethality (37, 38) and Dgcr8-deficient embryonic stem cells have defects in proliferation and differentiation (38, 39). In line with the latter data, our results indicate that reduced DGCR8 activity is antiproliferative in both transformed and primary cells (Fig. 5; data not shown). The characterization of the mechanism responsible for the antiproliferative action of DGCR8 will be described in detail elsewhere.[5] It is feasible that increased expression of DGCR8, like that found in Ing1-mutant cells, might promote proliferation and thus contribute to the transformed phenotype. Impaired processing of pri-miRNAs (40) and altered expression of microRNA processing proteins (41, 42) have been reported in human tumors. Interestingly, microarray data at the Oncomine Cancer Profiling database[6] show increased DGCR8 expression in several tumor types, such as melanoma, glioblastoma, or breast carcinoma. Of note, several of these reports indicate an inverse correlation between ING1 and DGCR8 expression in tumors such as invasive breast carcinoma or glioblastoma. In summary, by studying the global effect of Ing1 depletion in gene expression, we have identified a novel link between the tumor suppressor Ing1 and the microRNA machinery through the transcriptional control of DGCR8. This functional link identifies a novel connection between tumor suppressor proteins and microRNA biogenesis, potentially relevant for the contribution of Ing1 dysfunction to neoplastic transformation.

[5] D. Gómez-Cabello and I. Palmero, in preparation.
[6] http://www.oncomine.org

Disclosure of Potential Conflicts of Interest

No potential conflicts of interest were disclosed.

Acknowledgments

We thank Ana Dopazo and Fátima Sánchez-Cabo for excellent assistance with the microRNA microarray analysis, Gordon Peters for the gift of NARF cells, and Esther Martín-Garrido for the generation of the EMG cell line.

Grant Support

Spanish Ministry of Science and Innovation grant BFU06-10882 (I. Palmero).
The costs of publication of this article were defrayed in part by the payment of page charges. This article must therefore be hereby marked *advertisement* in accordance with 18 U.S.C. Section 1734 solely to indicate this fact.

Received 06/10/2009; revised 11/30/2009; accepted 12/08/2009; published OnlineFirst 02/23/2010.

References

1. Coles AH, Jones SN. The ING gene family in the regulation of cell growth and tumorigenesis. J Cell Physiol 2009;218:45–57.
2. Soliman MA, Riabowol K. After a decade of study-ING, a PHD for a versatile family of proteins. Trends Biochem Sci 2007;32:509–19.
3. Ythier D, Larrieu D, Brambilla C, Brambilla E, Pedeux R. The new tumor suppressor genes ING: genomic structure and status in cancer. Int J Cancer 2008;123:1483–90.
4. Kichina JV, Zeremski M, Aris L, et al. Targeted disruption of the mouse ing1 locus results in reduced body size, hypersensitivity to radiation and elevated incidence of lymphomas. Oncogene 2006; 25:857–66.
5. Coles AH, Liang H, Zhu Z, et al. Deletion of p37Ing1 in mice reveals a p53-independent role for Ing1 in the suppression of cell proliferation, apoptosis, and tumorigenesis. Cancer Res 2007;67:2054–61.
6. Coles AH, Marfella CG, Imbalzano AN, et al. p37Ing1b regulates B-cell proliferation and cooperates with p53 to suppress diffuse large B-cell lymphomagenesis. Cancer Res 2008;68:8705–14.
7. Garkavtsev I, Grigorian IA, Ossovskaya VS, Chernov MV, Chumakov PM, Gudkov AV. The candidate tumour suppressor p33ING1 cooperates with p53 in cell growth control. Nature 1998;391:295–8.
8. Tsang FC, Po LS, Leung KM, Lau A, Siu WY, Poon RY. ING1b decreases cell proliferation through p53-dependent and -independent mechanisms. FEBS Lett 2003;553:277–85.
9. Leung KM, Po LS, Tsang FC, et al. The candidate tumor suppressor ING1b can stabilize p53 by disrupting the regulation of p53 by MDM2. Cancer Res 2002;62:4890–3.
10. Gonzalez L, Freije JM, Cal S, Lopez-Otin C, Serrano M, Palmero I. A functional link between the tumour suppressors ARF and p33ING1. Oncogene 2006;25:5173–9.
11. Palacios A, Garcia P, Padro D, Lopez-Hernandez E, Martin I, Blanco FJ. Solution structure and NMR characterization of the binding to methylated histone tails of the plant homeodomain finger of the tumour suppressor ING4. FEBS Lett 2006;580:6903–8.
12. Palacios A, Munoz IG, Pantoja-Uceda D, et al. Molecular basis of histone H3K4me3 recognition by ING4. J Biol Chem 2008;283: 15956–64.
13. Pena PV, Davrazou F, Shi X, et al. Molecular mechanism of histone H3K4me3 recognition by plant homeodomain of ING2. Nature 2006; 442:100–3.
14. Pena PV, Hom RA, Hung T, et al. Histone H3K4me3 binding is required for the DNA repair and apoptotic activities of ING1 tumor suppressor. J Mol Biol 2008;380:303–12.
15. Shi X, Hong T, Walter KL, et al. ING2 PHD domain links histone H3 lysine 4 methylation to active gene repression. Nature 2006;442: 96–9.
16. Doyon Y, Cayrou C, Ullah M, et al. ING tumor suppressor proteins are critical regulators of chromatin acetylation required for genome expression and perpetuation. Mol Cell 2006;21:51–64.

17. Goeman F, Thormeyer D, Abad M, et al. Growth inhibition by the tumor suppressor p33ING1 in immortalized and primary cells: involvement of two silencing domains and effect of Ras. Mol Cell Biol 2005;25:422–31.
18. Kuzmichev A, Zhang Y, Erdjument-Bromage H, Tempst P, Reinberg D. Role of the Sin3-histone deacetylase complex in growth regulation by the candidate tumor suppressor p33(ING1). Mol Cell Biol 2002;22:835–48.
19. Skowyra D, Zeremski M, Neznanov N, et al. Differential association of products of alternative transcripts of the candidate tumor suppressor ING1 with the mSin3/HDAC1 transcriptional corepressor complex. J Biol Chem 2001;276:8734–9.
20. Palmero I, Serrano M. Induction of senescence by oncogenic Ras. Methods Enzymol 2001;333:247–56.
21. Kumar MS, Lu J, Mercer KL, Golub TR, Jacks T. Impaired microRNA processing enhances cellular transformation and tumorigenesis. Nat Genet 2007;39:673–7.
22. Stott FJ, Bates S, James MC, et al. The alternative product from the human CDKN2A locus, p14(ARF), participates in a regulatory feedback loop with p53 and MDM2. EMBO J 1998;17:5001–14.
23. Weinmann AS, Farnham PJ. Identification of unknown target genes of human transcription factors using chromatin immunoprecipitation. Methods 2002;26:37–47.
24. Abad M, Menendez C, Fuchtbauer A, Serrano M, Fuchtbauer EM, Palmero I. Ing1 mediates p53 accumulation and chromatin modification in response to oncogenic stress. J Biol Chem 2007;282:31060–7.
25. Han J, Lee Y, Yeom KH, Kim YK, Jin H, Kim VN. The Drosha-DGCR8 complex in primary microRNA processing. Genes Dev 2004;18:3016–27.
26. Shiohama A, Sasaki T, Noda S, Minoshima S, Shimizu N. Nucleolar localization of DGCR8 and identification of eleven DGCR8-associated proteins. Exp Cell Res 2007;313:4196–207.
27. Shaked H, Shiff I, Kott-Gutkowski M, Siegfried Z, Haupt Y, Simon I. Chromatin immunoprecipitation-on-chip reveals stress-dependent p53 occupancy in primary normal cells but not in established cell lines. Cancer Res 2008;68:9671–7.
28. Garkavtsev I, Kozin SV, Chernova O, et al. The candidate tumour suppressor protein ING4 regulates brain tumour growth and angiogenesis. Nature 2004;428:328–32.
29. Colla S, Tagliaferri S, Morandi F, et al. The new tumor-suppressor gene inhibitor of growth family member 4 (ING4) regulates the production of proangiogenic molecules by myeloma cells and suppresses hypoxia-inducible factor-1α (HIF-1α) activity: involvement in myeloma-induced angiogenesis. Blood 2007;110:4464–75.
30. Nozell S, Laver T, Moseley D, et al. The ING4 tumor suppressor attenuates NF-κB activity at the promoters of target genes. Mol Cell Biol 2008;28:6632–45.
31. Takahashi M, Seki N, Ozaki T, et al. Identification of the p33(ING1)-regulated genes that include cyclin B1 and proto-oncogene DEK by using cDNA microarray in a mouse mammary epithelial cell line NMuMG. Cancer Res 2002;62:2203–9.
32. Feng X, Bonni S, Riabowol K. HSP70 induction by ING proteins sensitizes cells to tumor necrosis factor α receptor-mediated apoptosis. Mol Cell Biol 2006;26:9244–55.
33. Denli AM, Tops BB, Plasterk RH, Ketting RF, Hannon GJ. Processing of primary microRNAs by the Microprocessor complex. Nature 2004;432:231–5.
34. Gregory RI, Yan KP, Amuthan G, et al. The Microprocessor complex mediates the genesis of microRNAs. Nature 2004;432:235–40.
35. Winter J, Jung S, Keller S, Gregory RI, Diederichs S. Many roads to maturity: microRNA biogenesis pathways and their regulation. Nat Cell Biol 2009;11:228–34.
36. Shi XB, Tepper CG, deVere White RW. Cancerous miRNAs and their regulation. Cell Cycle 2008;7:1529–38.
37. Stark KL, Xu B, Bagchi A, et al. Altered brain microRNA biogenesis contributes to phenotypic deficits in a 22q11-deletion mouse model. Nat Genet 2008;40:751–60.
38. Wang Y, Medvid R, Melton C, Jaenisch R, Blelloch R. DGCR8 is essential for microRNA biogenesis and silencing of embryonic stem cell self-renewal. Nat Genet 2007;39:380–5.
39. Wang Y, Baskerville S, Shenoy A, Babiarz JE, Baehner L, Blelloch R. Embryonic stem cell-specific microRNAs regulate the G_1-S transition and promote rapid proliferation. Nat Genet 2008;40:1478–83.
40. Thomson JM, Newman M, Parker JS, Morin-Kensicki EM, Wright T, Hammond SM. Extensive post-transcriptional regulation of microRNAs and its implications for cancer. Genes Dev 2006;20:2202–7.
41. Muralidhar B, Goldstein LD, Ng G, et al. Global microRNA profiles in cervical squamous cell carcinoma depend on Drosha expression levels. J Pathol 2007;212:368–77.
42. Sugito N, Ishiguro H, Kuwabara Y, et al. RNASEN regulates cell proliferation and affects survival in esophageal cancer patients. Clin Cancer Res 2006;12:7322–8.

ING Proteins in Cellular Senescence

Camino Menéndez, María Abad, Daniel Gómez-Cabello, Alberto Moreno and Ignacio Palmero*

Instituto de Investigaciones Biomédicas CSIC-UAM. Arturo Duperier, 4. 28029 Madrid, Spain

Abstract: Cellular senescence is an effective anti-tumor barrier that acts by restraining the uncontrolled proliferation of cells carrying potentially oncogenic alterations. ING proteins are putative tumor suppressor proteins functionally linked to the p53 pathway and to chromatin regulation. ING proteins exert their tumor-protective action through different types of responses. Here, we review the evidence on the participation of ING proteins, mainly ING1 and ING2, in the implementation of the senescent response. The currently available data support an important role of ING proteins as regulators of senescence, in connection with the p53 pathway and chromatin organization.

INTRODUCTION

Cellular senescence was first described by Leonard Hayflick in the 1960s, while studying the growth behavior of human embryo fibroblasts in culture. More than four decades later, senescence is not longer considered as a rarity of cells under tissue culture conditions and rather is increasingly viewed as a relevant antitumor barrier, at a similar level as apoptosis. Little over a decade ago, ING1, the founding member of the ING family was identified in a screening for tumor suppressor genes. As more members have been added to the family and we know more about their mechanism of action, there is mounting interest to understand the role of these proteins in tumor suppression. In this article we aim to review the role of ING proteins in the senescence response and the relevance of this link in their tumor protective action. First we will review the essentials of the current knowledge of the senescence response and then, with this background we will discuss the -often conflicting- evidence about the participation of members of the ING family in cellular senescence.

OVERVIEW OF CELLULAR SENESCENCE

The concept of cellular senescence has its origins in the seminal observations of Hayflick and Moorehead in 1961 [1, 2]. As he tried to propagate human embryonic fibroblasts, Hayflick observed that, despite keeping them under optimal growth conditions, the cells invariably reached a point, after a number of serial passages, where no net gain in cell number was obtained. Although these cells did not divide, they remained alive and metabolically active. Hayflick reasoned that the cessation in division reflected the loss of fitness of the cell population as they accumulated divisions and designated it "cell aging", alike to the process of aging in organisms, and later "cellular senescence". At the time, the generally accepted view was that normal cells could be indefinitely propagated *in vitro*, in part because of the early experience with tumor cell lines, and it took some time before the concept of limited proliferative potential was accepted. Currently, we know that the phenomenon Hayflick originally described is only one manifestation of a more general response to stress, present not only in cultured cells but also in live organisms, which is known as cellular senescence. For a more extensive description of this process, the reader is referred to several excellent recent reviews on senescence [3-5].

This antiproliferative response can be triggered by a long list of alterations in the normal cellular homeostasis, ranging from telomere dysfunction to oxidative stress or aberrant promitogenic signals [4, 5]. Although it was originally described and remains best characterized in fibroblasts of human and murine origin, senescence has also been described in a variety of other cell types both *in vitro* and *in vivo*, including melanocytes, lymphocytes, or epithelial cells.

The essential feature of the senescent phenotype is the absence of cell division. Cells driven into senescence do not divide and enter a state of stable cell-cycle arrest. Senescent cells most frequently accumulate at the G1 phase of the cycle, although there are also examples of arrest with increase of the G2/M population [4]. A number of specific features distinguish senescence from other similar non-proliferative states. One of them is its permanent character. Under normal conditions, once the cell has entered the senescent arrest, this is essentially irreversible and senescent cells are not responsive to extracellular mitogenic signals, distinguishing it from with quiescence. Although they do not divide, senescent cells are viable, they retain a normal metabolical activity and do not engage in programmed cell death. In fact, resistance to proapoptotic stimuli is another distinctive feature of most senescent cells. Apoptosis and senescence appear to be mutually exclusive outcomes to stress signals, but the mechanisms by which senescent cells acquire resistance to apoptosis are poorly understood. They might involve differential regulation of several pro or anti apoptotic genes, some of which could be mediated by p53 [4, 6].

A number of morphological markers define the senescent phenotype. Most of these have been best defined in fibroblasts, but generally also apply to other cell types. One of the

*Address correspondence to this author at the Instituto de Investigaciones Biomédicas CSIC-UAM. Arturo Duperier, 4. 28029 Madrid, Spain; Fax: +34 915854401; E-mail: ipalmero@iib.uam.es

1389-4501/09 $55.00+.00

most distinctive signs of senescence is a marked change in cell morphology, from the thin, elongated shape of normal non-senescent fibroblasts to a large, flattened morphology, with very extended cytoplasm and high density of vacuolae. Other features like enlarged nucleus, with prominent nucleoli, and multinucleated cells are usually observed. A very specific marker of senescent cells is the existence of a pH-specific Beta-Galactosidase activity, known as Senescence-Associated Beta Galactosidase or SA-BetaGal [7]. This activity is believed to arise from altered lysosomal structure in senescent cells and it is a widely used marker because its convenience in staining in cells or tissues [8].

The senescent phenotype can be induced by a variety of stimuli (Fig. **1**). The classical form of senescence - that originally described by Hayflick - is induced as a direct consequence of the accumulation of cell divisions, and it is triggered by telomere dysfunction. Telomeres are complex protective structures at the end of the linear eukaryotic chromosomes [9]. As a consequence of semi-conservative DNA replication, telomere length is progressively reduced with each round of cell division. Critically short or dysfunctional telomeres are recognized as double-strand DNA breaks by the surveillance cellular machinery and thus activate a DNA Damage Response (DDR) that ultimately results in the cell-cycle arrest characteristic of senescence [10, 11]. This form of senescence is referred to as replicative senescence, and it provides a mechanism to limit the proliferative life span of normal cells within limits compatible with tissue organization and organismal fitness. But an undistinguishable senescent phenotype can also be induced in cells that have not accumulated a critical number of divisions, if they are exposed to a list of intracellular or environmental stress signals. From these, the best characterized are oxidative stress, DNA damaging agents, or excessive mitogenic signals as those evoked by the expression of activated oncogenes [12] or high nutrient conditions typical of standard tissue culture conditions [13]. Collectively, these forms of senescence are known as premature senescence or stasis (stress and activated signaling-induced senescence) [14]. The relevance of the molecular machinery that mediates the cellular response to DNA damage (DDR) in the implementation of senescence has attracted a lot of interest in recent years. DNA damage has long been known to be one of the stimuli able to trigger senescence [15, 16]. More recently, it has been proposed that activation of the DDR response is a mediator of many different types of cellular senescence, including telomere or oncogene-induced senescence [11, 17, 18], although recent *in vivo* reports challenge this view [19, 20].

At the molecular level, all forms of senescence irrespective of their initial trigger ultimately activate a similar molecular machinery. In particular, two main signaling pathways are responsible for the implementation and maintenance of the senescent phenotype caused by different stimuli. These are the tumor suppressor pathways controlled by p53 and the retinoblastoma protein, Rb [3, 4, 14, 21]. Both proteins contribute, directly or indirectly to the proliferation arrest during senescence. The Rb protein plays a direct role in the control of the transition between the G1 and S phases of the cycle. Its phosphorylation by cyclin-dependent-kinases (cdk) releases a transcription block, mediated by the E2F

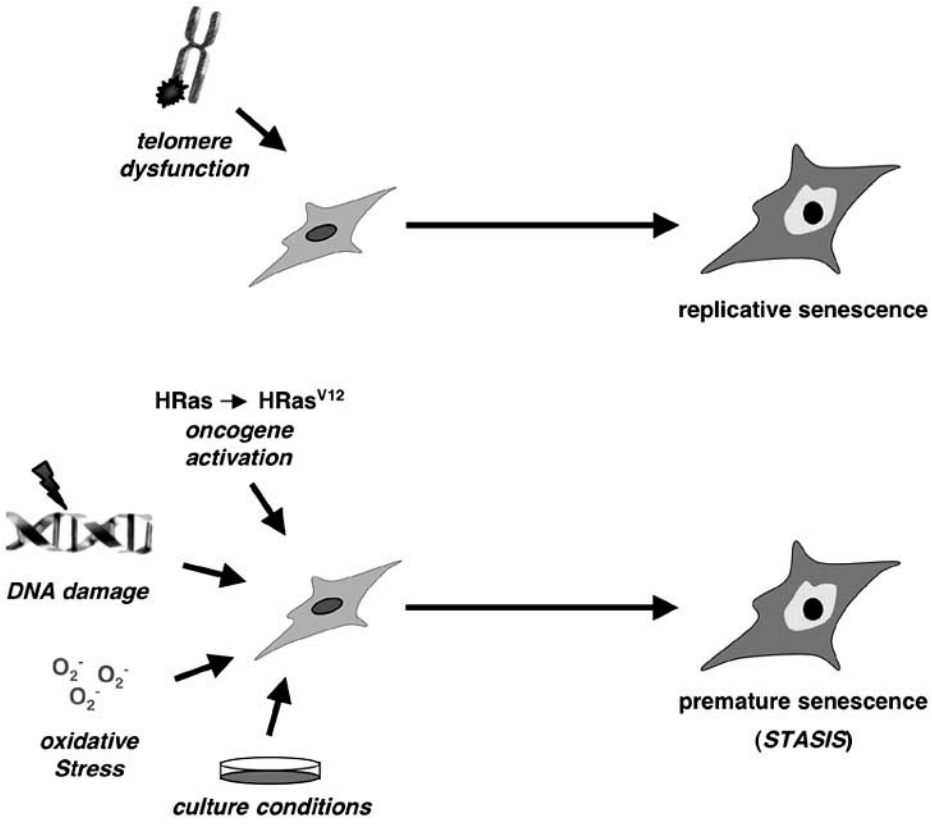

Fig. (1). Stimuli leading to the induction of cellular senescence.

factors, which results in the expression of genes required for S phase. During senescence, Rb typically accumulates in its inactive, non-phosphorylated state, blocking cell-cycle progression. Similarly, active p53 accumulates in senescent cells, leading to the transcriptional regulation of specific p53-target genes. Among these genes, the cdk-inhibitor p21CIP1, or GADD45 play an important role in the block of cell division during senescence. The regulation of both pathways during senescence relies mainly, but not exclusively, in the products of the INK4A-ARF locus, p16INK4A and ARF (p14ARF in humans and p19Arf in mice) [22, 23]. p16INK4A is a specific inhibitor of the G1 cyclin-dependent-kinases cdk4 and cdk6 that is pivotal for the control of the Rb pathway in this context [24, 25]. The other product of the locus, the ARF protein, is a positive regulator of the p53 pathway that acts primarily by increasing the stability of the p53 protein [26, 27]. ARF inhibits the binding and ubiquitin-mediated degradation of p53 by Mdm2, thus increasing the p53 protein pool and activity. The relative importance of the Rb or p53 pathways depends on many factors like the species, cell type, or senescence trigger. For instance, senescence in mouse embryo fibroblasts (MEF), either due to population doublings or oncogenic stress, is governed by the p19Arf-p53 axis. Arf levels are very low in presenescent MEFs and they increase dramatically as cells enter senescence, leading to p53 accumulation [28, 29]. Reinforcing the importance of these proteins in senescence in this cell type, independent ablation of p53 or Arf suffices to bypass different forms of senescence in mouse fibroblasts [12, 29, 30] and loss of one or another almost invariably accompanies their spontaneous immortalization. A more complex regulatory network is in action in human fibroblasts. Here, the p16-Rb pathway has a more prominent role than in mouse cells, and inactivation of both the p53 and Rb pathway is required to escape senescence [12, 31, 32]. The different stringency of the control of senescence between human and murine fibroblasts most likely accounts for their different behavior in terms of immortalization and transformation *in vitro*. While mouse fibroblasts become spontaneously immortalized very easily, immortalization of human fibroblasts is an extremely rare event, if at all possible [14]. Intriguingly, although p53 is a master regulator of senescence in both systems, the importance of ARF in p53 activation differs. As mentioned, ARF has an essential role in mouse fibroblasts senescence, but it does not appear to be a relevant player in the activation of p53 during senescence in human fibroblasts [32, 33]. Notwithstanding the relevance of ARF and p16 as major regulators of the p53 and Rb pathway in senescence, other regulators of both pathways should also be mentioned. For instance, p15INK4b, a protein related structurally and functionally to p16INK4a, has been shown to be a regulator of the Rb pathway in senescence in some settings [34]. With regard to p53, the kinases ATM and ATR which activate p53 in response to genotoxic stress, also significantly contribute to p53 activation in senescence triggered by telomere dysfunction, DNA damaging agents, or oncogene activation [11, 18].

Senescence is accompanied by a specific genetic program, with differential expression of a large list of genes. Several proteins involved in cell-cycle control show senescence-associated changes in expression. As mentioned above, negative regulators like p16INK4A, p21CIP or p19Arf are induced, while other positive regulators like cyclin A, or PCNA show reduced expression [35, 36]. The balance of positive and negative regulators ultimately leads to the cell cycle arrest characteristic of senescence. Apart from direct cell-cycle regulators, the list of genes with differential expression during senescence also includes several secreted proteins linked to inflammation, or degradation of extracellular matrix, like interleukins, chemokines and metalloproteases. Collectively, these soluble factors are believed to be responsible for the so-called "secretory phenotype" of senescence, which has been proposed to contribute to the reinforcement of senescence [4, 21, 37, 38] but also to clearance of senescent cells *in vivo* [39, 40], reviewed in [3, 4, 41].

Different types of evidence indicate that epigenetic control plays an important role in regulation of gene expression during senescence [42-44]. In some cell types, the global changes in chromatin structure associated with senescence lead to the appearance of new heterochromatin domains, associated to specific gene repression known as Senescence-Associated Heterochromatin Foci, or SAHFs (see below) [36, 45].

Senescence has been studied in detail in cells in culture for many years. However, the existence of this phenomenon in live organisms and its possible relevance in human cancer or aging has been a matter of considerable debate. Several observations have led to connect cellular senescence with tumor suppression. First, escape from senescence is a prerequisite for oncogenic transformation *in vitro*. This is evidenced by the well-established need of cooperating immortalizing events to allow the transformation of primary rodent cells by some oncogenes [14, 46, 47]. Also in support of this link, genes known to be critical regulators of senescence are frequently also involved in tumor protection. This is clearly the case of p53 and Rb, that have an essential role as master regulators of senescence and, at the same time are the most frequently inactivated tumor suppressors in human cancer [48]. The final proof for this link has been obtained in the last 5 years, with direct evidence supporting a role for senescence in tumor protection *in vivo*. Studying different experimental models of tumor progression, that include chemical skin carcinogenesis, melanomagenesis, or formation of lymphomas, several groups independently identified the presence of cells with senescence markers in benign lesions, but not in the more advanced malignant tumors [49-54]. These observations have led to a model where senescence is activated in premalignant lesions as a response to aberrant proliferative signals caused by activated oncogenes (Fig. **2**). Senescence imposes a proliferative block that, when effective, can impede the progression from premalignant to malignant tumors. According to this model, progression occurs when the senescence block is disabled by mutation of its regulators (reviewed in [3, 5, 55]). Further support to this model comes from recent experiments with murine genetically modified models with regulatable p53 activity. Reactivation of the p53 tumor suppressor in these mice leads to tumor regression that, in sarcomas, involves the activation of a senescence program [40, 56]. These findings clearly highlight the importance of senescence as an intrinsic tumor suppressor mechanism *in vivo*, in a similar level to apoptosis.

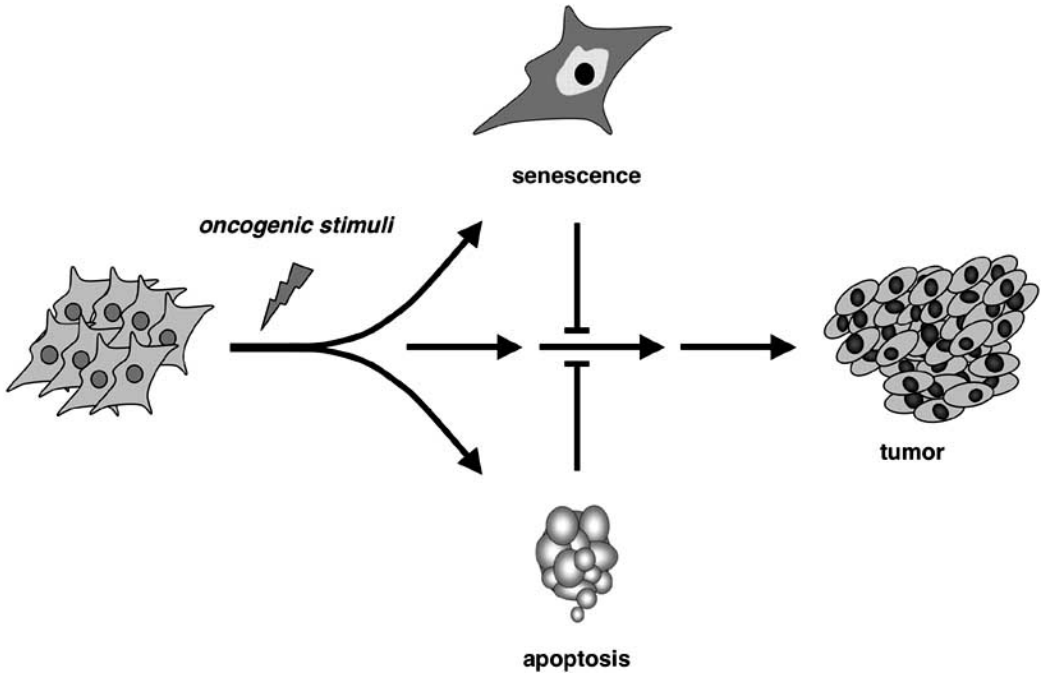

Fig. (2). Schematic depiction of the role of senescence in tumor suppression *in vivo*. See text for details.

INVOLVEMENT OF ING PROTEINS IN SENESCENCE

The ING proteins form a family of sequence related members, well conserved during evolution, with orthologs identified from yeast to human (reviewed in [57-62]). In mouse and human, there are 5 different ING loci distributed over the genome, some of which give rise to multiple protein products as a consequence of alternative splicing events [57]. Since the identification of the founding member ING1, over a decade ago, a substantial amount of evidence has accumulated that indicates that the ING proteins play an important role in tumor protective mechanisms, *via* their connection with the p53 tumor suppressor pathway and the chromatin regulation machinery. As mentioned above, activation of the p53 pathway and gene regulation *via* epigenetic mechanisms are both hallmarks of the senescence program, which itself constitutes an effective tumor suppressor barrier. Considering the connection of ING proteins with these processes and their role as putative tumor suppressors, it is not surprising that the connection between ING proteins and cellular senescence has generated interest.

The different studies investigating the role of ING proteins in senescence have focused mainly on the two cellular systems where cellular senescence has been most extensively studied, namely primary embryonic fibroblasts of human and murine origin. The first evidence suggesting a participation of ING proteins in senescence and control of *in vitro* life span was obtained soon after the identification of the founding member of the family, ING1. In a loss-of-function approach, Garkavtsev and colleagues [63] expressed a retroviral construct with antisense sequences against the 3' common exon of the ING1 locus in human fibroblasts of the Hs68 strain that were approaching senescence. Silencing of ING1 gene products achieved by the antisense construct resulted in a limited extension of the life span of these cells, beyond their normal physiological limit, but did not allow full immortalization, similarly to the bypass obtained in this cell type by inactivation of the p53 pathway. This observation suggested for the first time a role for ING proteins in control of cellular senescence.

A series of independent gain-of-function experiments have also contributed to define the role of ING proteins in this context. The most extensive evidence so far relates to the products of the ING1 locus. This locus can give rise, both in human and mice, to different protein isoforms, generated through splicing of alternative first exons to a common second exon [57]. Modest stable overexpression of the p33ING1 isoform (also known as ING1b or p33ING1b) in early passage IMR90 human fibroblasts causes a dramatic reduction in their division rate [64]. This antiproliferative response is accompanied by the acquisition of several of the above-described senescence-specific markers. In particular, it was shown that ING1-expressing fibroblasts acquired a senescent morphology, with extended cytoplasm, multiple nuclei and vacuolization. Also, the SA-BetaGal activity was significantly induced in ING1-expressing cells. Collectively, these results show that ectopic induction of p33ING1 can trigger an antiproliferative response in human fibroblasts indistinguishable from cellular senescence, and support a causal role for ING1 in the implementation of the senescence program in this cell type.

Similar results have been presented for ING2, the member of the ING family most closely related to ING1 [57, 65], which also indicate a role for this protein in senescence. Ectopic retrovirus-driven expression of ING2 in early passage MRC5 human fibroblasts was shown to be sufficient to enforce premature senescence in these cells, as evidenced by a cell-cycle arrest accompanied by the acquisition of flat morphology and induction of SA-BetaGal staining [66].

The above described overexpression experiments provide proof of the ability of ING proteins to implement senescence. But their physiological role as putative mediators of senescence under normal conditions can be examined more accurately with approaches where the function of endogenous INGs has been manipulated. In the case of ING1, several mouse models with defective Ing1 function have been described [67-69], providing genetically defined experimental settings to address this question. In one of these models [67], we targeted the murine *Ing1* locus by the insertion of a gene trap cassette in the intron between exon 1b and 1c, resulting in a dramatic reduction (over 90%) on the expression of the different products of the locus. Mouse embryonic fibroblasts from these animals were used to investigate their behavior with regard to senescence. While senescence due to population doublings and spontaneous immortalization did not appear to be altered in these cells, the deficiency in the *Ing1* locus resulted in a clear impairment in the induction of senescence triggered by oncogenic stress. Accordingly, Ing1-deficient MEFs expressing an activated Ras oncogene retained normal proliferation rates, and did not significantly induce markers of the senescence state, like flat morphology or SA-BetaGal activity. However, Ing1 deficiency was not sufficient to render mouse fibroblasts completely permissive to the expression of Ras, as they did not acquire characteristics of transformed cells. This set of experiments supports a role for the *Ing1* locus as a critical mediator of the senescent arrest caused by activated oncogenes in mouse fibroblasts. Strikingly, similar studies with another Ing1-mutant mouse models have yielded apparently contradictory results [68]. These authors generated mice mutant for the *Ing1* locus through a similar strategy, involving the integration in this locus of a "polyA-trap-type" gene trap cassette. In this study, the response of MEFs from these animals to the enforced expression of activated Ras was reported to be normal. At present, the reason for this discrepancy is not known. It is worth noting that the targeting strategies used in each case apparently led to different effects in the expression of Ing1 products. While the Ing1-mutant mice used by Abad *et al.* have reduced expression -but not complete absence- of all Ing1 transcripts, Coles *et al.* reported absence of the p33ING1b protein, but increased expression of the exon2-specific p24ING1c isoform in some tissues. Although other factors, like experimental setting or mouse genetic strain, might be relevant, it is tempting to speculate that these differences could mirror specific roles of the Ing1 isoforms in this context. Mice deficient for the *Ing1* locus by homologous recombination have also been generated [69]. In this case, the complete loss of all Ing1 isoforms has been reported. Clearly, the analysis of oncogene-induced senescence in this system could help clarify this issue.

The role of endogenous INGs has also been explored in senescence in human fibroblasts with genetic tools. As mentioned above, silencing of all ING1 products with an antisense construct results in a limited extension of life span [63]. We have also recently addressed the specific contribution of the p33ING1b product in this process by using RNA interference against the exon 1b in human fibroblasts (Abad *et al.*, submitted). Specific silencing of this transcript was sufficient by allow the bypass of oncogene-induced senescence in these cells, but the effect on replicative senescence has not been studied. In the case of ING2, the available data indicate a more complex picture. Stable knockdown of ING2 was originally reported to lead to an extension of life span of normal fibroblasts for a limited number of divisions [66], a phenotype similar to that described for ING1 silencing ([63], Abad *et al.* submitted), and consistent with the ING2 gain-of-function experiments. However, this is in contrast with a very recent report [70], where silencing of ING2 was obtained using transient expression of short interfering RNAs in telomerase-expressing fibroblasts. Unexpectedly, knockdown of ING2 under these conditions was not associated with bypass of senescence, as anticipated, but rather caused a senescent-like arrest. Clearly, more experiments are needed to clarify the role of ING2 in senescence.

ROLE OF ING PROTEINS IN REGULATION OF GENE EXPRESSION AND CHROMATIN DURING SENESCENCE

As mentioned, implementation of senescence is accompanied by specific gene expression changes, and some of these involve gene repression and heterochromatin formation. The importance of epigenetic control in regulation of gene expression in senescence is well established [42-44]. For instance, different drugs that affect histone modifications like acetylation, or DNA methylation status have been shown to induce senescence in different cell types [71, 72]. Also, several proteins with a well-defined role as chromatin regulators can control senescence, in many cases *via* the transcriptional regulation of the INK4a/ARF locus. Examples of these factors include Cbx7 [73], HDAC4 [74], or Bmi [75].

A number of reports support a possible role of ING proteins as regulators of gene expression through chromatin regulation during senescence. As mentioned above, different types of evidence support a model where ING proteins participate in transcriptional regulation through their association to complexes with chromatin-modifying activities, like HAT (histone acetyl transferase) or HDAC (histone deacetylase) [64, 76-80]. Specific recognisition of trimethylation of Lys4 of histone H3 (H3K4triMe), a mark of active chromatin, through their conserved PHD domain [81-83] would lead to the recruitment of the above mentioned complexes to the vicinity of specific gene targets, resulting in the activation or repression of these genes. Proof of the relevance of this function of ING proteins in implementation of senescence, was obtained as part of the characterization of the induction of senescent phenotype by ING1 in human fibroblasts. Deletion mutants of the protein were used in parallel in transcriptional assays *in vitro* and in induction of senescence. These studies revealed a clear correlation between the activity of ING1 mutants as transcriptional repressors *in vitro* and their ability to induce senescence [64], consistent with similar results in non-primary cells [78]. It is worth noting that ING1 and ING2 are closely related members of the ING family, and they constitute a distinct subfamily that acts primarily as transcriptional repressors [64, 76, 78, 79]. On the contrary, ING3, ING4 and ING5 seem to be preferentially linked to transcriptional activation [79]. Considering the demonstrated role of these two INGs in senescence and the apparent involvement of transcriptional repression in ING1-induced senescence, it is tempting to speculate that induction of se-

nescence is a feature of the "repressor INGs", associated to their ability to repress transcription. To elucidate this putative link between repression and induction of senescence by ING proteins, it would be extremely interesting to determine if a similar correlation between repression and senescence is true for ING2. Similarly, to examine the behavior of the "activator INGs", ING3, 4 and 5, in this context, would also be very informative.

Further insight in the link between chromatin regulation and induction of senescence by ING proteins has recently been obtained in experiments using point mutants in the PHD conserved domain of p33ING1 that are defective for the binding to the chromatin mark H3K4triMe (Abad *et al.*, submitted). In our assay, the histone-binding mutants showed a markedly reduced ability to trigger senescence, reinforcing the need for proper chromatin regulation by ING1 to induce this phenotype. Interestingly, the same mutants have been independently reported to be inactive in other functional assays for ING1, like apoptosis induction or DNA repair, indicating the existence of common molecular mechanisms underlying induction of these diverse responses by ING1 [84].

As mentioned above, in some cell types, the changes in chromatin structure associated with senescence can be visualized because of the appearance of the novo macroscopic regions of facultative heterochromatin, designated Senescence-Associated Heterochromatin Foci, or SAHFs [36, 45]. These structures have been characterized in detail in senescent human fibroblasts, although their presence has also been observed in some other cell types [49]. The SAHFs can be distinguished as hyperchromatic spots with DAPI staining, due to their compacted chromatin, and they are enriched in a number of heterochromatin specific markers, such as hypoacetylated histones, histone H3 methylated in Lysine 9 (H3K9Me), the heterochromatin protein1 (HP1) [36], the histone variant macroH2A [85], or HMGA proteins [45]. In turn, they are depleted in histone H1 [86] and several marks of active chromatin. SAHFs have been associated with transcriptional repression of specific cell-cycle genes, such as cyclin A or PCNA, in a process mediated by Rb and E2F factors [36]. SAHFs are distinct structures to DNA damage foci or telomere-associated damage, and they are considered to play an important role in establishing the irreversibility of the senescent phenotype through the establishment of a stable inactive chromatin structure in key proteins involved in the senescence cell-cycle arrest.

Given the involvement of ING proteins in transcriptional repression and chromatin control, there is an obvious interest in understanding the connection between ING proteins and senescence-specific global chromatin changes. In early studies using chromatin immunoprecipitation with antibodies against human ING1 proteins, it was shown that these proteins bind more avidly to chromatin in senescent human fibroblasts, relative to presenescent controls [87]. Conceivably, this behavior could be a reflection of increased levels of ING1 proteins in senescence, or alternatively indicate an increased affinity for chromatin in this setting. Although these results suggest a differential behavior of ING proteins in terms of chromatin binding in senescent fibroblasts, their connection with structures like the SAHFs is not clear. Enforced expression of either p47ING1a [88], or p33ING1b (Abad *et al.*, submitted) in early passage human fibroblasts results in formation of SAHFs. As SAHFs are very good markers of senescence, at the moment it is not possible to distinguish if this phenotype is due to direct roles of ING1 proteins in SAHF formation or merely reflect their ability to induce senescence. In a very recent report, Soliman *et al.* have presented evidence of the preferential binding of ING1 proteins to the promoter of the PCNA gene in senescent fibroblasts, by chromatin immunoprecipitation [88]. As indicated, PCNA is one of the loci silenced in SAHFs. Therefore this result might suggest a participation of ING1 proteins in gene repression in the context of these chromatin structures. However, it should be noted that ING1 proteins were not found in other SAHF-regulated loci, like cyclin A, and thus the generality of this finding remains to be tested. Interestingly, although it was found that expression of PCNA could be repressed by ectopic p47ING1a, the specific contribution of each ING1 isoform was not determined in the chromatin binding assays, opening the possibility for roles for both ING1 isoforms [87, 88]. We have also investigated the possible participation of ING1 proteins in SAHFs by immunofluorescence. We have failed to observe a significant colocalization of ectopic or endogenous ING1 proteins with SAHFs, suggesting that, although they might play a role in their establishment or maintenance, ING1 proteins do not seem to be a major stable component of the SAHFs (unpublished observations). Also, in experiments with mouse fibroblasts, we have found Ing1-dependent changes in the global chromatin structure of fibroblasts expressing oncogenic Ras [67]. SAHFs are not present in this cell type, but an increase in heterochromatinization was evident in Ras-senescent wild-type cells, and this was impaired in Ing1-deficient cells. These results further support a role for Ing1 in chromatin control during senescence, consistent with its proposed role in heterochromatin formation in other settings [89]. To our knowledge, the possible connection of ING2 with these senescence-specific chromatin changes has not yet been studied in human or murine cells.

FUNCTIONAL LINK OF ING PROTEINS TO P53 IN SENESCENCE

Activation of p53 is a hallmark of the senescent phenotype in many circumstances. Depending on the species and cell type, the particularities of the specific mechanism of p53 activation or even the relative weight of this tumor suppressor in the senescent arrest vary.

ING proteins have been implicated in the control of the p53 pathway through different mechanisms [58]. Physical association between p53 and ING proteins, with the exception of ING3, has been described based on co-immunoprecipitation experiments with ectopic proteins [66, 90, 91]. It has been proposed that ING proteins are functionally linked to the p53 pathway at several different levels of regulation, all of which are relevant to p53 activity during senescence. The regulation of p53 activity is under a strict control, to ensure that p53 levels are kept low in unstressed conditions and are promptly activated when required [92]. The essential step to control p53 activity is the regulation of p53 protein stability. Mdm2, itself a transcriptional target of p53,

is the major regulator of p53 protein levels. Several independent reports have shown that ING proteins are able to provoke a clear accumulation of p53 protein when overexpressed [65, 91, 93, 94]. At least in the case of ING1, this effect seems to arise from a direct action on the circuitry regulating p53 protein stability [95]. The p33ING1 protein can bind to the N-terminus of p53, in a region overlapping with the binding site for Mdm2, and therefore ING1 could help stabilize p53 by competing with Mdm2. Post-translational modifications of p53 also represent an essential mechanism of p53 regulation. Different residues in the p53 molecule are subject to modifications like phosphorylation, acetylation, methylation, or sumoylation, among others. The spectrum of modifications in each case acts in a combinatory manner to modulate p53 function [96]. The final outcome is believed to depend on factors like protein levels, differential binding to p53 targets or interaction with specific cofactors [97]. Apart form the effect on p53 stability, ING proteins can also participate in the establishment of post-translational modifications of p53, most notably acetylation. In a series of *in vitro* experiments, ectopic expression of different ING proteins has been shown to result in increased C-terminal acetylation of p53. This role in p53 regulation was first demonstrated for ING2 [65], and it has subsequently been shown for ING1 [98], ING4 and ING5 [91], albeit with different efficiencies [65]. ING proteins do not seem to have intrinsic enzymatic activity, rather they might promote acetylation of p53 or other proteins by acting as cofactors. In support of this model, biochemical analyses have shown association of ING proteins with acetylases like p300 or PCAF [77, 91] or deacetylases like SIRT1 or HDAC1 [76, 80, 98] all of which have the ability to regulate acetylation levels of p53. An additional level of functional interplay between p53 and ING proteins would be the role of ING proteins as transcriptional cofactors cooperating with p53 in gene regulation, possibly trough the recruitment of histone modifying complexes [99]. In support of this model, ectopic Ing1 and p53 require the presence of each other to elicit cellular responses and induction of p53 targets [90, 100]. One possible mechanism for the transcriptional cooperation between ING1 and p53 could relate to the functional connection between ING1 and ARF [100]. Besides its well-known function in control of p53 stability (see above), ARF can also cooperate with a number of transcriptional factors, including p53, acting in connection with histone modifying activities [27]. We found that ING1 required functional ARF for induction of cell-cycle arrest and activation of the p53 targets p21 and Mdm2, in the absence of effects on p53 protein stability, suggesting the existence of functional interplay between these proteins at the level of transcriptional control [100].

Since ING proteins appear to be linked to p53 in different ways, there has been an obvious interest in trying to decipher the connection between ING proteins and p53 in the context of senescence. The role of p53 is particularly relevant in senescence of murine fibroblasts. p53 protein levels are very low in presenescent non-stressed MEFs. A dramatic accumulation of the p53 protein, [25, 29] frequently accompanied by specific post-translational modifications [101] is readily observed in mouse fibroblasts as they enter oncogene-induced senescence. This accumulation is primarily due to the action of the p19Arf protein and its inhibition of Mdm2-mediated degradation of p53. As mentioned, ING1 has been functionally linked to ARF [100] and also to Mdm2-mediated p53 stabilization [95]. Consistent with an important role for Ing1 in p53 control, Ing1-deficient mouse fibroblasts fail to accumulate p53 as efficiently as their wild-type counterparts upon Ras expression [67]. This defective accumulation of p53 does not appear to be due to impaired induction of p19Arf in response to oncogenic Ras, as this p53 regulator shows a normal upregulation irrespective of the Ing1 status of the cells. Rather, it seems to reflect a reduced basal half-life of p53 in Ing1-mutant cells. The precise basis for this phenotype has not been unambiguously established. It could feasibly be explained through the direct effect *via* Mdm2 discussed above [95], although other indirect mechanisms cannot be ruled out. It should be noted that this defect in p53 activation seems to be restricted to this specific stress response [67, 69], and therefore, some undefined senescence-specific factors might be relevant. During senescence caused by different stimuli, most notably oncogenic stress, p53 not only accumulates but also undergoes specific post-translational modifications. Increased phosphorylation of Ser15 or Ser18 [6, 102] and increased acetylation of Lys373 and Lys382 [101] in the p53 molecule have been associated with implementation of senescence in different cellular types. As indicated above, acetylation is the post-translational modification of p53 most consistently linked to ING proteins. The potential relevance of p53 acetylation in the context of ING proteins and senescence has been so far only explored for ING2. Pedeux *et al.* [66] showed that ING2 forms a ternary complex with p53 and the acetyltransferase protein p300 in senescent human fibroblasts, but not in young fibroblasts, which could contribute to the accumulation of acetylated p53 typical of this setting. Conversely, silencing of ING2 by RNA interference in replicative senescent cells resulted in a decrease of the amount of acetylated p53 in these cells. Although these results indicate a critical role for ING2 in the regulation of p53 acetylation during senescence, how ING2 relates to the canonical machinery controlling p53 acetylation in senescence is not known. In the generally accepted model, adequate acetylation of p53 during oncogene-induced senescence requires the relocalization of p53 and the CBP protein to nuclear bodies, in a process mediated by the PML protein [101, 103]. In contrast, the co-localization of ING2 with PML or CBP has not been observed in senescence, suggesting that, whatever the exact mechanism, the observed effect of ING2 on p53 acetylation occurs *via* an alternative PML-independent mechanism [66]. It should also be mentioned that, although p53 acetylation has been linked to ING2 *in vitro*, a specific interaction between ING2 and phosphorylated p53 in senescent cells has also been observed [66].

As a further proof of the link of the INGs to p53 in the context of the senescent arrest, induction of senescence by ectopic INGs has been shown to require the presence of functional p53 in several settings. For example, in human fibroblasts, disabling of the p53 pathway by RNA interference is sufficient to allow the bypass of senescence triggered by ectopic expression of ING2 [66]. Surprisingly, senescence induced by silencing of ING2 in telomerised fibroblasts appears to occur in a p53-independent manner [70]. To add further complexity to this regulatory pathway, it has been

recently reported that ING2 is also a transcriptional target of p53, suggesting the existence of a complex regulatory feedback circuit between ING2 and p53 in the context of senescence [70]. As a further proof of the functional involvement of p53 in ING-induced senescence, enforced p33ING1b expression fails to trigger senescence efficiently in human fibroblasts where the p53 pathway is disabled by the expression of the oncoviral protein E6 (Abad *et al.* submitted), or in p53-null mouse embryo fibroblasts ([100] and unpublished observations).

An interesting issue is the possible specificity of different ING proteins or isoforms with regard to the type of senescence. A number of observations in different systems appear to suggest that the participitation of ING proteins in senescence might depend of the senescence trigger. For example, studies with human fibroblasts suggest that ING2 has markedly different roles depending whether senescence is elicited by oncogenes or due to the accumulation of divisions. While ING2 levels raise with increased population doublings and its silencing allows an extension of normal life span, ING2 levels are reduced upon Ras induced senescence, and this response is not affected by ING2 suppression. These data suggest that this ING protein might be a component of the regulatory circuit in action during replicative senescence, but does not seem to be involved in Ras-induced senescence [66]. In the case of murine Ing1, its deficiency in fibroblasts has a clear impact in oncogene-induced senescence while entry into senescence due to population doublings is not significantly affected. Although it has not been investigated directly, the data from mouse models with inactivation of the *Ing1* locus is also consistent with variant-specific roles of the products of this locus in senescence [67, 68]. A complex situation has been described for the alternative isoforms of the human ING1 locus, p47ING1a and p33ING1b. These variants are generated by splicing of two alternative first exons to a common exon, and accordingly share their C-terminus but differ in their N-terminus. The p47ING1a isoform is not as well characterized as ING1b, but biochemical studies suggest that they might have differential effects in histone acetylation [77]. In the context of replicative senescence of human fibroblasts, there is conflicting evidence about the effects on p33ING1b levels. There have been reports of upregulation of this isoform in late passage cells [63], but also of reduced expression in similar conditions [77, 88]. The available data about the alternative isoform p47ING1a in senescence is more limited, but also controversial. In a recent report [88], it was reported that the levels of the ING1a transcript and, to a lesser extent, p47ING1a protein increased during replicative senescence of human fibroblasts. In turn, during oncogene-induced senescence in the same cell type, p33ING1b protein levels are elevated, while those of ING1a do not change (Abad *et al.* submitted). Also, transient ectopic expression of ING1a was shown to induce a senescent phenotype in early passage human fibroblasts, while ING1b was mainly pro-apoptotic under these circumstances [88]. Taken together, these and the previously discussed evidence, would suggest that both ING1 isoforms can have a causal role in the implementation of cellular senescence. A summary of the evidence linking ING proteins to senescence is presented in Table **1**.

REGULATION OF ING PROTEINS IN SENESCENCE

The mechanisms underlying the regulation of ING proteins during senescence are not well defined. In the case of p33ING1b and ING2, the increase in protein levels during Ras-induced senescence or replicative senescence, respectively, is not accompanied by obvious changes in RNA levels [66] Abad *et al.*, submitted). This observation opens the possibility that post-translational mechanisms might be responsible, at least in part, for the accumulation of ING proteins in senescent cells. Such mechanisms have been recently described for p33ING1b, and they involve the phosphorylation of specific Serine residues, which in turn block p33ING1b degradation *via* the proteasome [104,105]. Interestingly, one of the kinases responsible for ING1 phosphorylation is ATM. This kinase is a major effector of responses to genotoxic stress, which has been implicated in the induction of senescence triggered by DNA damage. It would be very

Table 1.

	ING Protein	Experimental Approach	Senescence Phenotype	Cell Type	Reference
Gain of Function	ING1[a]	Transient overexpression	Induction of senescence	Human fibroblasts	[88]
	ING1[b]	Retroviral transduction	Induction of senescence	Human fibroblasts	[64]; Abad *et al.*, submitted
	ING2	Retroviral transduction	Induction of senescence	Human fibroblasts	[66]
Loss of Function	Ing1 locus[a]	Gene trap mutation	Bypass of oncogene-induced senescence	Mouse fibroblasts	[67]
	ING1[b]	Antisense	Extension of life span	Human fibroblasts	[63]
	ING1[b]	shRNA	Bypass of oncogene-induced senescence	Human fibroblasts	Abad *et al.*, submitted
	ING2	shRNA	Extension of life span	Human fibroblasts	[66]
	ING2[c]	siRNA	Induction of senescence	Human fibroblasts	[70]

a: Reduced expression of all Ing1 isoforms. b: Against the common exon of the ING1 locus. c: With ectopic expression of telomerase. Only reports where an effect on senescence has been described are included. See text for a more complete description.

interesting to determine if this level of control of ING function is in action during senescence.

ING PROTEINS AND SENESCENCE *IN VIVO*

As mentioned, senescence is increasingly regarded as an effective anti-tumor barrier *in vivo*. Therefore, an issue of extraordinary interest is how the evidence at the cellular level that we have discussed so far could translate to live organisms and, accordingly, which could be the possible role of ING proteins in the establishment of the senescence response *in vivo* and its implication in the context of tumor suppression. The most obvious tumor phenotype of mice deficient for the Ing1 locus is the increased predisposition to the formation of B-cell lymphomas, either spontaneously in aged animals or in response to irradiation [68, 69]. The relevance of senescence as a block to tumor formation has now been studied in a variety of experimental tumor models. Interestingly, one of them is the formation of T-cell lymphomas in mice driven by the expression of RasV12 in the T-cell compartment [49]. Induction of senescence and the concomitant block to tumor formation in this setting was found to depend on the histone-methylase Suv39h1, indicating the importance of proper chromatin regulation in this *in vivo* response. In a separate study, senescence has also been identified as a protective mechanism that prevents the formation of B-cell lymphomas in mice, mediated by telomere attrition [106]. With these data in mind, it is tempting to speculate that the increased appearance of B-cell lymphomas in Ing1-deficient animals might reflect the disablement of this protective barrier, due to the loss of Ing1 function. Currently, this is a largely unexplored field and clearly, more experiments are needed to address directly the possible participation of Ing1 in the implementation of senescence *in vivo* in this or other tumor types.

CONCLUDING REMARKS AND FUTURE DIRECTIONS

In this review, we have tried to summarize the growing evidence linking the ING family of tumor suppressors to the cellular senescence response. The picture that emerges from the data accumulated over recent years on this subject is still incomplete and sometimes contradictory. While the implication of ING proteins in the regulation of senescence appears to be firmly established, there are still many open questions that need to be solved. Collectively, the data support a model where ING proteins act as players in the complex molecular machinery that controls initiation and maintenance of cellular senescence, but their precise position in this circuitry and their crosstalk with other regulators or effectors still needs to be defined (Fig. **3**). Large part of the evidence coincides in pointing at ING proteins as important regulators of gene expression during senescence, *via* chromatin regulation. Many other factors have been previously implied at this level, probably reflecting the complexity of gene expression control required for the correct regulation of this response. The possible crosstalk of ING proteins with other senescence regulators at this level should be explored. Also, very little is known about the specific targets whose expression is controlled by ING proteins during senescence. The identification of these, for instance with expression profiling studies, would be of great interest. Similarly, the implication of the p53 pathway in this function of ING proteins seems also well established. This functional link to p53 should be investigated in more detail, specifically to obtain a better understanding of the molecular mechanism involved.

Obviously, the current data offers a partial view of a possibly complex role of ING proteins in senescence. A large part of the evidence linking ING proteins to senescence is based on overexpression experiments, and these should be

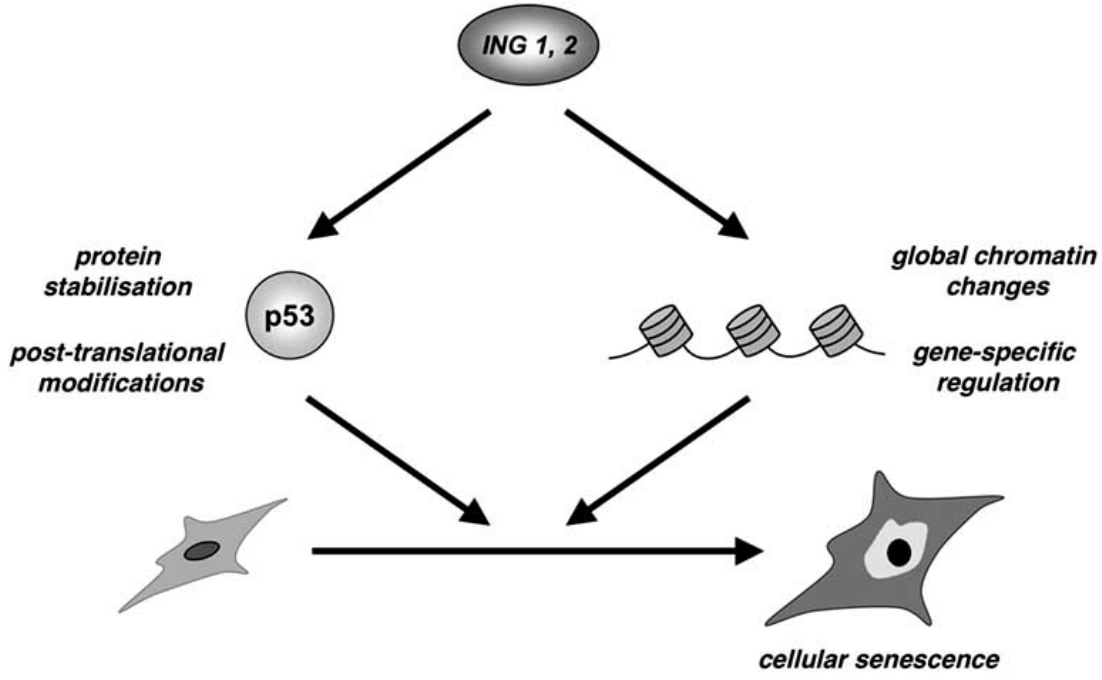

Fig. (3). Model for the implication of ING proteins in cellular senescence. See text for details.

interpreted with caution. Dominant negative effects caused by competition for limited interactors (like HDACs or H3K4triM), or sequestering of ING partners through dimerization are possible. Also, the level and type of ectopic expression –transient and acute or stable and moderate – should also be borne in mind when interpreting these results. Similarly, and in part related to the above, the specific roles of the isoforms of the human or murine ING locus in this context need further clarification. Experiments with genetically modified models, or isoform-specific genetic tools, should help clarify this issue. Hopefully, as more data accumulates, with more different and complementary experimental approaches, these issues should be progressively clarified.

Another open question is the putative involvement of ING proteins in senescence triggered by different stimuli. For instance, a possible role for ING1 as a mediator of telomere-driven senescence can be implied from the observation that ING1 protein accumulates in human senescent fibroblasts where telomeres are made dysfunctional by the expression of a dominant-negative form of the telomeric protein TRF [107]. Interestingly, all human ING loci, except ING3, are located in subtelomeric chromosomal regions, opening the possibility of their regulation in response to telomere dysfunction. Related to this, an additional standing issue is the possible link between ING proteins and DDR response during senescence. ING proteins can participate in different types of DNA repair, in part modifying chromatin structure [108, 109]. It would be interesting to determine the possible link of ING proteins with the DDR response in the context of senescence triggered by oncogenes, telomere attrition, or other stimuli. Although here we have discussed senescence mostly in the context of tumor suppression, it has also been suggested that senescence might be linked to organismal aging, either by deleterious effects of the accumulation of senescent cells in aging tissues or through the age-related depletion of stem cell pools [3, 4]. A possible role for ING proteins in this context and its possible implications in organismal aging is also a subject that deserves attention. And, last but not least, in light of the role of senescence as a tumor suppressor barrier *in vivo*, the potential relevance of the link of ING proteins to senescence in the context of human tumors is of paramount importance. A hint of this potential link could come from the study of the behavior in senescence assays of tumor-associated ING variants [84]. In summary, we are only starting to understand the connection between ING proteins and cellular senescence, and its implication in their tumor suppressor action. Clearly, additional work is warranted to better understand this complex scenario, with the hope that it might shed light on the role of ING proteins in tumorigenesis.

ACKNOWLEDGEMENTS

Work in the authors' laboratory has been funded by the Spanish Ministry of Science and Innovation, grant BFU06-10882, and the Fundación de Investigación Medica Mutua Madrileña.

REFERENCES

[1] Hayflick, L. and Moorhead, P.S. (1961) *Exp. Cell Res.*, **25**, 585-621.
[2] Hayflick, L. (1965) *Exp. Cell Res.*, **37**, 614-636.
[3] Collado, M.; Blasco, M.A. and Serrano, M. (2007) *Cell*, **130**(2), 223-233.
[4] Campisi, J. and d'Adda di Fagagna, F. (2007) *Nat. Rev. Mol Cell Biol.*, **8**(9), 729-740.
[5] Courtois-Cox, S.; Jones, S.L. and Cichowski, K. (2008) *Oncogene*, **27**(20), 2801-2809.
[6] Jackson, J.G. and Pereira-Smith, O.M. (2006) *Cancer Res.*, **66**(17), 8356-8360.
[7] Dimri, G. P.; Lee, X.; Basile, G.; Acosta, M.; Scott, G.; Roskelley, C.; Medrano, E. E.; Linskens, M.; Rubelj, I.; Pereira-Smith, O.; Peacocke, M. and Campisi, J. (1995) *Proc. Natl. Acad. Sci. U. S. A.*, **92**(20), 9363-9367.
[8] Collado, M. and Serrano, M. (2006) *Nat. Rev. Cancer*, **6**(6), 472-476.
[9] Blasco, M.A. (2005) *Nat. Rev. Genet.*, **6**(8), 611-622.
[10] Herbig, U.; Jobling, W.A.; Chen, B.P.; Chen, D.J. and Sedivy, J.M. (2004) *Mol. Cell*, **14**(4), 501-513.
[11] d'Adda di Fagagna, F.; Reaper, P.M.; Clay-Farrace, L.; Fiegler, H.; Carr, P.; Von Zglinicki, T.; Saretzki, G.; Carter, N.P. and Jackson, S.P. (2003) *Nature*, **426**(6963), 194-198.
[12] Serrano, M.; Lin, A.W.; McCurrach, M.E.; Beach, D. and Lowe, S.W. (1997) *Cell*, **88**(5), 593-602.
[13] Sherr, C.J. and DePinho, R.A. (2000) *Cell*, **102**(4), 407-410.
[14] Drayton, S. and Peters, G. (2002) *Curr. Opin. Genet. Dev.*, **12**(1), 98-104.
[15] Di Leonardo, A.; Linke, S.P.; Clarkin, K. and Wahl, G.M. (1994) *Genes Dev.*, **8**(21), 2540-2551.
[16] Roninson, I.B. (2003) *Cancer Res.*, **63**(11), 2705-2715.
[17] Bartkova, J., Rezaei, N., Liontos, M., Karakaidos, P., Kletsas, D., Issaeva, N., Vassiliou, L. V., Kolettas, E., Niforou, K., Zoumpourlis, V. C., Takaoka, M., Nakagawa, H., Tort, F., Fugger, K., Johansson, F., Sehested, M., Andersen, C. L., Dyrskjot, L., Ornтoft, T., Lukas, J., Kittas, C., Helleday, T., Halazonetis, T. D., Bartek, J. and Gorgoulis, V. G. (2006) *Nature*, **444**(7119), 633-637.
[18] Di Micco, R.; Fumagalli, M.; Cicalese, A.; Piccinin, S.; Gasparini, P.; Luise, C.; Schurra, C.; Garre, M.; Nuciforo, P. G.; Bensimon, A.; Maestro, R.; Pelicci, P. G. and d'Adda di Fagagna, F. (2006) *Nature*, **444**(7119), 638-642.
[19] Christophorou, M.A.; Ringshausen, I.; Finch, A.J.; Swigart, L.B. and Evan, G.I. (2006) *Nature*, **443**(7108), 214-217.
[20] Efeyan, A.; Garcia-Cao, I.; Herranz, D.; Velasco-Miguel, S. and Serrano, M. (2006) *Nature*, **443**(7108), 159.
[21] Campisi, J. (2005) *Cell*, **120**(4), 513-522.
[22] Gil, J. and Peters, G. (2006) *Nat. Rev. Mol. Cell Biol.*, **7**(9), 667-677.
[23] Kim, W.Y. and Sharpless, N.E. (2006) *Cell*, **127**(2), 265-275.
[24] Serrano, M.; Hannon, G.J. and Beach, D. (1993) *Nature*, **366**(6456), 704-707.
[25] Serrano, M. (1997) *Exp. Cell Res.*, **237**(1), 7-13.
[26] Sherr, C.J. (2001) *Nat. Rev. Mol. Cell Biol.*, **2**(10), 731-737.
[27] Sherr, C.J. (2006) *Nat. Rev. Cancer*, **6**(9), 663-673.
[28] Zindy, F.; Quelle, D.E.; Roussel, M.F. and Sherr, C.J. (1997) *Oncogene*, **15**(2), 203-211.
[29] Palmero, I.; Pantoja, C. and Serrano, M. (1998) *Nature*, **395**(6698), 125-126.
[30] Kamijo, T.; Zindy, F.; Roussel, M.F.; Quelle, D.E.; Downing, J.R.; Ashmun, R.A.; Grosveld, G. and Sherr, C.J. (1997) *Cell*, **91**(5), 649-659.
[31] Huot, T. J.; Rowe, J.; Harland, M.; Drayton, S.; Brookes, S.; Gooptu, C.; Purkis, P.; Fried, M.; Bataille, V.; Hara, E.; Newton-Bishop, J. and Peters, G. (2002) *Mol. Cell Biol.*, **22**(23), 8135-8143.
[32] Voorhoeve, P.M. and Agami, R. (2003) *Cancer Cell*, **4**(4), 311-319.
[33] Wei, W.; Hemmer, R.M. and Sedivy, J.M. (2001) *Mol. Cell Biol.*, **21**(20), 6748-6757.
[34] Malumbres, M.; Perez De Castro, I.; Hernandez, M.I.; Jimenez, M.; Corral, T. and Pellicer, A. (2000) *Mol. Cell Biol.*, **20**(8), 2915-2925.
[35] Stein, G.H. and Dulic, V. (1995) *Bioessays*, **17**(6), 537-543.
[36] Narita, M.; Nunez, S.; Heard, E.; Narita, M.; Lin, A.W.; Hearn, S.A.; Spector, D.L.; Hannon, G.J. and Lowe, S.W. (2003) *Cell*, **113**(6), 703-716.

[37] Acosta, J. C.; O'Loghlen, A.; Banito, A.; Guijarro, M. V.; Augert, A.; Raguz, S.; Fumagalli, M.; Da Costa, M.; Brown, C.; Popov, N.; Takatsu, Y.; Melamed, J.; d'Adda di Fagagna, F.; Bernard, D.; Hernando, E. and Gil, J. (2008) *Cell*, **133**(6), 1006-1018.
[38] Kuilman, T.; Michaloglou, C.; Vredeveld, L.C.; Douma, S.; van Doorn, R.; Desmet, C.J.; Aarden, L.A.; Mooi, W.J. and Peeper, D.S. (2008) *Cell*, **133**(6), 1019-1031.
[39] Krizhanovsky, V.; Yon, M.; Dickins, R.A.; Hearn, S.; Simon, J.; Miething, C.; Yee, H.; Zender, L. and Lowe, S.W. (2008) *Cell*, **134**(4), 657-667.
[40] Xue, W.; Zender, L.; Miething, C.; Dickins, R.A.; Hernando, E.; Krizhanovsky, V.; Cordon-Cardo, C. and Lowe, S.W. (2007) *Nature*, **445**(7128), 656-660.
[41] Campisi, J. (2003) *Nat. Rev. Cancer*, **3**(5), 339-349.
[42] Narita, M. (2007) *Br. J. Cancer*, **96**(5), 686-691.
[43] Funayama, R. and Ishikawa, F. (2007) *Chromosoma*, **116**(5), 431-440.
[44] Adams, P.D. (2007) *Gene*, **397**(1-2), 84-93.
[45] Narita, M.; Narita, M.; Krizhanovsky, V.; Nunez, S.; Chicas, A.; Hearn, S.A.; Myers, M.P. and Lowe, S.W. (2006) *Cell*, **126**(3), 503-514.
[46] Ruley, H.E. (1983) *Nature*, **304**(5927), 602-606.
[47] Land, H.; Parada, L.F. and Weinberg, R.A. (1983) *Nature*, **304** (5927), 596-602.
[48] Lowe, S.W.; Cepero, E. and Evan, G. (2004) *Nature*, **432**(7015), 307-315.
[49] Braig, M.; Lee, S.; Loddenkemper, C.; Rudolph, C.; Peters, A. H.; Schlegelberger, B.; Stein, H.; Dorken, B.; Jenuwein, T. and Schmitt, C. A. (2005) *Nature*, **436**(7051), 660-665.
[50] Chen, Z.; Trotman, L. C.; Shaffer, D.; Lin, H. K.; Dotan, Z. A.; Niki, M.; Koutcher, J. A.; Scher, H. I.; Ludwig, T.; Gerald, W.; Cordon-Cardo, C. and Pandolfi, P. P. (2005) *Nature*, **436**(7051), 725-730.
[51] Collado, M.; Gil, J.; Efeyan, A.; Guerra, C.; Schuhmacher, A. J.; Barradas, M.; Benguria, A.; Zaballos, A.; Flores, J. M.; Barbacid, M.; Beach, D. and Serrano, M. (2005) *Nature*, **436**(7051), 642.
[52] Courtois-Cox, S.; Genther Williams, S.M.; Reczek, E.E.; Johnson, B.W.; McGillicuddy, L.T.; Johannessen, C.M.; Hollstein, P.E.; MacCollin, M. and Cichowski, K. (2006) *Cancer Cell*, **10**(6), 459-472.
[53] Dankort, D.; Filenova, E.; Collado, M.; Serrano, M.; Jones, K. and McMahon, M. (2007) *Genes Dev.*, **21**(4), 379-384.
[54] Michaloglou, C.; Vredeveld, L. C.; Soengas, M. S.; Denoyelle, C.; Kuilman, T.; van der Horst, C. M.; Majoor, D. M.; Shay, J. W.; Mooi, W. J. and Peeper, D. S. (2005) *Nature*, **436**(7051), 720-724.
[55] Prieur, A. and Peeper, D.S. (2008) *Curr. Opin. Cell Biol.*, **20**(2), 150-155.
[56] Ventura, A.; Kirsch, D. G.; McLaughlin, M. E.; Tuveson, D. A.; Grimm, J.; Lintault, L.; Newman, J.; Reczek, E. E.; Weissleder, R. and Jacks, T. (2007) *Nature*, **445**(7128), 661-665.
[57] He, G.H.; Helbing, C.C.; Wagner, M.J.; Sensen, C.W. and Riabowol, K. (2005) *Mol. Biol. Evol.*, **22**(1), 104-116.
[58] Shi, X. and Gozani, O. (2005) *J. Cell Biochem.*, **96**(6), 1127-1136.
[59] Soliman, M.A. and Riabowol, K. (2007) *Trends Biochem. Sci.*, **32**(11), 509-519.
[60] Gunduz, M.; Gunduz, E.; Rivera, R.S. and Nagatsuka, H. (2008) *Curr. Cancer Drug Targets*, **8**(4), 275-284.
[61] Ythier, D.; Larrieu, D.; Brambilla, C.; Brambilla, E. and Pedeux, R. (2008) *Int. J. Cancer*, **123**(7), 1483-1490.
[62] Coles, A.H. and Jones, S.N. (2009) *J. Cell Physiol.*, **218**(1), 45-57.
[63] Garkavtsev, I. and Riabowol, K. (1997) *Mol. Cell Biol.*, **17**(4), 2014-2019.
[64] Goeman, F.; Thormeyer, D.; Abad, M.; Serrano, M.; Schmidt, O.; Palmero, I. and Baniahmad, A. (2005) *Mol. Cell Biol.*, **25**(1), 422-431.
[65] Nagashima, M.; Shiseki, M.; Miura, K.; Hagiwara, K.; Linke, S. P.; Pedeux, R.; Wang, X. W.; Yokota, J.; Riabowol, K. and Harris, C. C. (2001) *Proc. Natl. Acad. Sci. U. S. A.*, **98**(17), 9671-9676.
[66] Pedeux, R.; Sengupta, S.; Shen, J. C.; Demidov, O. N.; Saito, S.; Onogi, H.; Kumamoto, K.; Wincovitch, S.; Garfield, S. H.; McMenamin, M.; Nagashima, M.; Grossman, S. R.; Appella, E. and Harris, C. C. (2005) *Mol. Cell Biol.*, **25**(15), 6639-6648.
[67] Abad, M.; Menendez, C.; Fuchtbauer, A.; Serrano, M.; Fuchtbauer, E.M. and Palmero, I. (2007) *J. Biol. Chem.*, **282**(42), 31060-31067.
[68] Coles, A.H.; Liang, H.; Zhu, Z.; Marfella, C.G.; Kang, J.; Imbalzano, A.N. and Jones, S.N. (2007) *Cancer Res.*, **67**(5), 2054-2061.
[69] Kichina, J.V.; Zeremski, M.; Aris, L.; Gurova, K.V.; Walker, E.; Franks, R.; Nikitin, A.Y.; Kiyokawa, H. and Gudkov, A.V. (2006) *Oncogene*, **25**(6), 857-866.
[70] Kumamoto, K.; Spillare, E. A.; Fujita, K.; Horikawa, I.; Yamashita, T.; Appella, E.; Nagashima, M.; Takenoshita, S.; Yokota, J. and Harris, C. C. (2008) *Cancer Res.*, **68**(9), 3193-3203.
[71] Ogryzko, V.V.; Hirai, T.H.; Russanova, V.R.; Barbie, D.A. and Howard, B.H. (1996) *Mol. Cell Biol.*, **16**(9), 5210-5218.
[72] Munro, J.; Barr, N.I.; Ireland, H.; Morrison, V. and Parkinson, E.K. (2004) *Exp. Cell Res.*, **295**(2), 525-538.
[73] Gil, J.; Bernard, D.; Martinez, D. and Beach, D. (2004) *Nat. Cell Biol.*, **6**(1), 67-72.
[74] Berns, K.; Hijmans, E. M.; Mullenders, J.; Brummelkamp, T. R.; Velds, A.; Heimerikx, M.; Kerkhoven, R. M.; Madiredjo, M.; Nijkamp, W.; Weigelt, B.; Agami, R.; Ge, W.; Cavet, G.; Linsley, P. S.; Beijersbergen, R. L. and Bernards, R. (2004) *Nature*, **428** (6981), 431-437.
[75] Jacobs, J.J.; Kieboom, K.; Marino, S.; DePinho, R.A. and van Lohuizen, M. (1999) *Nature*, **397**(6715), 164-168.
[76] Skowyra, D.; Zeremski, M.; Neznanov, N.; Li, M.; Choi, Y.; Uesugi, M.; Hauser, C. A.; Gu, W.; Gudkov, A. V. and Qin, J. (2001) *J. Biol. Chem.*, **276**(12), 8734-8739.
[77] Vieyra, D.; Loewith, R.; Scott, M.; Bonnefin, P.; Boisvert, F. M.; Cheema, P.; Pastyryeva, S.; Meijer, M.; Johnston, R. N.; Bazett-Jones, D. P.; McMahon, S.; Cole, M. D.; Young, D. and Riabowol, K. (2002) *J. Biol. Chem.*, **277**(33), 29832-29839.
[78] Kuzmichev, A.; Zhang, Y.; Erdjument-Bromage, H.; Tempst, P. and Reinberg, D. (2002) *Mol. Cell Biol.*, **22**(3), 835-848.
[79] Doyon, Y.; Cayrou, C.; Ullah, M.; Landry, A. J.; Cote, V.; Selleck, W.; Lane, W. S.; Tan, S.; Yang, X. J. and Cote, J. (2006) *Mol. Cell*, **21**(1), 51-64.
[80] Binda, O.; Nassif, C. and Branton, P.E. (2008) *Oncogene*, **27**(24), 3384-3392.
[81] Pena, P.V.; Davrazou, F.; Shi, X.; Walter, K.L.; Verkhusha, V.V.; Gozani, O.; Zhao, R. and Kutateladze, T.G. (2006) *Nature*, **442**(7098), 100-103.
[82] Shi, X.; Hong, T.; Walter, K. L.; Ewalt, M.; Michishita, E.; Hung, T.; Carney, D.; Pena, P.; Lan, F.; Kaadige, M. R.; Lacoste, N.; Cayrou, C.; Davrazou, F.; Saha, A.; Cairns, B. R.; Ayer, D. E.; Kutateladze, T. G.; Shi, Y.; Cote, J.; Chua, K. F. and Gozani, O. (2006) *Nature*, **442**(7098), 96-99.
[83] Palacios, A.; Munoz, I.G.; Pantoja-Uceda, D.; Marcaida, M.J.; Torres, D.; Martin-Garcia, J.M.; Luque, I.; Montoya, G. and Blanco, F.J. (2008) *J. Biol. Chem.*, **283**(23), 15956-15964.
[84] Pena, P. V.; Hom, R. A.; Hung, T.; Lin, H.; Kuo, A. J.; Wong, R. P.; Subach, O. M.; Champagne, K. S.; Zhao, R.; Verkhusha, V. V.; Li, G.; Gozani, O. and Kutateladze, T. G. (2008) *J. Mol. Biol.*, **380**(2), 303-312.
[85] Zhang, R.; Poustovoitov, M. V.; Ye, X.; Santos, H. A.; Chen, W.; Daganzo, S. M.; Erzberger, J. P.; Serebriiskii, I. G.; Canutescu, A. A.; Dunbrack, R. L.; Pehrson, J. R.; Berger, J. M.; Kaufman, P. D. and Adams, P. D. (2005) *Dev. Cell*, **8**(1), 19-30.
[86] Funayama, R.; Saito, M.; Tanobe, H. and Ishikawa, F. (2006) *J. Cell Biol.*, **175**(6), 869-880.
[87] Vieyra, D.; Toyama, T.; Hara, Y.; Boland, D.; Johnston, R. and Riabowol, K. (2002) *Cancer Res.*, **62**(15), 4445-4452.
[88] Soliman, M.A.; Berardi, P.; Pastyryeva, S.; Bonnefin, P.; Feng, X.; Colina, A.; Young, D. and Riabowol, K. (2008) *Aging Cell*, **7**(6), 783-794.
[89] Xin, H.; Yoon, H.G.; Singh, P.B.; Wong, J. and Qin, J. (2004) *J. Biol. Chem.*, **279**(10), 9539-9546.
[90] Garkavtsev, I.; Grigorian, I.A.; Ossovskaya, V.S.; Chernov, M.V.; Chumakov, P.M. and Gudkov, A.V. (1998) *Nature*, **391**(6664), 295-298.
[91] Shiseki, M.; Nagashima, M.; Pedeux, R. M.; Kitahama-Shiseki, M.; Miura, K.; Okamura, S.; Onogi, H.; Higashimoto, Y.; Appella, E.; Yokota, J. and Harris, C. C. (2003) *Cancer Res.*, **63**(10), 2373-2378.
[92] Vousden, K.H. and Lane, D.P. (2007) *Nat. Rev. Mol. Cell Biol.*, **8**(4), 275-283.
[93] Zeremski, M.; Hill, J.E.; Kwek, S.S.; Grigorian, I.A.; Gurova, K.V.; Garkavtsev, I.V.; Diatchenko, L.; Koonin, E.V. and Gudkov, A.V. (1999) *J. Biol. Chem.*, **274**(45), 32172-32181.

[94] Nagashima, M.; Shiseki, M.; Pedeux, R.M.; Okamura, S.; Kitahama-Shiseki, M.; Miura, K.; Yokota, J. and Harris, C.C. (2003) *Oncogene*, **22**(3), 343-350.
[95] Leung, K.M.; Po, L.S.; Tsang, F.C.; Siu, W.Y.; Lau, A.; Ho, H.T. and Poon, R.Y. (2002) *Cancer Res.*, **62**(17), 4890-4893.
[96] Bode, A.M. and Dong, Z. (2004) *Nat. Rev. Cancer*, **4**(10), 793-805.
[97] Murray-Zmijewski, F.; Slee, E.A. and Lu, X. (2008) *Nat. Rev. Mol. Cell Biol.*, **9**(9), 702-712.
[98] Kataoka, H.; Bonnefin, P.; Vieyra, D.; Feng, X.; Hara, Y.; Miura, Y.; Joh, T.; Nakabayashi, H.; Vaziri, H.; Harris, C. C. and Riabowol, K. (2003) *Cancer Res.*, **63**(18), 5785-5792.
[99] Murphy, M.; Ahn, J.; Walker, K.K.; Hoffman, W.H.; Evans, R.M.; Levine, A.J. and George, D.L. (1999) *Genes Dev.*, **13**(19), 2490-2501.
[100] Gonzalez, L.; Freije, J.M.; Cal, S.; Lopez-Otin, C.; Serrano, M. and Palmero, I. (2006) *Oncogene*, **25**(37), 5173-5179.
[101] Pearson, M.; Carbone, R.; Sebastiani, C.; Cioce, M.; Fagioli, M.; Saito, S.; Higashimoto, Y.; Appella, E.; Minucci, S.; Pandolfi, P. P. and Pelicci, P. G. (2000) *Nature*, **406**(6792), 207-210.
[102] Webley, K.; Bond, J.A.; Jones, C.J.; Blaydes, J.P.; Craig, A.; Hupp, T. and Wynford-Thomas, D. (2000) *Mol. Cell Biol.*, **20**(8), 2803-2808.
[103] Ferbeyre, G.; de Stanchina, E.; Querido, E.; Baptiste, N.; Prives, C. and Lowe, S.W. (2000) *Genes Dev.*, **14**(16), 2015-2027.
[104] Garate, M.; Campos, E.I.; Bush, J.A.; Xiao, H. and Li, G. (2007) *FASEB J.*, **21**(13), 3705-3716.
[105] Garate, M.; Wong, R.P.; Campos, E.I.; Wang, Y. and Li, G. (2008) *EMBO Rep.*, **9**(6), 576-581.
[106] Feldser, D.M. and Greider, C.W. (2007) *Cancer Cell*, **11**(5), 461-469.
[107] Li, G.Z.; Eller, M.S.; Firoozabadi, R. and Gilchrest, B.A. (2003) *Proc. Natl. Acad. Sci. U. S. A.*, **100**(2), 527-531.
[108] Cheung, K.J.; Jr. and Li, G. (2002) *Exp. Cell Res.*, **279**(2), 291-298.
[109] Kuo, W.H.; Wang, Y.; Wong, R.P.; Campos, E.I. and Li, G. (2007) *Exp. Cell Res.*, **313**(8), 1628-1638.

Received: February 20, 2009 Revised: March 3, 2009 Accepted: March 4, 2009